CSIRO
Exploration & Mining

ACARP
Australian Coal Association Research Program

ACARP PROJECT C9021
EXPLORATION AND MINING REPORT 976C

BOWEN BASIN SUPERMODEL 2000

Joan Esterle[1] and Renate Sliwa[1]
with contributions from Guy Le Blanc Smith[1],
Joel Yago[1], Ray Williams[2], Shuxing Li[3] and
Roussos Dimitrakopoulos[3]

August 2002

OPEN REPORT

CSIRO Exploration & Mining
PO Box 883, Kenmore, Queensland, Australia 4069

[1] CSIRO Exploration & Mining
[2] GeoGAS Systems Pty Ltd
[3] W HBryan Mining Research Centre

ACARP

Australian Coal Association Research Program

DISCLAIMER

No person, corporation or other organisation ("person") should rely on the contents of this report and each should obtain independent advice from a qualified person with respect to the information contained in this report. Australian Coal Research Limited, its directors, servants and agents (collectively "ACR") is not responsible for the consequences of any action taken by any person in reliance upon the information set out in this report, for the accuracy or veracity of any information contained in this report or for any error or omission in this report. ACR expressly disclaims any and all liability and responsibility to any person in respect of anything done or omitted to be done in respect of the information set out in this report, any inaccuracy in this report or the consequences of any action by any person in reliance, whether wholly or partly, upon the whole or any part of the contents of this report.

EXECUTIVE SUMMARY

The aim of the Supermodel 2000 project was to deliver a regional three-dimensional model of the Moranbah-German Creek Coal Measures along the western limb of the Bowen Basin from integrated mine-scale databases and regional basement geology. It provides a snapshot of the available data and knowledge as at December 2000 and provides the first set of regional maps showing coal seam thickness and interburden distributions in the context of structure and basin evolution. This model is the framework from which to examine the relationships between structure, interburden character, stress and gas contents that will aid in regional area selection and local hazard recognition for coal resource extraction. The approach is novel in that it is the first time since initial exploration that a formalized approach to data sharing and presentation at this scale has been implemented.

The approach of the project was to quilt together a "Supermodel" consisting of three regional tiles (**Northern**: Wards Well to Grosvenor; **Middle**: Peak Downs to Norwich Park; and **Southern**: German Creek to Kestrel mines) that display the regional and local structure of the main mineable seams, their thickness and splitting patterns and their interburden thickness distributions. A regional correlation schema of the coal seams across all tiles was developed to implement this approach. Where available, the sedimentary character of the interburden was included to project ground conditions due to the distribution of weak and strong lithologies and their association with tectonic structures. Within this framework, the distribution of virgin gas content and composition was examined to identify domains of similarity with respect to depth and interpreted permeability using coal rank, type and cleat orientation with respect to regional horizontal stress.

Data consisted of mine site drilling (37,250 drill holes) in which coal seams had been logged, open cut and underground mapping of faults, joints and coal cleat, available geophysics (seismic, aeromagnetics, and gravity) and stress measurements. Gas content data came from exploration drilling (415 drill holes) and is presented as full seam composites normalized to 15% ash at 20º C and 101.3 kPa for the Goonyella Middle seam in the northern tile and the German Creek seam in the southern tile.

The results are:

- A structural interpretation of faulting style, severity and timing within the coal measures that is underpinned by an assessment of regional basement structure and available stress measurements;
- The recognition of basement controls on the thickness distribution and splitting patterns of coal seams and their interburden character along the western limb of the basin;
- Predictive relationships between the distributions of weak lithologies and jointed and faulted ground adjacent to strong sandstone dominated roof;
- Predictive relationships between low to high gas domains, seam structure, projected permeability and stress;

- Regional correlations of seams and a series of isopach maps of superseams and interburdens for each of the tiles.

The above relationships are presented in a series of maps and cross sections that are described in this report and contained in a poster set included on CD. Super-seam correlations are provided for the Goonyella Lower-Dysart-German Creek-Lilyvale seam and the Goonyella Middle-Harrow Creek-Aquila/Tieri seam, which are the main mineable seams in this region. Also included in digital format are maps of super-seam structure, thickness and splitting patterns and interburden distributions. Where data were dense enough, seam thickness and interburden maps of the stratigraphically higher intervals to the P-Pleiades seam and the Goonyella Upper seam are also included.

This project had the support of the coal industry, in particular BHP Billiton Mitsubishi Alliance, North Goonyella Coal Pty Ltd, Oaky Creek Coal Pty Ltd, Anglo Coal Pty Ltd, Capricorn Coal Management Ltd, Pacific Coal Pty Ltd, Kestrel Coal Pty Ltd, Santos Ltd and CH4 Pty Ltd, who provided invaluable data, ideas, in-kind support and/or finance. The Queensland Department of Natural Resources and Mines also provided access to regional data and open file information. Geoscience Australia provided access and use of regional gravity data. Invaluable discussions were also held with Chris Fielding of University of Queensland. Two honours theses (Ronan, 2000 and Hill, 2000) were supported as part of this project.

TABLE OF CONTENTS

LIST OF TABLES

LIST OF FIGURES

1 INTRODUCTION

Significant downtime in underground coal mining occurs due to unpredicted faulting and associated poor ground conditions, high stress and high gas levels. This uncertainty can result in substantial monetary losses due to delays in production schedules, changes in mine plans, and loss of coal reserves. These mining issues are geologically derived and controlled by the geological history of a basin during sediment deposition and subsequent burial and coalification. Many of the structural features manifested in the sedimentary coal measures can be tracked back to basement dislocations and subsequent reactivation throughout their deposition and burial history, but few have pursued these relationships due to the difficulties of acquiring and integrating large and disparate regional data sets with mine scale information. This study integrates such a dataset for the extensively mined Late Permian Moranbah and German Creek Coal Measures (CM) that outcrop and are mined along the western limb of the Bowen Basin in central Queensland Figure 1.

Along the western limb, open cut mine exposures and well more than 38,000 company drill holes from 11 operating mines intersect the coal measures within a corridor around 200 km long and 10 km wide. The basic stratigraphy (Figure 2) of these coal measures and lateral continuity of coal seams was determined from analysis of coal exploration drilling conducted by the then Queensland Department of Mines (summarized in Koppe, 1978) and by Utah International (Milligan, 1971). Since that time, a number of regional and detailed minescale studies of the sedimentology of the coal measures have added detail and knowledge to our understanding of their origins (summarised in Michaelsen, 1999). Simply stated, the coal measures mined along the western limb record the transition from the fluvio-deltaic Moranbah CM in the north, to the paralic or marginal marine German Creek CM in the south deposited within the basin during the onset of foreland loading.

Valuable regional studies of the structure and tectonics of the basin had been conducted by the Queensland Department of Natural Resources and Mines, Geoscience Australia and the CSIRO. Hammond and Mallett (1987) used detailed high wall mapping and accessory analyses of drilling data to develop a regional appraisal of structural domains in the Bowen Basin. At that time mine sites were just moving towards computerised modelling and drilling density down dip of high walls was sparse. Hence, the results are not readily transferable to mine site models and required a substantial update in light of the greater data density available today. By combining the currently available datasets, a better visibility of individual features, trends and scales of zones of faulting can be achieved.

The integration of sedimentary and structural models at the minescale developed predictive relationships between poor ground conditions, faulting and the margins of sandstone bodies in the Moranbah CM (LeBlanc Smith and Esterle, 1998; Kelly et al, 2001). This allows structural discontinuities to be forecast where drilling density is too sparse to resolve faulting. By integrating a series of adjoining leases, better identification of the geometry of sandstones can be obtained to project into greenfields areas.

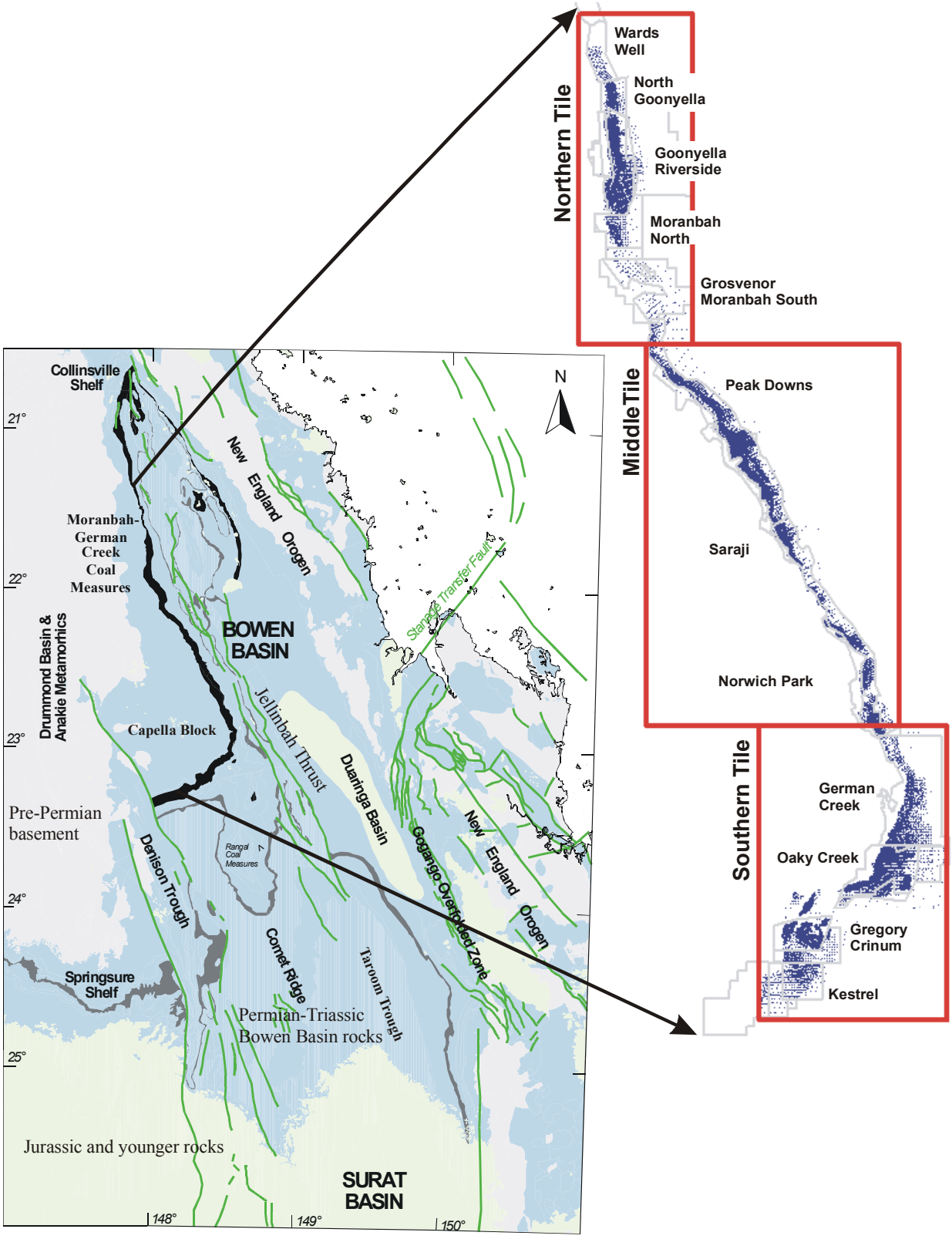

Figure 1 Location maps showing the outline of Permian coal measures outcrop and the Supermodel tiles coverage of mining leases and available company drilling data along the western limb of the central Bowen Basin, Queensland. Major basin elements and regional faults (green lines) are shown (black – Moranbah/German Ck coal measures, blue – Early and Late Permian sedimentary rocks, green – Triassic sedimentary rocks, grey-basement and cover rocks).

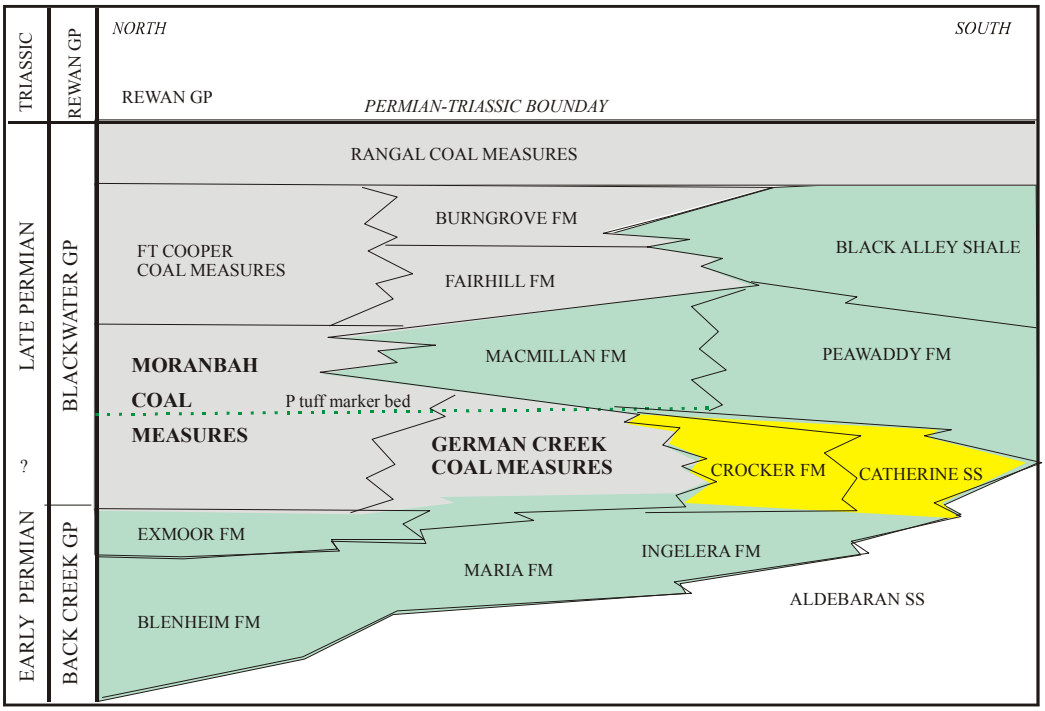

Figure 2 Stratigraphic framework for the Moranbah-German Creek Coal Measures. Modified after Draper, 1990 and Falkner and Fielding, 1993 and Michaelson, 1999.

With the increase in underground mines and the increasing depths of operating mines, coal seam gas also became an issue for the western limb of the basin. Based on minesite studies, the first regional picture for gas distributions in the Moranbah CM was developed by Williams (Williams et al, 2000). Williams identified domains of similar gas behaviour with depth and suggested that domain boundaries were related to geological features.

The Supermodel 2000 project has integrated these different data streams into a regional geological framework that can be used to understand variability at the minescale. It provides a snapshot of the available data and knowledge as at December 2000 and provides the first set of regional maps showing coal seam thickness and interburden distributions in the context of structure and basin evolution. This model is the framework from which to examine the relationships between structure, interburden character, stress and gas contents that will aid in regional area selection and local hazard recognition for coal resource extraction.

The report is organised to present different aspects and scales of Bowen Basin coal measure geology and its impact on mining through maps and descriptive text about the maps. Included in digital format is a poster set that highlights the main findings described in the following sections. These should be plotted and displayed to provide information for geologists, engineers and generalists interested in coal geology.

1.1 Products

The products from Supermodel 2000 include this report that describes the data and tools used to generate the model and derivative maps and cross sections, a set of 6 posters with the following themes:

- Regional Structure and evolution of the Bowen Basin
- Interburden character
- Geological controls on coal seam gas distribution
- Northern tile coal seam and interburden geology
- Middle tile coal seam and interburden geology
- Southern tile coal seam and interburden geology;

Maps are also included in digital format and, for contributors only, DXF overlays of structure and infrastructure, and locatable model grids.

1.2 Acknowledgements

This project could not have been conducted without the support of ACARP and the coal industry. In particular, we thank BHP Billiton Mitsubishi Alliance, North Goonyella Coal Pty Ltd, Oaky Creek Coal Pty Ltd, Anglo Coal Pty Ltd, Capricorn Coal Management Ltd, Pacific Coal Pty Ltd, Kestrel Coal Pty Ltd, Santos Ltd and CH4 Pty Ltd and their operations. Individuals who assisted in this process include mine site geologists, consultants, government geologists and researchers as follows: Stuart Argent, Jared Armstrong, Jim Beeston, Mark Biggs, Frans Bos, Tim Britten, Roger Buzzacott, Bob Coutts, Bob Cranstoun, John Crossley, Paul Damen, Doug Dunn, John Draper, Andrew Falkner, Chris Fielding, Richard Fry, Nigel Godfrey, Nick Gordon, Rod Hammond, Darren Holden, Paul Jones, Jochen Kassan, Bill Koppe, Andrew Laws, Eric Lohe, Dennis MacManus, Cliff Mallett, Mark Manners, Dave Mathew, Ted Milligan (deceased), Ken Preston, Ian Price, Harry Seitlinger, Ray Smith, Diane Sommer, John Thrift, Andrew Willson. Our monitors for this project were Andrew Willson, Doug Dunn and Peter Forrestal. Our apologies for many omissions.

1.3 External data copyright notes

This product Supermodel 2000 incorporates data that are:

The Data (Australian National Gravity Database) has been used in Supermodel 2000with the permission of Geoscience Australia. Geoscience Australia has not evaluated the Data as altered and

incorporated within Supermodel 2000, and therefore gives no warranty regarding its accuracy, completeness, currency or suitability for any particular purpose.

Limited End-user licence provided by Geoscience Australia: You may use Supermodel 2000 to load, display, print and reproduce views obtained from the Data, retaining this notice, for your personal use, or use within your organisation only.

Visit the Geoscience Australia website (www.ga.gov.au) to download the most current version of the Data and to obtain an Unlimited Licence. An Unlimited Licence permits you to create a Derivative Product, and to distribute the Data or Derivative Product to third parties.

2 METHODOLOGY

The study area was confined to the western limb of the basin and it was subdivided into three regional tiles: northern, middle and southern (Figure 1). A total of 38220 boreholes with interpreted and correlated coal seams for the Moranbah-German Creek measures were used to build the models across the three tiles. The surface elevation and bases of weathering, water table and Tertiary were also available for these holes. Each of these logs contained a down-hole geophysical suite (density, gamma ray, and calliper with variable availability of sonic and neutron) and data were available either digitally or in paper-format. Approximately 20,000 drill holes to determine oxidation lines for the different seams were excluded from the database.

Down-hole geophysics was used to check correlations where necessary and to interpret and correlate gross interburden lithologies in the Northern and Southern Tiles where one-on-one studies were conducted for geotechnical assessment. Drilling data and geophysical wire line log profiles were loaded into Paradigm Geophysical Geolog6 software for display, correlation and analysis. Calibration of drill hole geophysics was conducted with reference to available core and high wall exposures (examples shown in Figure 3 and Figure 4).

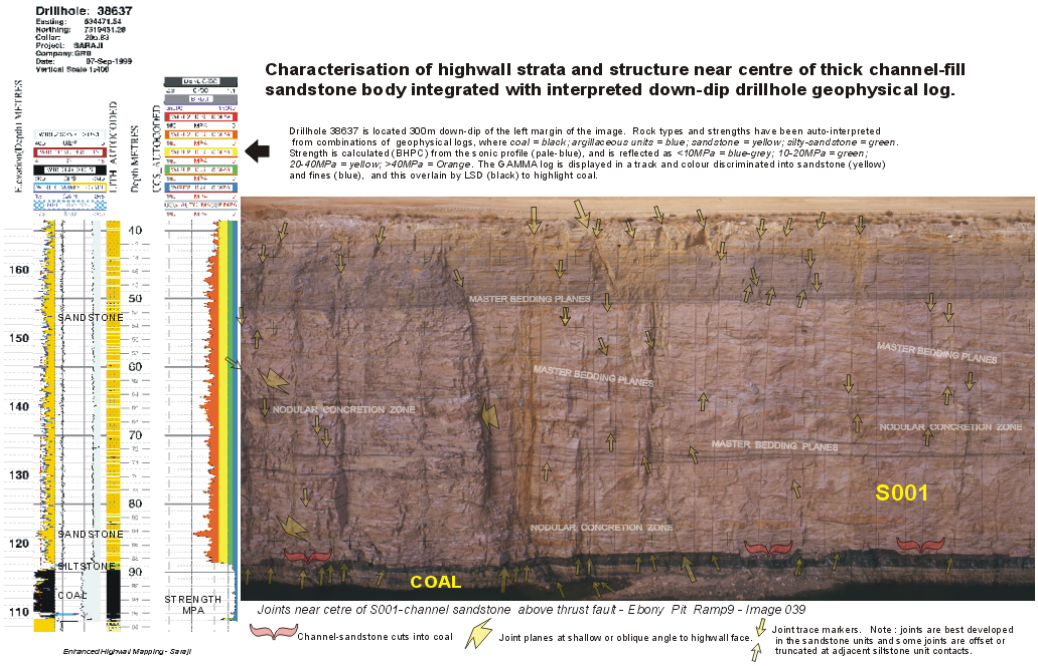

Figure 3 Characterisation of geophysical drill hole log with high wall strata and structure near centre of thick channel-fill sandstone body overlying the Dysart Seam. Ebony pit, Saraji Mine (from Sliwa and Le Blanc Smith, 2000).

Characterisation of Ebony Ramp 9 highwall strata and structure with down-dip drillhole geophysical logs.

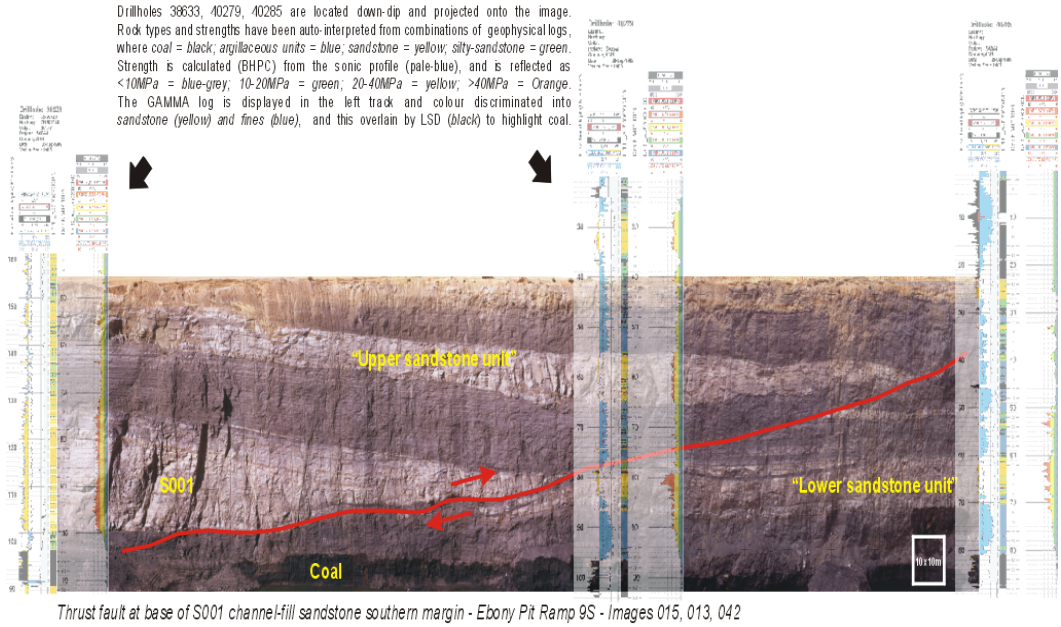

Figure 4 Characterisation of geophysical drill hole logs with high wall strata and structure at margin of channel-fill sandstone body overlying the Dysart Seam. Ebony pit, Saraji Mine. Note thrust fault is deflected by thick sandstone and breaks through sandstone where it is <10m thick (from Sliwa and Le Blanc Smith, 2000).

Stratigraphic correlation and coding for principal coal seams honoured mine site nomenclature. Access to numerous mine databases, personnel and reports greatly facilitated this collaborative work. Stratigraphic unit picks were checked and loaded into Mincom Minescape4 ^{TM} -Stratmodel software and, where data permitted, 3D sedimentary models were generated for the principal lithologies in the northern and southern tiles.

Structural mapping of faults, joints and cleat were obtained from operating open cut and underground mines and from regional geological surveys (Hammond and Mallett, 1987; Mallett et al, 1988; Queensland Dept. of Mines, 1988). Fault interpretations from recently acquired 2D and 3D seismic were also included where available. Faults and joints were characterized by their type and severity (discussed in Section 4) and placed into a temporal and spatial sequence with respect to the evolution of the Bowen Basin. Present-day stress measurements were obtained from mine sites and from publicly available reports (Enever et al, 1987; Hillis et al, 1999).

Virgin gas data for the Goonyella Middle seam in the Northern Tile and the German Creek seam in the Southern Tile were obtained from the mine sites. All gas data were compiled and validated by Ray Williams of GeoGAS Pty Ltd., and reported to a common basis for whole seam composites (see Section 6). Actual values are not reported here due to confidentiality concerns. However, the trends in the data are presented by contour maps that give some insight into geological controls that might be used as predictors of high gas domains that will create drainage and management issues.

Regional ground gravity and aero-magnetics were obtained from Geoscience Australia and the Queensland Geological Survey (Queensland Department of Natural Resources and Mines) and used to interpret regional structural trends, areas of intrusions and basement controls on the depositional and deformational history of the coal measures.

All digital borehole geophysical data are stored in Paradigm Geolog6 ™ software that was used to assist in lithologic interpretation and correlation of interburden sedimentary units. The coal seam and interburden models were built and queried in Mincom Minescape4 ™ geological modelling software. Intellicad ™ was used for DXF overlays of structure. Final map production was created in Surfer 7 ™ and exported as JPG or WMF formats for inclusion in the report and poster set.

3 REGIONAL CONTEXT

Renate Sliwa

3.1 Evolution of the northern Bowen Basin

The following discussion of the regional setting of the Moranbah/German Creek Coal Measures is set within the context of the broader Bowen Basin framework, which was derived in collaboration with Chris Fielding and Rod Holcombe of the University of Queensland, and is discussed and referenced in detail in Fielding et al, 2000.

The Bowen Basin evolved above a basement of Early Palaeozoic metamorphic and sedimentary rocks of the Drummond Basin and Anakie Block (see time-space plot in Figure 5). It initiated with rifting in the early Permian resulting in a series of isolated fault-bounded basins filled with volcanics and sediments (eg. Lizzie Creek Volcanics, Reids Dome Beds). Once rifting ceased by the Middle Permian, thermal relaxation took over as the mechanism for subsidence, and marine conditions dominated the Basin until the Late Permian (eg. Back Creek Group, Tiverton Formation). The progressive filling of the basin and deposition of widespread thick coal measures (eg. Moranbah-German Creek CM and Rangal CM) mark the onset of foreland loading during the Latest Permian, which controlled subsidence in the basin until its closure during the Middle Triassic.

A series of later events added structural complexity to the coal measures. These include the propagation of thrust faults into the western basin during the Middle Triassic, intrusion of sills and dykes in the Mid-Cretaceous, uplift and joint formation in the Late Cretaceous and major volcanic activity in the Tertiary.

These events are described in more detail in the following sections.

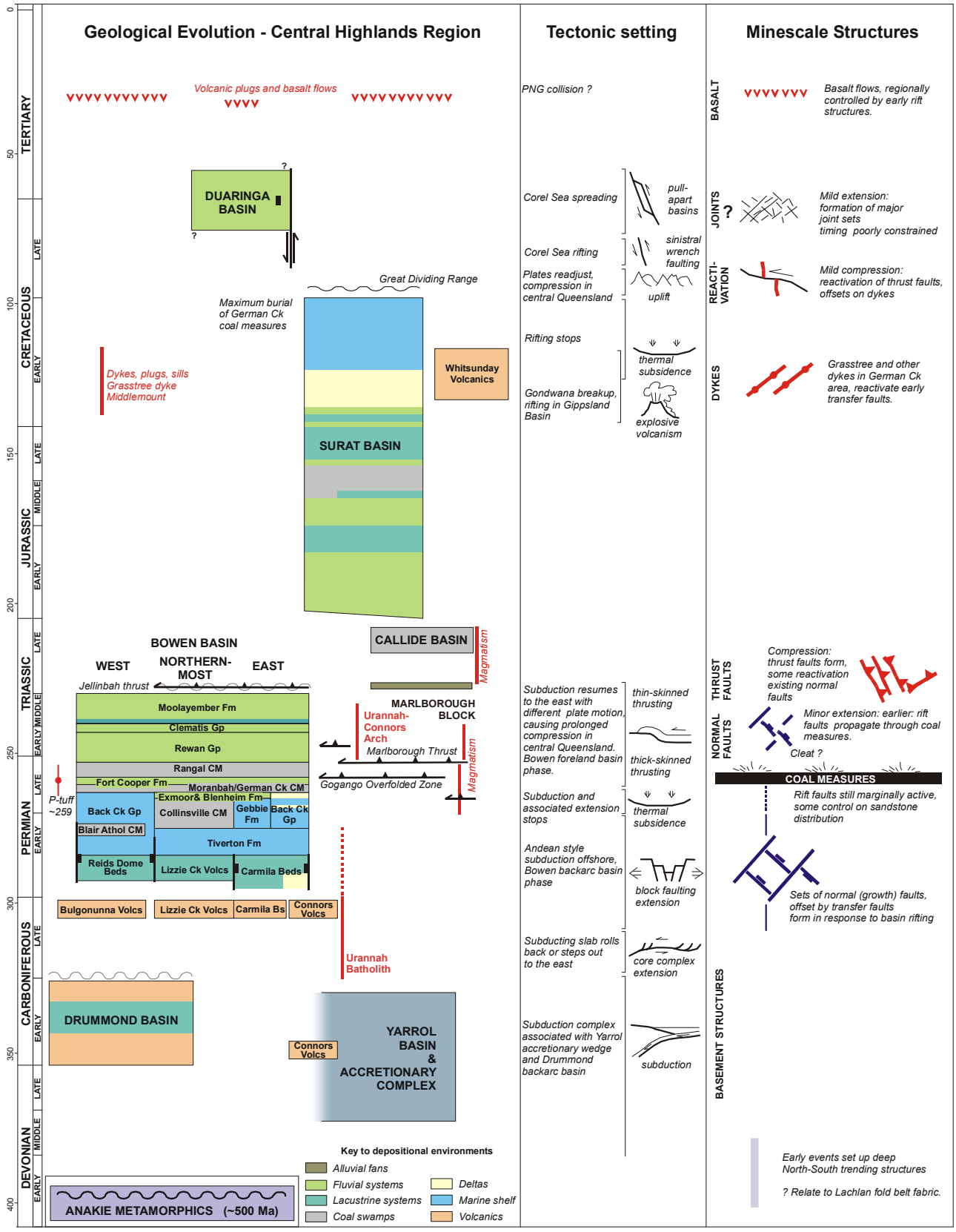

Figure 5 Time-space plot for the Bowen Basin and selected surrounding rocks.

3.1.1 Early Permian – Extension

Events prior to the Early Permian shaped the basement to the Bowen Basin and set up some of the larger scale basement structures, particularly those with NS trends. After a regional metamorphic event (Anakie Metamorphics), a subduction complex developed along the eastern Australian continental margin. This included the New England Orogen accretionary complex exposed along the present day coastline and the Drummond back-arc basin that underlies the Bowen Basin. This episode of subduction terminated when the subducting slab rolled back or stepped offshore during the Late Carboniferous.

A new subduction complex formed to the east of the older one, positioning the present day Central Highlands in a back arc rift setting. Thus the early phase of the Bowen Basin formed a series of isolated non-marine, NS to NW trending grabens and half-grabens (eg. the Denison Trough). Outside these basins NE trending normal and NW trending transfer faults have been inferred from aeromagnetic data and from reactivated fault patterns. The extensional fault systems subsequently influenced the deposition and deformation of the Late Permian coal measures. Deposition within these isolated basins was associated with significant volcanic activity and locally the formation of thick coal measures (eg. Blair Athol CM).

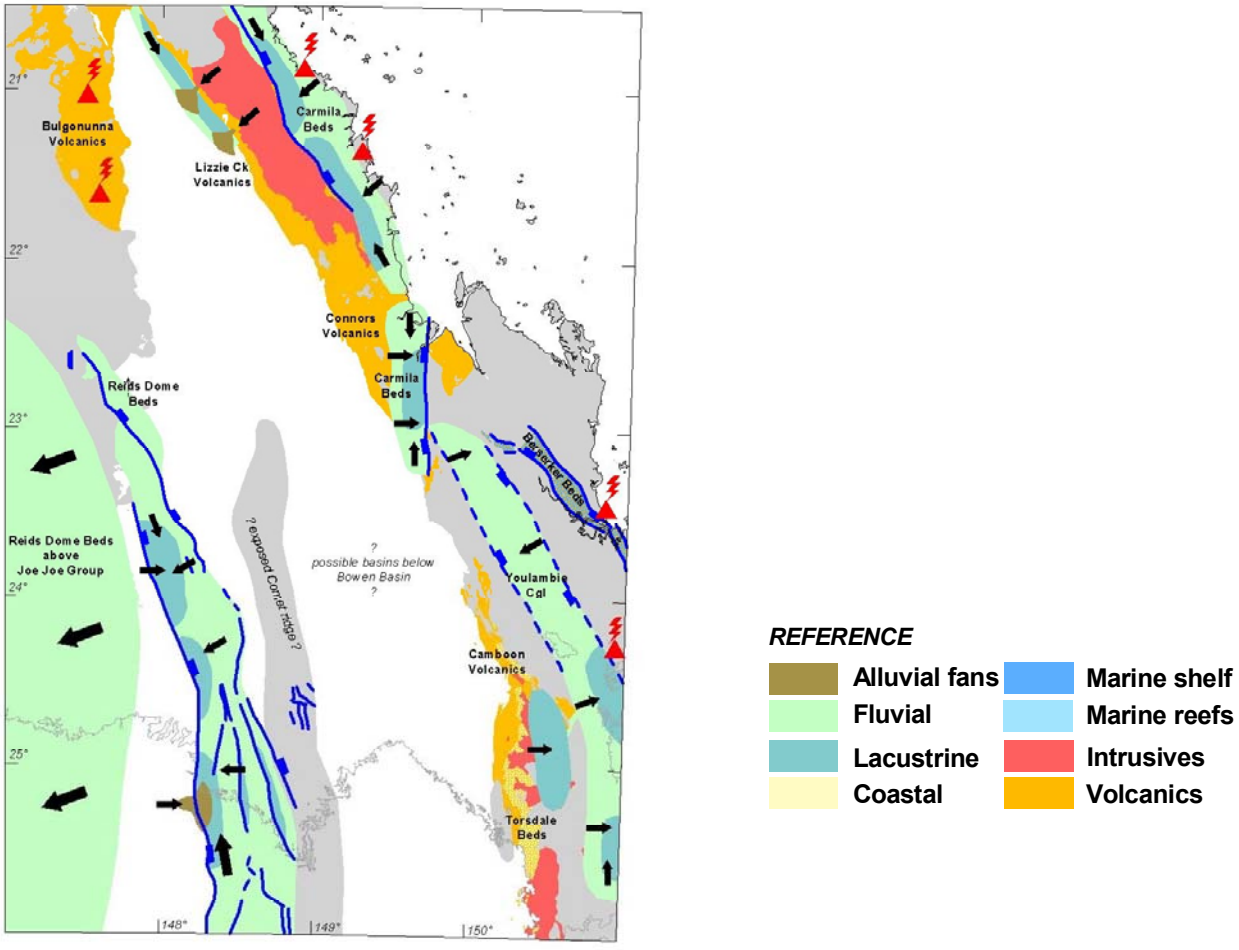

Figure 6 Palaeogeography and active structural framework for the Early Permian. The reference colours in the legend are used for Figure 7 to Figure 13.

3.1.2 Late Permian – Thermal subsidence

A change in plate tectonic conditions to the east caused the end of rift extension in the Bowen Basin. Now thermal subsidence was the main basin-forming mechanism causing a major marine transgression, and the complete flooding of the Bowen Basin. The maximum extent of marine conditions in the basin was reached during this time, resulting in the deposition of the Maria Formation and its equivalents. Coastal conditions with sediments fed from the west are interpreted for the western limb of the basin.

Renewed subduction with different plate movement vectors in the east set up a prolonged period of compression in central Queensland, during which the Bowen Basin acted as a foreland basin. The onset of this event is marked by the initiation of unstable marine slopes in east, associated with submarine debris flows (Barfield Formation).

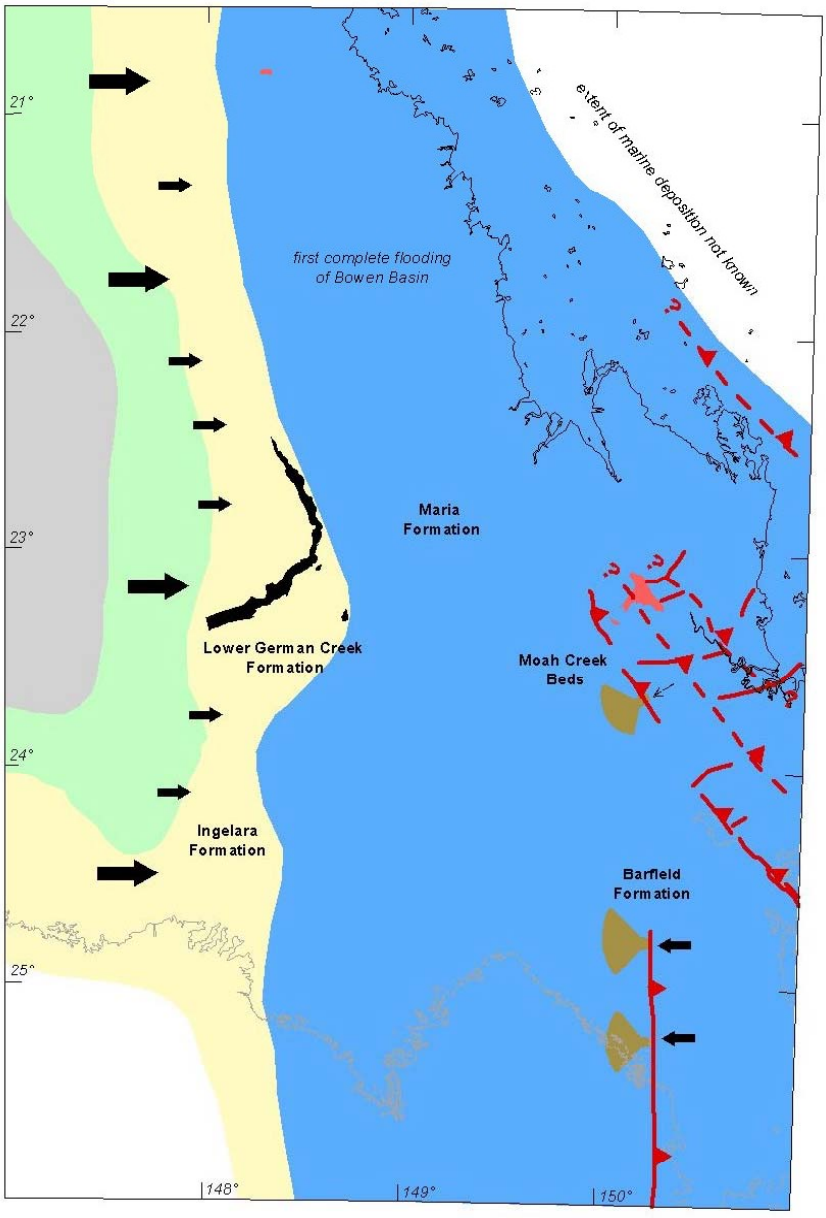

Figure 7 Palaeogeography and active structural framework for the Late Permian.

3.1.3 Late Permian – Onset of foreland loading

The onset of foreland loading was marked by uplift and resurgence of volcanism to the east, and the progressive infilling of the basin from the north. Extensive and thick coals developed during this time (Moranbah/German Creek CM). The normal/transfer rift fault systems were still mildly active at depth and had some control on the distribution of sandstone bodies in the coal interburdens. The character of the coal seams and their interburdens are examined in more detail in Section 5.

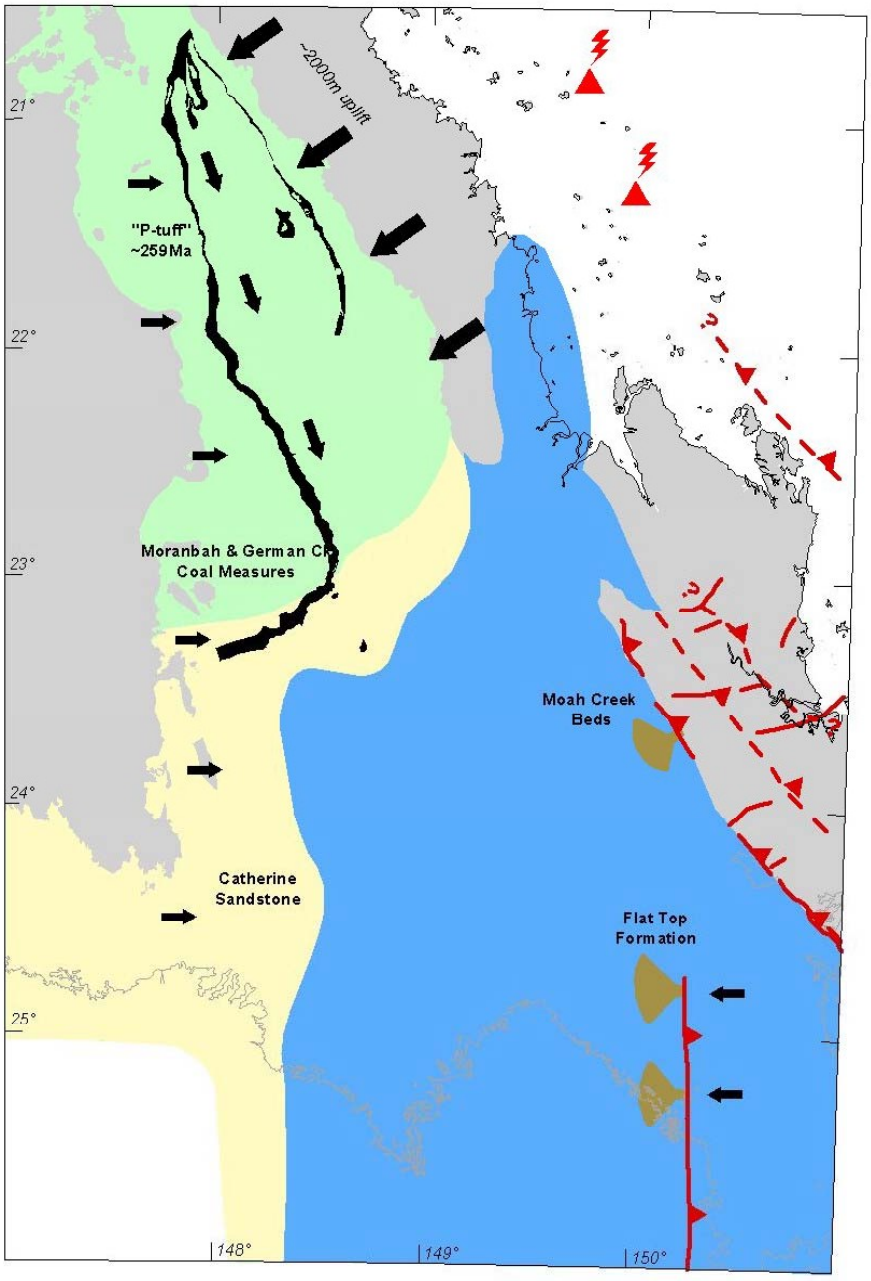

Figure 8 Palaeogeography and active structural framework for the Late Permian.

3.1.4 Late Permian – Foreland loading

During the main phase of foreland loading, thrusting built up the Gogango Overfolded Zone in the east (Holcombe et al, 1997). By this time marine conditions were restricted to the south of the basin. The Fort Cooper Formation and its equivalents are widespread and contain thick carbonaceous sediments and high ash coal with abundant tuff.

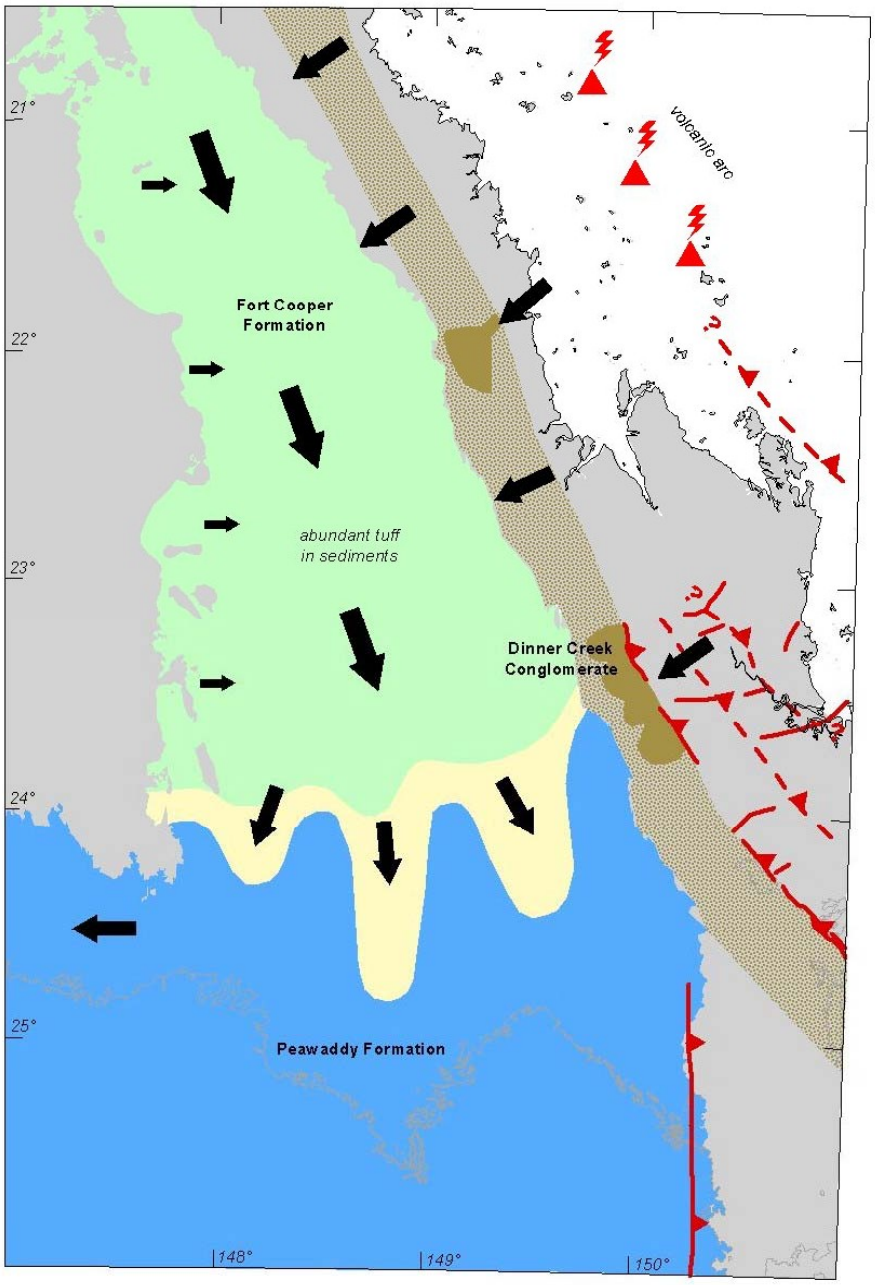

Figure 9 Palaeogeography and active structural framework for the Late Permian.

3.1.5 Latest Permian – Foreland loading

The further emplacement of major thrust sheets maintained foreland loading. Deposition was characterised by non-marine, lithic sediments with widespread development of thick, complex coals. During this time some areas in the western Bowen Basin were under mild extension, causing the early Permian normal faults and some much older structures to reactivate and propagate through the coal measures.

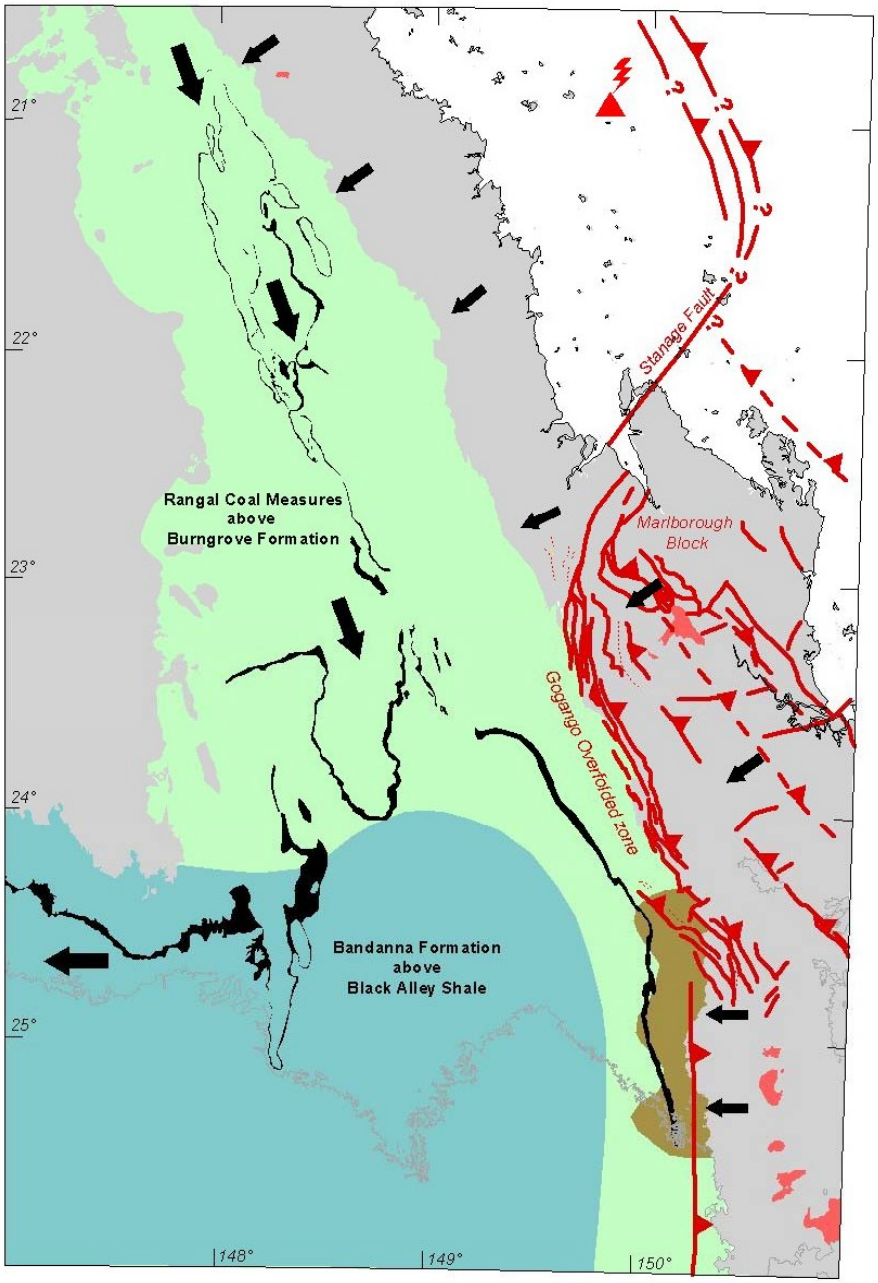

Figure 10 Palaeogeography and active structural framework for the Latest Permian.

3.1.6 Middle Triassic – Basin closure

The final phase of the Bowen Basin was dominated by lithic sediments derived from volcanic sources to the north and west, before further compression resulted in propagation of thin skinned thrust faults through the entire basin (eg. the Jellinbah Fault). The thrust faults and reactivation of normal faults in the mines are correlated with this event. The coal measures achieved maximum burial during this time, with relatively high geothermal gradients (Shibaoka and Bennett, 1976; Beeston, 1986).

Subsequently the Surat Basin developed over the Bowen Basin throughout the Jurassic and Early Cretaceous.

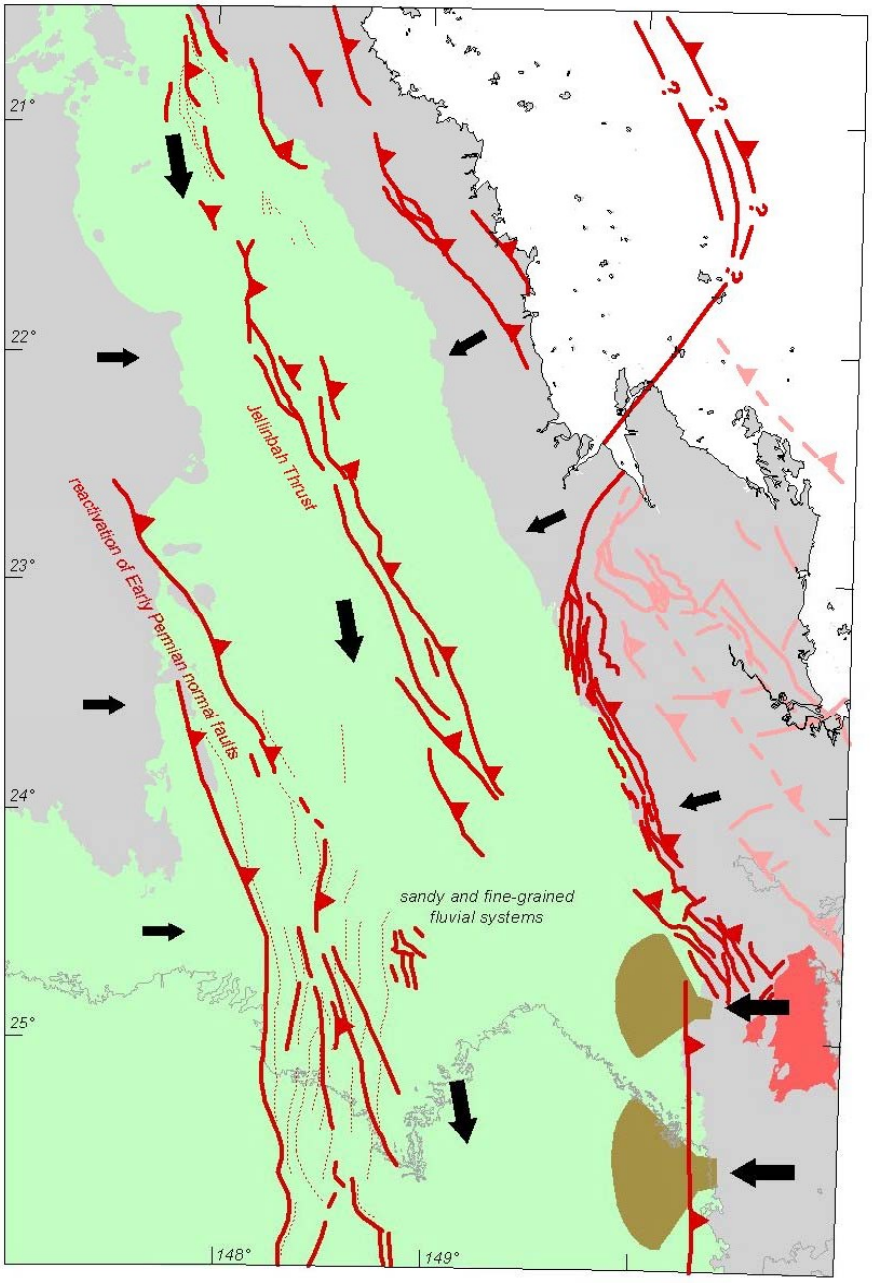

Figure 11 Palaeogeography and active structural framework for the Middle Triassic.

3.1.7 Cretaceous –Igneous activity and uplift

The break-up of the Gondwana super-continent resulted in a marine transgression in the Surat Basin, formation of the fault-controlled Styx Basin, extensional volcanism and the intrusion of abundant dykes, sills and plugs into the Permian coal measures. Mild reactivation of shallow faults and movement along bedding planes occurred at this time.

A period of compression followed, causing broad folds in the Surat Basin and up to 1500 m of uplift in the eastern Bowen Basin (Raza et al, 1998). Geothermal gradients in the Surat Basin are interpreted to have been much lower than in the Bowen Basin (Shibaoka and Bennett, 1976). The new incised land surface in the western Bowen Basin is preserved as the Tertiary unconformity later filled in by sediments and basalts.

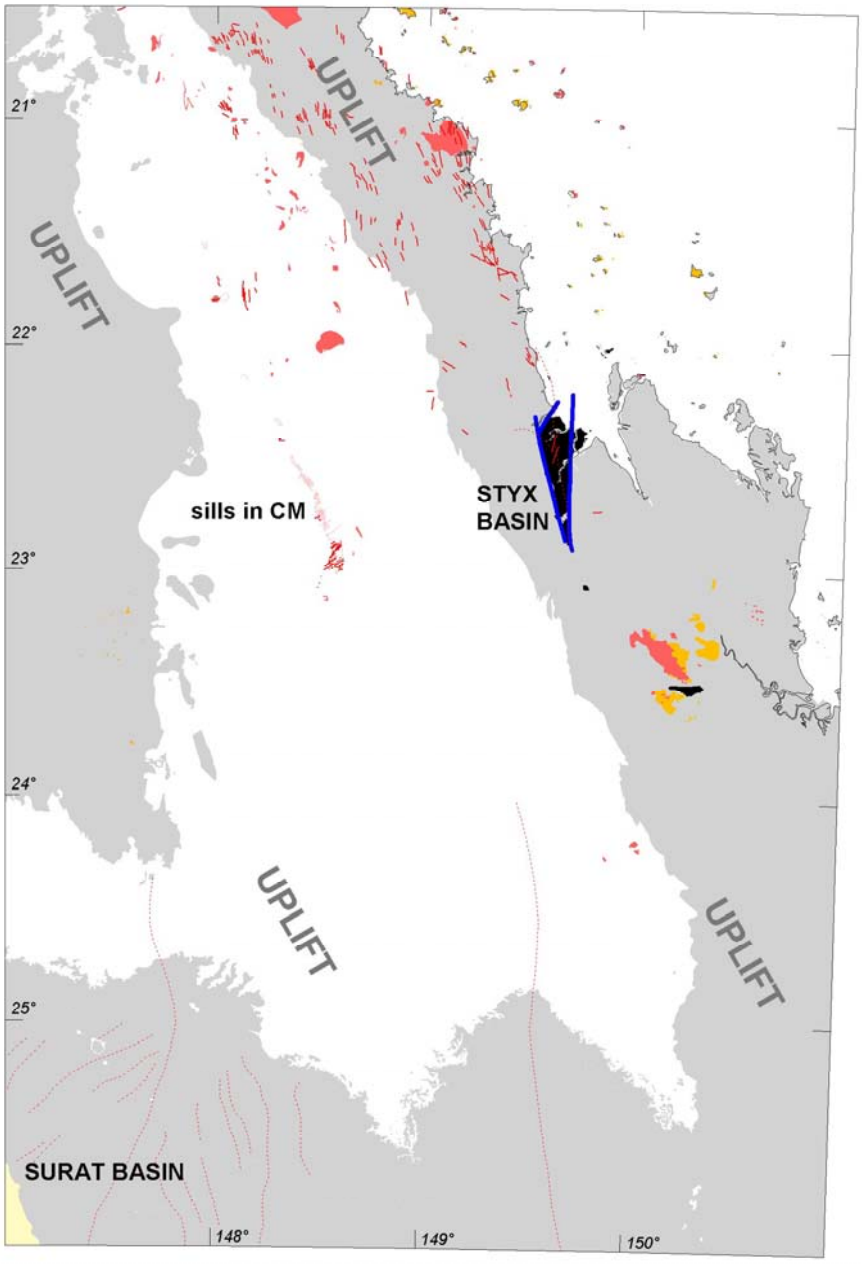

Figure 12 Palaeogeography and active structural framework for the Early Cretaceous.

3.1.8 Late Cretaceous to present – Uplift and volcanism

Extensional conditions prevailed during the rifting and opening of the Coral Sea, associated with regional strike slip faulting and formation of pull-apart basins (eg. Duaringa Basin). Although poorly constrained by overprinting relationships, the formation of most joint sets is likely to correlate with this event.

Collision and accretion of terranes in Papua New Guinea (PNG) dominate the tectonic setting and stress distribution of central Queensland during the Tertiary to present. During this collision, large volumes of basaltic lava extruded, and older structures were reactivated.

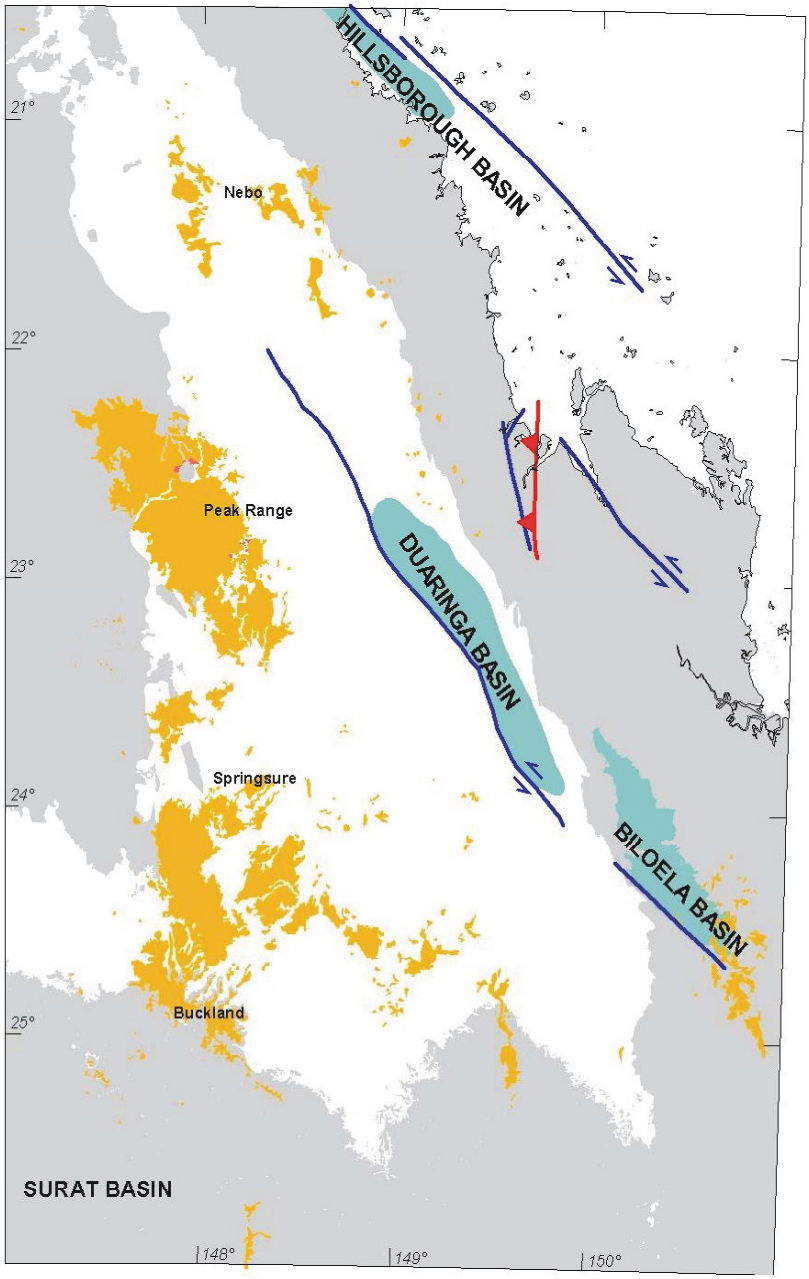

Figure 13 Palaeogeography and active structural framework for the Late Cretaceous to present.

3.2 Regional basement structure

3.2.1 Shape of the Bowen Basin floor

The nature and age of the crust beneath the Bowen Basin can only be inferred from exposed rocks outside the basin area and a deep seismic survey acquired by Geoscience Australia, as exploration drilling to date has not penetrated the basin succession away from its immediate margins.

The oldest dated rocks within the region are within the Neoproterozoic Anakie inlier (age of metamorphism) and the Marlborough ophiolite, suggesting that the crust underlying the Bowen Basin may be at least of this age (Scheibner and Veevers, 2000). Other units that appear to continue underneath the basin are the Carboniferous intrusive rocks of the Urannah-Connors Arch to the east and the Drummond Basin succession to the west. Interpretations of the regional deep seismic survey suggest that most of the rocks underlying the basin are part of the Lachlan orogen, but does not differentiate between basin fill and older metamorphic basement (Korsch et al*,* 1997).

The regional gravity image of Australia (Figure 14; Geoscience Australia, 2002) measures the bulk density of approximately the top 5-10 km of the earths crust, and is therefore a guide to the geometry of the basement of the Bowen Basin. It contrasts dense regions with mafic crystalline rocks close to the surface (reds/whites) against less dense regions with either thick sedimentary succession at the surface or less dense granitoids at depth (blues/purples).

The gravity image clearly highlights the main basement compartments of the Bowen Basin. The Comet Ridge, Taroom Trough and Collinsville Shelf are particularly recognizable as basement highs or lows. At higher resolution, the distribution of high and low density areas beneath the western Bowen Basin does not correlate well with the outcrop pattern or thickness distributions of the Permian sediments, which suggests that the gravity signature is derived from a combination of the Bowen and Drummond Basin successions over a heterogenous metamorphic/igneous basement.

Despite this, several gravity anomalies in the Supermodel area are interpreted as active basement blocks during the deposition of the coal measures. The most important one is a basement high in the Northern Tile that controlled the coal seam splitting patterns and the distribution of thin to thick stacked seams and sandstone units (discussed in Section 5), as well as influencing the orientation and distribution of normal and thrust faults.

Outside the exposed basin area, the dominant grain of the image consists of northwest trending “ridges” and “valleys” in the gravity signature. The ridges generally correlate with large near surface or outcropping intrusions, while some of the valleys are fault-bounded basins (eg. Duaringa Basin). This northwest trending fabric was enhanced during the Late Permian to Middle Triassic Hunter-Bowen compression that is responsible for the thrust faulting in the Supermodel area.

As well as the general basement shape, the gravity image also shows numerous lineaments, mostly trending Northeast. These are discussed in a broader Australian context below.

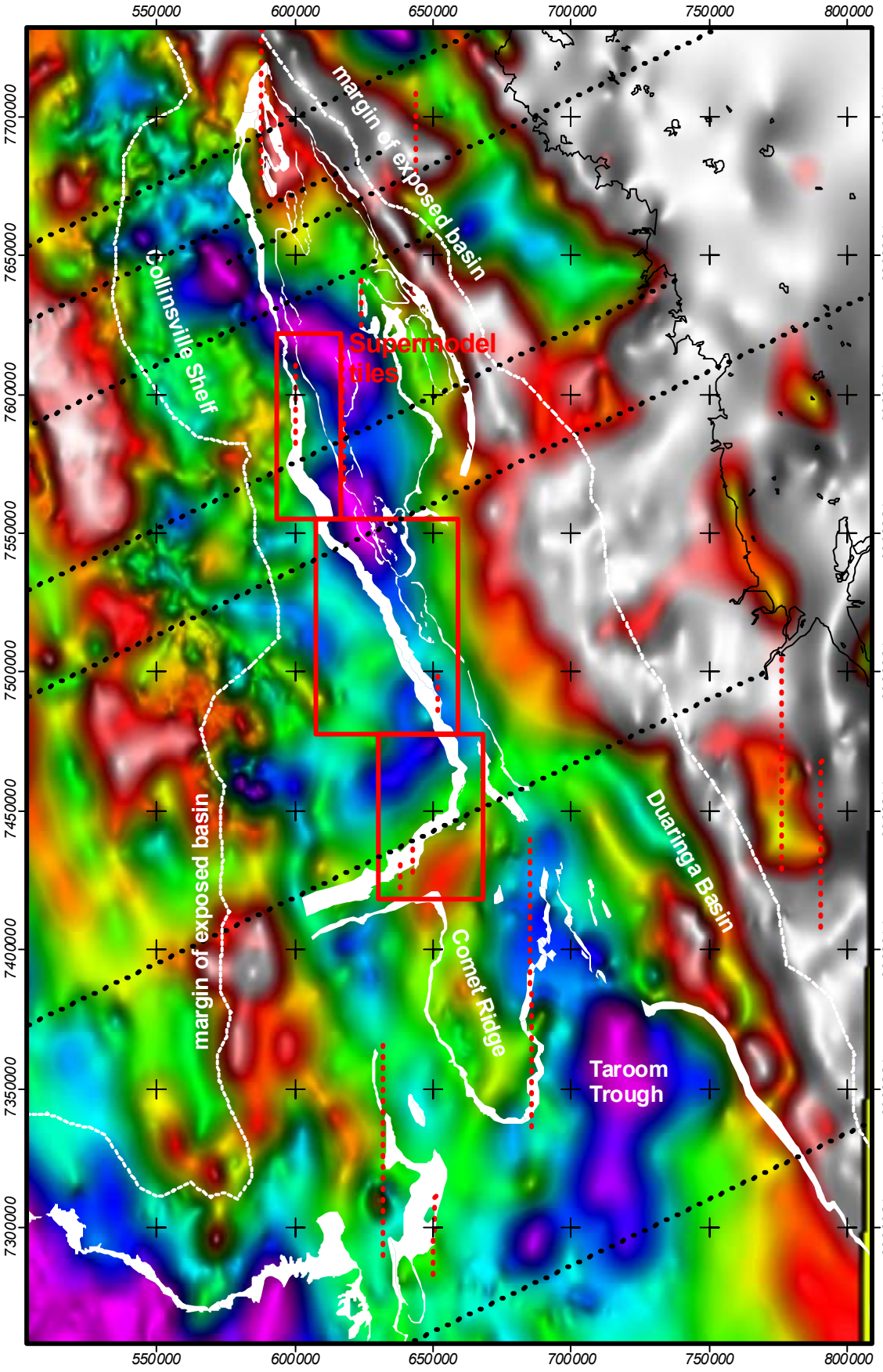

Figure 14 Geoscience Australia Bouguer gravity image of Bowen Basin (White/red: high; blue/purple: low). White overlay: Permian Coal Measures, Dotted lines: interpreted basement structures.

3.2.2 Regional grain and lineaments

The Supermodel structural synthesis (see Section 4) shows how important deep basement structures are to the distribution and orientation of faults and dykes within the coal measures. Once a deep-seated structure is formed in the earth's crust it will nearly always reactivate during subsequent deformation rather than let new structures form. This section will briefly characterize the major deep crustal structures in eastern Australia and relate them to observed structures in the Bowen Basin.

A cursory interpretation of the regional gravity data over eastern Australia (Geoscience Australia, 2002) shows several sets of lineaments and structural grain that can also be identified in the Supermodel area of the Bowen Basin (Figure 15).

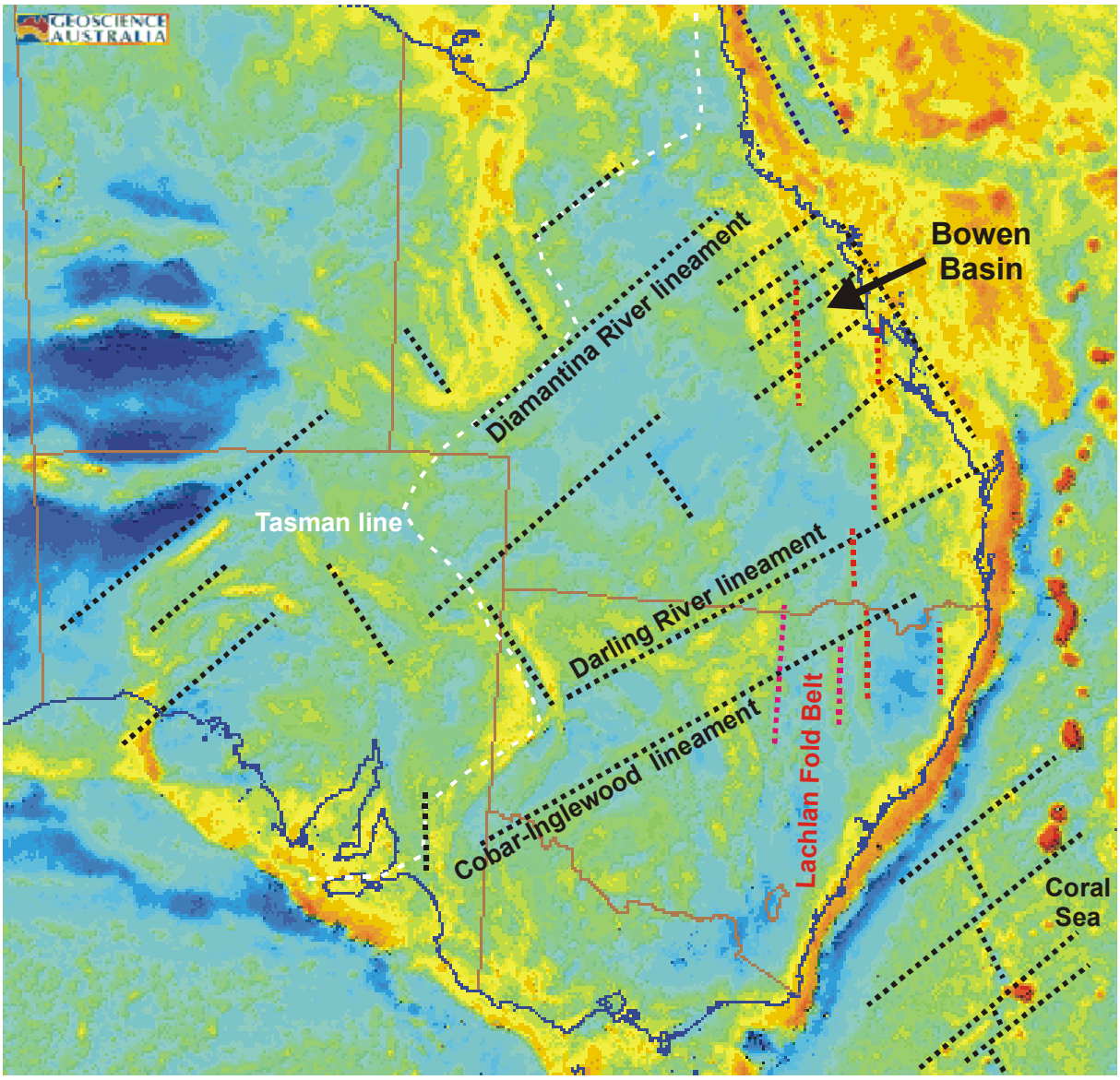

Figure 15 Regional gravity map of Australia with overlay of major lineaments (dotted lines) that are important to the northern Bowen Basin.

Northeast and northwest lineaments and northwest structural grain

Northeast trending lineaments and the conjugate northwest trending lineaments (represented by black dotted lines in Figure 15) present a very strong fabric across eastern Australia. These lineaments formed and reactivated during several events over a large time span (Scheibner and Veevers, 2000; Murray et al*,* 1989) For example:

- The Diamantina lineament is part of the Tasman line, a rift cutting across the continent during the Late Proterozoic).
- The Darling River and Cobar-Inglewood lineaments were most active during the Carboniferous, partitioning deformation of the Lachlan Fold Belt in New South Wales.
- Late Cretaceous to Early Tertiary sea-floor spreading patterns in the Coral Sea also exhibits the regional NE and NW orientations (Veevers et al, 1991).

In the Bowen Basin region the northwesterly orientations are parallel to the present coastline, but are also preserved in the structural grain imposed by the Hunter-Bowen orogeny (eg. Jellinbah thrust fault) and early basin controlling faults such as the normal faults at a margins of the northern Denison Trough (see Bowen Basin Solid Geology 1:500 000 map).

The northeasterly trends are subtler. They were identified as a series of corridors (Mallett et al*,* 1988) partitioning compartments with consistent geology and structural style. They were termed "corridors" because:

"… because, although many significant structures are influenced by them and reflect their presence, no single discrete feature normally characterises them."

The criteria developed as indicators of corridors included closures of map scale folds or lateral shifts in their axes, zones of increased fault disruption, steps in the boundaries of basin elements or structural zones (e.g. Comet Ridge) and lines of intrusive bodies along their length.

While the presence of these structures is indisputable, their main periods of reactivation were during the early parts of Basin evolution (shape of the basin), during the Hunter-Bowen compression (compartmentalization of folding and faulting) and during the Cretaceous and Tertiary intrusive events. There is little evidence for any major activity on these structures during the deposition of the Moranbah-German Creek CM. However, northeast and northwest trends observed within the sandstone body distributions in the Northern Tile suggest some local fault control on subsidence and position of channels (Esterle et al*,* 1998).

North-south lineaments

North-south trending lineaments (represented by the red dotted lines in Figure 15) are shorter than the northeast trending ones, and are confined to eastern Australia. They are only weakly defined in the regional gravity data, but stand out in the outcropping geology. They are defined either by the edges of major geological units such as the northwestern and southeastern margins of the exposed Bowen Basin, or major basin and basement structures including the southern Denison Trough, the Comet

Ridge, the eastern bounding fault of the Styx Basin and sections of the Jellinbah and Moonie Faults. **In the Supermodel area this basement trend is important as it is correlated with the mapped larger normal and thrust fault systems**.

The inheritance of these structures by the New England Orogen and Bowen-Sydney basins, suggests that these structures are at least of early Palaeozoic age. The confinement of these north-south structures to eastern Australia suggests that they relate to the regional structural grain imposed by the Lachlan Orogen.

4 REGIONAL TO MINESCALE STRUCTURE

Renate Sliwa

4.1 Structural elements

Detailed fault characteristics are best determined from mapping in the open cut pits where 3D geometries and overprinting relationships are exposed. Mapping of open cut pits was outside the scope of the Supermodel project, thus the following summary relies strongly on detailed pit mapping by Lohe & Sullivan (1992), and prior mapping experience from selected mines in the area.

4.1.1 Compaction structures

Small normal faults are common in fine-grained rock units, beneath more massive sandstone bodies. Due to their small scale they are only observed in outcrop and drill core, and are difficult to interpret from widely spaced exploration-drilling data. However, their presence can be predicted from the distribution of geotechnically massive sandstone units in the interburden.

The faults have short strike lengths and typically dip at 50° toward the centre of the overlying massive unit. Their vertical penetration is less than or equal to the thickness of the overlying massive unit (Figure 16). The faults throws are influenced by the slope of the lower contact of the overlying unit, the steeper the contact, the greater the throw. This suggests that these structures are most severe around the margins of massive sandstone bodies in the interburden.

The faults are typically annealed, suggesting that they formed during compaction, as a result of accommodation beneath geotechnically massive sandstone bodies. They are the earliest structures mapped in the coal measures.

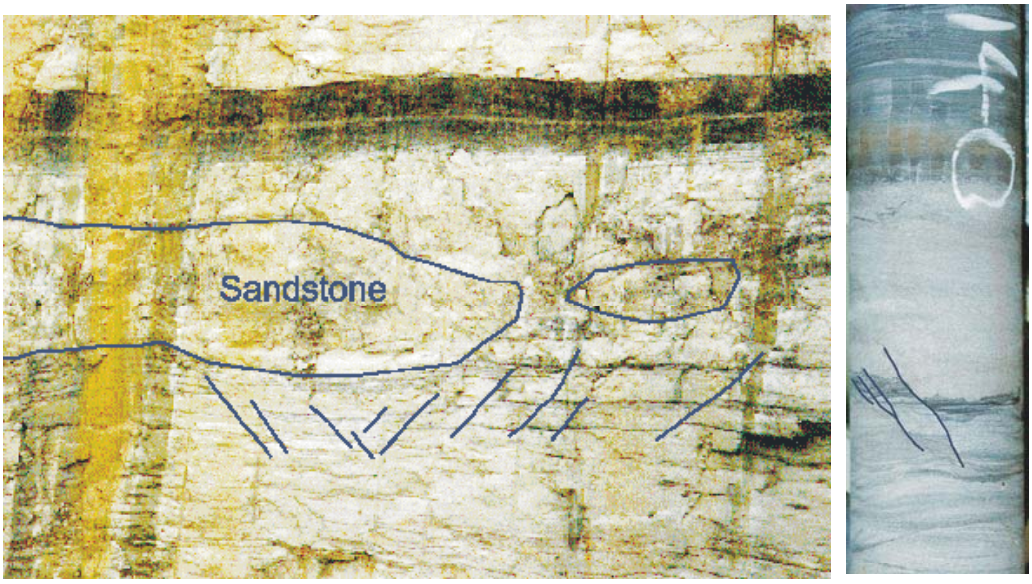

Figure 16 Small normal faults below a geotechnically massive sandstone body, in outcrop and in drill core (Goonyella).

4.1.2 Normal faults

Two classes of normal faults, persistent steep ones and non-pervasive moderately dipping ones, have been observed in the open cut pits. The steep normal faults are generally vertically persistent, transecting the entire height of the high wall (Figure 17, Figure 18), with throws ranging from centimetres to 80 m. Individual fault segments are up to several hundred metres in strike-length, combining to form regionally significant fault zones that can be traced for >12 km. Apparent mismatch of geology on either side of the faults, and complex termination structures near the top of the high walls suggest a component of strike-slip movement. These faults can be interpreted in the context of basement geometry and structural evolution. Reverse reactivation is common and lead to local broadening of the fault damage zone. All normal faults, including reactivated ones are truncated by the Tertiary unconformity.

Moderately dipping normal faults are less common and, similar to compaction faults, are only observed in outcrop. These faults occur in clusters and have small vertical extent (Figure 19). Most resulted from accommodation around complex thrust faulting.

Figure 17 Steep normal fault transecting high wall.

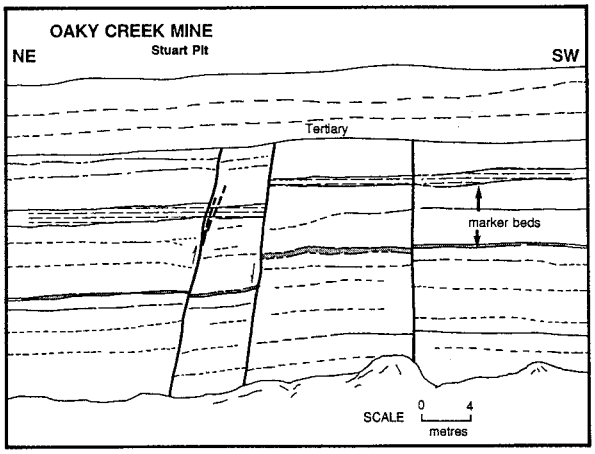

Figure 18 Steep normal and reactivated normal faults at Oaky Ck. (from Lohe and Sullivan, 1992).

Figure 19 Moderately dipping normal faults forming in response to accommodation above a major thrust fault (Goonyella).

4.1.3 Thrust faults

The Supermodel area is positioned about 12-15 km west of the Jellinbah thrust fault, a regional structure with approximately 600-800 m throw, which transects the Bowen Basin from Collinsville to south of Blackwater. It is a thin-skinned thrust where all component thrusts join a detachment that shallows out at 3 to 5 km depth. Supermodel is positioned well within the footwall of this structure (Figure 20), and shows only relatively minor faulting, that none-the-less mimic the style of the regional structure. All mapped thrust faults are interpreted as subsidiary structures to the Jellinbah thrust fault.

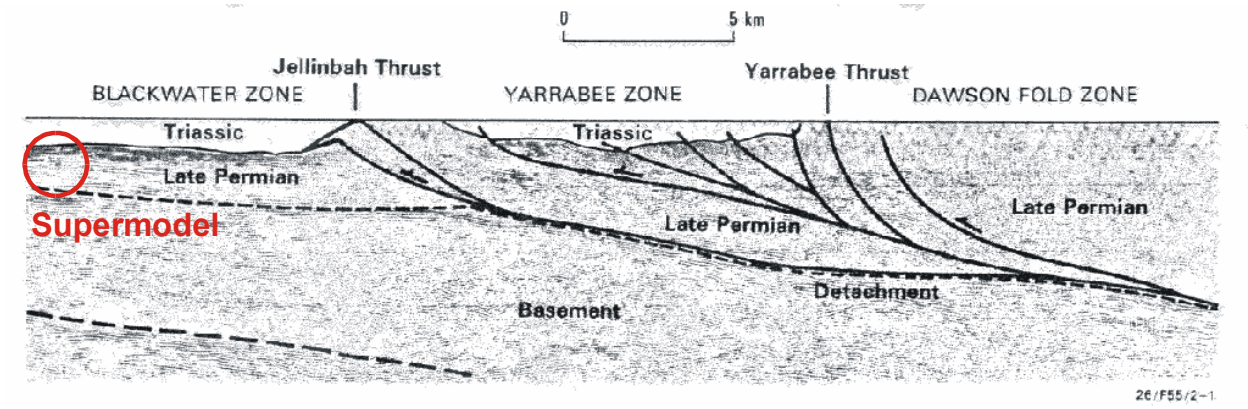

Figure 20 Part of Geoscience Australia deep seismic line BMR8901BB (from Geoscience Australia web page) showing the geometry of the Jellinbah thrust zone and its position relative to Supermodel.

In the coal measures thrust faults are less abundant than normal faults, but form some of the most damaging structures. Individual faults range in strike length from tens of metres to several kilometres with throws ranging from centimetres to tens of meters. Thrust faults commonly form in broad thrust zones that can be traced for up to 25 km.

Thrust faults are the most complex structures within the coal measures. The fault geometry typically includes sub-horizontal thrust flats, particularly within or at the top of coal seams, and moderately to steeply dipping thrust ramps with well developed hanging wall anticlines (Figure 22). Complex thrust duplex structures are common and are usually particularly well developed where thrust faults overprint and interfere with existing normal faults (Figure 23).

Thrust faults overprint the normal faults, but are also clearly cut by the Tertiary unconformity.

Figure 21 Thrust flat and sidewall ramps exposed in high wall (South Blackwater). The hanging wall has moved toward the viewer.

Figure 22 Thrust fault with well-developed fault-bend fold in the hanging wall (Goonyella).

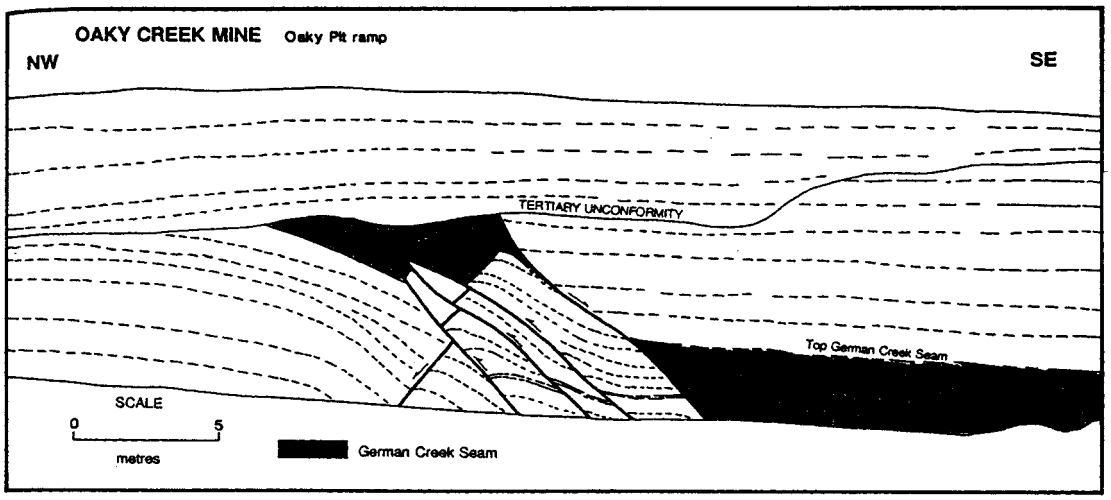

Figure 23 Complex geometry caused by the interference of normal and thrust faults at Oaky Ck (from Lohe and Sullivan, 1992).

4.1.4 Joints

Joints are abundant in the interburden between the coal seams in all the open cut and underground pits of the study area. Many different joint sets occur, some with regional significance, such as northeast and northwest trending ones, and some with localized controls, such as thrust ramps. The vast majority of these joint sets dip steeply or vertically, which may reflect a bias in the sampling, particularly in underground mapping of mine roofs with limited three dimensional exposure.

The spacing of joints and their vertical persistence depends strongly on the lithology in which they occur. Joints within thick geotechnically massive sandstone units are commonly widely spaced single planes, which transect the entire unit (Figure 24), while the same joints in finer grained rock units generally consist of confined zones of fracturing (Sliwa and Le Blanc Smith, 2000). Mapping in the roof of underground mines at Oaky Creek (Figure 25) compiled by Esterle et al (2002) has shown that joint spacing increases significantly in areas of fine grained weak roof lithologies.

Figure 24 Major vertical joint set in sandstone unit (Saraji).

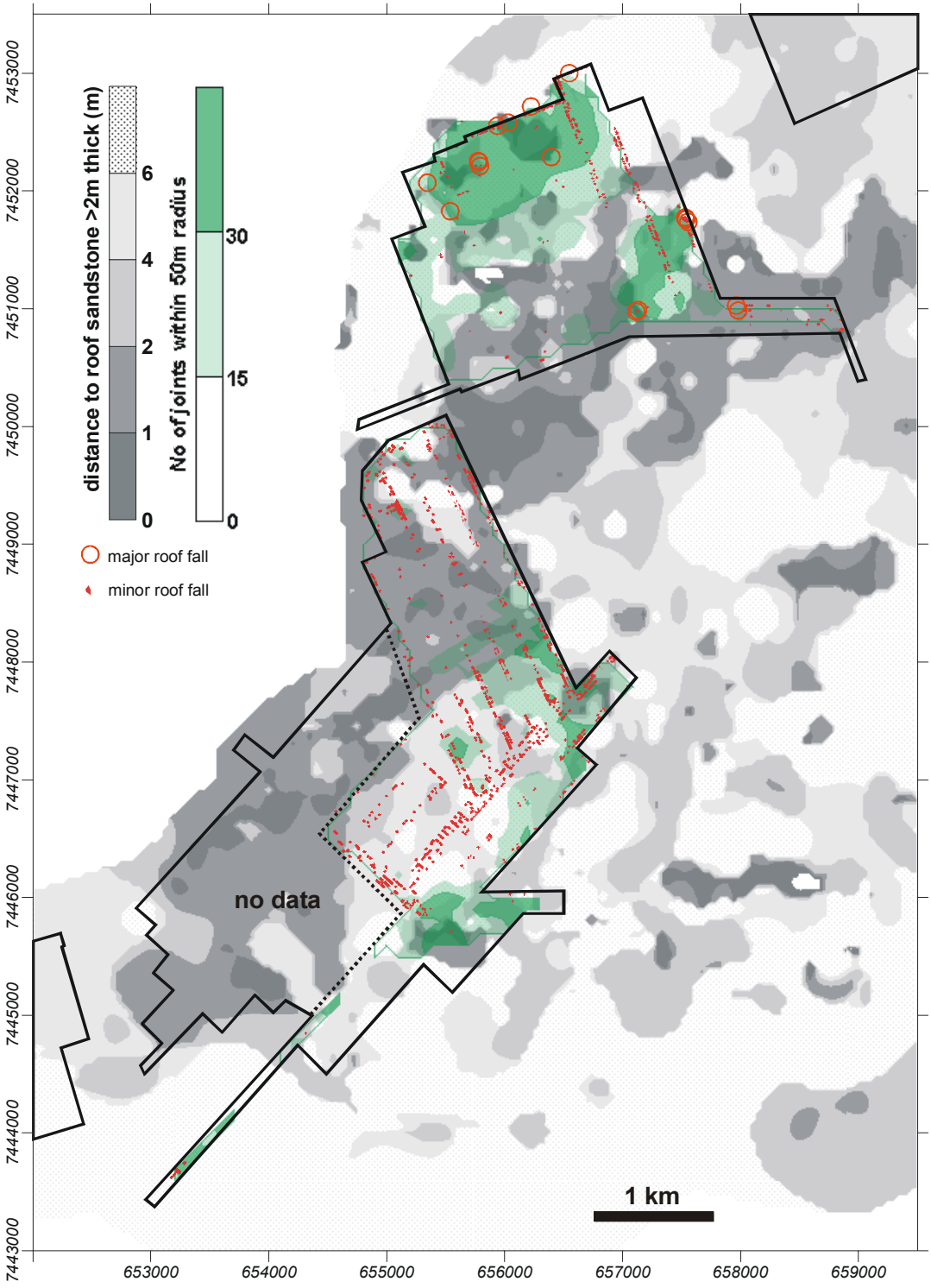

Figure 25 Relationships of roof falls, joint density and distribution of weak and strong roof lithologies at Oaky Creek Mine (from Esterle et al*, 2002).*

4.1.5 Dykes

Dykes occur sporadically throughout the Supermodel area, but are most common in German Creek where a regionally significant, northeast trending, set of dykes occurs. These dykes occur in swarms up to 1 km across and about 2 km apart. Individual dykes are generally vertical and 0.1 m to 2.4 m wide (Ward et al*,* 1997). Dyke segments are generally less than 1 km in length, but overlap en-echelon

to form narrow structures that can be traced for up to 10 km along strike. Dykes can be vertically persistent but are commonly offset by bedding plane shear faults (Figure 26).

Figure 26 Steep dyke offset by bedding plane shear (Goonyella).

Dyke intrusion and bedding plane shear are intricately linked. Work at German Creek (Smith, 1996) shows that some of the dykes were faulted by an in-seam shear zone while they were still hot and ductile. They produce a coked halo on the opposite side of the slip plane after movement, and blebs of dyke material get caught up in the shear zone.

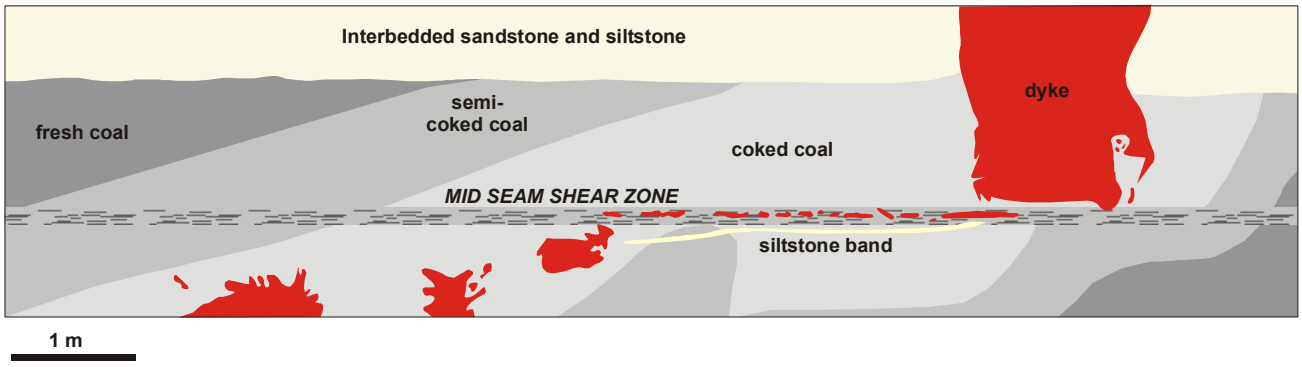

Figure 27 Complex relationships between mid-seam shear zone and intruding dykes at German Creek (from Smith, 1996).

4.1.6 Bedding plane shear and fault reactivation

Shearing parallel to bedding is common throughout the study area. Most underground mines have recorded shearing within or near the top of the working seams. In the high walls the most reliable indicators are offsets on dykes (Figure 26) and large joint sets. There is also evidence for the reactivation of thrust faults that are sub-parallel to bedding. Figure 28 shows this relationship where most of the thrust faulting precedes the intrusion of the dyke, but a small movement on one of the low angle thrust faults offsets the dyke.

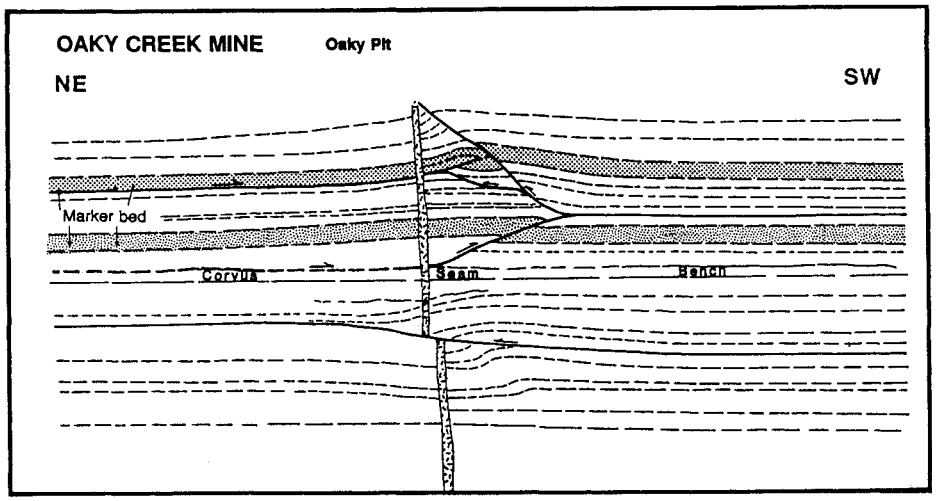

Figure 28 Relative timing of dyke intrusion and thrust fault reactivation (from Lohe and Sullivan, 1992).

4.1.7 Cleat

Cleat data for various seams were compiled from Pattison et al (1995), Faraj (1997) and from existing underground mapping. The following characterisation is extracted from Pattison et al (1995).

Face and butt cleat are ubiquitous in all coal seams throughout the Supermodel area, and are perpendicular to bedding. Face cleat spacing is typically 1-10 mm in the bright bands, and 5-30 mm in duller bands. Most commonly cleat patterns are orthogonal to sinusoidal with the butt cleat perpendicular to the face cleat. Locally there is little distinction in character between face and butt cleat.

A second generation of moderately dipping cleat locally overprints the regional fabric. It is either associated with thrust faults (eg. Saraji, Le Blanc Smith, pers. Comm.) or with bedding plane shears (eg. Goonyella, Sliwa and Le Blanc Smith, 2001). In the Goonyella exploration adit these cleats are associated with strongly striated bedding planes, and dip moderately toward the interpreted movement direction of the bedding plane shear, consistent with a genetic link between the structures.

Pattison et al (1995) noted that cleats in the German Creek coal measures are generally less mineralised than those in the Rangal coal measures, where illite and kaolinite are common in the face cleats and carbonate is common in the butt cleat. The carbonate mineralisation is clearly younger than the clay minerals. Radiometric dates of illite cleat infill suggested that it had formed between 245-220 Ma (Faraj quoted in Pattison et al, 1995), possibly associated with significant intrusive and

metasomatic activity to the east of the Basin. The later carbonate mineralisation is less well constrained in time, but is possibly linked to the magmatic activity during the mid-Cretaceous.

The regional distribution of cleat orientation and its relationship to joints, faults and regional stress is discussed below.

4.2 Regional distribution and timing

Detailed structures including faults, dykes, joints and cleat were compiled from exploration drilling, seismic, and field mapping interpretations by mine site geologists. For Supermodel only faults with >1 m throw were synthesized to create a coherent fault interpretation for the whole of study area. All faults with more than 1 m throw were assessed against all available interpretations, adjusted where necessary and then classified by fault type (i.e. thrust or normal fault) and throw. The results are presented in a series of maps throughout this chapter. Please refer to Figure 29 for symbol reference.

In addition to the structural synthesis presented in this chapter, the mapped faults of the Southern Tile were statistically analysed using stochastic simulations, to test for the presence or regionally consistent fractal characteristics of fault distributions, throws and strike orientations. The results of this independent analysis are presented in APPENDIX 2.

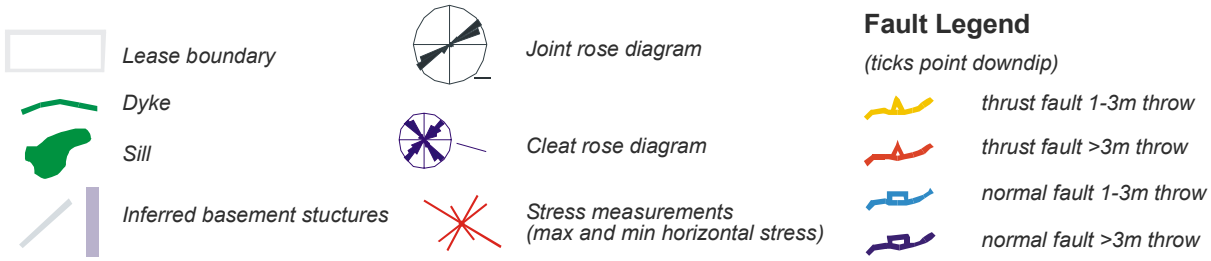

Figure 29 Legend for all maps following in this section.

4.2.1 Faults and dykes

Compilation maps showing the distribution of faults dykes and sills in the three tiles of the Supermodel area are presented in Figure 30 to Figure 32.

In the **Northern Tile** (Figure 30) thrust faulting is the most dominant fault style. One major thrust system can be traced for >30 km throughout Goonyella to Wards Well. The system trends NS, possibly ramping up above a NS basement structure at depth (purple zone on Figure 30a). Two further systems occur toward the east, spaced ~2.5 km apart. Individual thrust fault segments have long strike lengths (up to 3 km) where they trend NS, but break into short en-echelon segments where the strike

of the system swings to NW or NE. Short thrust faults also occur in NW trending zones and provide linkage between the larger systems.

Three sets of normal faults occur in the Northern Tile, trending northwest, northeast and east-west. The northwest trending faults are the most common. East-west trending normal faults occur in 2 to3 km wide zones in North Goonyella and Moranbah North. The spacing between these zones is about 20 km, similar to spacing between east-west trending fault zones in the Middle Tile.

There is a strong link between the distribution of the smaller thrust fault segments and the presence of strong sandstone channel complexes above the Goonyella Middle seam (Figure 30b). Larger thrust faults wrap around and ramp up along the margins of these sandstone bodies, while larger normal terminate against them. The abundance of smaller faults increases strongly in areas of weak roof lithologies, particularly at North Goonyella and Moranbah North.

Mining in the **Middle Tile** (Figure 31) is all by open cut. Thus only larger faults that have an impact on open pit mining were mapped in this tile. The structural style is similar to the Northern Tile. Most normal faults trend northeast, and some northwest. Thrust faults generally trend northeast, parallel to the regional Jellinbah thrust system that occurs 12 km to the east of the mine areas. Reactivated north-south and east-west basement structures locally influence the orientation of both normal and thrust faults. Note that the spacing between east-west basement structures is 20 km, similar to the Northern Tile.

The distribution of faults in the **Southern Tile** (Figure 32) contrasts with that in the north. Northwest-trending normal faults are abundant at Oaky Ck and German Ck, with northeast-trending faults confined to narrow (1 km), but widely spaced (3 to 5 km) zones. This orthogonal relationship is interpreted as a reactivated Early Permian rift fault pattern at depth. Large north-south trending thrust and normal faults are prominent at Kestrel and Crinum. They occur along strike of the eastern boundary structure of the Denison Trough, and are interpreted to be the result of the same reactivated deep basement structure.

A major gravity lineament passes through the Southern Tile, but has little control on the distribution of faulting or folding. However it is parallel to the Grasstree dyke, a large Cretaceous structure.

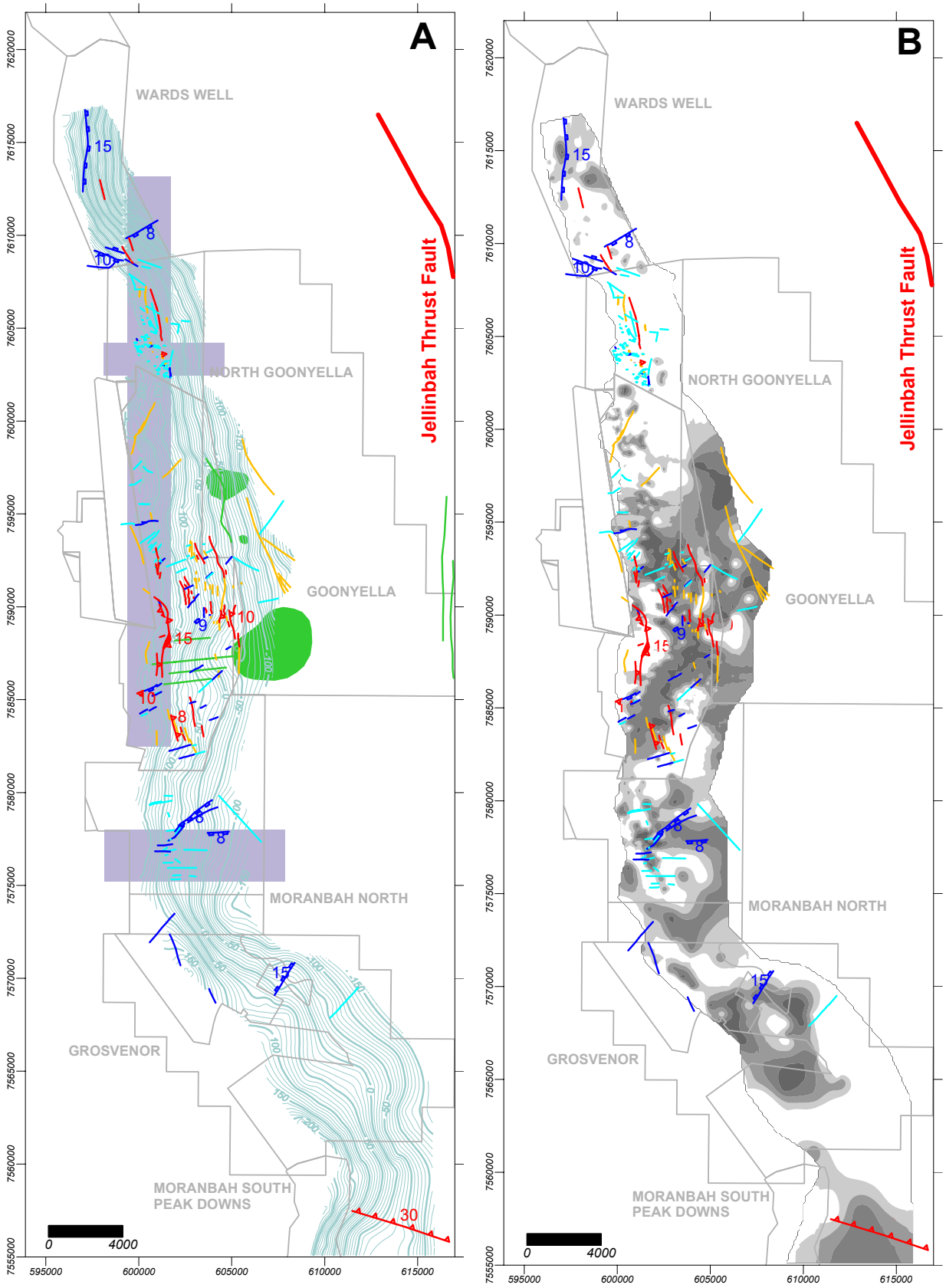

Figure 30 Faults with >1 m throw mapped in the GMS of the Northern Tile, shown with a) GMS structure contours, and b) distribution of major channel sand bodies (dark grey tones) above GMS.

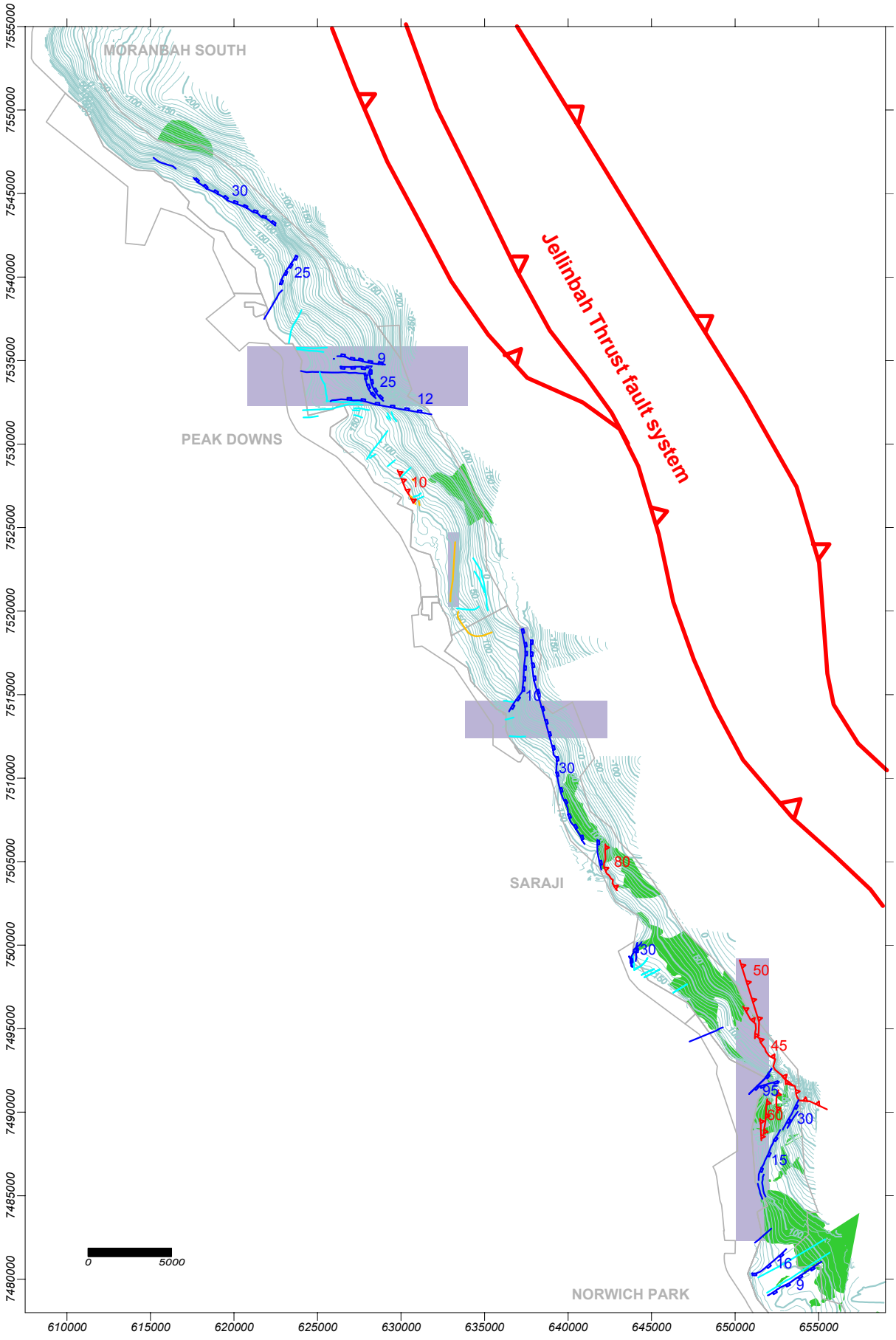

Figure 31 Faults with >1 m throw mapped in the Dysart seam of the Middle Tile, shown with structure contours of Dysart seam floor.

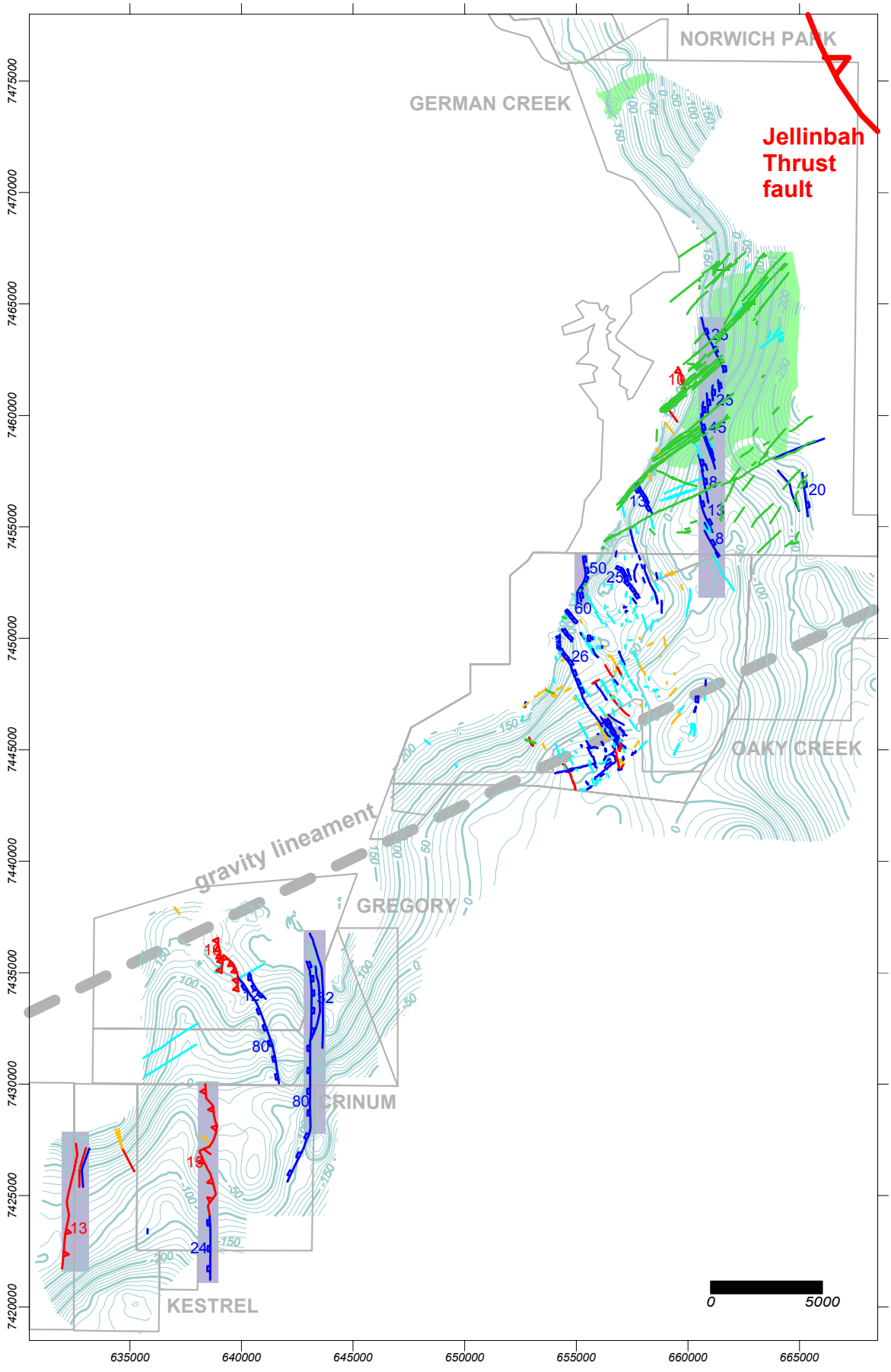

Figure 32 Faults with >1 m throw mapped in the German Creek seam of the Southern Tile, shown with structure contours of German Creek seam floor.

4.2.2 Joints and cleat

In the context of this discussion on the regional distribution of cleat and joints in the Supermodel area, cleats are defined as opening-mode fractures within the coal seams, while joints are fractures within the interburden rocks. The majority of mapped cleats and joints are sub vertical or vertical, as discussed in section 4.1.7 above. Locally occurring cleat overprints and moderately dipping joint sets are discussed here. Rose diagrams summarizing the joint and cleat orientations for local areas in the northern, middle and Southern Tiles are presented in Figure 33 to Figure 35.

In the **Northern Tile** (Figure 33), joints were compiled for the North Goonyella and Moranbah North underground workings. In each area there is a single dominant joint set trending WNW at North Goonyella and east-west at Moranbah North. These sets are parallel to the orientation of the dominant local faults.

Cleat roses are compiled from Faraj (1997) who mapped the high wall faces at Goonyella-Riverside. Face cleats are more prominent than butt cleats, and gradually swing from a northwesterly trend in the north through east-west to southwest in the south. This swing coincides with the presence of a gravity high (dashed line), which has been interpreted as a basement block that was active during deposition of the coal measures and later deformation (see section 5).

In the **Middle Tile** (Figure 34), joints were mapped at Saraji (Sliwa and Le Blanc Smith, 2000). The roses show the presence of several joint sets across a small area, which is relatively free of larger faults. Fracture patterns developed within thick strong sandstone units control the joint patterns in the finer grained units.

Cleat roses are again compiled from Faraj (1997), where butt cleats were not differentiated from face cleats. If the assumption is made that face and butt cleats are generally perpendicular but easily switch orientation in response to subtle changes in the stress field, the Middle Tile can be interpreted as an area where two cleat sets are present and interfere locally. In the north at Peak Downs the dominant cleat set trend NNE and WNW, while in the south at Norwich Park, the dominant set is NNW and ENE. In the southern Peak Downs/northern Saraji area bimodal distributions suggest that both sets are present. The changeover in the two domains lies just to the north of a gravity high (dashed lines) again suggesting a basement control on the cleat distribution.

In the **Southern Tile** (Figure 35), joints were compiled from underground mapping at German Creek, Oaky Creek and Crinum. Two major joint sets occur: northwest and northeast. The northwestern joint set is dominant at Oaky Creek, an area of prominent northwest trending faults, while the northeastern joint set is present in all three mines and parallel the second most important fault orientation.

Cleat roses in the Southern Tile were compiled from Faraj (1997), and they are consistent with mapping by Pattison et al (1995). Both face and butt cleat are shown on the diagrams. The cleats are more consistent across the Southern Tile than the middle and Northern Tile, with northeast and northwest trends dominant. The northeast trending cleats are strongest in the Oaky Creek area, suggesting that there may be a link between the distribution of cleats and joints in this tile.

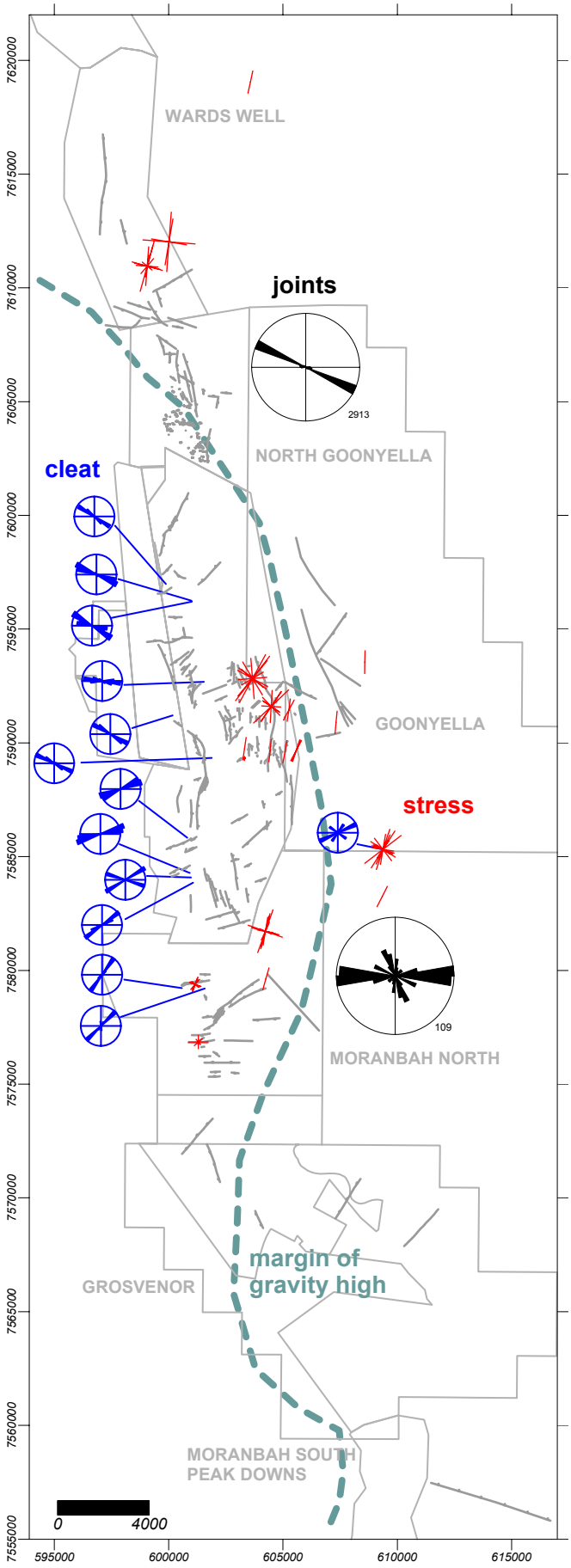

Figure 33 Distribution of joints (black), cleat (blue) and horizontal stress (red) in the Northern Tile.

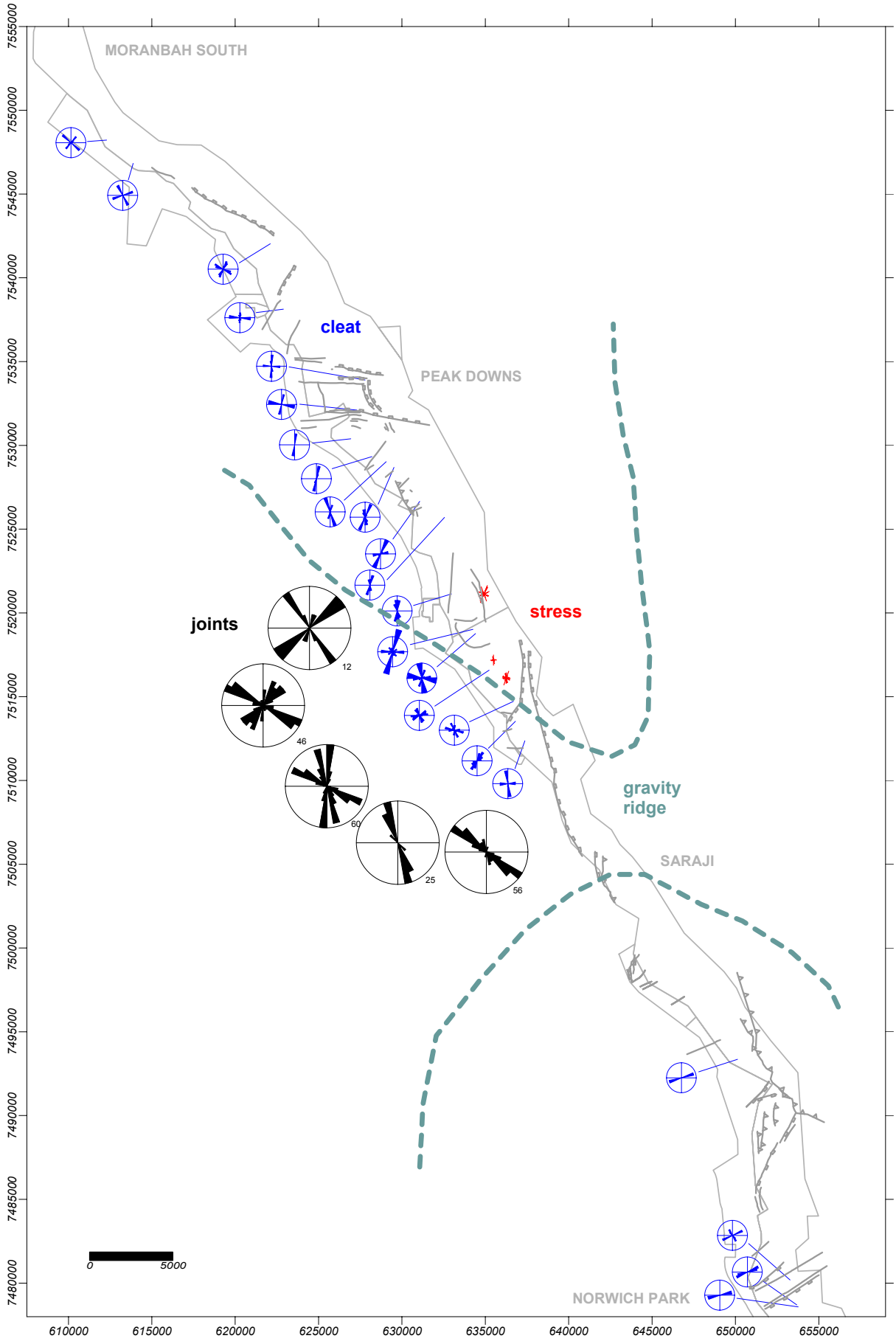

Figure 34 Distribution of joints (black), cleat (blue) and horizontal stress (red) in the Middle Tile.

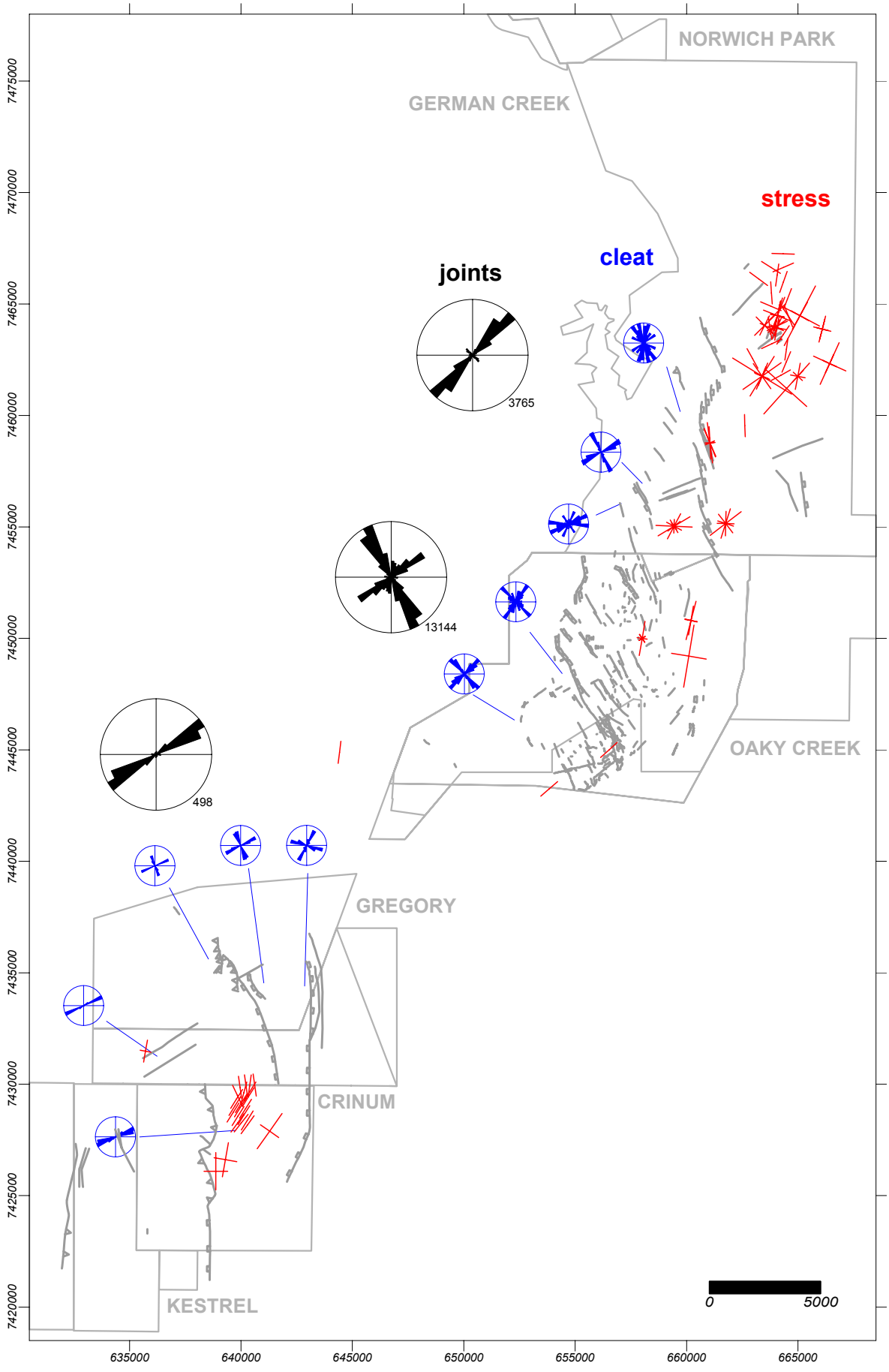

Figure 35 Distribution of joints (black), cleat (blue) and horizontal stress (red) in the Southern Tile.

Underground mine mapping at Oaky Creek shows that although joints and cleat have similar orientations, there are significant differences in the distribution of these structures (Figure 36). Face and butt cleats show a consistent orientation throughout the mine, whereas joints form distinct domains where one orientation is dominant over all the others. These domains cannot be directly linked to the presence of individual faults in the area, but are parallel to the main fault orientations.

Joints and cleat most likely formed at different times during the regional evolution under different stress regimes, separated by at least two major phases of faulting (see sections 4.1.4 and 4.1.7). Cleats formed early in a relatively unfractured rock mass, allowing them to respond consistently to the stress field at the time, which was influenced by basement structure. Joints formed a lot later, within a faulted and pre-strained rock mass, in a non-directional extensional stress field. In this case the strongest control on joint orientations is pre-existing fabric, rather than the orientation of the stress field, causing the strong domains.

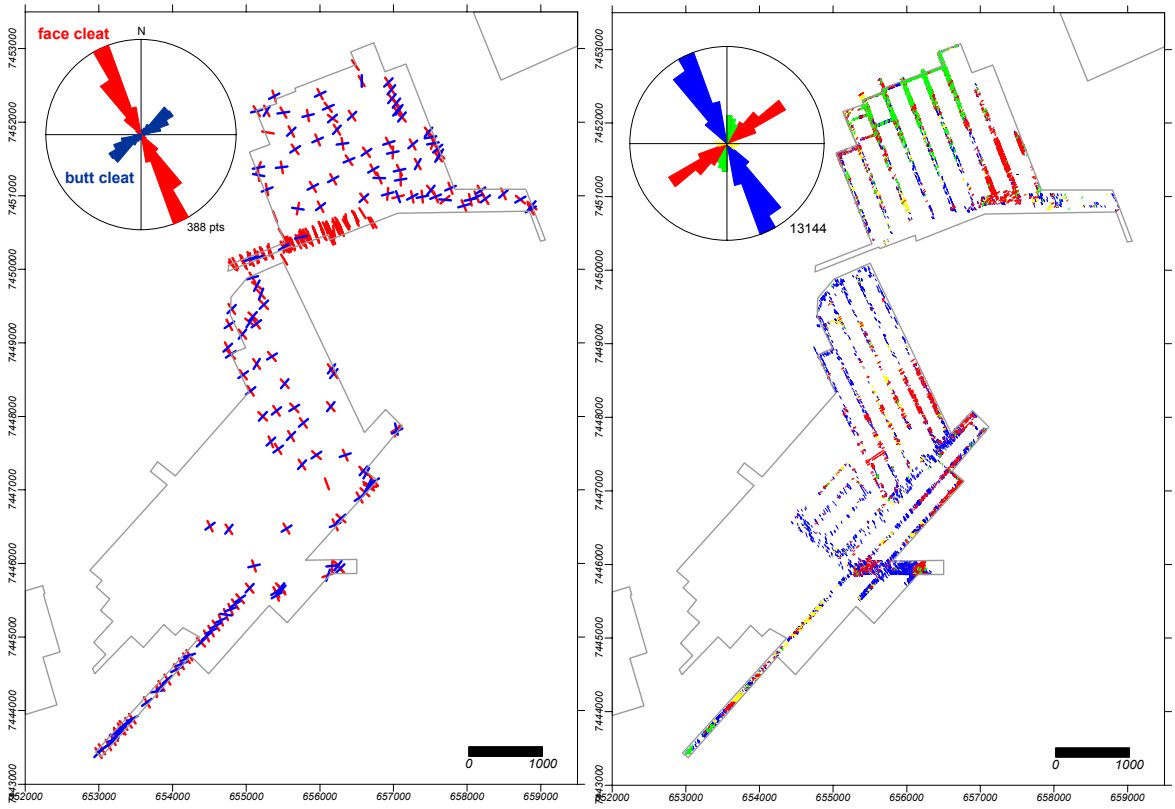

Figure 36 Cleat and joint set distribution at Oaky Creek underground mines. Orientations of map symbols are colour coded as shown on the rose diagrams.

In conclusion the main controls on cleat orientation are subtle basement features and its control on the orientation of the stress field at the time. Similar relationships have been documented and modelled for coals Wyoming that were deformed during the Tertiary (Laubach et al, 1998).

Joints formed during uplift in an extensional stress regime where the maximum and minimum horizontal stresses are very similar. Hence the orientation of the fractures that form is most strongly controlled by pre-existing anisotropies in the rock mass.

4.2.3 Timing relationships

In order to integrate the observed structural elements into the regional evolution and basement structure, relative and absolute timing relationships need to be established. From the review of data and above discussion we know that:

- Widely spaced north-south and east-west as well as more common northeast and northwest trending structural patterns exert control on all structures within the coal measures, and are interpreted to predate their deposition.
- No growth faults have been identified within the Moranbah-German Creek Coal Measures. However, the distribution of thick channel complexes in the interburden of the Northern Tile suggests some weak activity on basement structures at depth (Le Blanc Smith and Esterle, 1998).
- Normal faults of regional significance show northeast or northwest trends that seem to reactivate an earlier basement fabric.
- Normal faults are completely brittle and propagated through fully lithified rocks. They occur at least as high in the stratigraphy as the Rangal Coal Measures.
- Where thrust and normal faults interfere with each other, thrust faults overprint the normal faults.
- Thrust faults within the Supermodel area are related to the regional-scale Jellinbah thrust system, which propagated into the basin during the Mid Triassic.
- Normal and thrust faults, dykes and most reactivation on these structures are truncated by the Tertiary unconformity.
- Small intrusions in the region, including dykes and sills at German Creek are geochemically related and some have been dated as Early Cretaceous (Pattison, 1990).
- Dyke intrusion is coeval with bedding plane shear. However some of the bedding plane shear and thrust fault reactivation postdates the dykes.
- Cleat mineralisation has been dated at 245-220 Ma (Faraj quoted in Pattison et al, 1995). This mineralisation has not been found in the vertical joint sets.

These relationships are summarized in Figure 37 and suggest that the north-south and east-west as well as the northeast and northwest trending basement structures are older than Late Permian and exerted a mild control on the distribution of sediments during Late Permian deposition, but not enough to form growth faults. The fully lithified rocks underwent first a mild extension resulting in abundant normal faults, and then compression resulting in the less abundant but more severe thrust faults by Mid-Triassic.

Dykes intruded during the early Cretaceous associated with bedding plane shear and mild fault reactivation. Some fault reactivation and jointing may be as young as Tertiary, but there is no field evidence for structures to cross the Tertiary unconformity.

Joints are the most poorly constrained structures in the study area. However their spatial distributions are generally parallel to the main faults nearby, suggesting that they are younger. They are most likely related to the Late Cretaceous uplift.

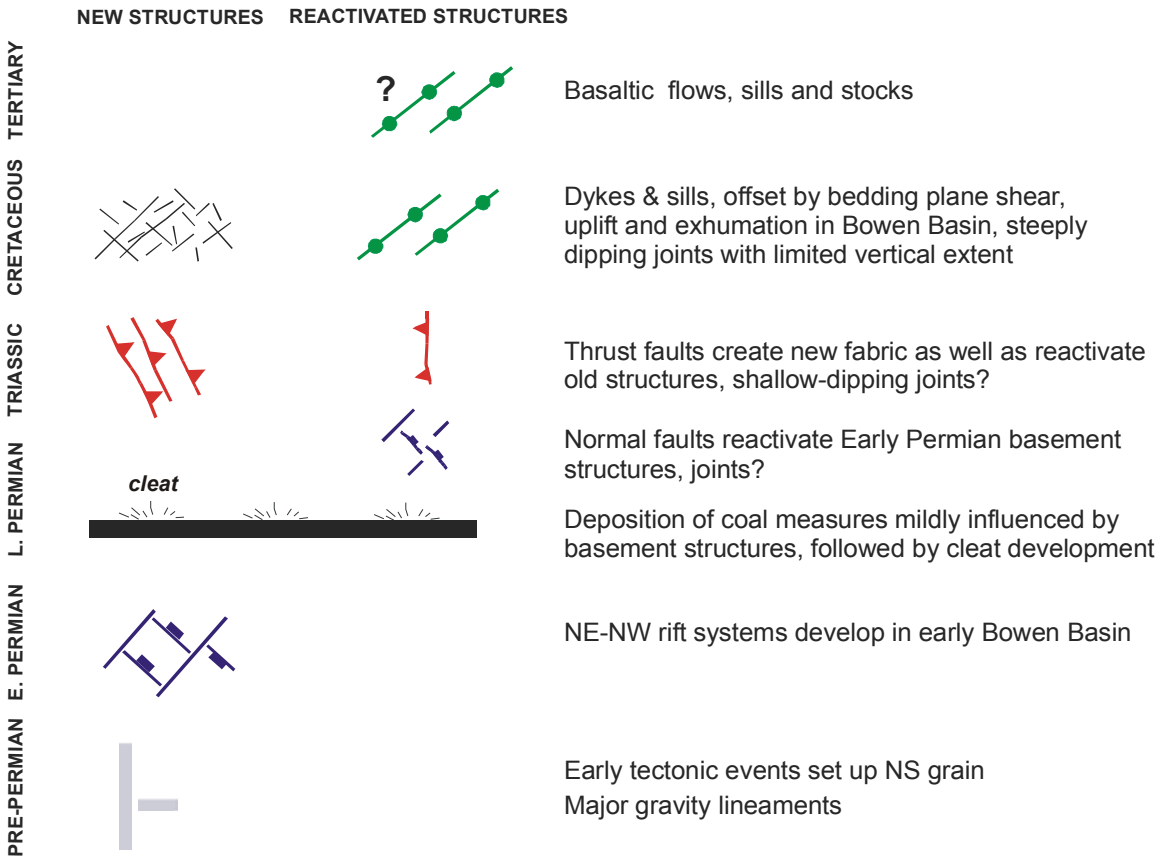

Figure 37 Suggested evolution of structural elements in the Supermodel area.

4.3 Stress

Data for modern day stress were compiled from existing mine mapping and borehole measurements. The aim was to investigate the regional variation in horizontal stress magnitude and orientation, and to assess local controls such as nearby faults.

No attempt was made in this discussion to evaluate the relative quality of data determined by a broad range of measurement techniques, which included:

- *Overcoring*. This technique yields minimum and maximum horizontal compressive stress magnitudes and orientations (σHmin and σHmax) in vertical boreholes. In horizontal

boreholes drilled underground overcoring can also yields the vertical stress and the true orientations of all three major stress axes in space.

- *Hydraulic fracture analysis*. This technique yields σHmax and σHmin magnitudes and orientation as well as rock strength estimates. It assumes the burial stress component to be vertical. This was the most common technique in the Supermodel data.
- *Borehole breakouts* measured on acoustic scanner logs. This technique yields σHmax orientations, but no magnitudes.
- *Mine mapping.* These are a series of stress determinations on samples from underground workings at Kestrel. Note that these data include the effects of stress redistribution due to mining.

Only a few measurements recorded the vertical stress and its orientation, which is up to 23° off vertical at Goonyella. Therefore in the following discussion the assumption is made that the vertical stress plunges at 90°.

4.3.1 Tectonic stress component

As a component of the horizontal stress is a result of vertical loading, σHmax increases with depth (Figure 38a). To normalize the stress measurements for regional comparisons a procedure as outlined by Charleson and Gray (1999) for German Creek was applied. The assumption was made that the rock mass is laterally constrained so that conditions are elastic, and no creep deformation processes are taking place. In this case the vertical stress (σ_v) due to self-weight was calculated at a rate of 0.025 MPa/m depth, and the earth pressure coefficient (K_0) was chosen at 0.25. The component of maximum horizontal stress due to tectonic forces (σHTmax) was calculated as

$$\sigma HTmax = \sigma Hmax - \sigma_v * K_0$$

The results are plotted in Figure 38b, and highlight that the tectonic stress component is far greater than the component induced by loading, as expected for crustal conditions under compression (Pusch, 1995).

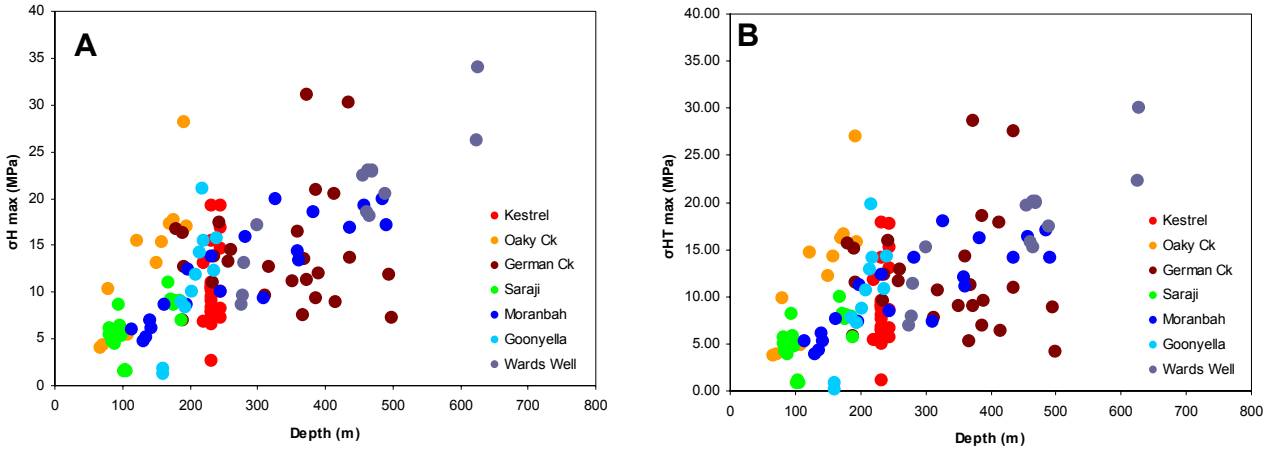

Figure 38 Relationships between a) σHmax and b) σHTmax with sample depth.

4.3.2 Stress magnitude distribution

There are two variables that are important to discuss in a regional context. One is the maximum horizontal tectonic stress (σHTmax), and the other is the ratio between the maximum and minimum horizontal tectonic stresses (σHTmax /σHTmin). The latter is an indicator for the presence and severity of shear stress.

Both these variables and the stress orientations vary considerably within individual boreholes. This is very common for boreholes in a variety of environments and host rocks (Pusch, 1995), and has been noted in the Bowen Basin (Enever, 1992). It highlights the importance of local controls on the stress distribution, such as rock elasticity, faults, joints and lithological boundaries that are prone to bedding parallel shear.

For a regional assessment of σHTmax and σHTmax /σHTmin, both variables are plotted (Figure 39) against the north-south distribution of the samples. There is no clear trend in the distribution or the range of magnitudes of σHTmax. Only Saraji appears to have lower stress magnitudes, but this could be a sampling issue. All three surveyed holes are close together, and shallow. The distribution also shows no clear trend within the mine site areas (Figure 33 to Figure 35 above).

Stronger relationships emerge in the distribution of the σHTmax /σHTmin ratio. Most data vary between 0.3 and 2.5 across the Supermodel area, but ratios in excess of 2.5 are only present in the Southern Tile, particularly at German Creek and Oaky Creek.

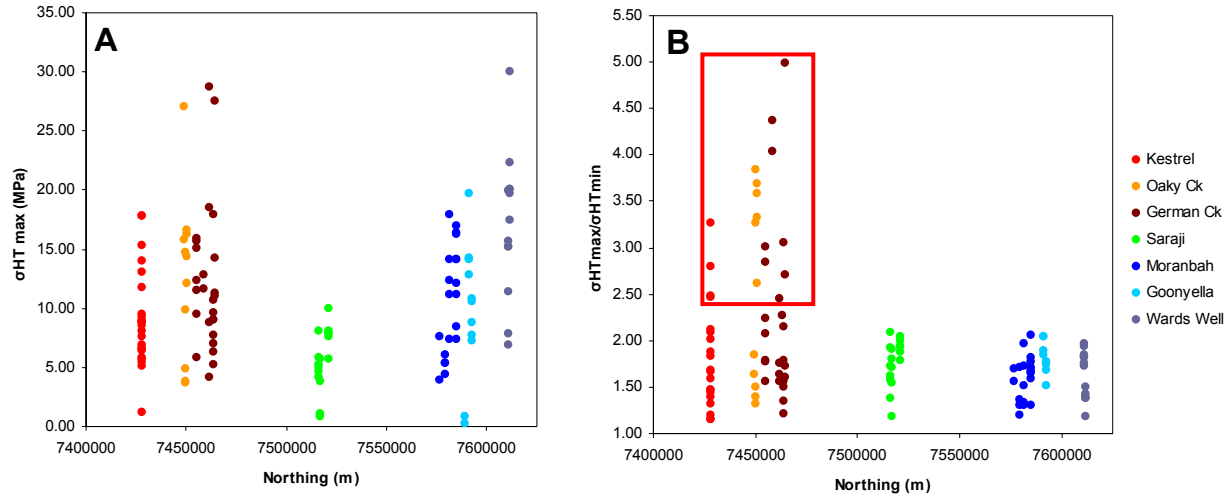

Figure 39 North-south distribution of a) σHtmax and b) σHTmax /σHTmin. Anomalously high ratios occur at German Ck and Oaky Ck mines (red outline).

Plotting these high ratios on a map of the Southern Tile shows that most plot interspersed with the other stress data. However, at least two of the high ratios occur near major structures (Figure 40), one near the Grasstree dyke (A) and one near a major north-south trending normal fault system (B). Note that the orientation of σHTmax at these positions is parallel to the structures, discordant with the regional trend.

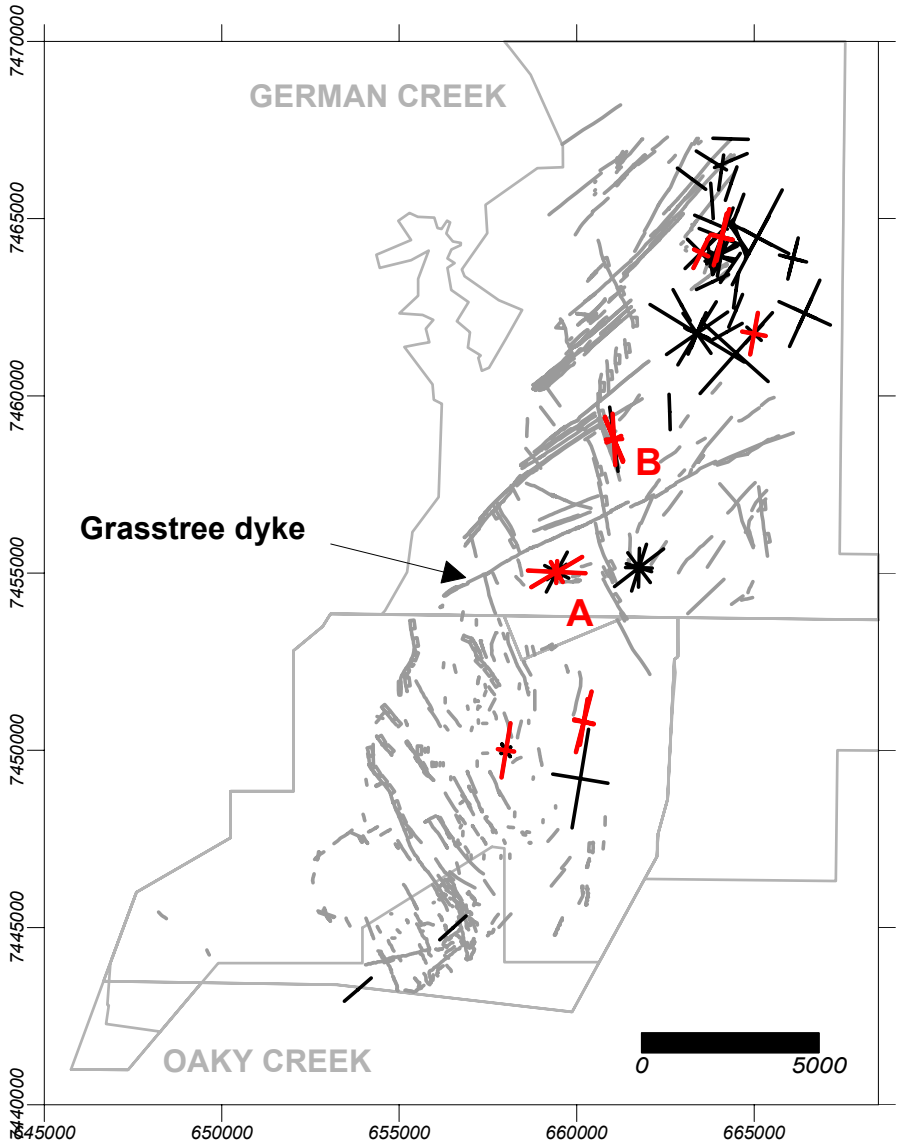

Figure 40 Map of northern part of Southern Tile showing σHTmax /σHTmin ratios above 2.4 (red). Other stress measurements are shown for reference (black).

The occurrence of high stress ratios and anomalous σHTmax trends in the Southern Tile may be interpreted as a result of the high structural complexity, and the presence of strong inherited fault patterns in this area.

4.3.3 Regional stress orientation

The predominant orientation for the maximum horizontal stress for all three tiles in the Supermodel area is NNE (Figure 41). The greater variability of data in the Middle Tile may just reflect the sparseness of data in this area. These results are in agreement to those compiled by Enever et al (1987), and Hillis et al (1999) for the Bowen Basin, and for several other regions across Australia including the Northern Territory and New Guinea.

Hillis et al (1999) conclude that this stress orientation is consistent with the predicted σHTmax from existing plate boundary-force models, and that hence the stresses in the Bowen Basin are most likely

controlled by plate boundary forces resulting from the collision of New Guinea with the Indo-Australian plate. New, more sophisticated numerical plate boundary-force models also corroborate this conclusion (Zhao and Müller, 2001).

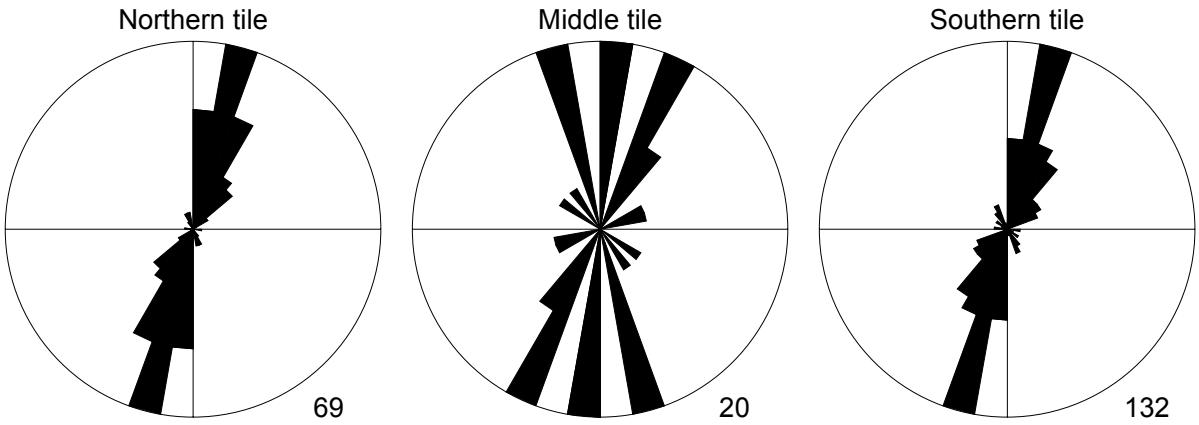

Figure 41 Orientation of maximum horizontal stress in the northern, middle and Southern Tiles. The number of measurements in each tile is indicated below each rose diagram. Stress orientations were corrected to AMG North by subtracting 9.5° from magnetic north.

5 SEDIMENTARY FRAMEWORK

Joan Esterle, Renate Sliwa and Guy Le Blanc Smith

5.1 Overview

The stratigraphic and sedimentary framework of the Moranbah and German Creek coal measures in the Supermodel area was derived from published and company reports and supplemented by CSIRO studies conducted for specific mine sites. The contribution of the Supermodel project is the creation of regional scale maps of the coal seam thickness and splitting patterns, interburden thickness maps and their integration with regional structure to determine the mechanics of basin fill and subsequent deformation of the sedimentary sequence.

The stratigraphic framework of the coal measures was established by regional mapping and by extensive coal exploration drilling (Figure 2, Milligan, 1975; Koppe, 1978, Draper, 1990). The transition from the Moranbah CM in the north to the German Creek CM in the south records the southerly progradation from fluvial and upper delta plain sedimentation to paralic or marginal marine sedimentation that formed during a period of foreland loading. Together they form a clastic wedge intercalated with laterally continuous coal seams that split and coalesce for some 250 km along the strike of the basin. In the north near Collinsville, the Moranbah CM are over 537 m thick (drill core Drake 26 cited in Michaelson, 1999); to the northeast at Kemmis Creek they are 760 m thick (Koppe, 1978); to the south and southwest they thin to less than 20 m over the Comet Ridge and Capella Block (Figure 96; Prouza and Park, 1973). Throughout, the interburdens of the Moranbah CM are sandstone-dominated, but drilling in the thick northeastern portion records clast-supported conglomerates in the lower part of the sequence. Here the coal seams are numerous (up to 24) but thin and widely spaced (50 to 100 m) relative to the western limb of the basin.

The coal measures are underlain by and pass laterally to the south into sequences of marine-derived sandstones and siltstones. The MacMillan Fm records a marine transgression that ingressed partially into the basin prior to the main phase of foreland loading and southerly progradation of terrestrial conditions that resulted in the accumulation of the thick, high ash and tuffaceous coal seams of the Fort Cooper Fm and its equivalents during the Late Permian. Thrusting built up the Gogango Overfolded Zone in the east, providing abundant clastic input to the basin (Holcombe et al*,* 1997). Foreland loading was maintained by further emplacement of major thrust sheets from the east and sedimentation was characterised by non-marine, lithic sediments with widespread development of the Rangal coal measures prior to basin closure and subsequent deformation in the Triassic. The basin strata plunge gently to south and east and show increasing levels of burial coalification and deformation to the east (Beeston, 1986).

The open cut mine exposures and dense drilling intersecting the coal measures within the 200 km long and 10 km wide mining corridor provided more detailed information about the internal architecture of the coal-capped sedimentary interburdens (Godfrey, 1978 and 1985; Johnson, 1984; Falkner and Fielding 1992, 1993; Michaelson, 1999, among others). The clastic interburden sediments of the Moranbah CM are characterized by variably bedded, thin to thick (up to 60 m where amalgamated)

sandstones that are intercalated with heterolithic fine grained and thinly bedded sandstones, siltstones and claystones that are interpreted to have formed in environments varying from broad (2 to 4 km) fluvial and upper delta-plain channel belts and adjacent floodplain deposits varying from wedge to sheet-like overbank, lobate crevasse-splays to open lakes. The framework grains of these sediments are characterized petrologically by abundant volcanolithics and minor quartz interpreted to have been sourced from the volcanoplutonic arc shedding sediments from the northeast (Jensen, 1971; Baker et al*,* 1993; Michaelson and Henderson, 2000).

Martini and Johnson (1987) envisaged the Permian age environment for the Bowen Basin to be similar to that of the Canadian Hudson Bay lowlands where vast cold climate mires, lakes and very low-gradient stable floodplains episodically traversed by an anastomosing (branching and reconnecting) semi-permanent system of multiple splay-channel complexes, which drained southwards into a marine basin. The system grew through a process of cyclic crevasse splay accretion and periodic channel avulsion accompanied by synchronous differential compaction of thick underlying peats. Splay and channel initiation appears linked to subtle movements on basement structures, which periodically formed new gradients of advantage across extensive peat deposits. Early avulsion deposits present as thin fine-grained “overbank” sheet splays and lacustrine facies, which locally matured into larger heterolithic accretionary splay and channelized systems separated by substantial peat islands.

The clastic interburden sediments of the coal-bearing German Creek CM are also sandstone dominated, but on average are characterized by thinner (4 to 20 m) sandstone sequences interbedded with carbonaceous mudstones. The sandstones, particularly in the upper part of the sequence, commonly contain indicative marine ichnofossils and body fossils. Thicker sandstone units have geometries ranging from narrow and sinuous channels, to lobes and sheets that are interpreted to have formed in paralic environments such as distributary channels that often prograde over their lobate mouth bars, and near shore bars and sheets reworked by longshore drift (Falkner and Fielding, 1993). The petrologic character of the sandstones is quartz-rich. Based on palaeocurrent analyses, the provenance of these sandstones is thought to be from the continental block or craton to the west, although their quartz-rich nature was probably enhanced by a loss of labile grains during coastal reworking (Michaelson and Henderson, 2000).

The aggradation and resulting sand accumulation rates varied as a function of sediment supply and accommodation space controlled either internally by subsidence, due either to differential compaction of underlying fine-grained sediments and peat or tectonic movement of underlying lithologies, or externally by changes in base level due to sea level fluctuations. The thick (1 to 11 m) and extensive coal seams that punctuate the clastic sequence represent a prolonged absence of sediment influx in the areas of peat accumulation. The clastic interburden and coal seam thickness distributions are described more fully in the following tile sections, but briefly outlined here to give the reader a regional context from which to examine the detailed maps. The mechanisms thought to be influential in the formation and subsequent deformation of the coal measures is discussed in a summary section.

5.2 Principal coal seams and markers

Figure 42 demonstrated the four major "superseams" that occur for more than 200 km along the western limb of the Bowen Basin. Similar correlations were first proposed and presented from government and BHP-Billiton Pty. Ltd. drilling (Utah Development Company; Milligan, 1975; Devey, 1983). These superseams have been used by Michaelsen (1999) to define major stratigraphic sequence boundaries that represent widespread periods of non-deposition of clastic sediments across the basin. The study area contains a sequence of coal seams which has a cumulative coal thickness of 20-30 metres in the north and progressively thins to the south and pinches-out near the southern margins of the sedimentary wedge (Figure 43). They are separated by intervals containing siltstones, carbonaceous mudstones, tuffaceous strata, and a series of offset- and vertically stacked sandstone units (Figure 48 and Figure 49,). Interburdens vary in thickness from less than 1 m to more than 60 m. The coals provide time-stratigraphic markers and they vary from 3 to 11 m thick, locally split and coalesce. The most persistent superseams in stratigraphic order from oldest to youngest are:

- Lower Superseam (Goonyella Lower – Dysart - German Creek Seams).
- Middle Superseam (Goonyella Middle - Harrow Creek – Aquila Seams);
- 'P-tuff' a regional tuffaceous unit (locally coupled with the P-Superseam);
- P-Superseam (P Seams – Pleiades Seam); and
- Upper Superseam (Goonyella Upper Seams).

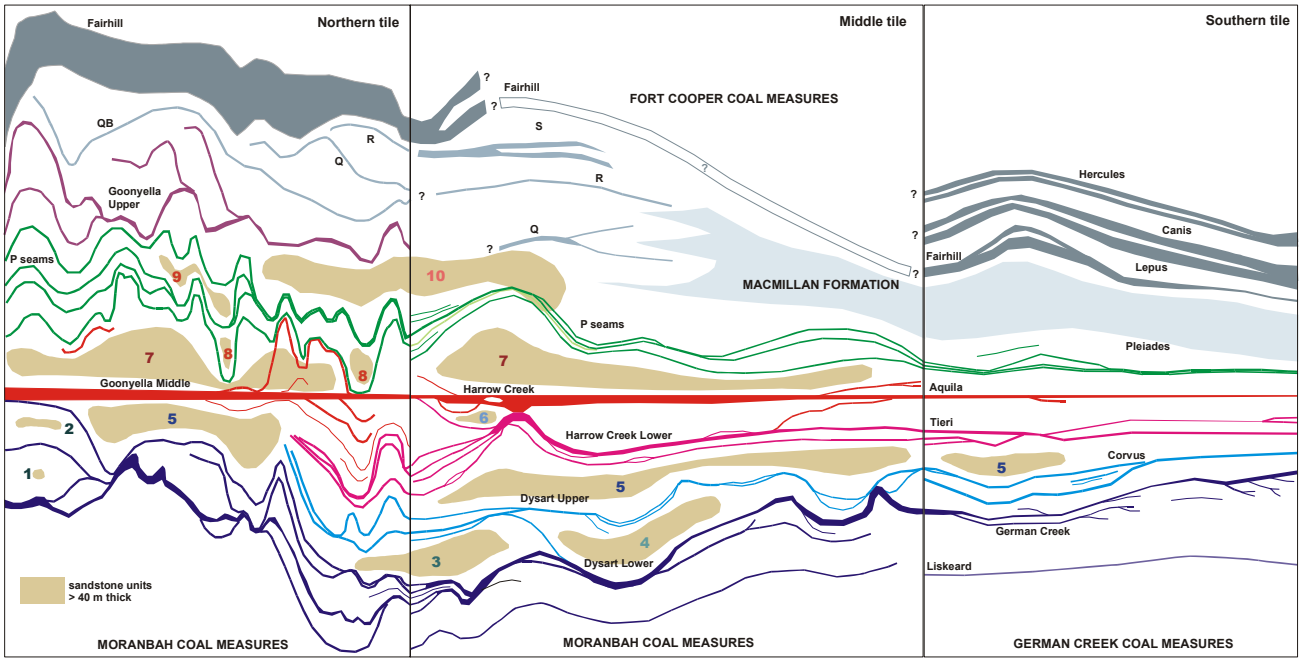

Figure 42 regional correlation sections through the Supermodel 2000 tiles showing the general thickness and splitting patterns of the major "superseams" over a section length of 200km. Datum is the Goonyella Middle seam and its lateral equivalents. Major sandstone units in the interburdens are numbered and referred to in Figure 97.

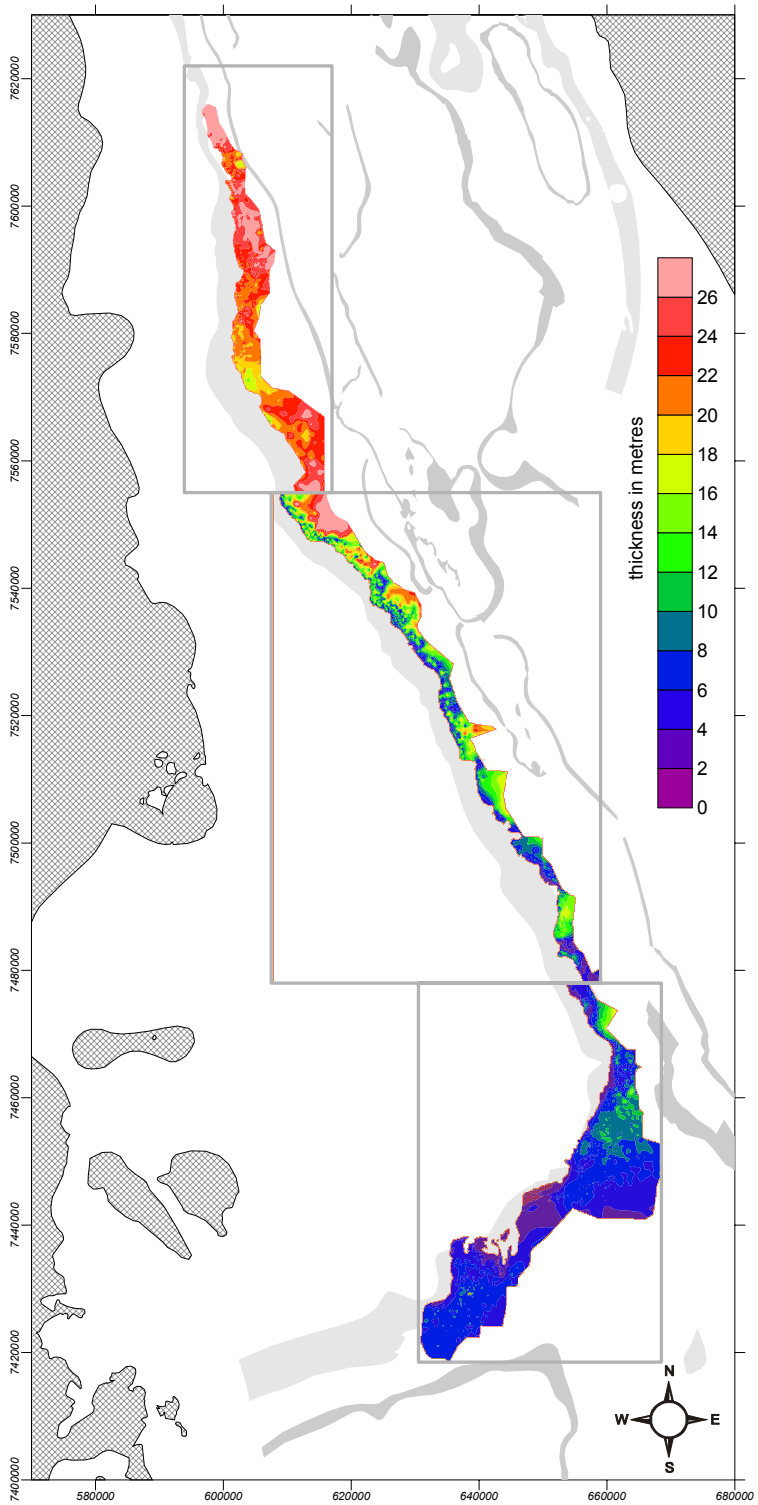

Figure 43 cumulative coal-only thicknesses in the Moranbah-German Creek CM from the lower to upper superseams along the western limb of the basin.

The **Lower Superseam** is the Goonyella Lower-Dysart-German Creek seam. In the north of the Supermodel area, this seam attains 12 m in thickness and it thins to the north and south by multiple episodes of splitting. The seam or its equivalent has been identified in drill core to the east at South Kemmis Creek and is 8 m thick (cited in Michaelson, 1999). Split lines are variably oriented and shaped depending on their origin from clastic influx from coastal transgressions, splays or channel belts (see maps in Section 5.3 to 5.5). Floor splits in the Lower Superseam are commonly oriented

northeast, parallel to palaeo-shoreline, suggesting the punctuated accumulation of the peat mires as the system prograded seaward. Roof splits tend to be more variable and reflect the influx of clastic sediments as the channel systems prograded seaward and buried the peats. In the Southern Tile, the equivalent German Creek (Lilyvale) seam thins from 5 m to less than 1m, although the seam is interpreted to continue some 50 km further to the south and southeast (Prouza and Park, 1973). Split lines in the Southern Tile commonly trend north-northeast, parallel to the interpreted paleo-shoreline.

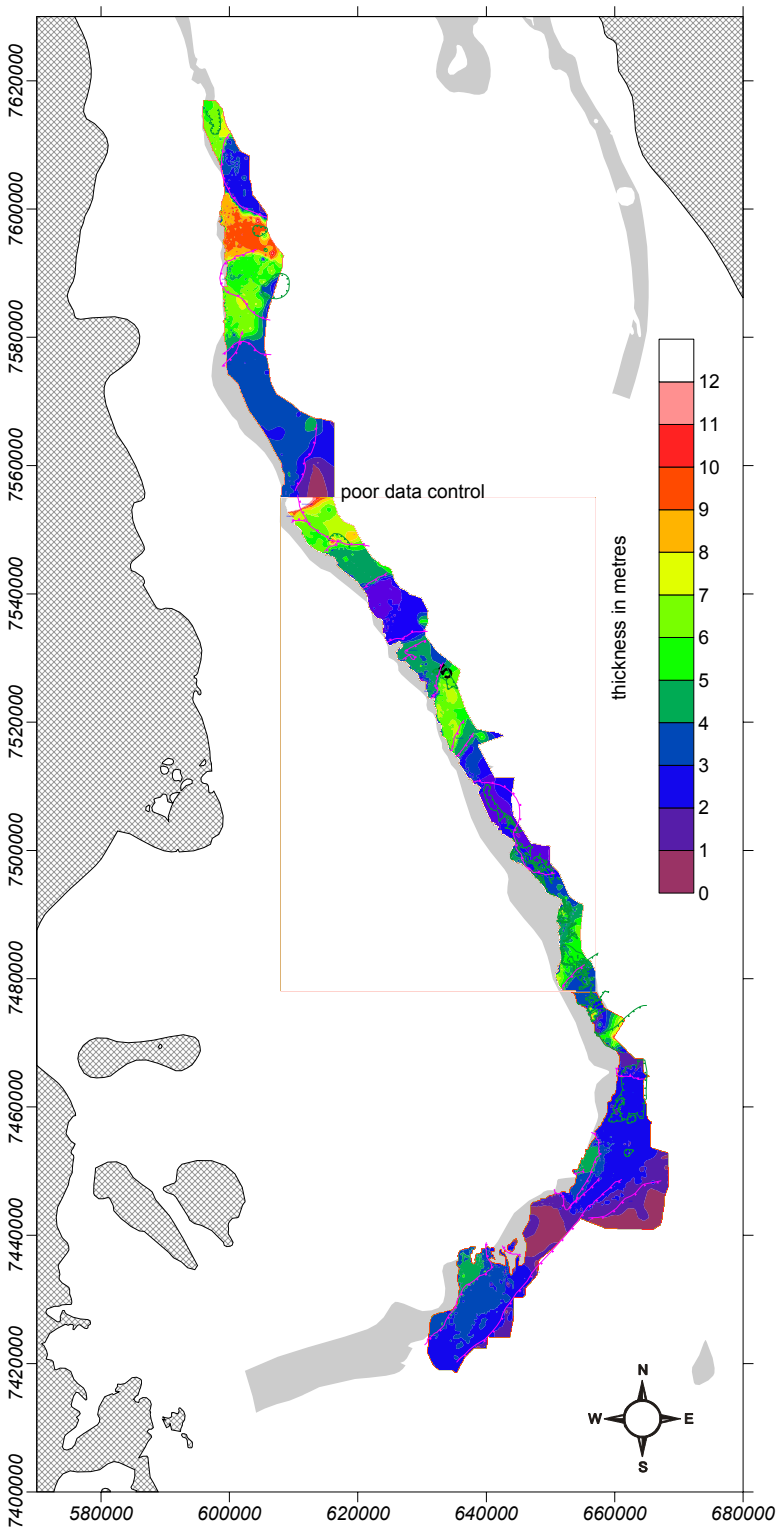

Figure 44 Lower Superseam thickness overlain by split lines (pink) and sill outlines (green).

The **Middle Superseam** is the Goonyella Middle-Harrow Creek-Aquila seam. Similar to the lower, it also attains 12 m in thickness in the Northern Tile and, in the data set, thins southward by splitting. "Z" splitting, where thin seam splits from an underlying seam and merges with an upper seam, is common for this seam, particularly in the Middle Tile. Also in the Middle Tile, the thin seams of the Harrow Creek Lower merge with the main Harrow Creek seam to form a thick, but laterally restricted seam in Peak Downs mine. Drilling between the tiles was too sparse to determine whether the Harrow Creek lower seams emanate from the splits of the Dysart Upper or just initiate in this area adjacent to major clastic channel systems. Split lines in the northern and Middle Tile define southerly oriented trunk channel belts with adjacent minor channels and splay deposits. In the Southern Tile the seam splits and thins into the Aquila seam.

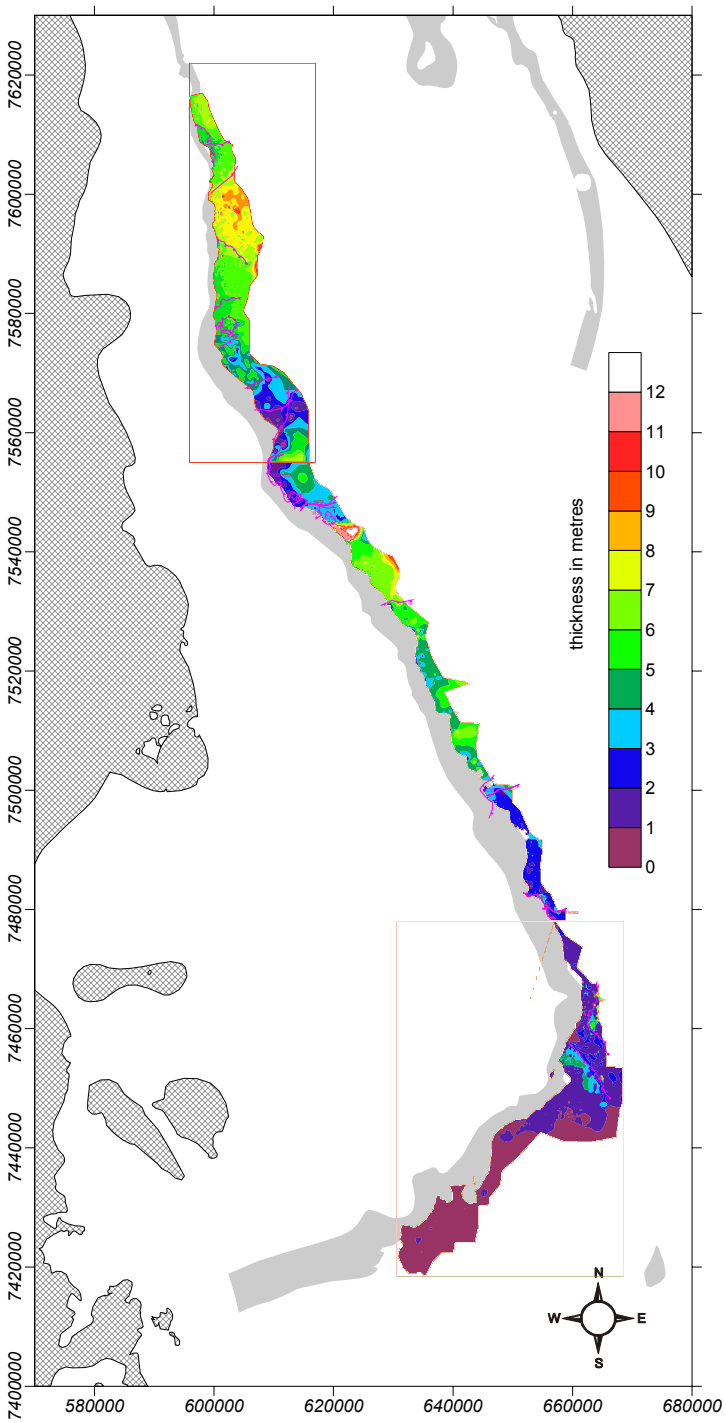

Figure 45 Middle Superseam thickness map overlain by split lines.

Unlike the underlying superseams, the **P superseams** merge southward forming a relatively thick seam horizon (up to 5 m) in the Middle Tile, but split and thin southward towards the palaeo-shoreline. The P-Pleiades horizon contains the "**P-Tuff**" which is an important stratigraphic marker unit (recently given the stratigraphic name "Platypus Tuff" by Michaelson and Henderson, 2001).

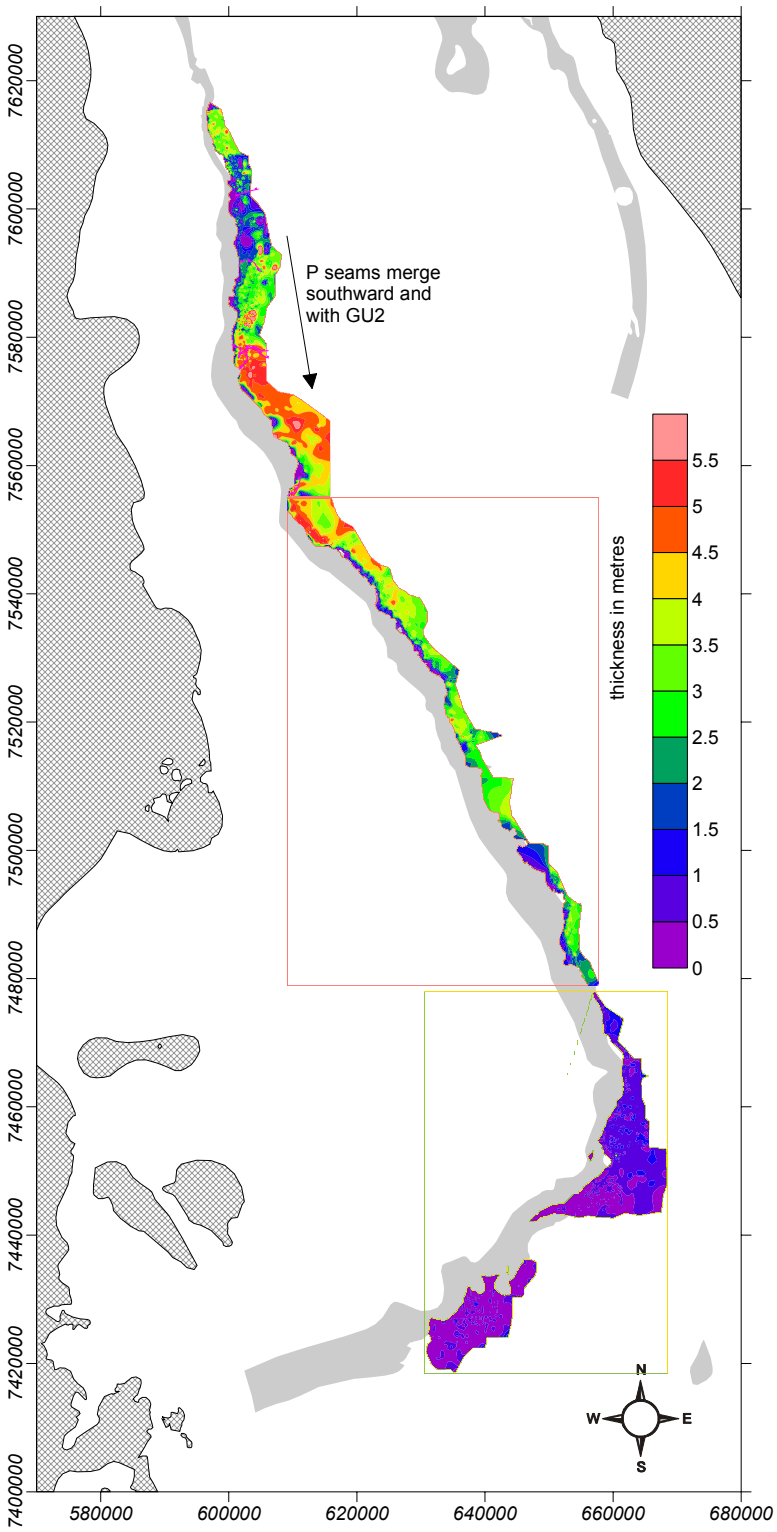

Figure 46 cumulative thicknesses of P seams, inclusive of the GU2 seam prior to merger in the southern part of the Northern Tile.

Although it is overlain by thinner seams (Q, R and S), the **Upper Superseam** that caps the study interval is the Goonyella Upper seam. The Upper Superseam reaches 6 m where merged in the Northern Tile, but it exhibits complex splitting patterns to the north and south. A lower leader seam merges with the P Superseam towards the south of the Northern Tile (GU2/GR with the Pleiades Lower seam). Split lines in the upper superseam continue the trend of thick, broad channel/splay belt complexes oriented southward. This seam thins and tapers to the south into the marine McMillan Fm in the Middle Tile. Its correlation with the mapped Q seam in this tile is uncertain.

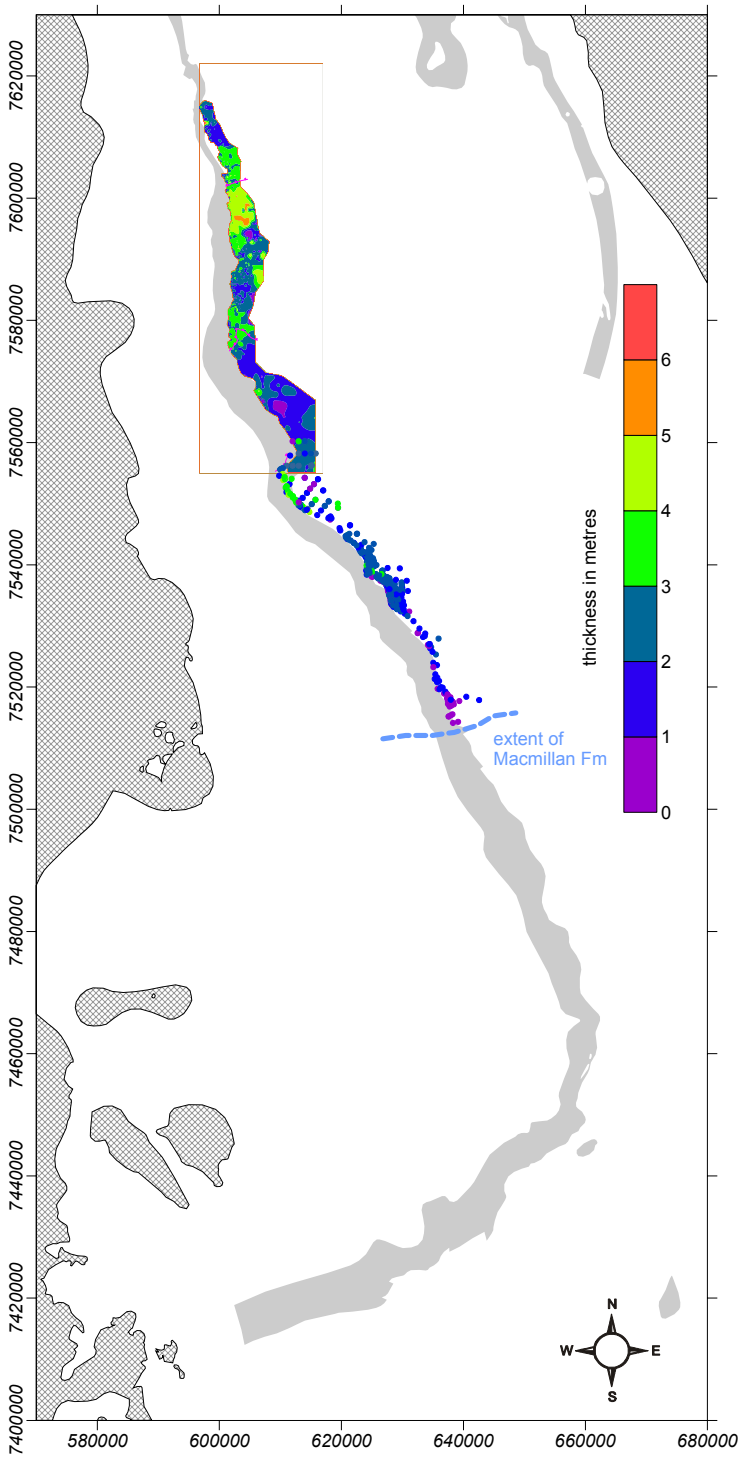

Figure 47 Thickness isopach of the Upper Superseam. Its thickness is represented by postings of the Goonyella Upper and Q seam in the Middle Tile due to uncertain correlation. Nevertheless, the upper seams thin and pinch out into the MacMillan formation to the south.

The distribution of seams and interburdens are described in detail across each of the tiles in the following sections. Seam thickness isopach maps are presented as respective superseam architectures where rider and leader seams are considered part of the interburden after they diverge from the foundation superseam. Split lines are annotated with ticks pointing in the direction of divergence. The summary discussion places these areas back into the regional framework.

5.3 Northern tile

The results for the Northern Tile model demonstrate the inter-relationship between the distribution of thick coal seams, seam splitting, thick sandstone channel complexes and basement fabric (Esterle et al, 2001, LeBlanc Smith and Esterle, 1998, LeBlanc Smith and Yago, 2000). Three laterally continuous coal seams, the Goonyella Lower (GL), Middle (GM) and Upper (GU) and their subordinate seams occur within an approximately 300 m thick sequence of the Moranbah CM. Seams vary from <5 m to 11 m thick and are separated by 15 to 60 m of interburden.

Seams split and merge along strike, but areas of thick merged seams tend to occur over areas of stable basement domains interpreted from regional gravity. Marginal to these areas, seams split and are interspersed with thick, multi-storey sandstone bodies. Sandstone depositional style in the Moranbah CM is commonly a composite of accretionary splays and channel-fills that range from 1 m to 55 m thick and up to 3 km wide; some with mapped lengths in excess of 15 kilometres (Figure 48). Mine exposures show sandstone-siltstone packages that are enclosed by coal and characterized by large low-angle accretionary foresets with fine-grained to silty toe-sets, which are attributed to cyclic (seasonal) depositional pulses that filled accommodation space created by progressive differential compaction of underlying peat layers (up to 60 m thick, Figure 49). Successive clastic packages predominantly display an offset-stacking pattern both laterally and up stratigraphic section. Vertical stacking of thick (>40 m) multi-storied sandstone bodies is more isolated but occurs in locations that are underlain by sequences characterized by the thickest (>8 m) coal seams. Vertical stacking of thinner sandstones and thinner coals also occurs and is interpreted as related tectonically controlled subsidence off the margins of stable basement platforms.

Figure 48 Lenticular cross-section of 35m thick amalgamated crevasse-splay channel unit dominated by medium- to coarse-grained cross-stratified lithic sandstone. Goonyella Mine Ramp 4 South high wall (75m high).

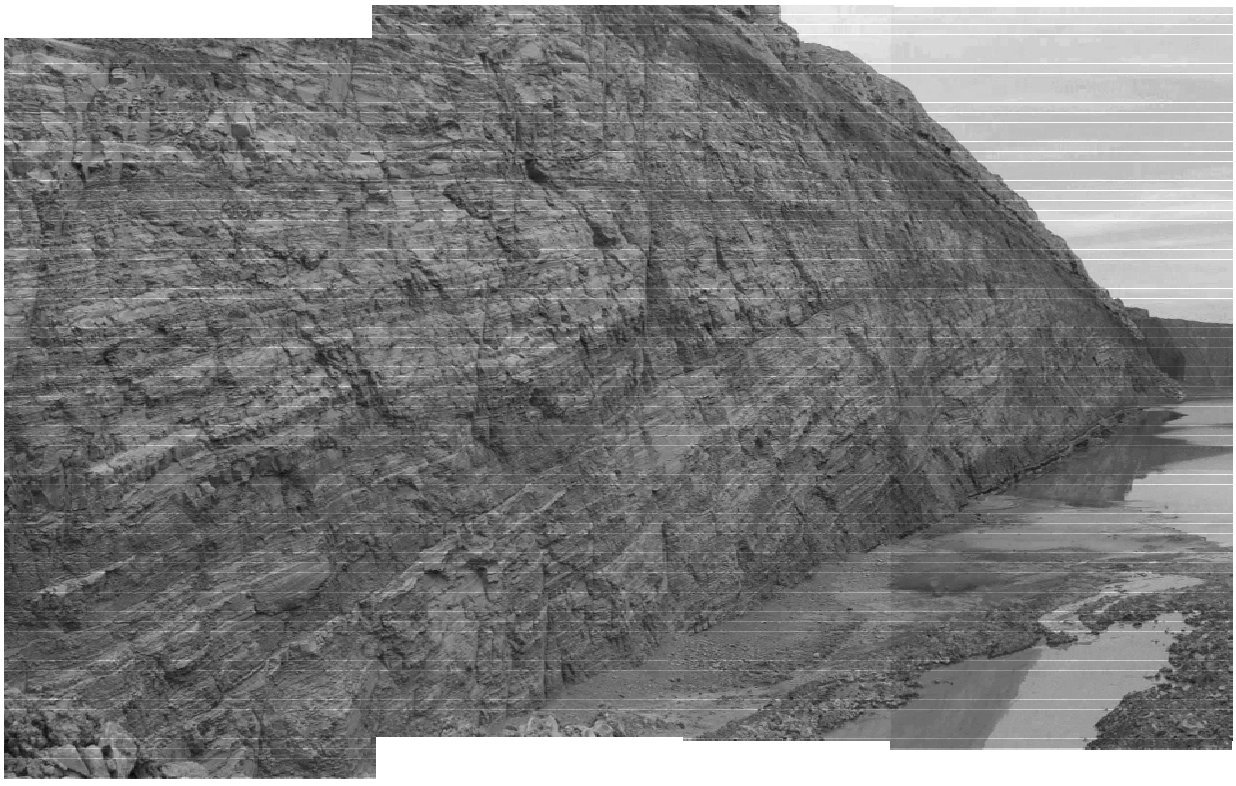

Figure 49 Large-scale heterolithic accretionary cross-stratified units overlying Goonyella Middle Seam. The high wall is 70m high. Location – Goonyella mine ramp 6 south.

Subsequently, the depositional fabric and the basement structure played a major role in partitioning deformation within the coal measures. Domains of consistent normal fault and cleat orientations appear to be bounded by the same margins of the basement high that controlled the distribution of thick sandstone bodies. During later deformation, thrust faults tended to deflect around the more competent sandstone bodies (Figure 50).

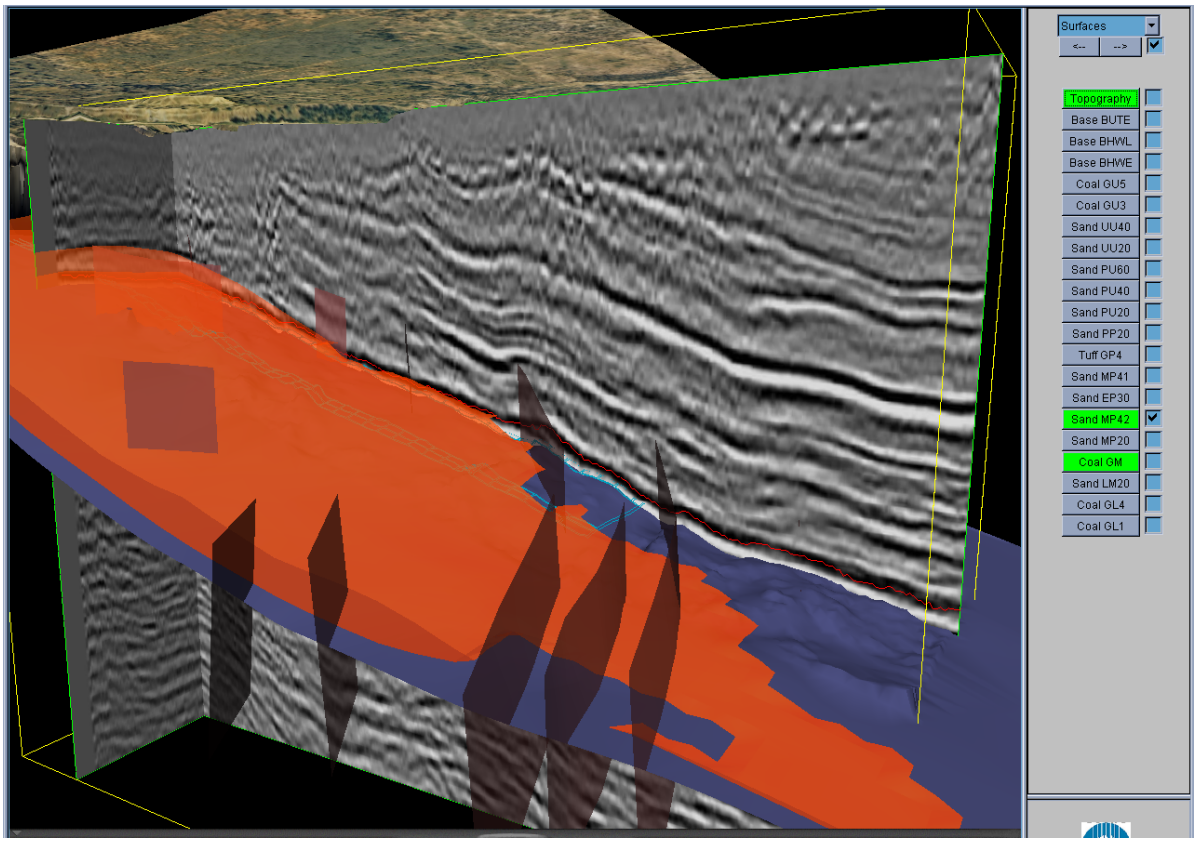

Figure 50 Example of zone of structure concentration and deflection around the margins of a lenticular 35m thick "stiff" roof sandstone unit (outlined in red) that overlies the working coal seam (blue-grey). Offsets in the depth-converted 3-D seismic reflectors clearly resolve structure and stratigraphic contacts (Goonyella Mine down-dip of Ramp 4 High wall, Le Blanc Smith and Caris, unpublished).

The thickness and splitting patterns for the Moranbah coal seams in the Northern Tile are demonstrated in a NS cross section (Figure 51) that uses the GM seam as a datum.

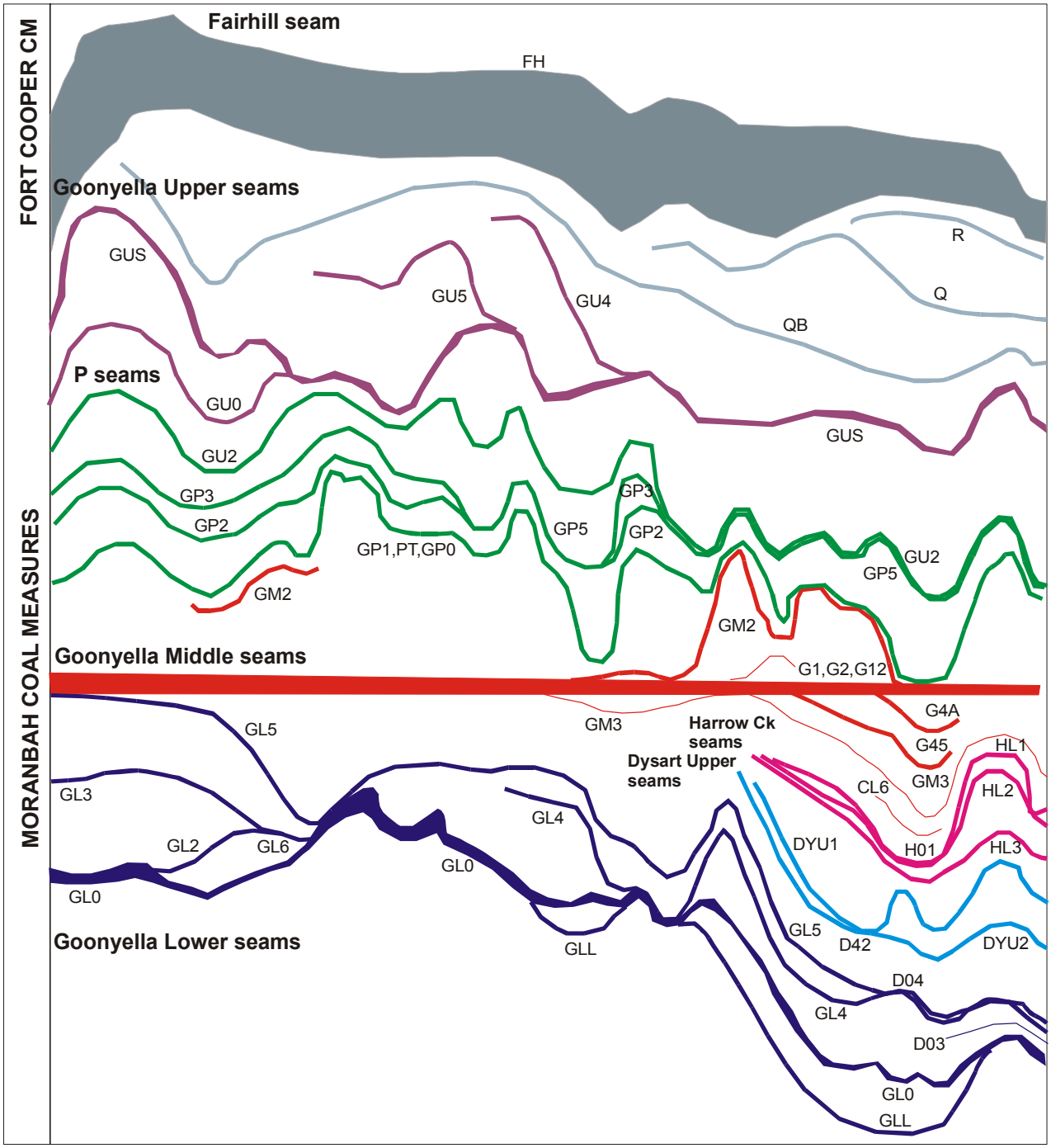

Figure 51 Schematic correlation of coal seams in the Northern Tile

A north-south cross section through the combined sedimentary/structural model demonstrates the regional and local variability in coal seam thickness and splitting character, sandstone distribution, deformation in the Permian coal measures, and the levels of Tertiary incision and infill. A broad east-west trending regional anticline dominates the area and it coincides with a regional gravity high. On its crest the GL and GM seams are thick (>8 m) and close (15 to 30 m) to one another. To the north and south of the limbs of the antiform, the GL and GM seams split into a series of thinner seams.

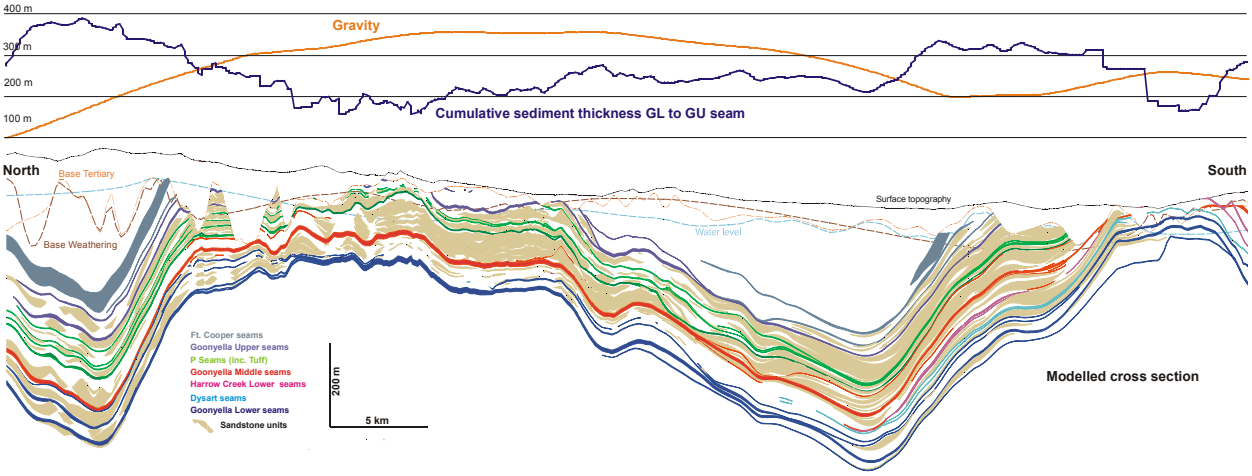

Figure 52 Seam and sand body structure in Northern Tile

In the crest area of the regional anticline the dip of the strata is gentle, around 3° to the east. To the north in North Goonyella and to the south in the Grosvenor area the axis of regional-scale folding swings from an E to a NE strike (Figure 65). In the limbs of the anticline the dip of the strata steepens to about 5°. Areas of thick Tertiary incision and infilling with sediments and basalts are associated with these areas.

Local folding occurs with wavelength of 4 to 6 km. The departures of roof and floor splits from the GM seam are often associated with the hinges of the folds, as is the thinning of the GM to P Tuff interval. Outcrop-scale folding and faulting occurs within the individual seams. Distribution of these features is controlled by the larger structures and the interburden makeup of the coal measures.

5.3.1 Topography and infrastructure

The topography reflects the surface drainage of the southerly draining Isaac River system. At the time of this report two underground mines were in operation at North Goonyella and Moranbah North and an exploration adit extracted at the extensive open cut operations at Goonyella.

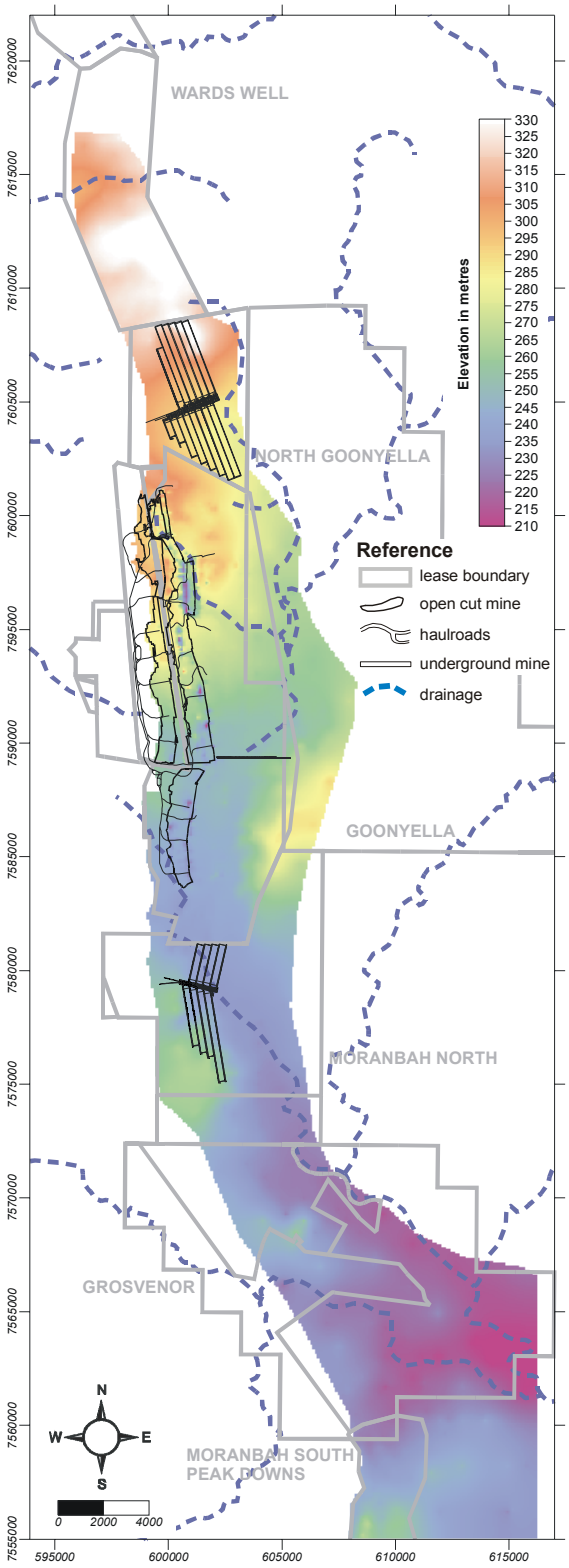

Figure 53 Topography and infrastructure

5.3.2 Base of Tertiary

The base of Tertiary surface reflects the drainage system imposed during Late Cretaceous uplift and incision. The Tertiary sequence is thickest in the north and south of the tile in NW and SW trending belts. Basalt infill is thickest in these areas.

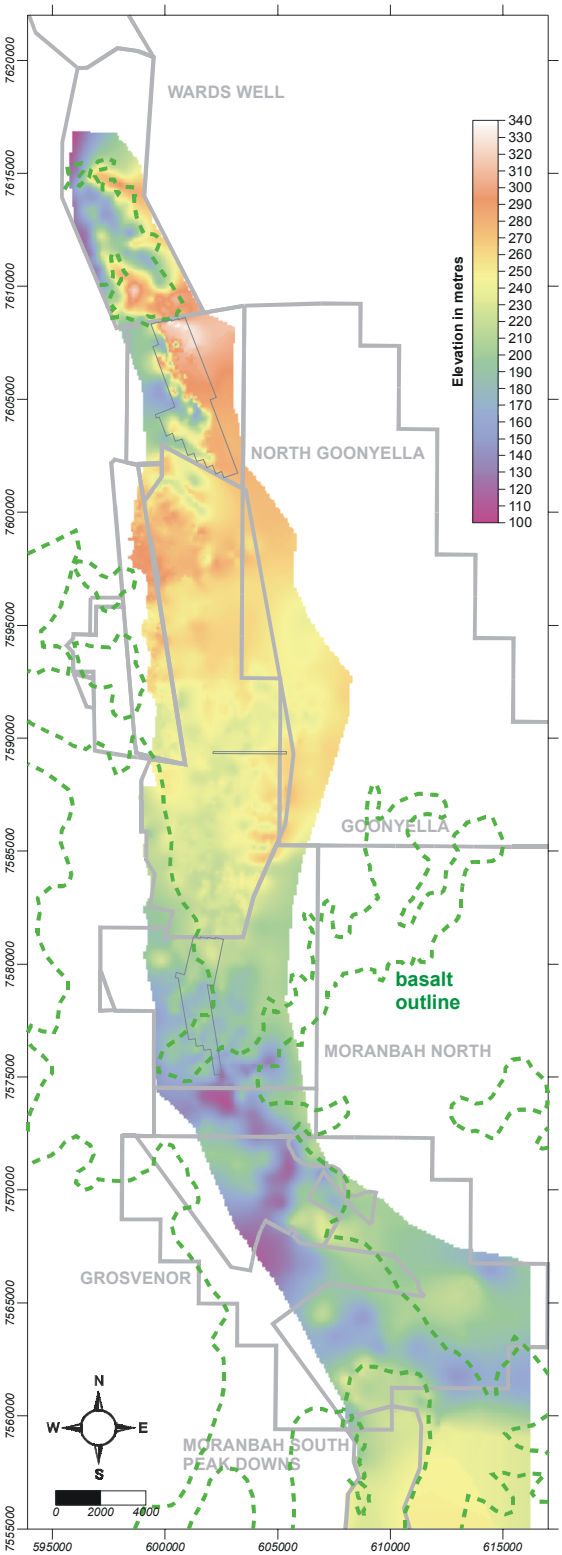

Figure 54 Base of Tertiary overlain by mapped distribution of basalt. Basalts present in North Goonyella but not mapped.

5.3.3 Goonyella Lower seam thickness

The GL seam is thickest, >8 m, in the north of the tile forming a pod 8x10 km in area. The main seam thins to the north and south by splitting. In the south, split lines reflect SSW trending, stacked channel belt sequences. In the north splitting reflects arcuate lobes infilled by heterolithic sediments. These lobate sedimentary bodies are interpreted as large splays that debouch from the main channel into open, but relatively shallow bodies of water on the floodplain. The Dysart seams, not included in this isopach, emanate from the roof of the GL seam to the south and merge to form the thick Dysart Lower seam that is mined in the Middle Tile.

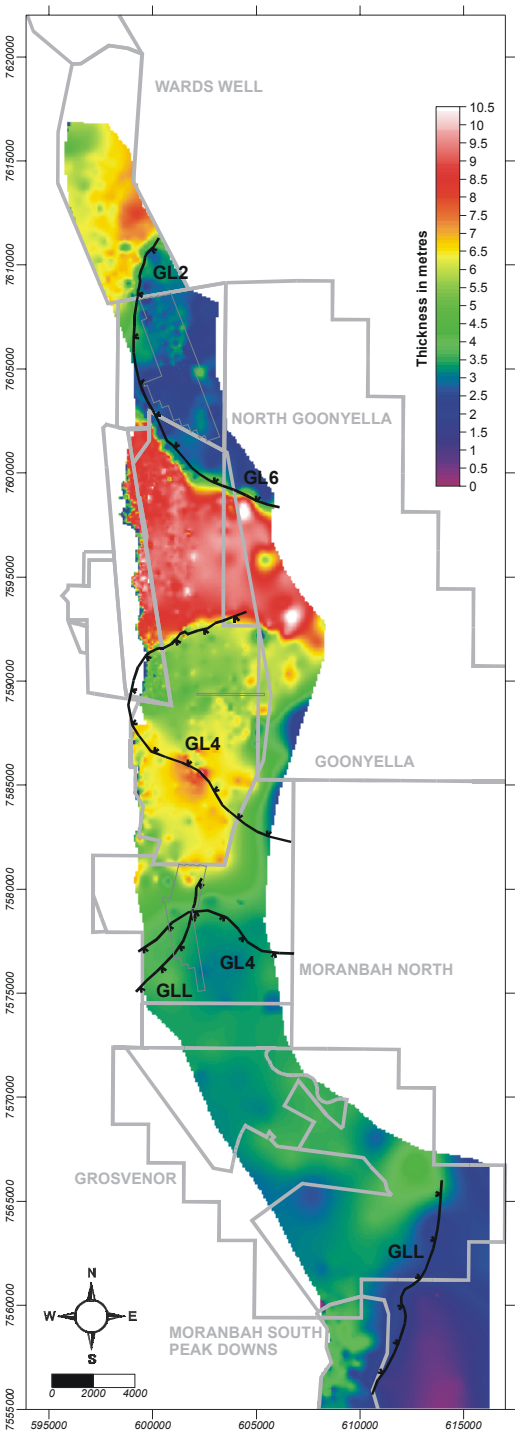

Figure 55 Goonyella Lower seam thickness overlain by split lines.

5.3.4 Goonyella Lower to Middle interburden thickness

The GL to GM interburden thickness varies from 15 to 150 m. The interburden is thinnest in the northern area where the GL and GM seams are thickest. Interburden thickness increases substantially to the south and includes a package of thick, stacked channel sandstones intercalated with the splits of the Dysart Lower and Harrow Creek Lower coal seams. The first influx of clastic sediment as manifested by the GL4 split is a large splay emanating from the east. Above the GL4 are a series of thin to thick sandstone units varying from lobate splays and sheet sandstones to channelized belts trending generally southward.

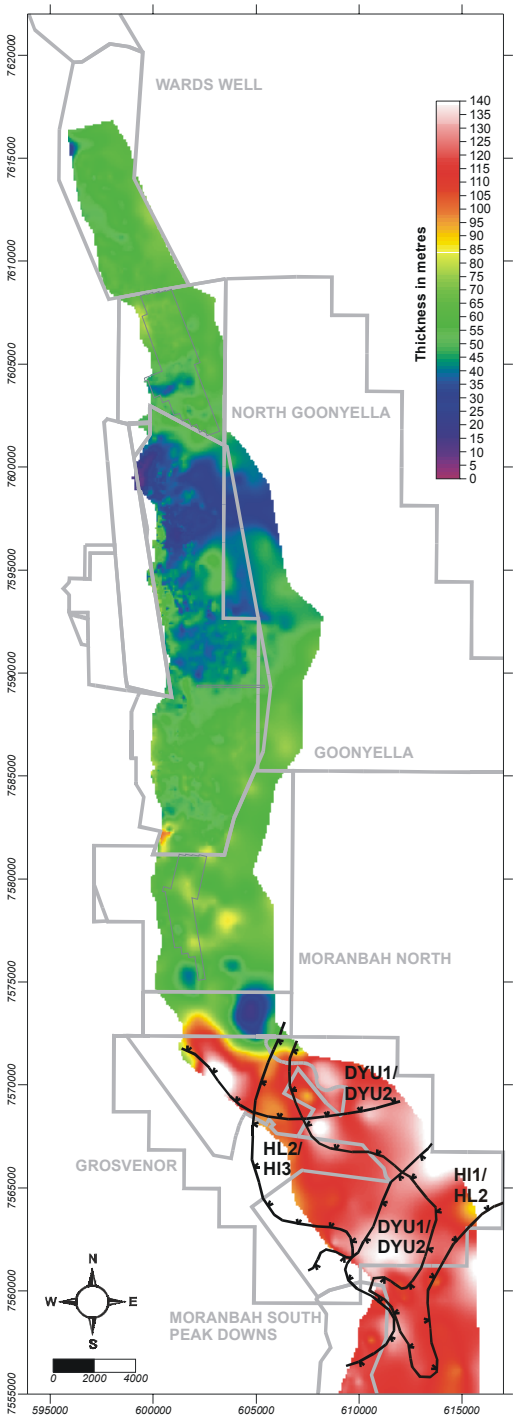

Figure 56 Goonyella Lower to Middle interburden thickness overlain by split lines.

5.3.5 Goonyella Middle seam thickness

The GM seam is thickest in the same location as the GL seam, forming a 12x14 km pod thicker than 8 m. The seam thins by splitting from the base and roof, as well as general tapering of middle plies. To the south, where subsidence is greatest, the main seam also splits. Split lines again generally exhibit a NE or NW orientation, although some radial splits occur. The Harrow Creek Lower seams (not included in GM seam) develop to the south and diverge upward from the GL and Dysart seams to join with Harrow Creek main seam in the Middle tile.

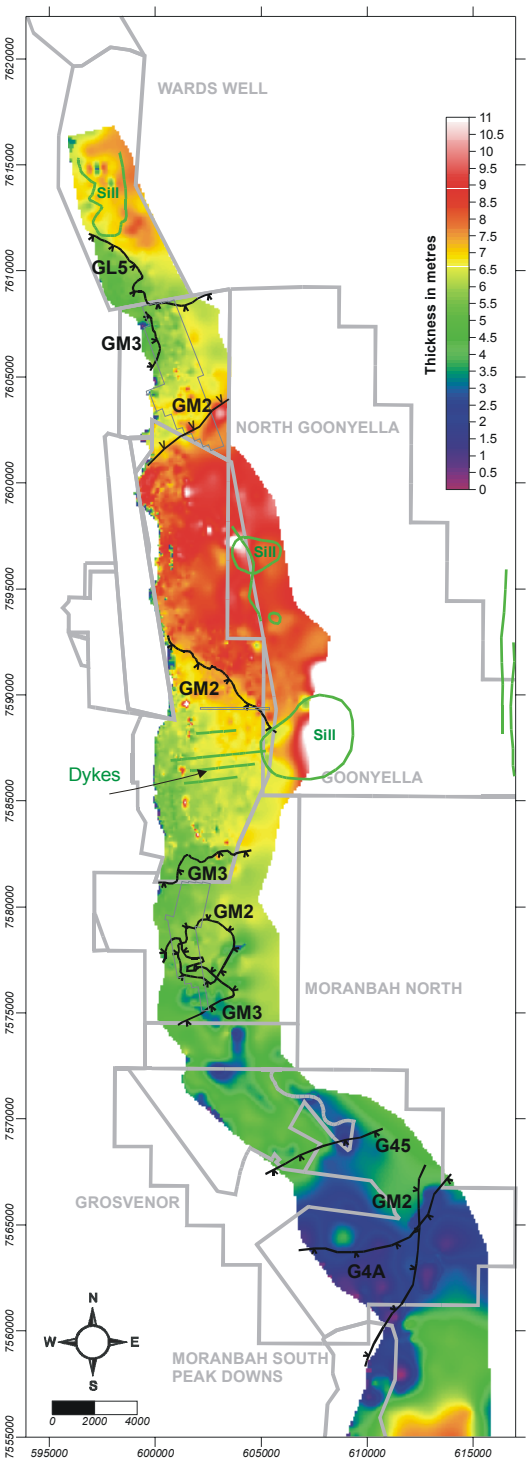

Figure 57 Goonyella Middle seam thickness overlain by split lines.

5.3.6 Goonyella Middle to P tuff interburden

The GM to P Tuff interburden thickness reflects a major southerly draining channel belt approximately 3-4 km wide and more than 25 km long. The system is compartmentalised by the seam splits. Where thick (>20 m), the interburden is generally dominated by sandstone units comprising stacked channel belts. Where thin (<10 m), the interburden is mudstone dominated and commonly contains fossilised tree stumps and abundant carbonaceous or coaly horizons. Convergences of the GM and P Tuff horizon ("peat islands") are spaced roughly 4 to 6 km apart in the study area and broadly define the margins of the local southerly striking channel system.

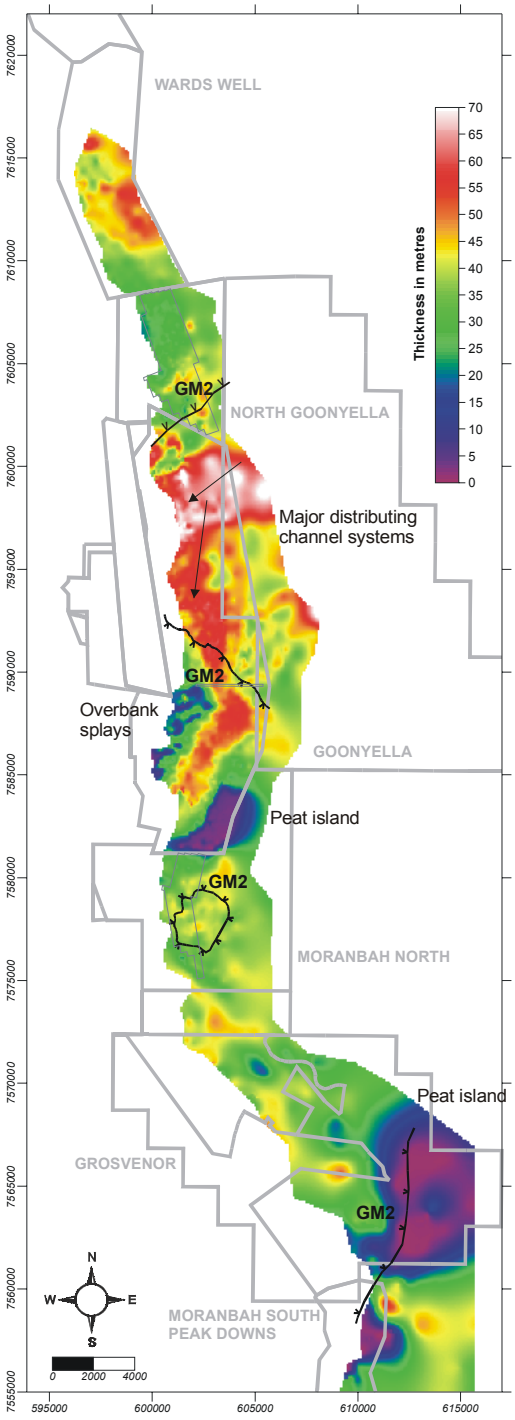

Figure 58 Goonyella Middle to P tuff interburden overlain by GM roof splits.

5.3.7 P tuff thickness

The P Tuff horizon consists of a 1 to 3 m thick fine- to coarse-grained tuff sandwiched between two thin (1-1.5 m) coal seams. In places it thickens up and defines final channel fills and lobes that mimic the distribution of the underlying sandstone channels. Where it is thin and clay-rich, the tuff is commonly root penetrated which suggests deposition in a relatively shallow but ponded floodplain.

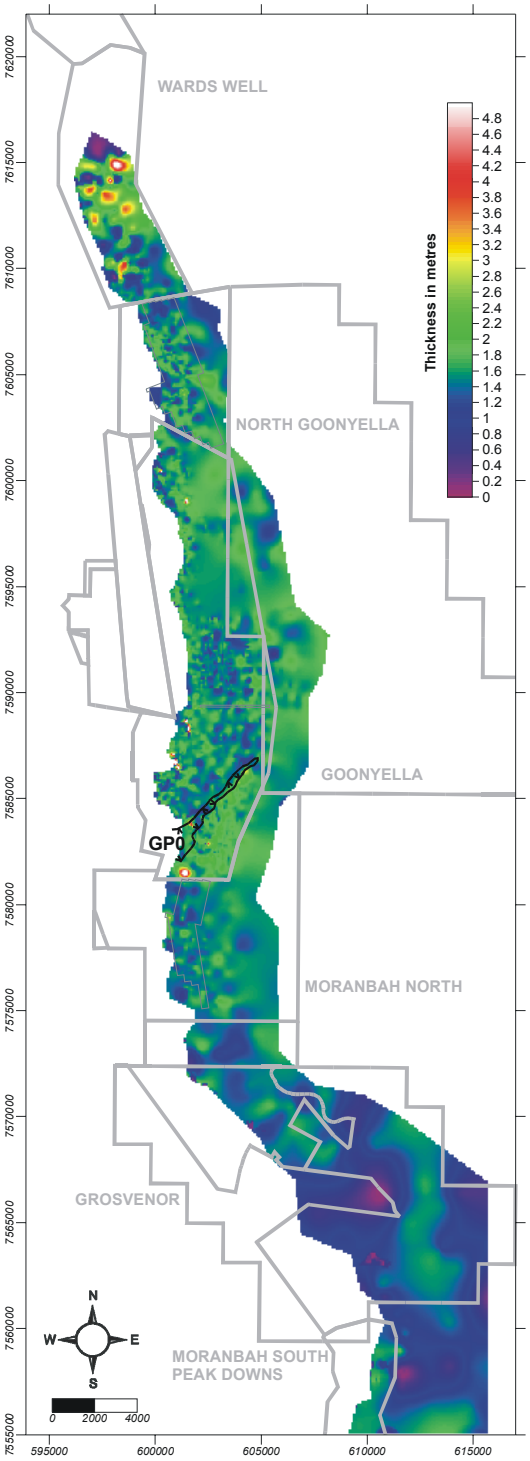

Figure 59 P tuff thickness.

5.3.8 P tuff to Goonyella Upper seam interburden

The thickness of this interburden is offset to that of the underlying GM to P Tuff interburden, except in the north at Wards Well. Rapid lateral variation is common (see cross section in Figure 51). The interburden between seams consist of thin sheet to lobate sandstones overlain by thicker channel belts fine upward into carbonaceous siltstones capped by the coal seams. In the Goonyella area, thick sandstones in this interval are offset relative to those of the underlying GM to P Tuff interburden. To the north and south, thick interburdens stack above those in the underlying interburdens to the GL seam.

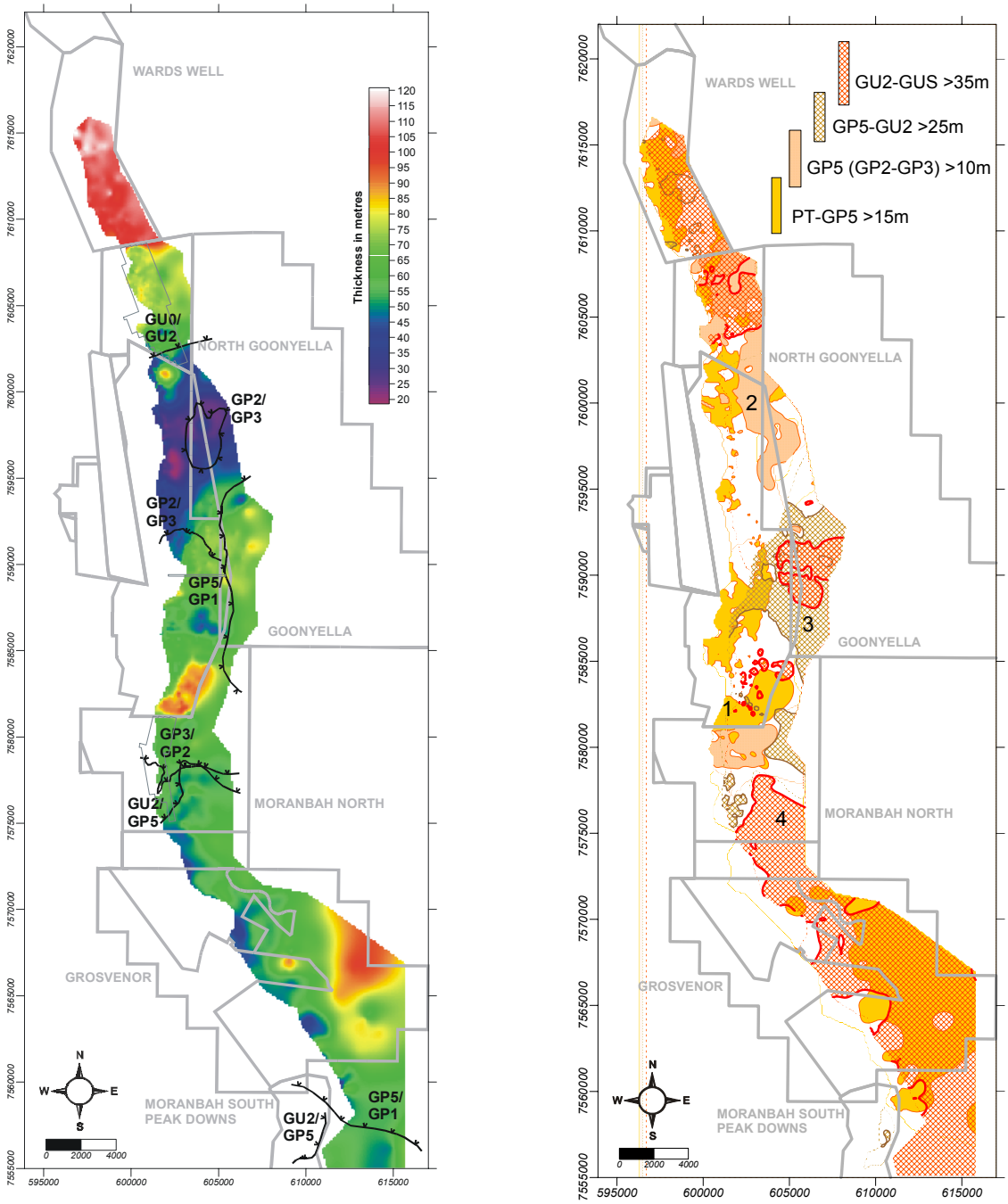

Figure 60 P tuff to Goonyella Upper seam interburden. A) isopach of interburden; B) sequential stacking of interburdens where thick. 1=lowest; 4=highest interburden.

5.3.9 Goonyella Upper seam thickness

The GU seam follows the thickness distribution patterns observed in the GL and GM seams and forms a thick pod in the same area. This pod is thinner than those of the other seams, up to 7 m. The lower split of the GU seam merges with the P seams to the south.

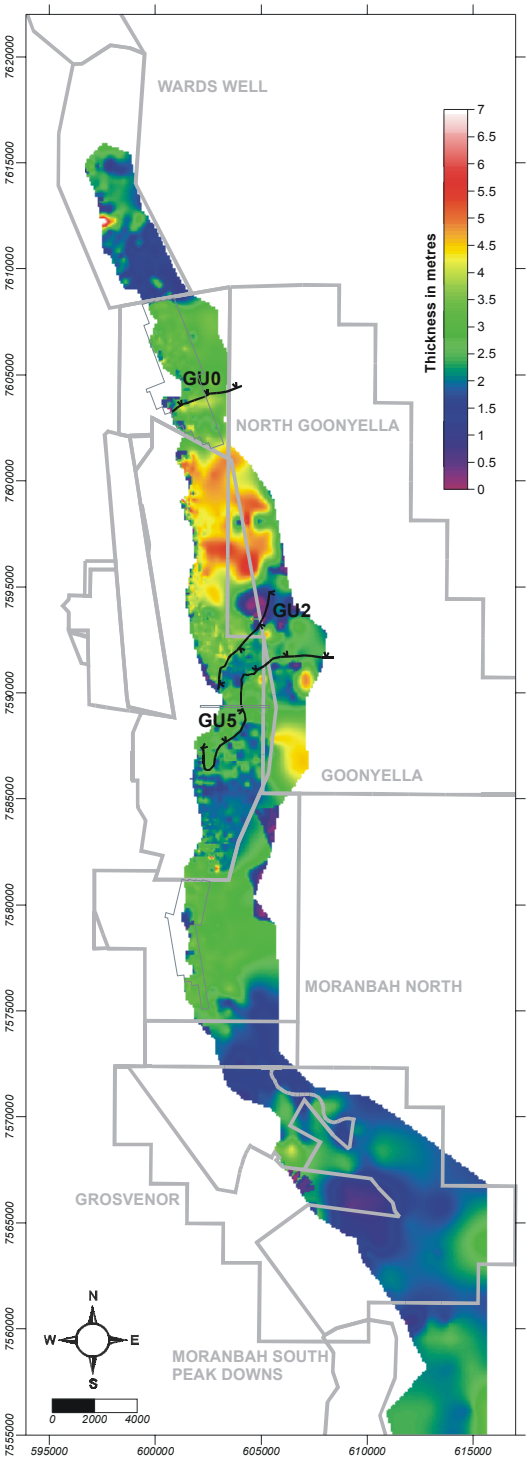

Figure 61 Goonyella Upper seam thickness overlain by split lines.

5.3.10 Facies distribution GM to P tuff

A 'roof zone' map was constructed for the stratigraphic interval most likely to participate in goafing or overburden blasting for the Goonyella Middle seam currently mined in this tile. Vertical sequences in sandstone distribution were interpreted from borehole geophysics and qualitatively grouped into one of six zones shown on the map. When overlain by interpreted fault systems, the zone map can be used to determine domains of similar roof conditions and potentially hazardous conditions.

Although sandstones occur throughout the Permian sequence, the thickest (60 m) and most widespread units (2 to 3 km wide and more than 25 km long) occur in the GM to P Tuff interburden. They are predominant in the area overlying thick GL and GM seams in the Goonyella Riverside lease. The thick, amalgamated sandstones (Zones A and B) occur in S to SW oriented belts that represent a prolonged depocentre of channelized flow.

Thick sandstones also occur over the Moranbah North lease but exhibit a different distribution. Here they are oriented west and southwestward, emanating as narrow channels that splay westward and distribute into smaller lobes or channels. Another set of thick sandstones occurs over the Grosvenor lease, but data are too sparse for patterning.

The thick channels taper rapidly into the adjacent fine-grained facies of Zones D to F and minor channels and splays occur in D. To the north of Goonyella Riverside the GM to P Tuff interval stays consistently thick (30 to 45 m), but is dominated by weaker siltstones and mudstones facies with minor sandstone channels. This facies is dominant over North Goonyella whereas minor channels occur in Ward's Well.

In the south of Goonyella Riverside, the GM to P Tuff interval undulates and the channel sandstones circumnavigate an "island" of slow deposition and low subsidence where the P Tuff occurs within 10 m of the GM seam. The P Tuff actually merges with the GM seam in the southeast of Grosvenor. These islands define the margins of the major channel system and overly areas of stacked channel sequences occurring within the splits of the GL seam.

During deformation these more competent sandstones acted as impediments to the upward migration of thrust faults. As a result, the faulting is more common on the margins of sandstone channels. This relationship provides a predictive, albeit empirical model for the prediction of faulted ground where data are dense enough to define channel geometries, but too sparse to adequately assess faulting.

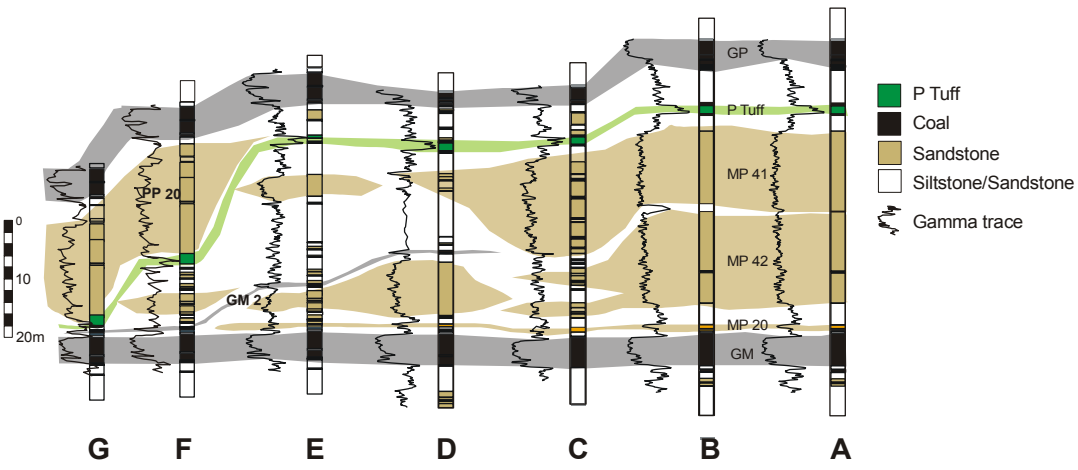

Figure 62 Facies definition for map shown in Figure 63.

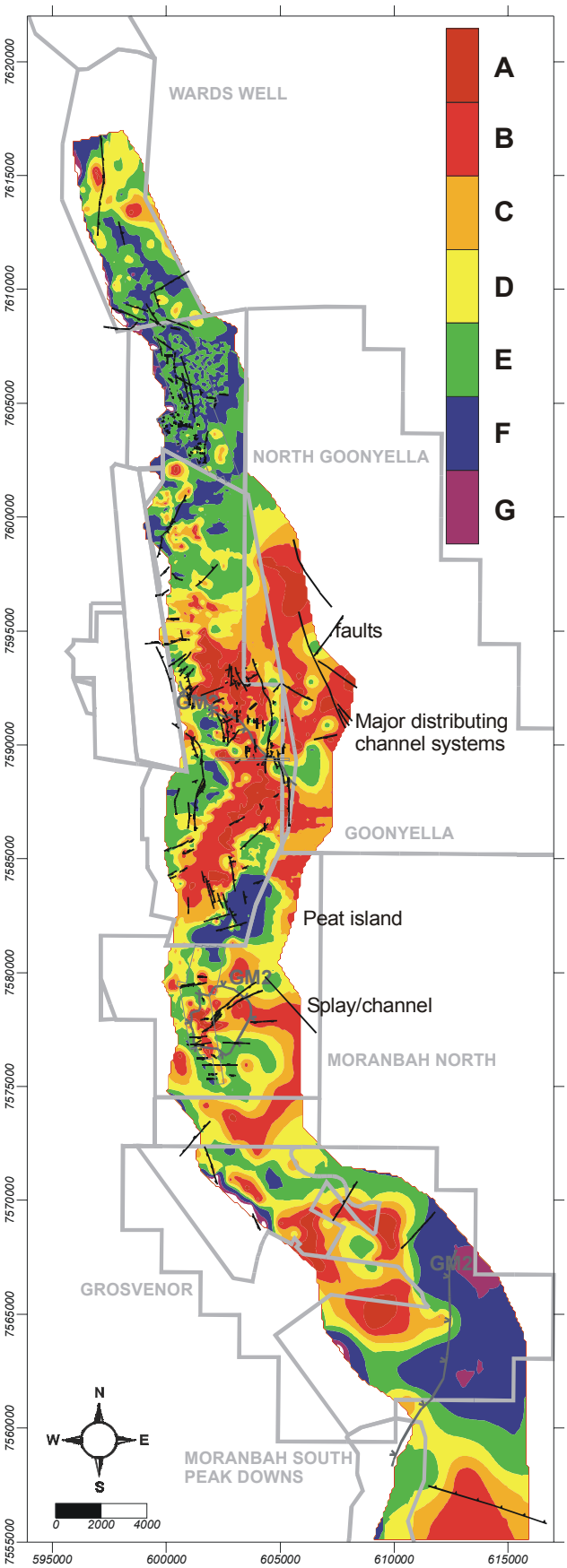

Figure 63 Facies distribution between GM and P tuff in the Northern Tile.

5.3.11 Sediment accumulation relative to basement

The thickest accumulation of sediments and coal between the GL and GU seams is associated with gravity lows suggesting sustained subsidence on the margins of a basement platform. Fewer, but thicker coal seams within the GL to GU sequence are associated with the gravity high suggesting that a relatively stable basement platform extended throughout deposition of the coal measures. The number of seams increases as the main seams split off the margins of the platform.

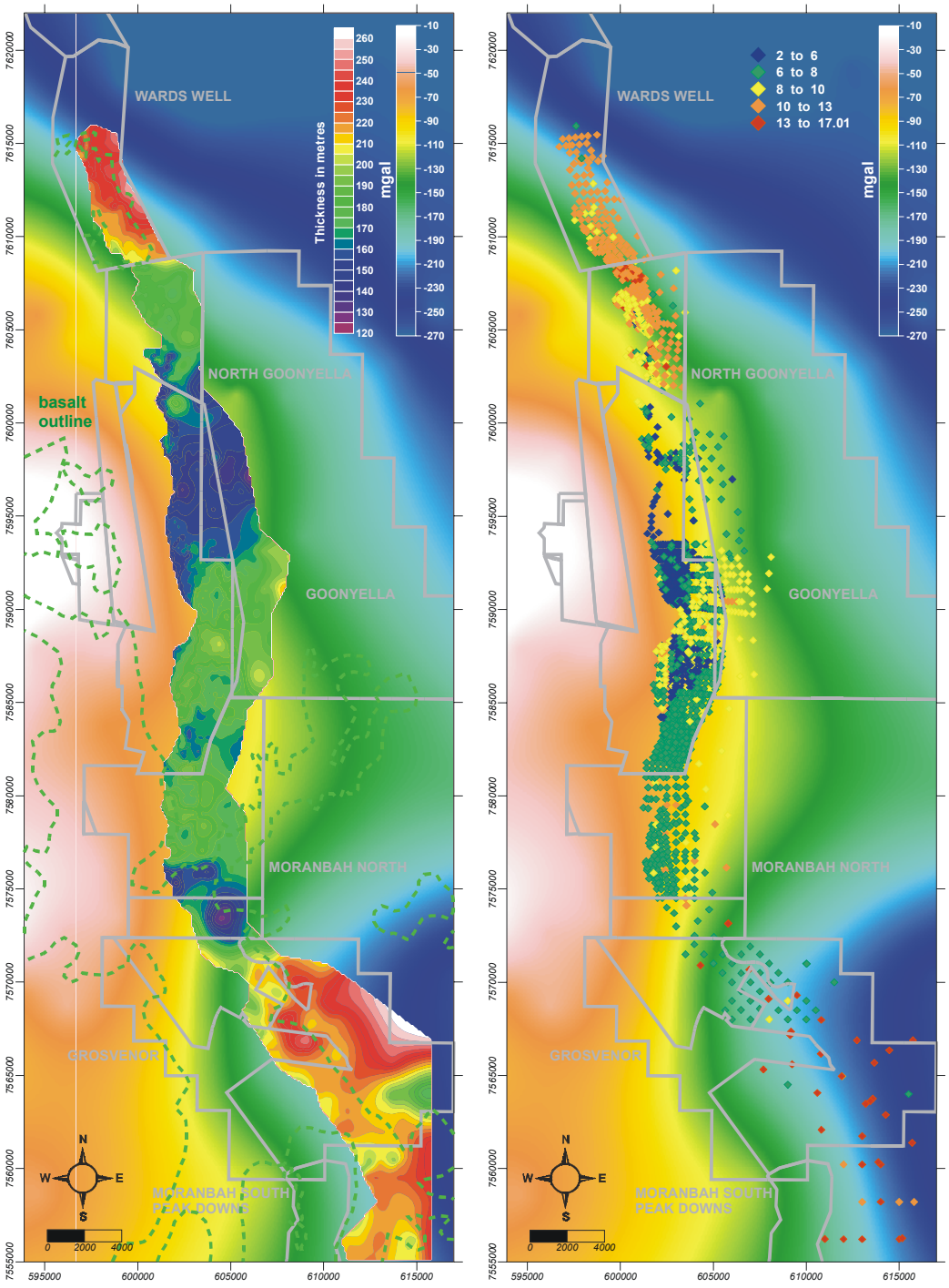

Figure 64 Cumulative thickness and number of coal seams shown relative to regional Bouguer gravity

Present day GM seam floor structure contours tighten around the margin of the basement high, suggesting that the basement block also created an impasse to later folding of the coal measures. Face cleat also swings from NW to SW coinciding with the crest of the regional antiform, as well as the basement platform.

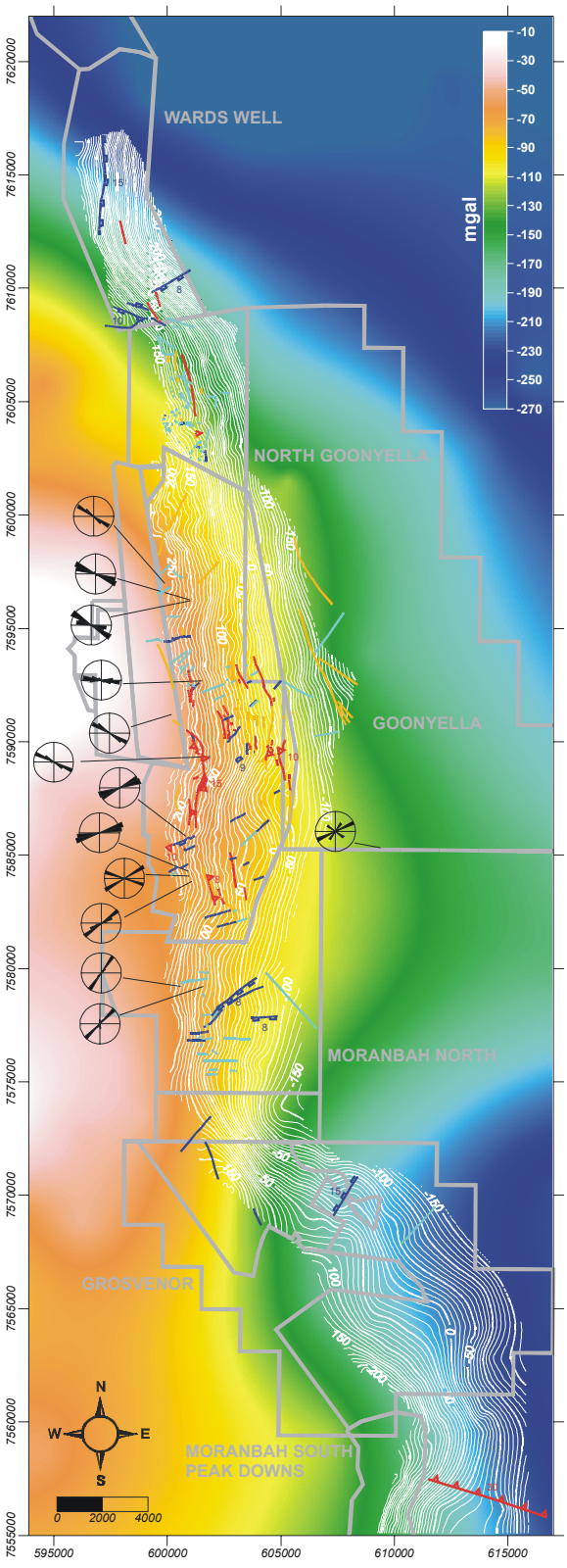

Figure 65 Structure of GM seam and structure relative to regional Bouguer gravity.

5.3.12 Summary discussion of Northern Tile

The thick amalgamated sandstone channel complexes (Zones A and B on zone map) in the GM to P Tuff interval tend to occur within broad synforms on the crest of the regional anticline. This is most evident at Goonyella Riverside and Moranbah North. Above this stratigraphic interval, sandstones are thinner and more widespread throughout up to the GU seam. Sparse drilling above this sequence suggests that another series of thick amalgamated sandstones occurs above the GU seam in this area.

During the deposition of the Moranbah CM, major volumes of sediment were supplied from the north and northeast, forming a series of coal-capped alluvial sequences (Fielding et al, 2000). The thickest and merged coal seams occur in an area interpreted as relatively stable during deposition and are flanked by significant splitting associated with the margins of a basement platform observed in the gravity image. Seam splitting occurs when the site of peat accumulation is inundated by sediment-laden water and, after sediments are deposited, peat mires reoccupy the site. As a result, the sites of maximum peat accumulation are delicately balanced between areas that are topographically "high" and those that are topographically "low", and hence easily inundated. Prolonged and repeated subsidence is interpreted in the areas of the gravity lows, resulting in more complex splitting and interfingering with channel sandstones, particularly in the GL seam. The above scenario is applicable to the GL and GM seam sequence, but a different mechanism may have controlled subsidence for deposition of the very thick, amalgamated channel system that occurs in the roof of the GM seam. Here the few hundred metres of peat and mud (allowing for a 10:1 compaction ratio from peat to coal and 7:1 to mudstone) began to compact relative to the flanking channel sands, creating accommodation for the progressive avulsion of the channel depocentre across the platform.

Hence, the palaeotopography that controlled the juxtaposition of thick coals and thick sandstones was influenced locally by differential compaction, but in the long term by differential subsidence across these basement blocks. Subsidence would be lower over stable basement blocks, creating the platform for the repeated accumulation of thick peats. Subsidence would be higher, or exhibit sporadic changes in rate on unstable flanks, resulting in vertical stacking of thin coals and thicker sandstones throughout the Permian.

During the Triassic, the Hunter-Bowen Orogeny resulted in a major NE-SW shortening event. Although the most significant deformation occurred on the eastern margin of the southern Bowen Basin, comparatively smaller thrusts propagated to the west throughout the northern basin. These include the Jellinbah Thrust system that bounds the eastern margin of the study area and many of the smaller (1 to 10 m displacement) thrusts mapped within the coal mines. Although there is an association of smaller thrusts propagating through the sequence around the more massive sandstone channels, the deep and large-scale control on these structures suggests that their position is more likely controlled by older basement structures.

It is also suggested that hinge zones around this basement block were reactivated during Cretaceous uplift and erosion. Areas of deepest incision and subsequent Tertiary infill, in particular by basalt, occur in NE and SE trending valleys that parallel the hinge zones.

5.4 Middle Tile

The model for the Middle Tile also demonstrates the relationships between the distribution of thick coal seams, seam splitting, thick sandstone-dominated interburdens and basement fabric.

The lower seams of the Moranbah CM are exposed and mined in the Middle tile. Here the lowest Dysart seams are the stratigraphic equivalents of the Goonyella Lower seam to the north and the German Creek seam to the south (Figure 66). The Harrow Creek seams are equivalent to the Goonyella Middle seam and split to the south to form the Aquila and Tieri seams. The P Tuff is mapped sporadically within the P seams, although it continues to the south within the equivalent Pleiades seams. The Goonyella Upper seam is no longer mapped as such, and from our interpretation it is often coded as Q seam at mine sites in the Middle Tile. However, the upper R and S seams are correlative and continue southward until they pinch out towards the MacMillan Fm that is the transgressive marine sequence.

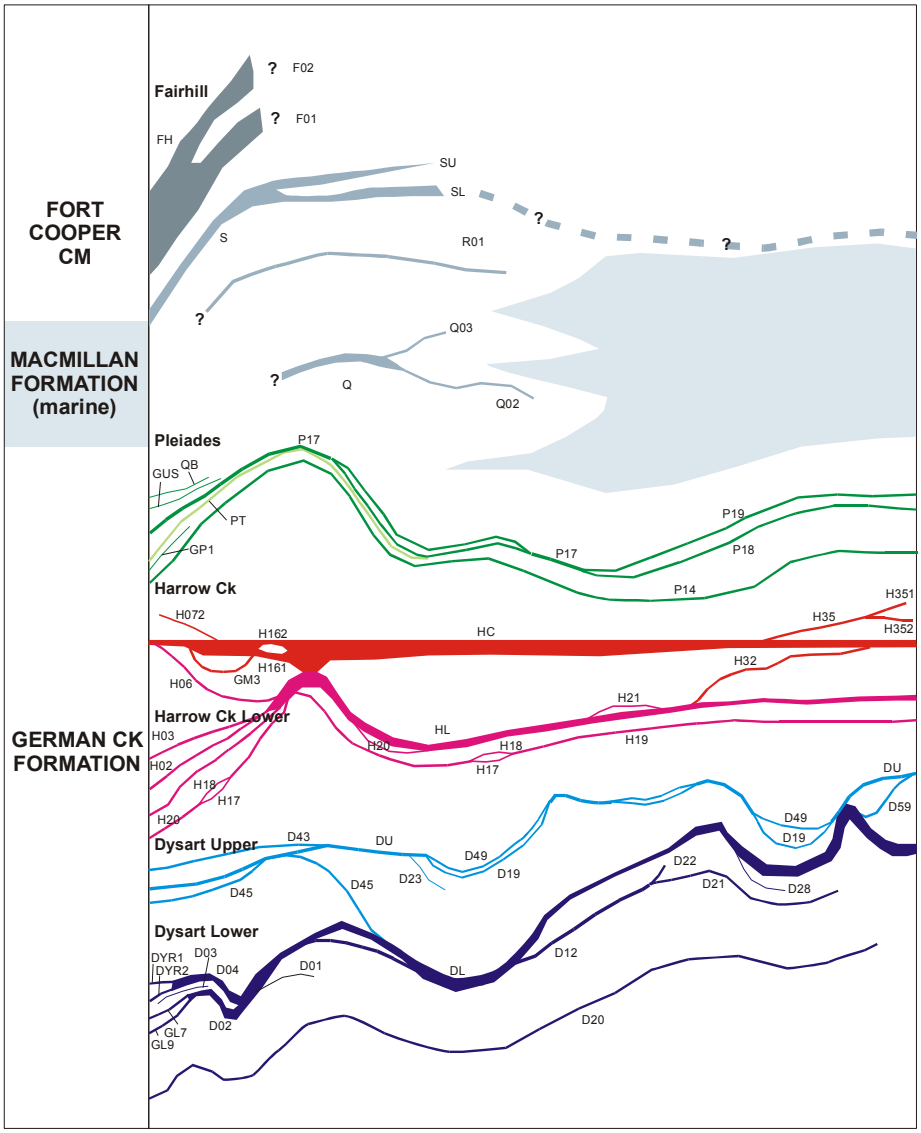

Figure 66 Schematic correlation of coal seams in the Middle Tile.

All seams dip eastward, varying from around 4 to 6 degrees, but are steeper locally in faulted areas. As observed in the coal seam isopach maps, the split lines trend both easterly and southerly, defining either narrow straight channels or broad and sinuous channels that encroach over terminated peat deposits. The latter tend to trend southerly. Faulting in the Middle Tile is dominated by normal faults that trend either NE or SE. Thrust faults occur in the Peak Downs and Saraji areas, often associated with thicker sandstone channels in the interburden.

The north-south cross section and structure map (Figure 67) of the Middle Tile model demonstrate the regional and local variability in coal seam thickness, interburden distribution and deformation in the Permian coal measures. The graph above the section shows profiles for the regional gravity and DL to P17 cumulative coal and interburden thickness. The section demonstrates the lateral continuity of the main mineable seams, the Dysart Lower seam and Upper seam, and the Harrow Creek seam where it forms a thick unsplit pod. Splitting patterns are most complex in the north where the cumulative thickness of the coal measures is thick, but simplify to the south where the coal measures thin towards the palaeo-shoreline.

Local folding occurs with wavelength of 4 to 6 km, with north-northeast trending fold axes. The eastern limbs of the folds are commonly faulted by either normal or thrust faults. Outcrop-scale folding and faulting occurs within the individual seams. Distribution of these features is controlled by underlying larger structures and the presence of thick sandstone units in the interburden of the coal measures.

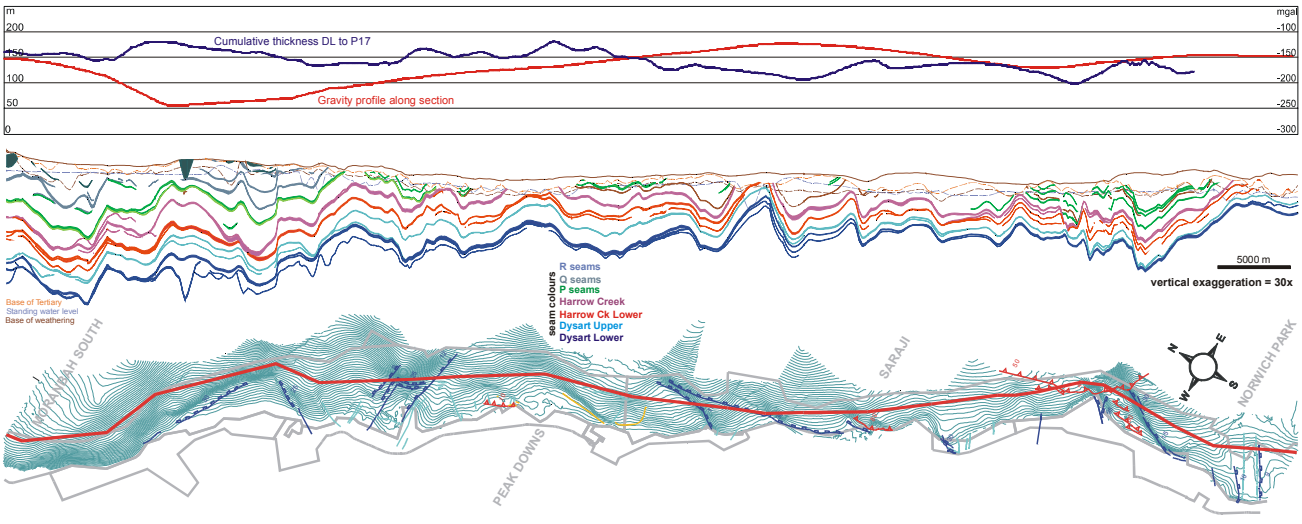

Figure 67 Coal seam structure of Middle Tile.

5.4.1 Topography and infrastructure

Three extensive open cut mines, Peak Downs, Saraji and Norwich Park, operate in the Middle Tile. A trial underground mine operated in the Harrow Creek seam at Peak Downs in the 1980's and down-dip exploration drilling has been conducted at all three mines. The topographic map shows the general decrease in surface elevation towards the south.

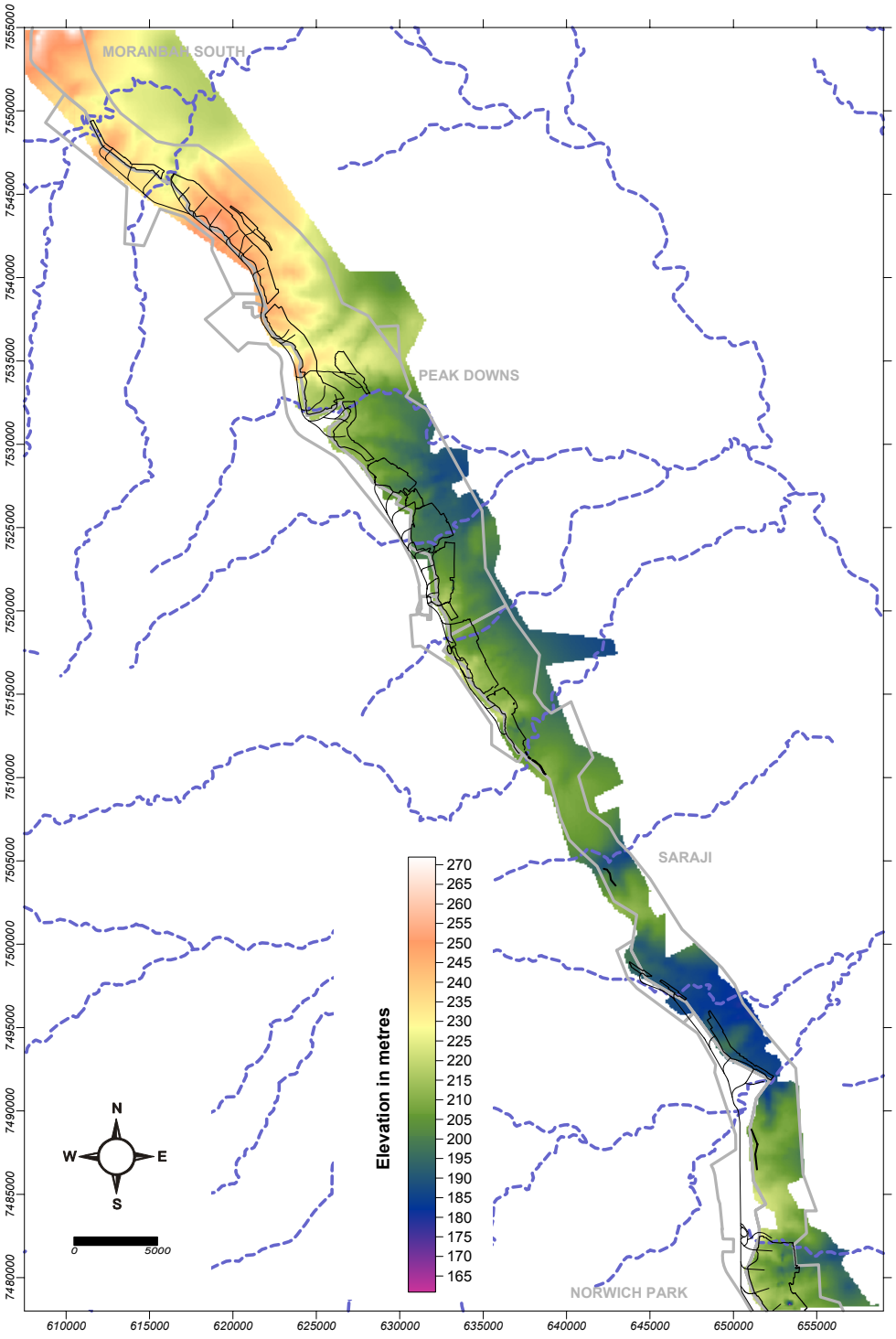

Figure 68 Topography and infrastructure (legend as in Figure 53).

5.4.2 Base of Tertiary

The elevation of the Tertiary unconformity mimics the present day topography, highlighting the longevity of this basic topography. Unlike in the northern and Southern Tiles, the Tertiary is thin (<30-50 m) and free of basalts. There are, however, abundant sills within the coal seams, especially in the southern half of the area.

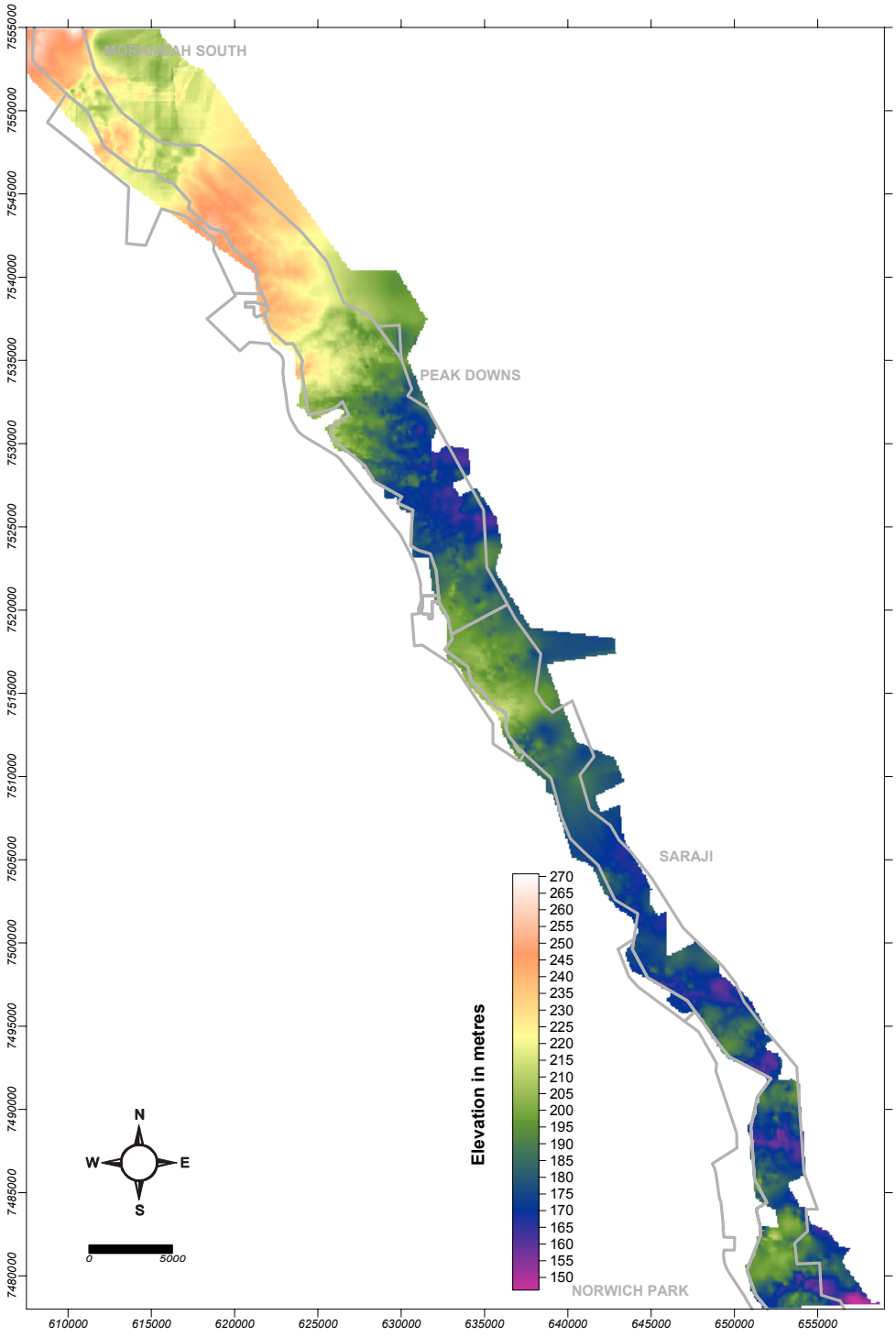

Figure 69 Base of Tertiary.

5.4.3 Dysart Lower seam thickness

The Dysart Lower seam (DL) is the thickest and most extensively mined seam in the Middle Tile. The Goonyella Lower splits and the Dysart rider seams from the Northern Tile merge in the Middle Tile. Splitting patterns reveal small to large-scale channel systems oriented easterly (narrow straight belts) or southerly (broadly sinuous belts). Thick (>5 m), non-split pods of coal around 10x5 km in area occur on each lease, spaced approximately 10-15 km apart. The seam contains abundant intrusions in the south.

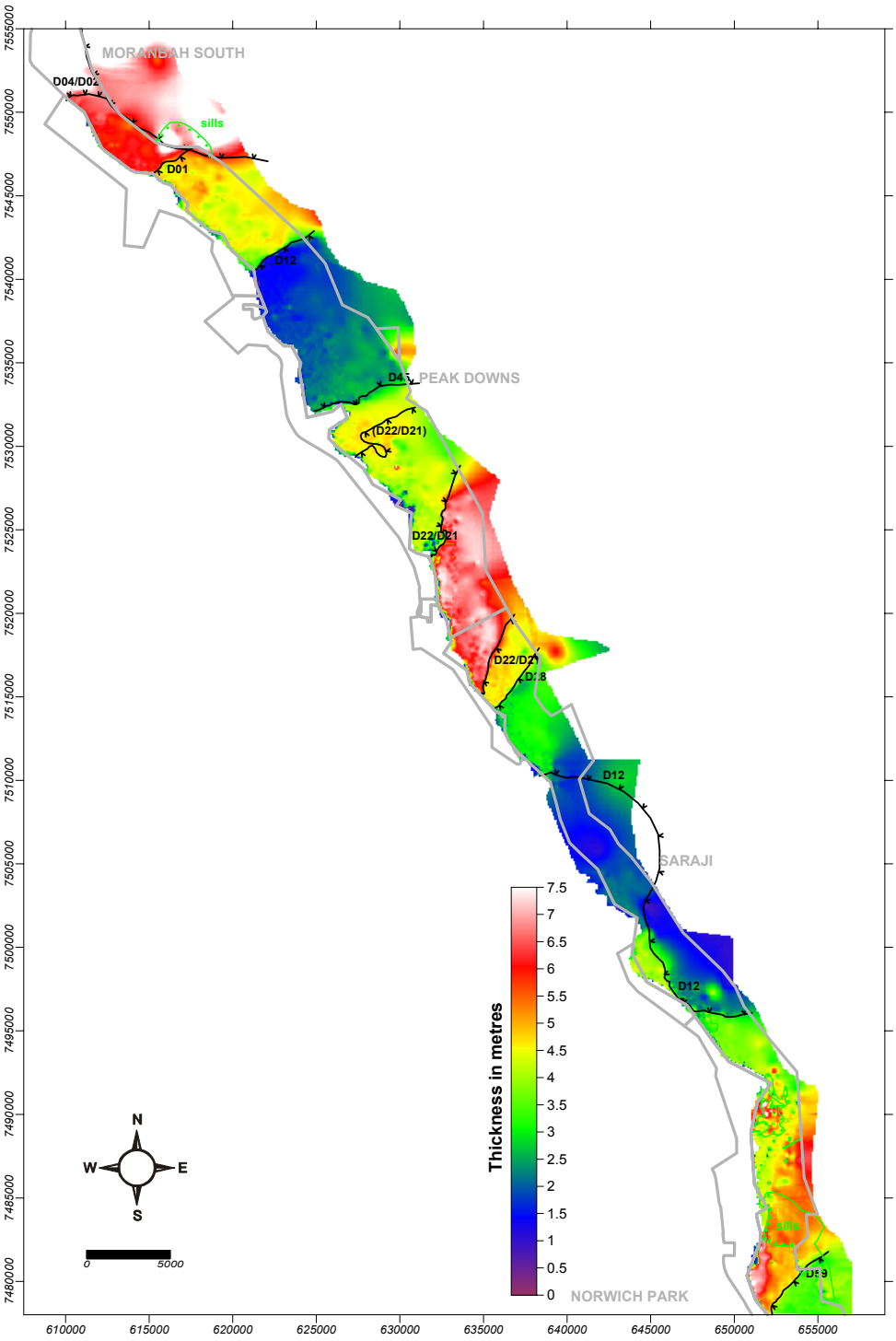

Figure 70 Dysart lower seam thickness overlain by split lines.

5.4.4 Dysart Lower to Dysart Upper interburden thickness

The DL to Dysart Upper seam (DU) interburden thins generally southward from >40 m to <16 m. Where thick, the interburden is sandstone dominated but may contain a series of thinner coal seams. The seam splits exhibit a pattern known as "Z splitting" where a floor split from an upper seam (DU split D45) merges with the roof of a lower seam (DL). This offset is best observed in the cross section in Figure 66. Thesis mapping in this interval at Norwich Park mine identified lagoonal and distributary channel/amalgamated mouth bar facies (Hill, 2000; Ronan, 2000).

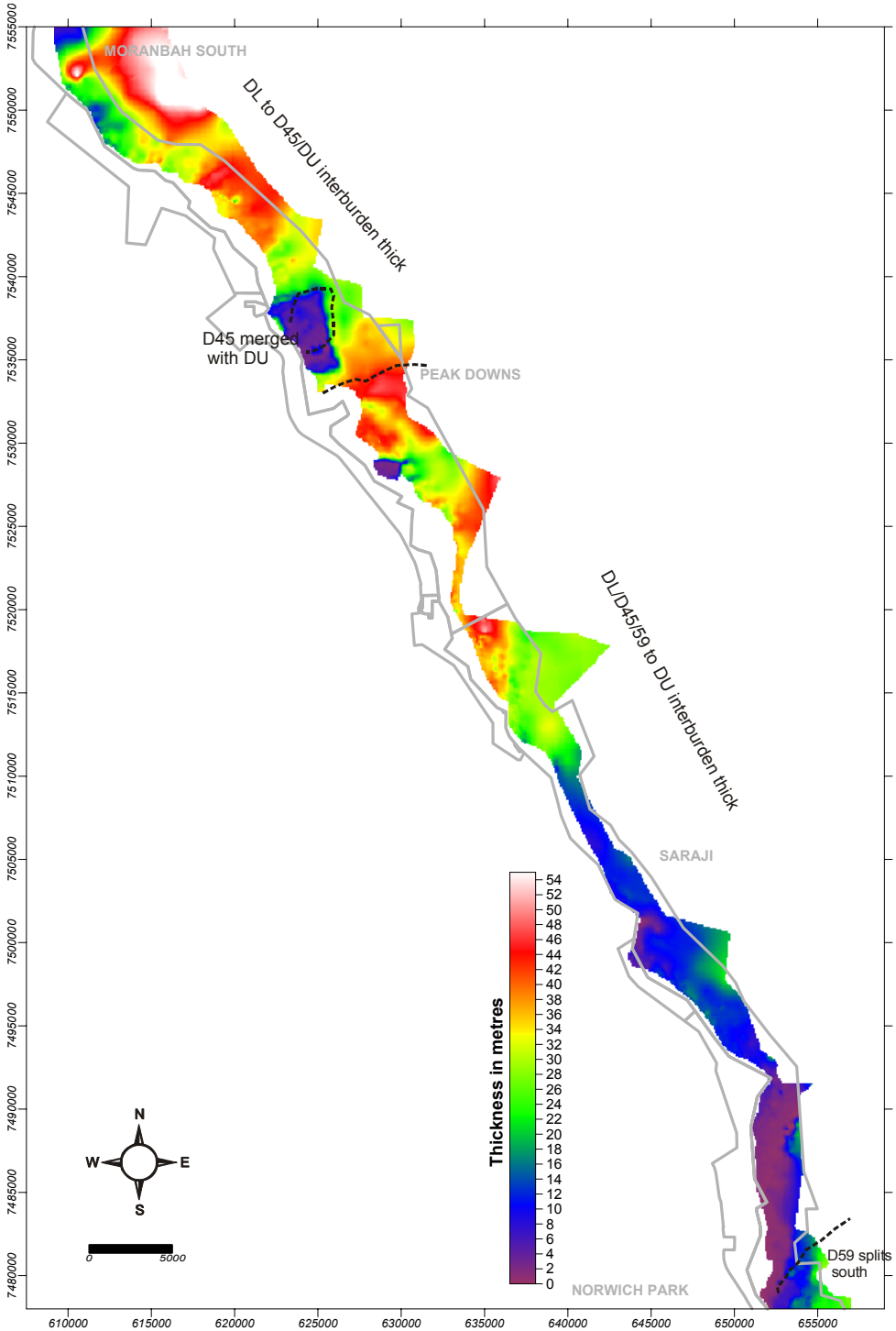

Figure 71 Dysart Lower to Dysart Upper interburden thickness

5.4.5 Dysart Upper seam thickness

The DU is thinner than the DL, reaching thicknesses >3 m in restricted areas. Seam splits reflect narrow east-west or southwest trending channels occurring mid-seam. The seam contains abundant intrusions in the south.

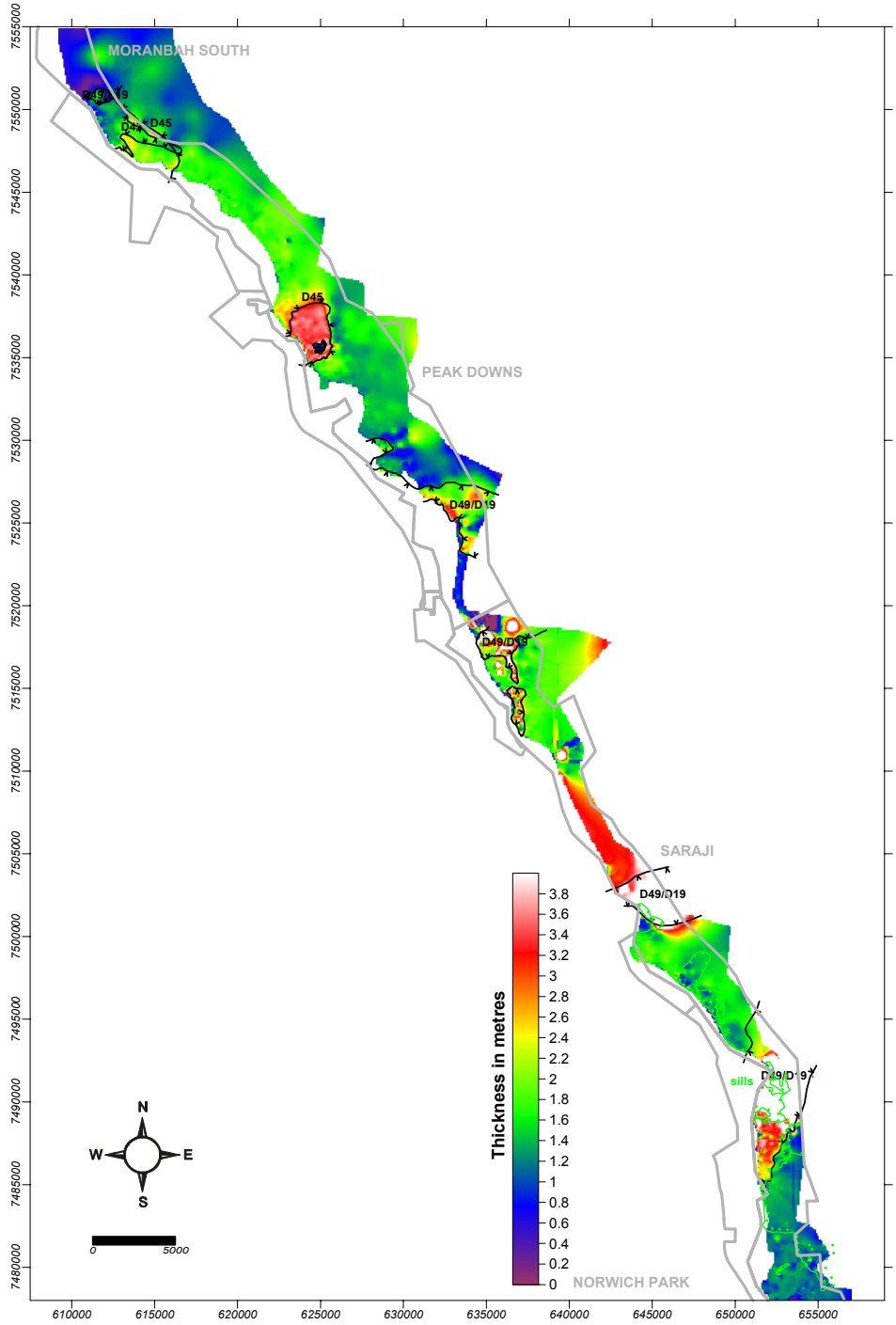

Figure 72 Dysart Upper seam thickness overlain by split lines.

5.4.6 Dysart Upper to Harrow Creek Lower seam interburden

The DU to Harrow Creek Lower seam (HL) interburden varies from <20 m to 60 m thick. Where it is thick it reflects a broadly sinuous, southerly trending channel belt system. A narrow channel belt occurs in this interval in the Norwich Park mine.

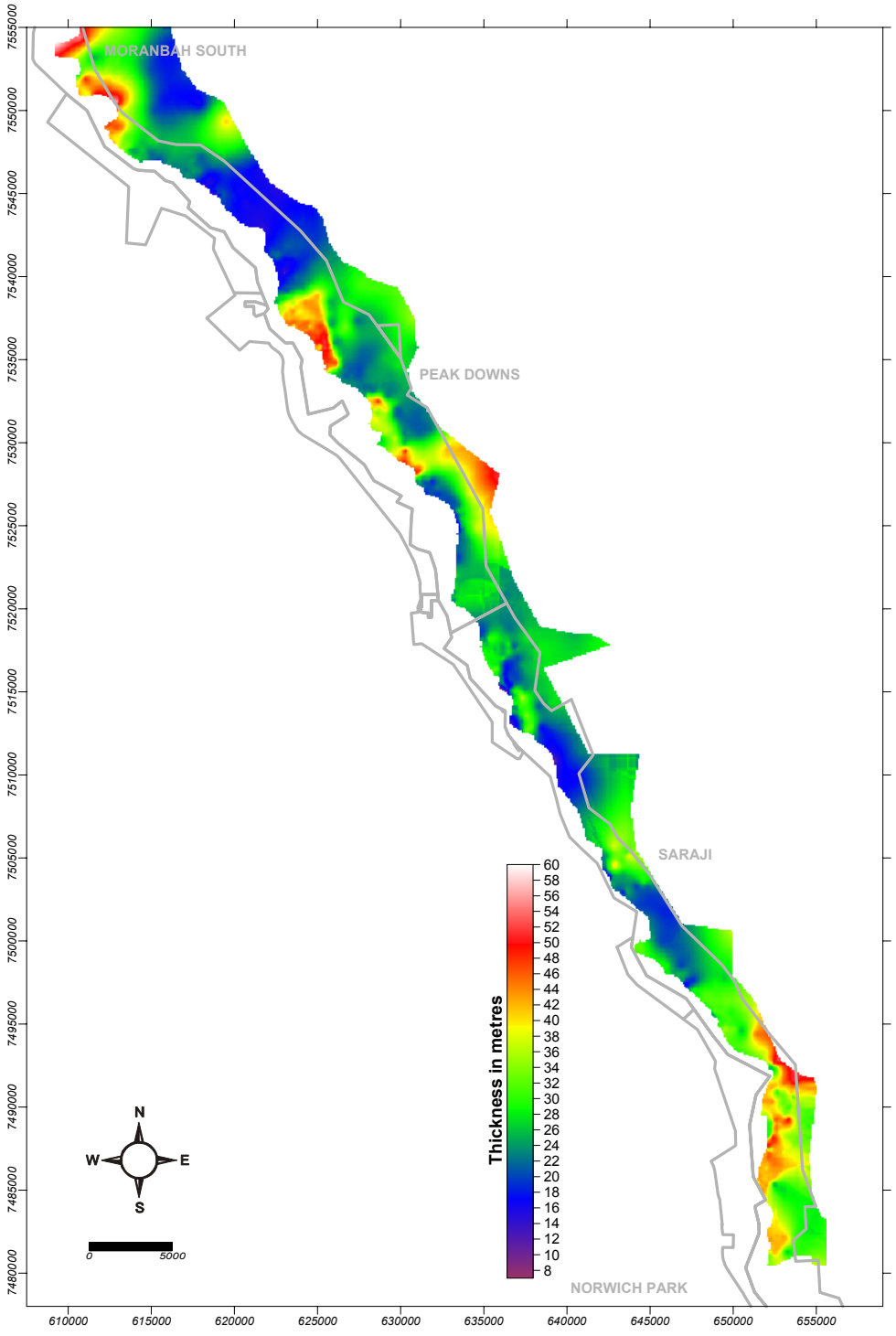

Figure 73 Dysart Upper to Harrow Creek Lower seam interburden

5.4.7 Harrow Creek Lower seam thickness

The HL is thickest in the north and thins to <2 m to the south where it merges with the Tieri seams of the Southern Tile (German Creek Formation).

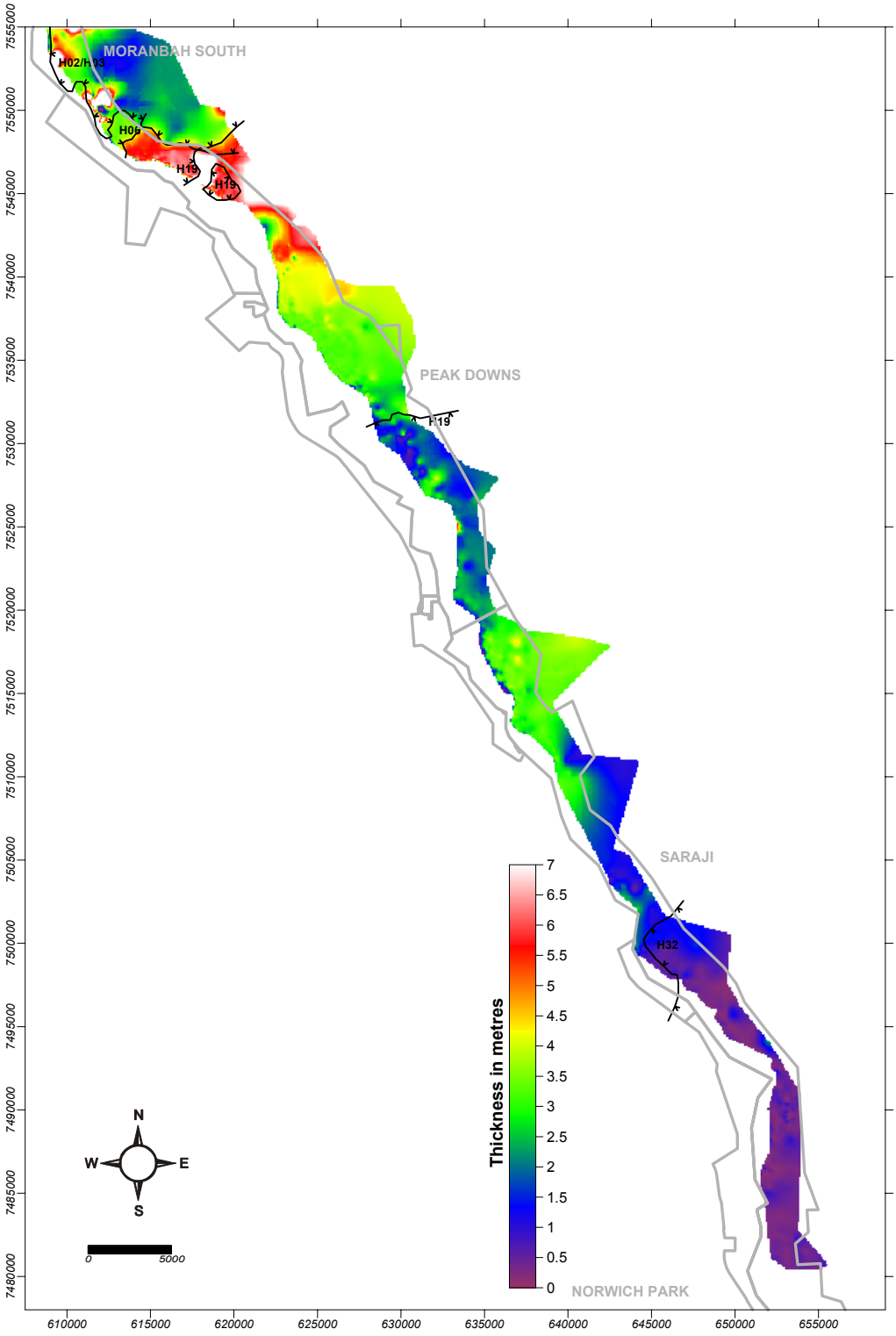

Figure 74 Harrow Creek Lower seam thickness

5.4.8 Harrow Creek Lower to Harrow Creek (upper) seam interburden

The HL to Harrow Creek seam (HC) interburden is controlled by splitting patterns in the HL. The thickest interburden (>40 m) occurs in the northern end of the tile. Offset stacking and "Z" splitting in seams is also common. The sequence thins substantially towards the Southern Tile as palaeo-conditions stabilized towards the coastal plain.

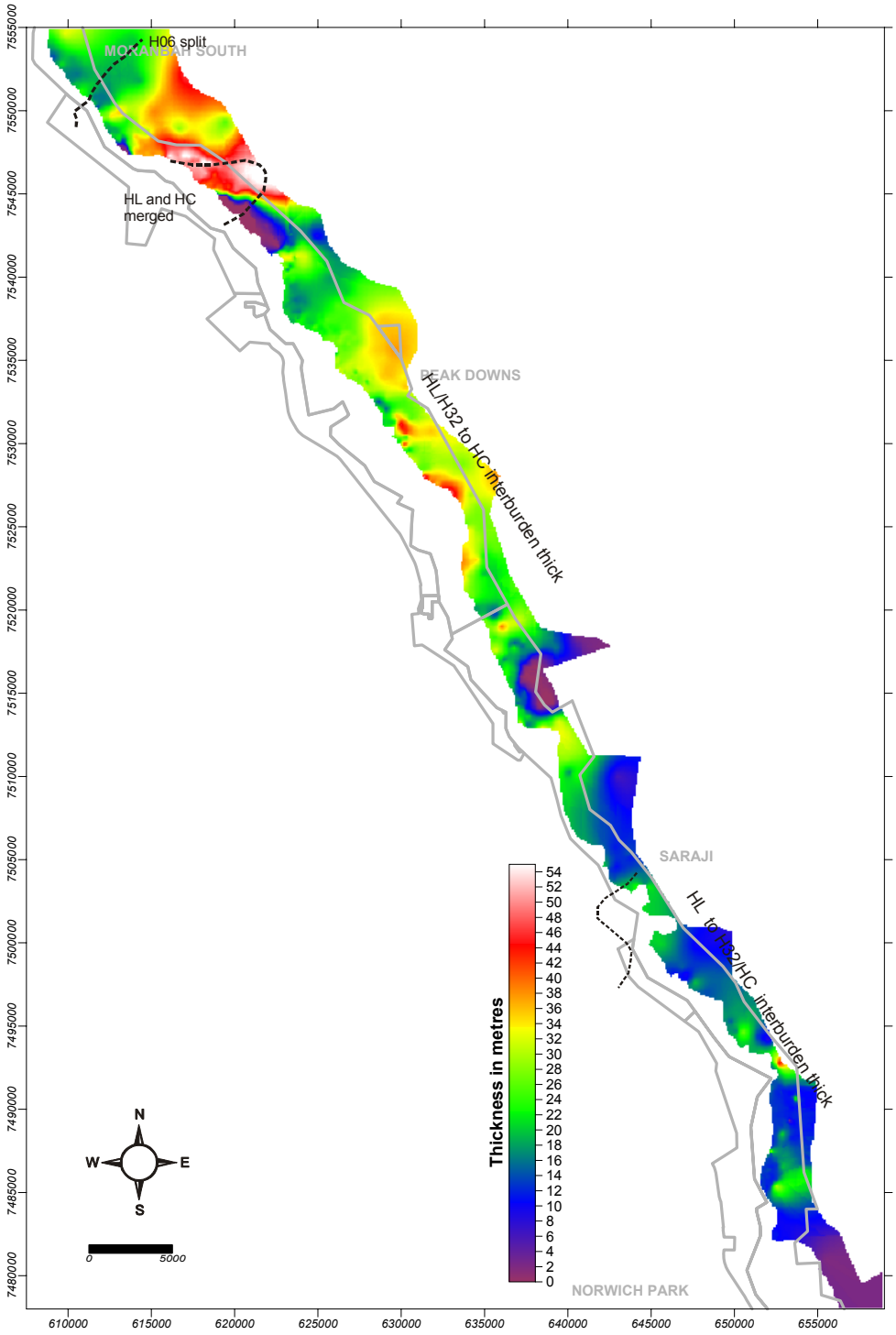

Figure 75 Harrow Creek Lower to Harrow Creek (upper) seam interburden overlain by split lines.

5.4.9 Harrow Creek (upper) seam thickness

The main Harrow Creek seam splits to the north and south. Where merged it is >10 m thick and forms a pod in the same geographic location where underlying DU and DL are thick. To the south, the seam thins and merges into the Aquila seams that are stratigraphically part of the German Creek Formation. The seam is intruded in the southern leases.

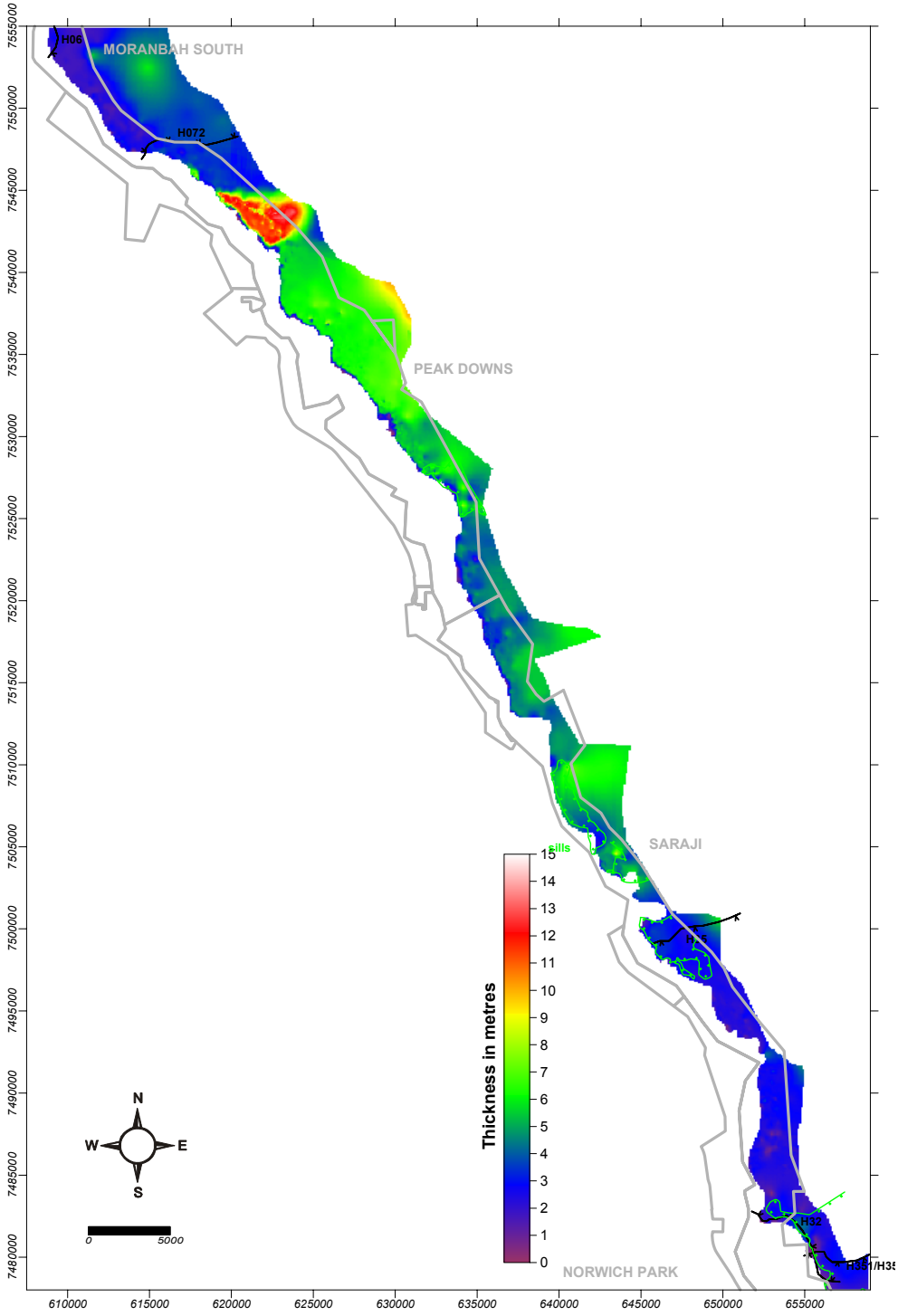

Figure 76 Harrow Creek (upper) seam thickness.

5.4.10 Harrow Creek to P seam (P17) seam interburden

This interburden is relatively thick, >30 m, across the Middle Tile, but it does contain some thicker (>50 m) that contain channelized sandstone units. Data were sparse to properly characterize this interval but high wall mapping by Falkner and Fielding (1993) suggest easterly to southerly trending channel systems that are a continuation of the major belts observed in the GM to P Tuff interval in the Northern Tile.

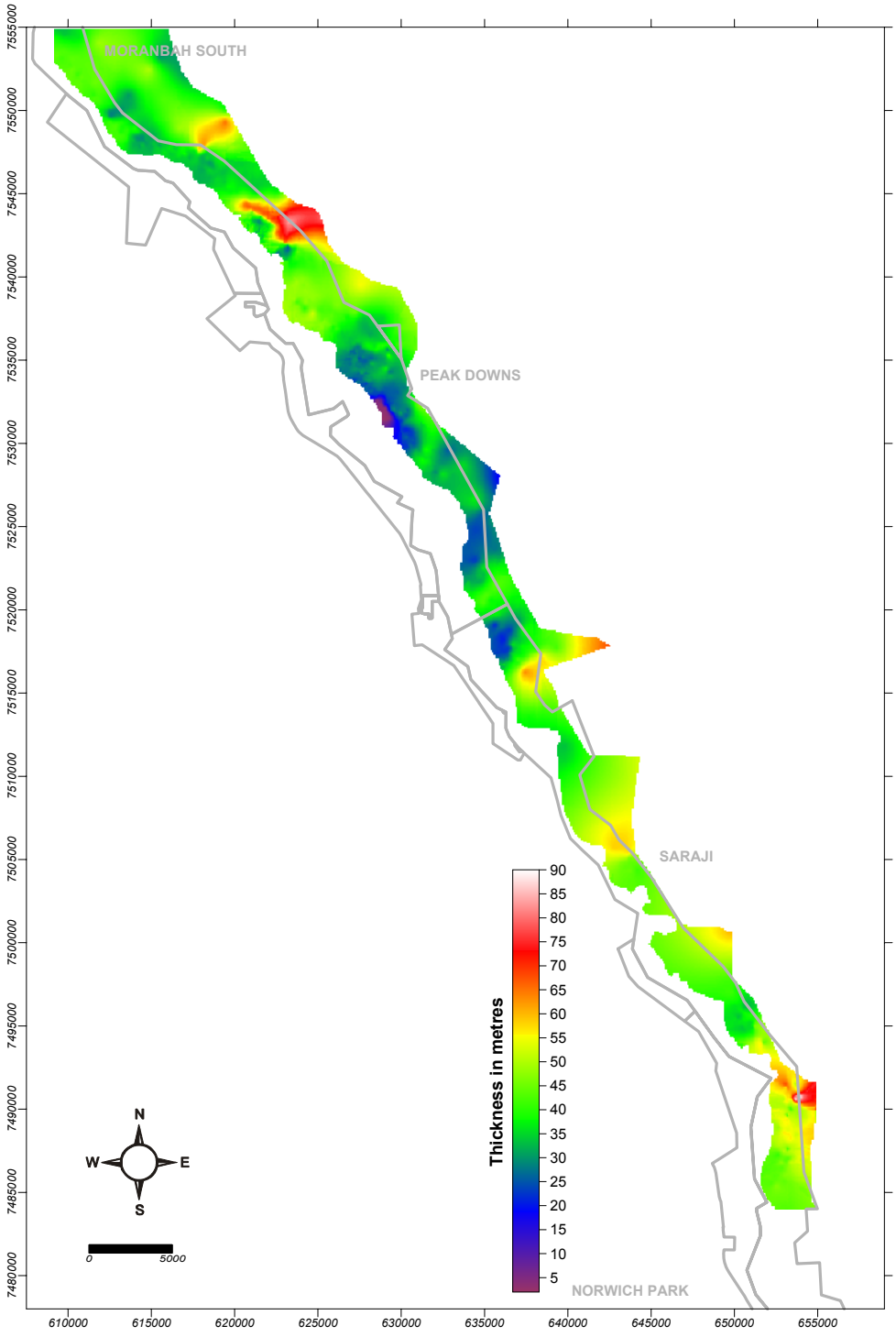

Figure 77 Harrow Creek to P seam (P17) seam interburden.

5.4.11 Sediment distribution and stacking patterns

The map in Figure 78 overlays the thickest part of all individual coal seam interburdens. Although lithologies were not discriminated within the Middle Tile dataset, thick interburdens tend to be sandstone-dominated and therefore, highlight sandstone body stacking patterns. Generally offset stacking is predominant in the succession below the HL (greens) and above the HL (reds). However, vertical stacking occurs between the two sequences in the northernmost part of the tile, which is consistent with rapid subsidence above a gravity low as noted in the Northern Tile data and in this tile (Figure 79).

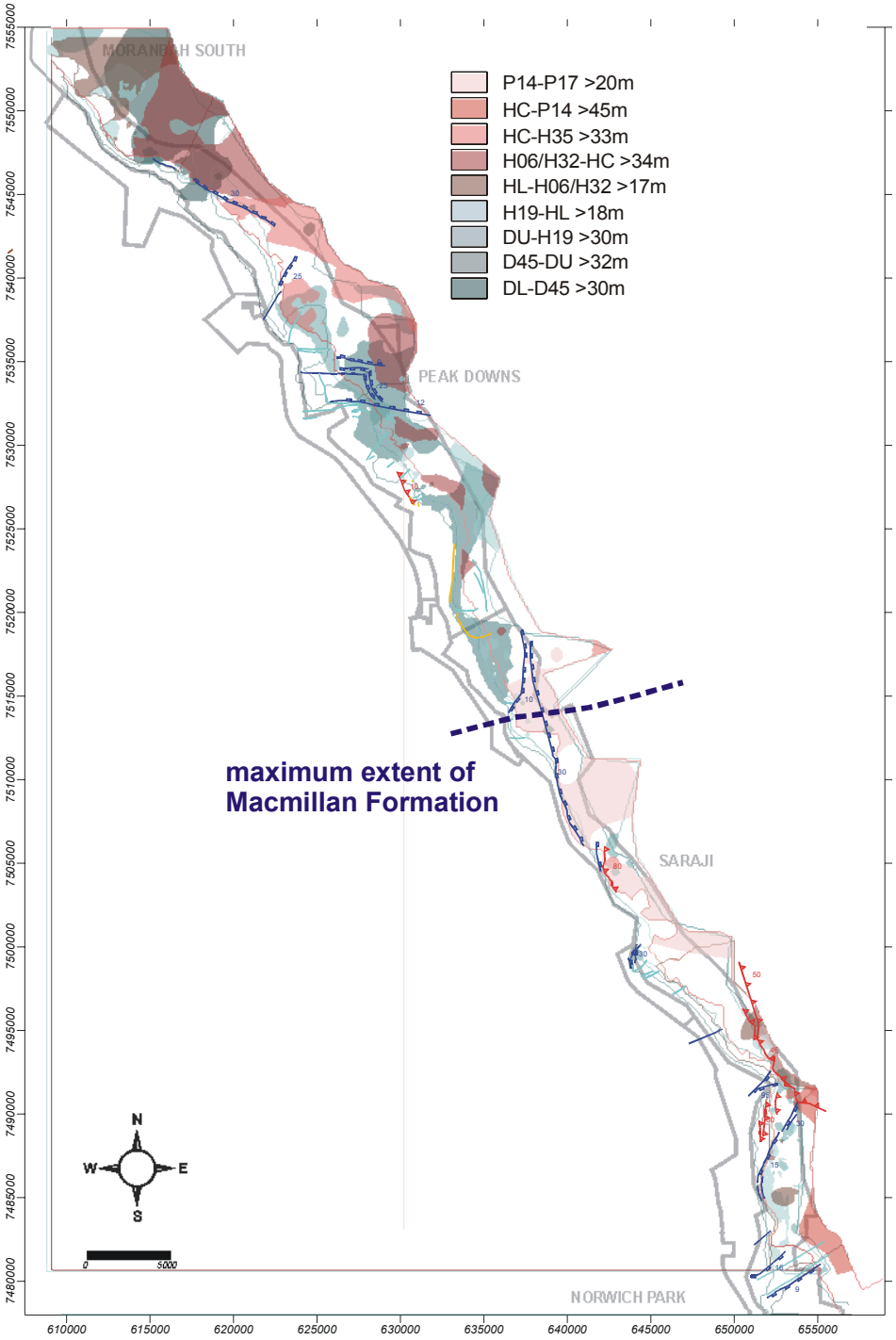

Figure 78 Synthesis of main sandstone distribution patterns in the Middle Tile.

Note also that extensive thick sands below the HL are restricted to north of the gravity bridge (Figure 79). This also coincides with the northernmost extent of the marine Macmillan Formation, above the German Creek CM, suggesting that this gravity bridge is an important basement structure active throughout the deposition of the Moranbah/German Creek CM.

The map also explores the relationship between the distribution of sandstone units and faulting. However, there is no consistent thickening of sediments along normal faults, which would suggest that the structures were active during deposition. There is however a link between the margins of the sandstone units and thrust faulting, particularly in the southern part of the tile.

5.4.12 Sediment accumulation relative to basement

In the Middle Tile sediment accumulation is also broadly controlled by differential subsidence in the basement as inferred from the regional gravity (Figure 79). The coal measures exhibit complex splitting patterns and thick cumulative thickness in the north where a deep gravity low occurs, but the total sequence from the base of the DL to the top of the P 17 seam thins to the south as they pass over a "gravity bridge" and interfinger with the cratonically derived and reworked quartz-rich and micaceous sediments of the German Creek Formation. This gravity bridge is interpreted as an important basement structure as it marks the southernmost extent of thick, extensive sandstone units below the Harrow Creek Lower seam, and the northernmost extent to the Macmillan Formation as well as to abundant intrusives (sills and dykes) within the main coal seams.

Opposite to the trend observed to the north, the sedimentary pile does not increase in thickness over the gravity low south of Saraji. However, this gravity low corresponds to the occurrence of abundant sills within the main coal seams, and an anomalous increase in vitrinite reflectance in this area. This suggests that this gravity low may be caused by a granitoid intrusion at depth.

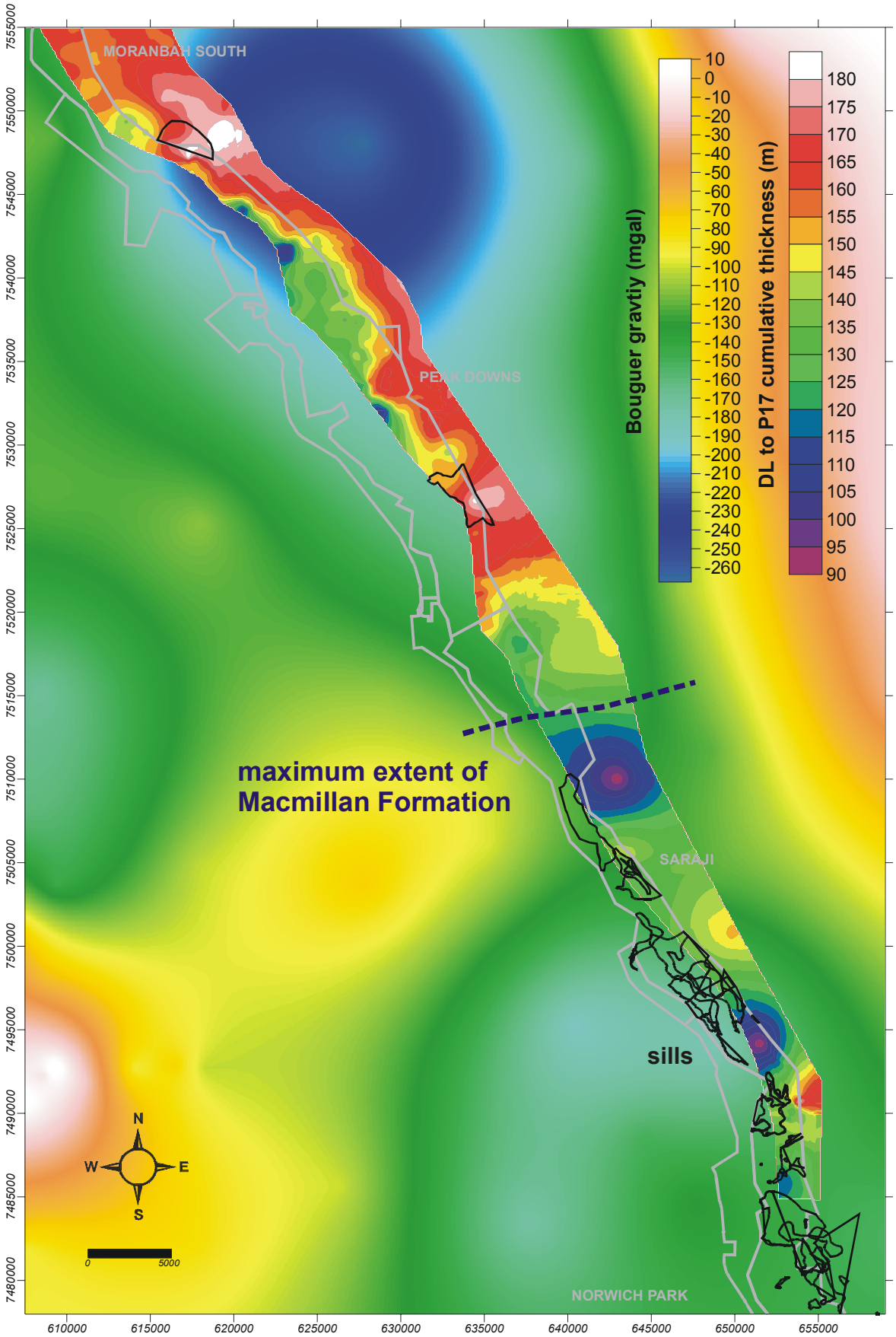

Figure 79 Cumulative thickness from DL to P17 seam over regional Bouguer gravity.

5.5 Southern Tile

The Southern Tile encompasses four mine sites (German Creek, Oaky Creek, Gregory-Crinum and Kestrel) that extract the German Creek - Lilyvale coal seam by open cut and underground long wall methods. The Aquila seam is also extracted by open cut methods.

The German Creek Formation varies in thickness from 95 m to 155 m and thins southward in the direction of the palaeo-shoreline. Seams vary in thickness from <1 m to >4 m, and thin by splitting. Split lines below the German Creek seam generally trend NE-SW. In contrast, up through the sequence the orientation of splits shifts to the S and SE. The correlation diagram is shown in Figure 80.

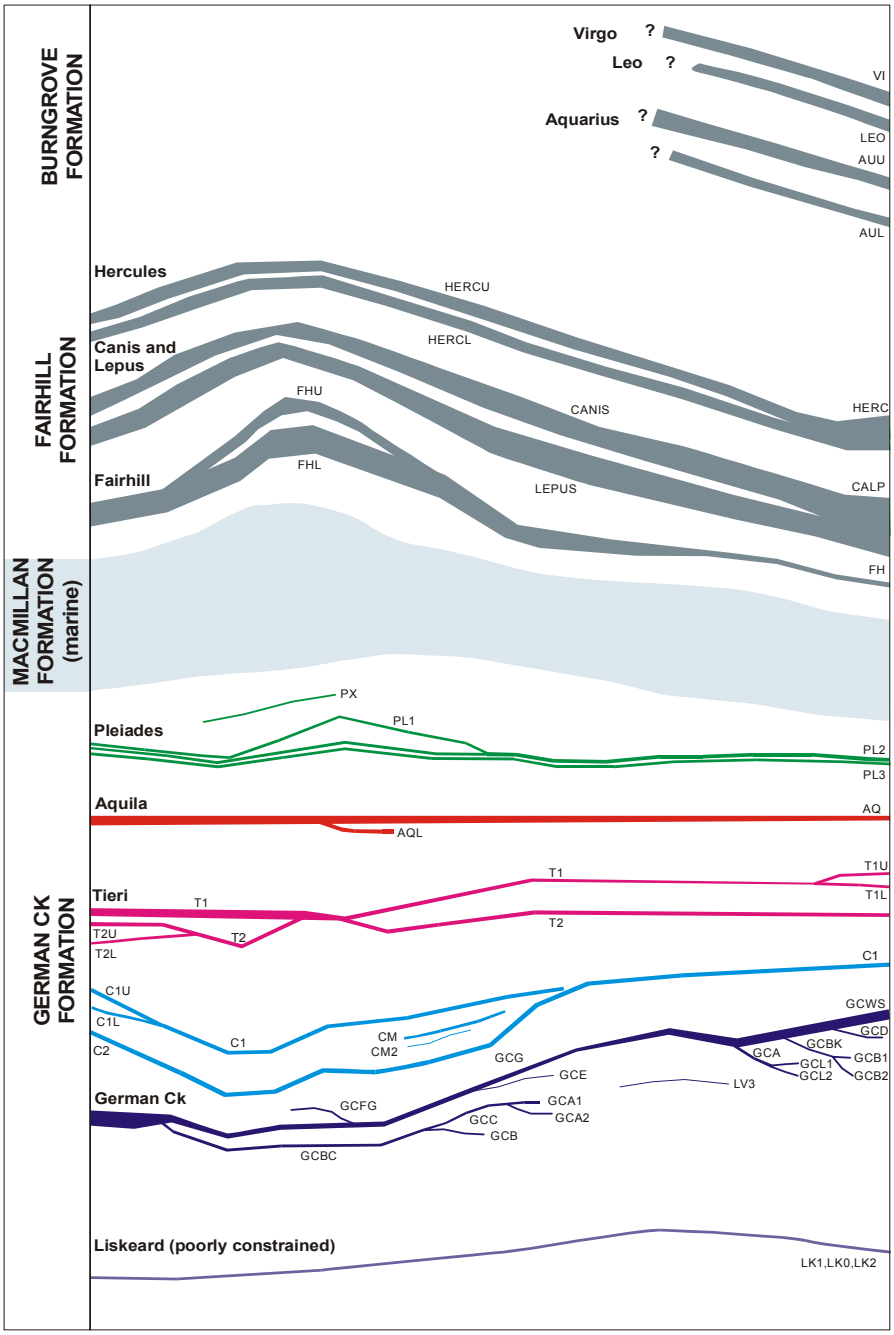

Figure 80 Schematic correlation of coal seams across Southern Tile.

In the southern areas the paralic (marginal marine) influences are marked with the intercalation of strata containing marine fossils in the upper part of the sequence (particularly above the Corvus seam). The sequence is dominated by sandstones that vary from southerly and easterly trending low to high sinuosity channels and northeasterly trending belts, commonly separated by carbonaceous and locally bioturbated sandy argillitic units, which are attributed to fluctuating deposition and minor tidal influence in a coastal setting (Falkner and Fielding, 1993). In this area, the sandstones in the lower part of the sequence are characterized by thinly interbedded, fine-grained sandstone and siltstone with ripple cross lamination and wave ripples (interdistributary bay and bay fill sequences) that are commonly overlain by or adjacent to erosively based, fine to coarse grained sandstone with variable siltstone partings that exhibits epsilon to trough cross bedding and ripple cross lamination (distributary channel). They are often tabular in outcrop (Figure 81). In some areas lobate sheet sandstones that emanated as mouth bars debouching from, and later traversed by, a distributary channel represent the bay-fill. The seaward margin of these sandstones are often reworked by longshore drift into cleaner, more quartzose sandstone bars that trend southwest.

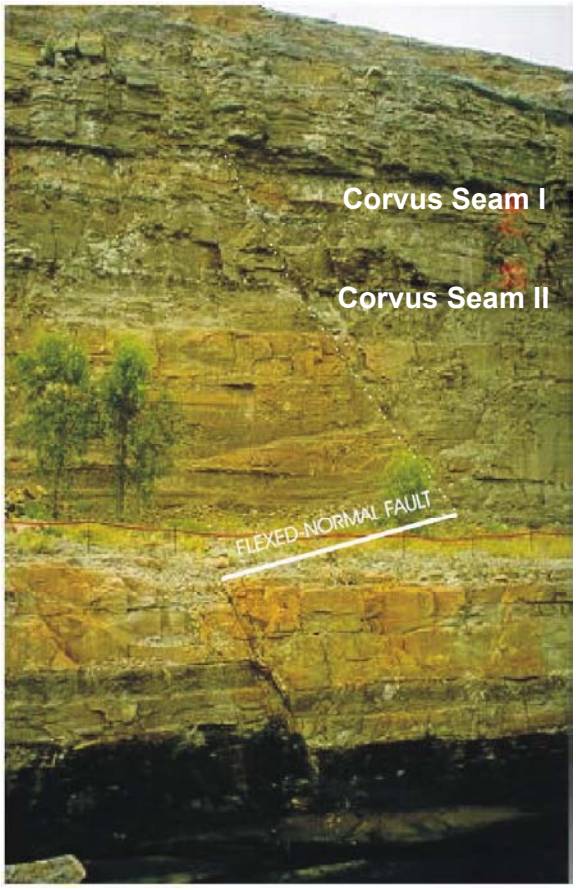

Figure 81 Exposure of roof strata of German Creek seam showing normal fault.

Interburden distribution patterns in the southern part of the tile (south of Oaky Creek) consistently show long, straight, NE trending belts of multi-storey, amalgamated sandstone units, that stack and "on lap" progressively up section. One exception to this pattern is the Tieri 2 to Tieri 1 interburden that is interpreted to contain a well-developed distributary channel system. The depositional environment for these interburden intervals is interpreted to be that of a distributary bay. Well-sorted,

quartz-rich sands abundant above the Tieri seam suggest that the deposition is influenced by a near-shore coastal environment (Falkner and Fielding, 1993).

Interburden distribution patterns in the northern part of the tile (German Creek and Oaky Creek) are more complex. The interval directly overlying the German Creek seam is still influenced by coastal conditions similar to the southern part of the tile. Successive interburdens show well-developed, large-scale channel belt and distributary channel/mortar systems that trend EW and NS respectively. Sediments accommodated within the interburdens show clear pattern of offset stacking with successive units stacking toward the north and northeast in response to the marine transgression.

The SE-stepping successive lower splits of the German Creek seam record a regional regression that culminated in the deposition of the German Creek seam. Northwesterly on lap of sandstone units in the immediate roof of the German Creek seam and the progressively northern offset stacking of successive channel belts record the regional transgression, which culminated with the deposition of the marine Macmillan Formation.

The Southern Tile is positioned over a major swing in strike of the Moranbah/German Creek CM from NNW to SW. A change in regional dip from 6° at Norwich Park to sub horizontal at Oaky Creek back to 6° near Kestrel accompanies the swing in strike.

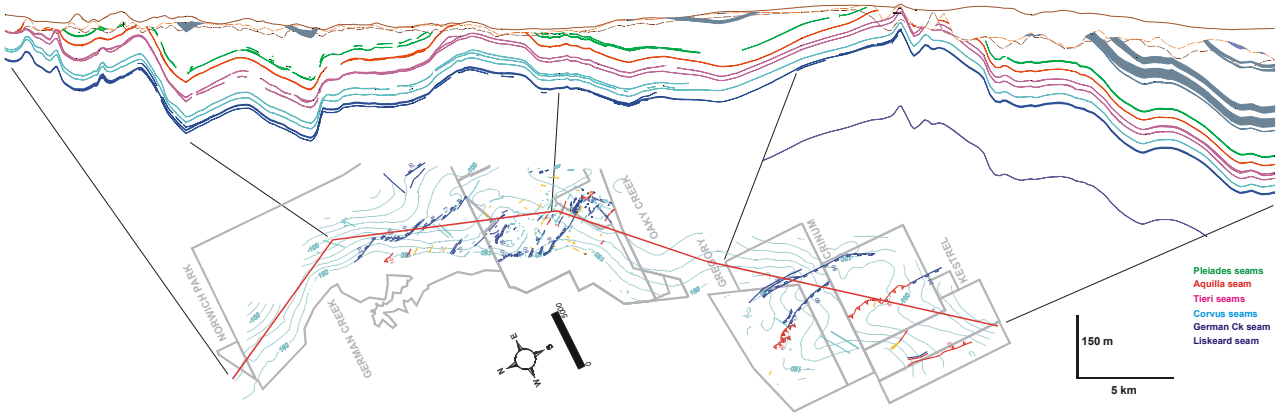

Figure 82 Cross section of Southern Tile showing seam structure.

The cross section in Figure 82 is broadly parallel to the strike of the coal measures and therefore reflects the subregional-scale folding pattern of the strata. Folding is open and gentle with a wavelength of approximately 5 km. The strike of the fold axes varies around the regional swing in the strata at Oaky Creek mine.

The cross section highlights the general thinning of the coal measures and the reduction of the number of coal seams from north to south. The coal seams are consistently parallel to each other, and splitting is less common than in the middle and Northern Tiles. The interburden thicknesses average between 20 and 30 m, substantially less than those to the north, but do show anomalous thickening that define the shape of the depositional systems.

5.5.1 Topography and Tertiary cover

The topography reflects the surface drainage of the eastward draining Mackenzie River system. At the time of this report seven underground mines were in operation at German Creek, Oaky Creek, Crinum and Kestrel. Open pit operations are extracting the German Creek and Aquila seams at German Creek, Oaky Creek and Gregory mine sites.

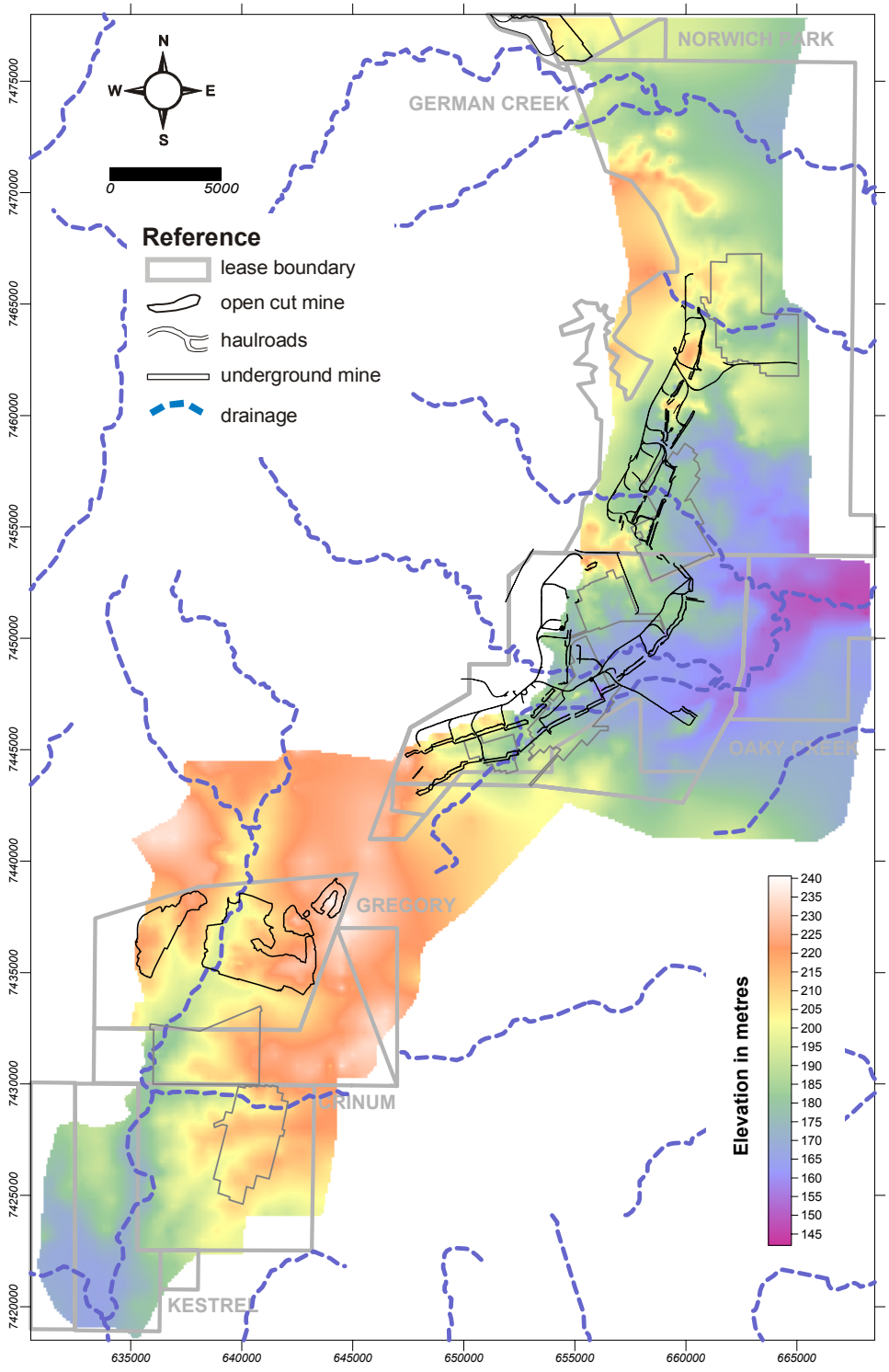

Figure 83 Topography and infrastructure of the Southern Tile.

5.5.2 Base of Tertiary

The shape of the Late Cretaceous erosional surface is similar to the present day topography, which shows that the Mackenzie River drainage system has remained stable since this time.

The main differences between the two surfaces are deep incisions at Kestrel, which were valleys filled by basalt (outlined in green hatch lines). During subsequent erosion these valleys became inverted.

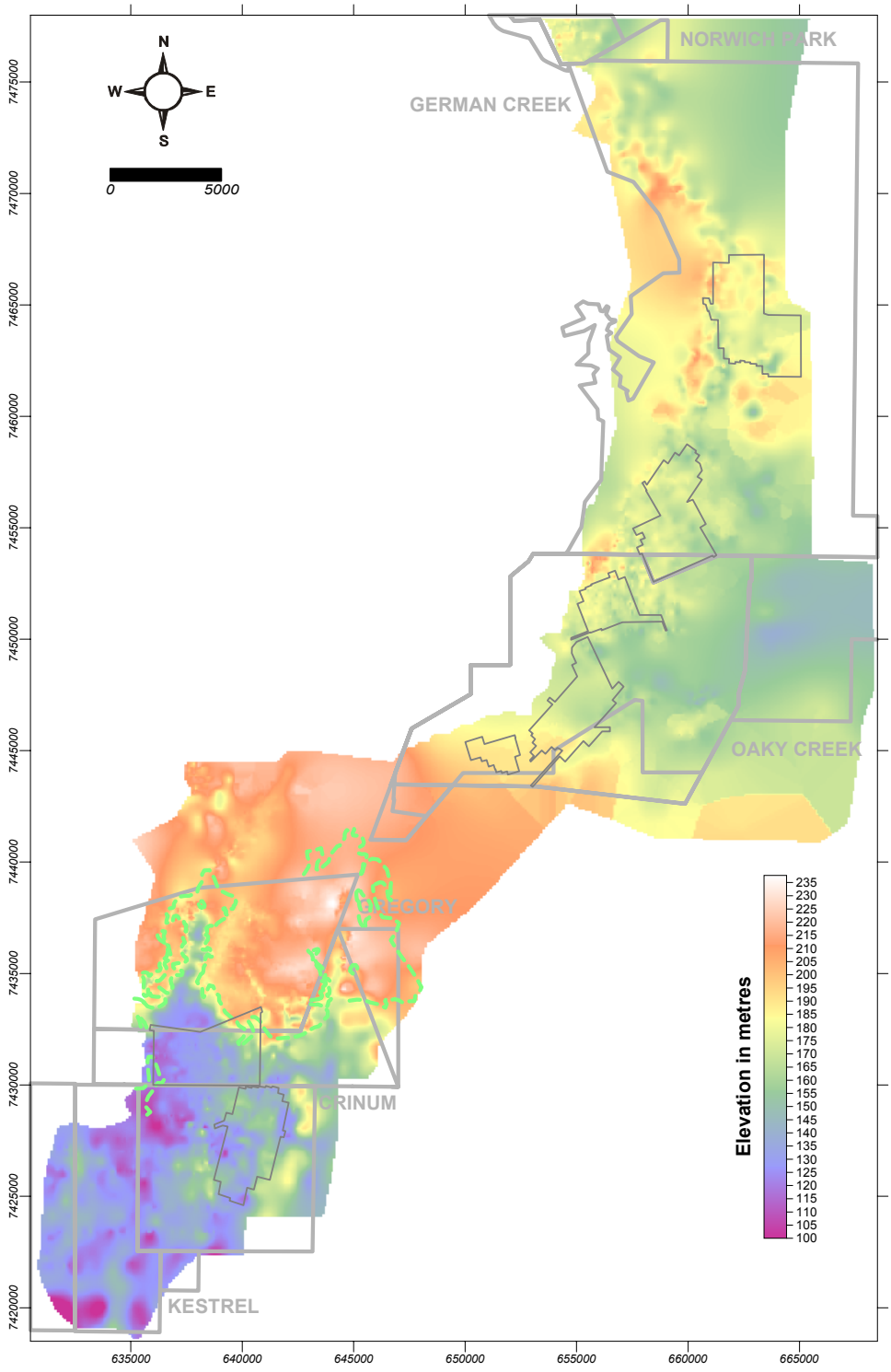

Figure 84 Base of Tertiary unconformity for Southern Tile overlain by basalt outlines (green line).

5.5.3 German Creek seam thickness and structure

The German Creek seam shows two thick (>4 m) pods in the Oaky Creek and Gregory lease areas. In the north of German Creek the seam is anomalously thick due to intrusion. It thins by splitting from the bottom of the seam to the southeast and to the north. The straight trend of the split lines, their northeasterly orientation and successive stepping to the southeast suggests a southeasterly regression of the coastline just prior to the deposition of the German Creek seam.

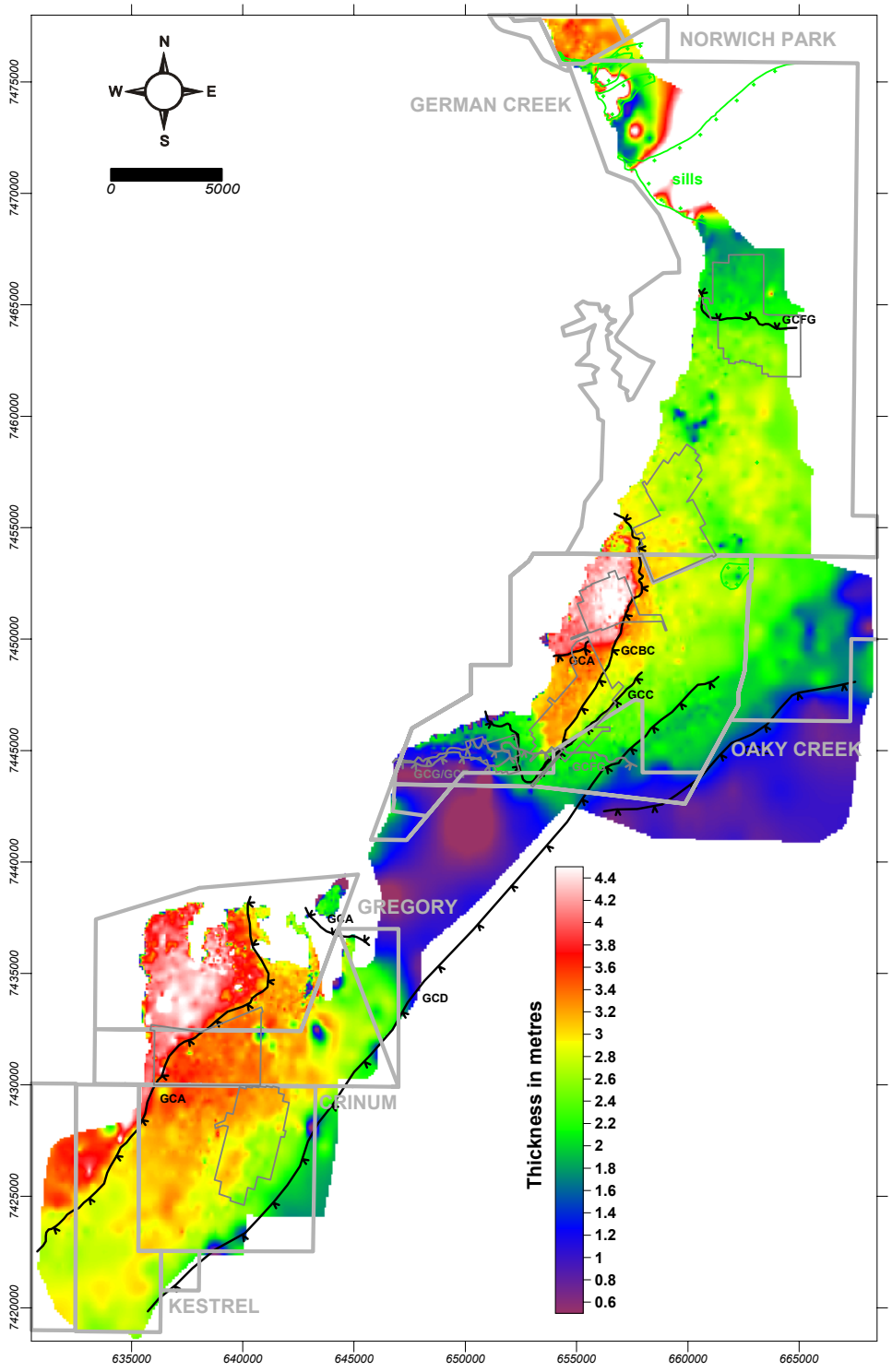

Figure 85 German Creek seam thickness with overlain splits lines and sills.

5.5.4 German Ck to Corvus 2/1 interburden thickness

This interval is variable from south to north and characterised by ENE-trending distributary channel sandstones with mouth bars that are reworked into shoreline parallel bars and ridges in the south (Gregory to Kestrel mine), an anomalously broad and thick (>25 m) SE trending channel between Gregory and Oaky Creek mine site, a broad amalgamated mouth bar that has also been reworked into shoreline parallel bars down dip over Oaky Creek, and SE-trending major and minor distributary channel belts at German Creek and further north. The thickest sediment accumulation occurs over thick pods of German Creek seam. The anomalously thick (up to 40 m) pile of sediments accumulated between Oaky Creek and Gregory on top of very thin coal, suggesting this may represent a major coastal passage feeding the palaeocoastline. These interpretations corroborate field mapping conducted by Falkner and Fielding (1993) and increase our knowledge of the geometry of these deposits.

Detailed work at Kestrel mine demonstrates the northwesterly incursion of successive sandstone bodies during this interval (Figure 87, Figure 88).

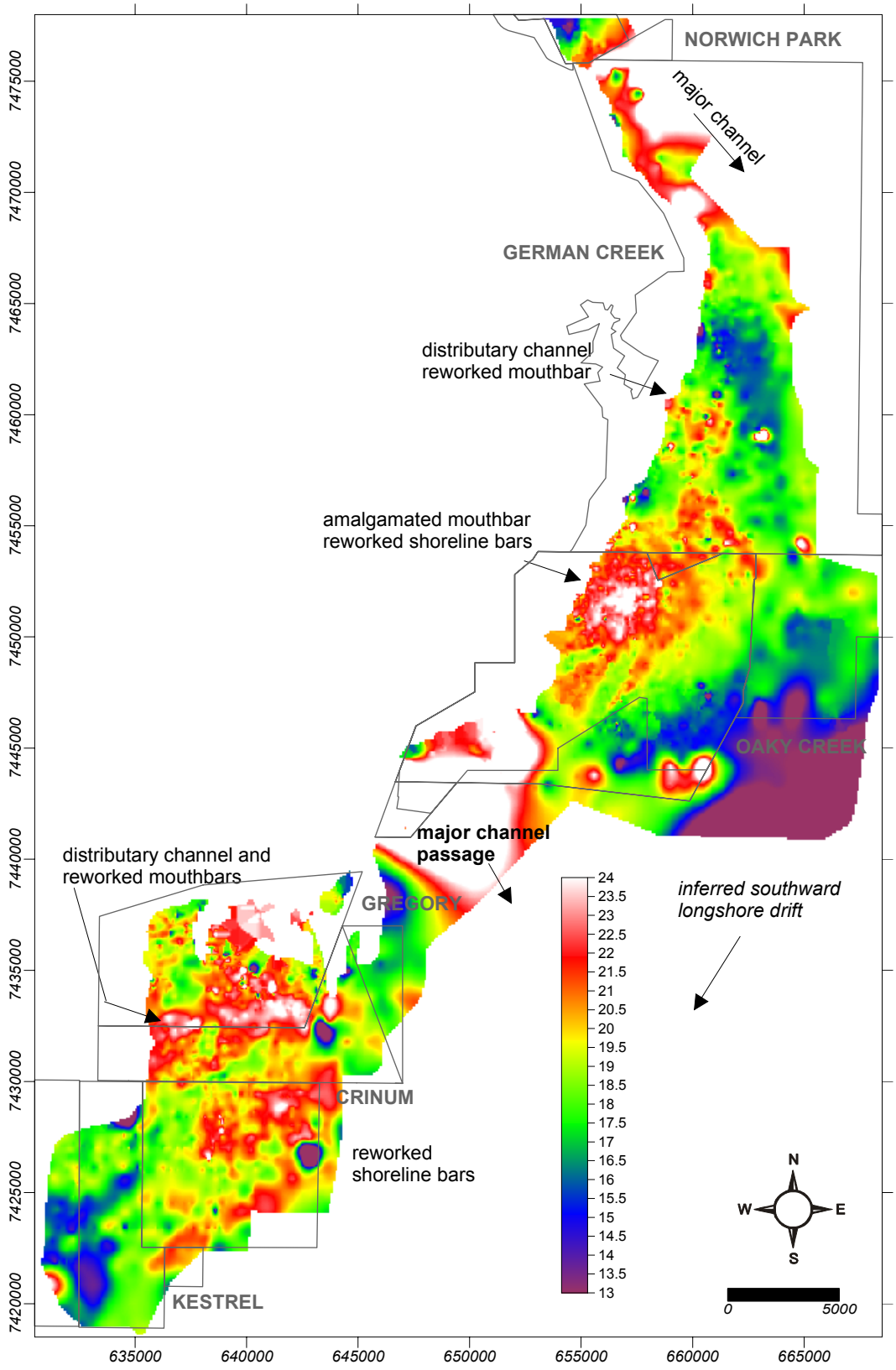

Figure 86 German Creek to Corvus 2/1 interburden thickness distribution.

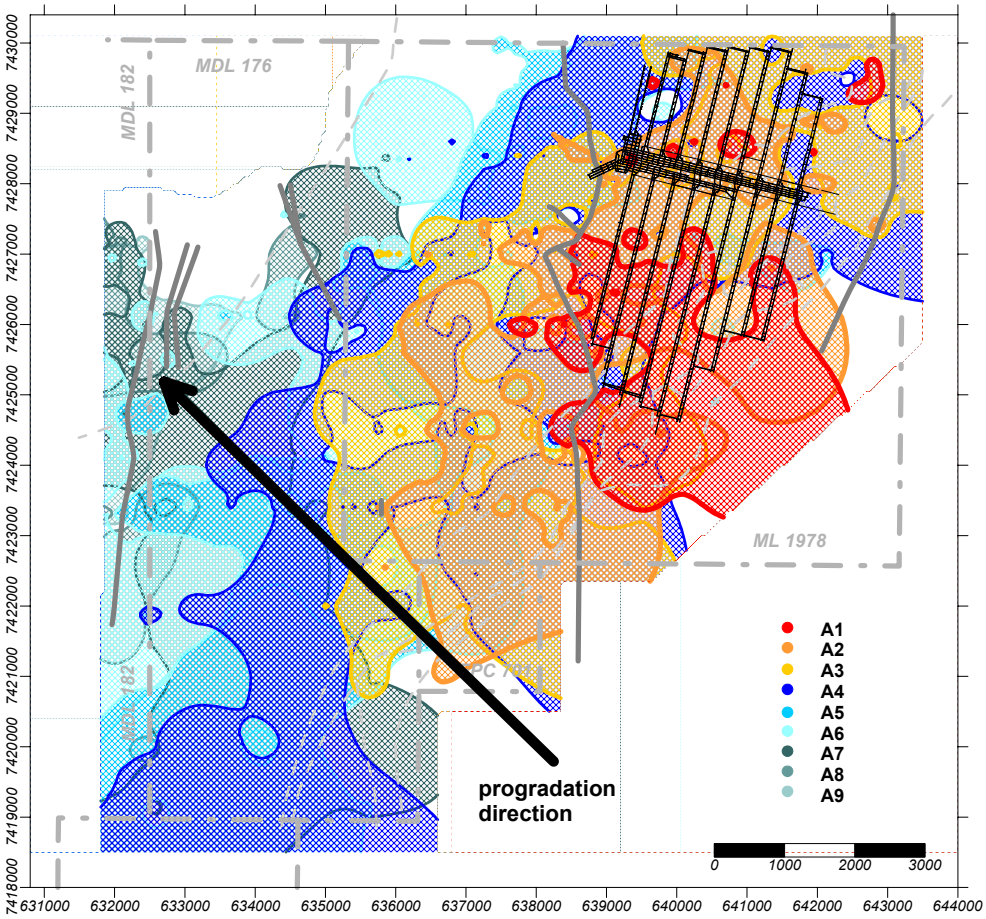

Figure 87 areal distributions of sandstones in the German Creek to Corvus interval at Kestrel Mine demonstrating on lapping as a function of sea level rise. A1 is at the base and A9 at the top.

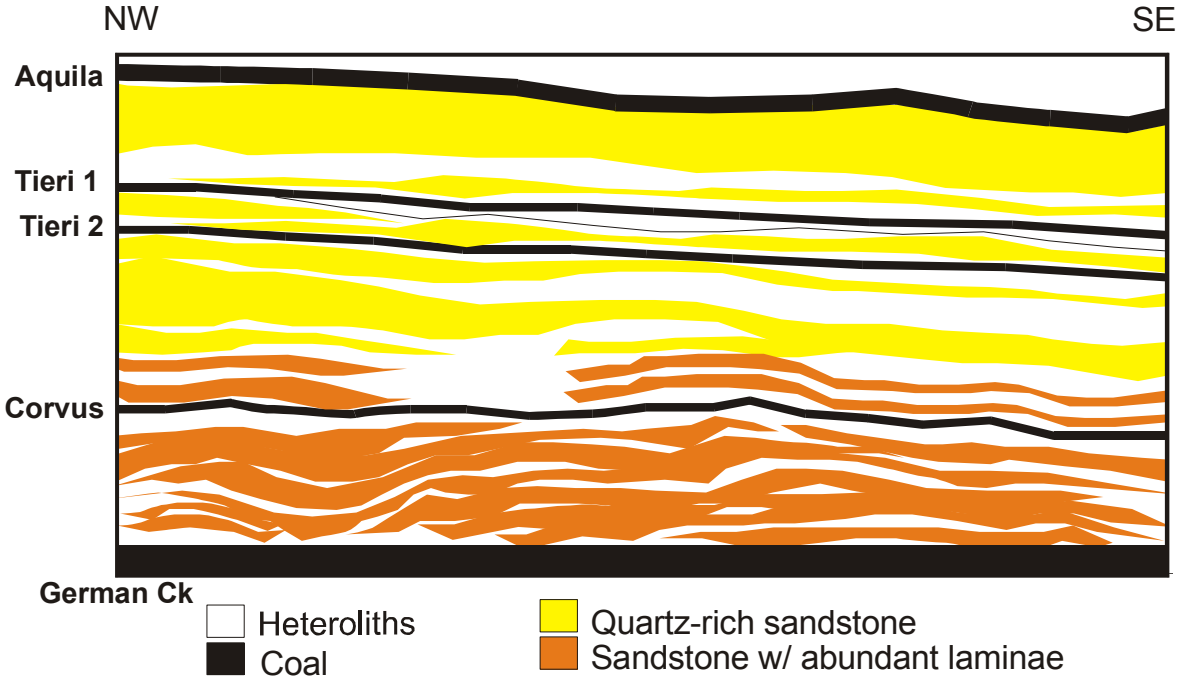

Figure 88 Schematic cross section through Kestrel lease demonstrating on lapping nature of sandstones in the German Creek to Corvus interval.

5.5.5 Corvus 2 to Corvus 1 interburden thickness

The Corvus 2 and 1 seams converge south of Oaky Creek, thus the C2-C1 interburden only occurs in the north of the tile. Both Corvus seams are thicker than 1 m in the split area. The interval is marked by an easterly trending distributary channel complex that builds sequentially eastward over the Oaky Creek lease connecting to a NS trending sandstone belt of unknown origin (? shoreline sandstone or southerly draining channel belt).

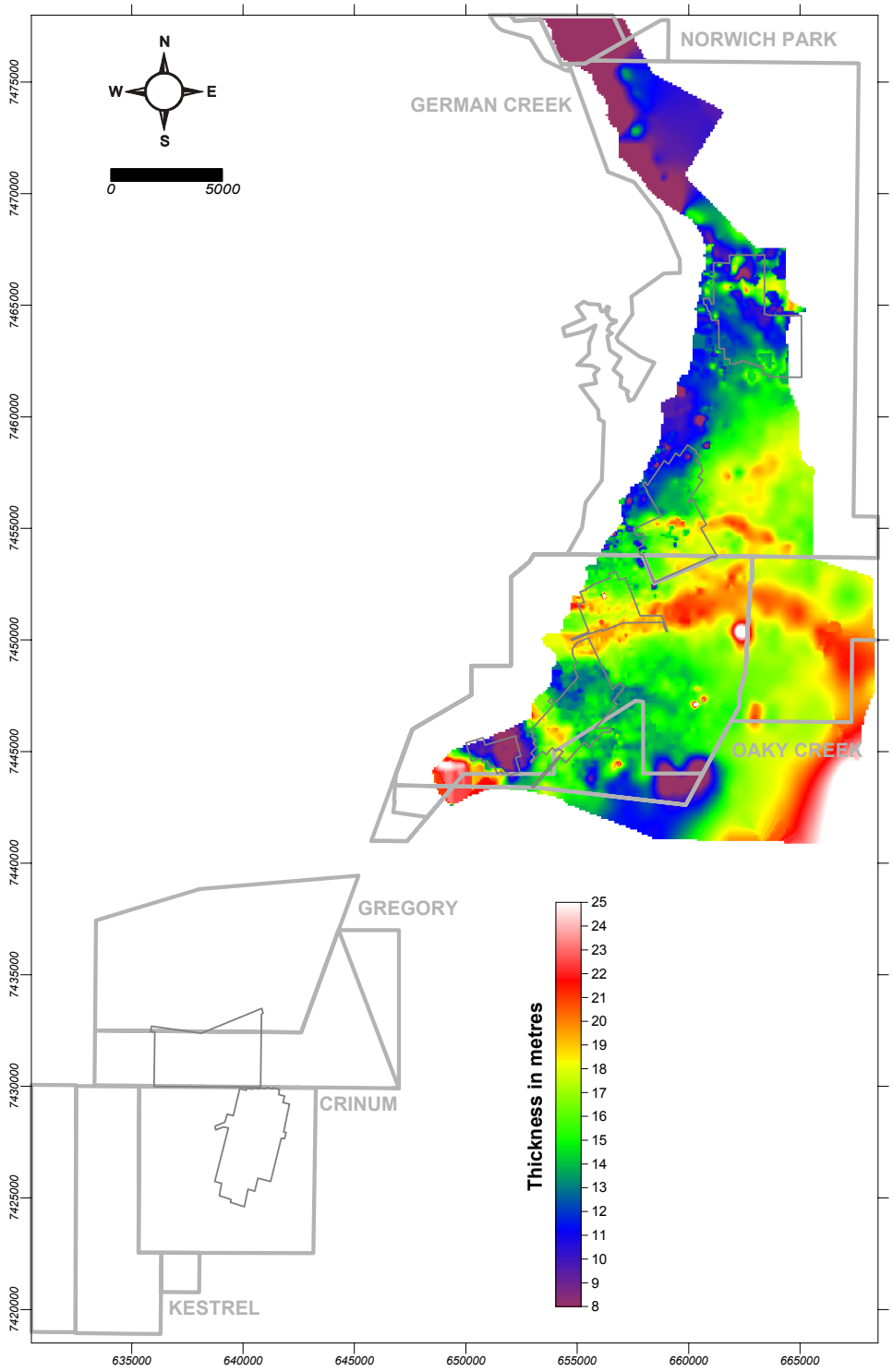

Figure 89 Corvus 2 to Corvus 1 interburden thickness distribution.

5.5.6 Corvus 1 to Tieri 2 interburden thickness

This interval is thickest in German Creek (>35 m) and thins to the south. Interburden interpretations were not conducted for German Creek, but in the Oaky Creek mine site, this interval consist of thin (<5 m) but widespread sheet like sandstones intercalated with thicker heterolithic units and capped by a relatively thick (>10 m) sandstone that forms a southward trending channel. In contrast, 5 to 10 m thick sheet sandstones with straight NE-trending margins, suggesting deposition in a coastal environment, dominate the south. Note that the large channel system in the C1/C2 interval is overlain by thin interburden in this interval.

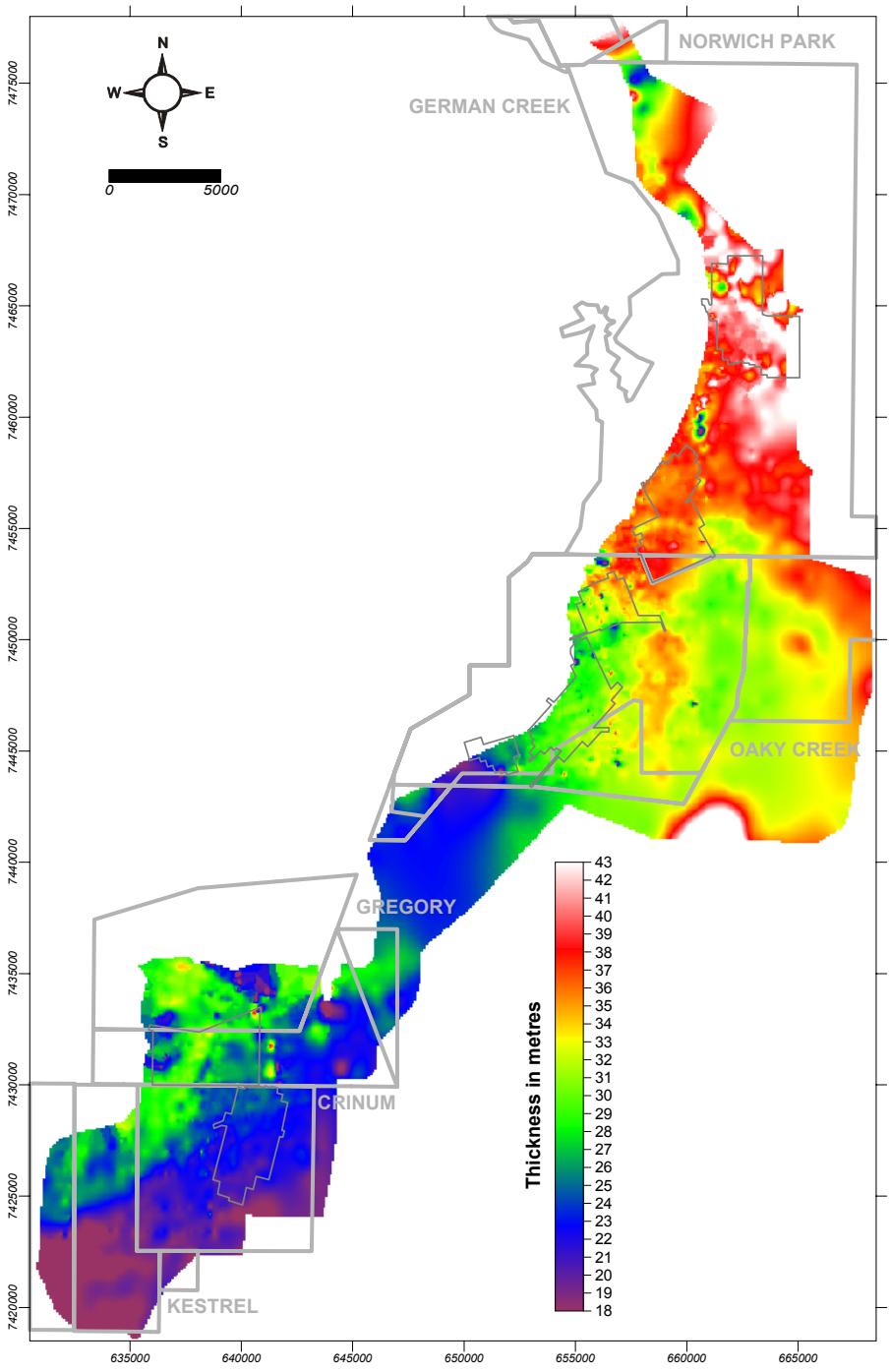

Figure 90 Corvus 1 to Tieri 2 interburden thickness distribution.

5.5.7 Tieri 2 to Tieri 1 interburden thickness

The focus of deposition shifted to the south during this interval. A broad complex channel belt formed in the Gregory/Kestrel area suggests deposition of a narrow but meandering channel belt across its underlying mouth bar. A smaller, NE-trending channel belt occurs in the German Creek lease area.

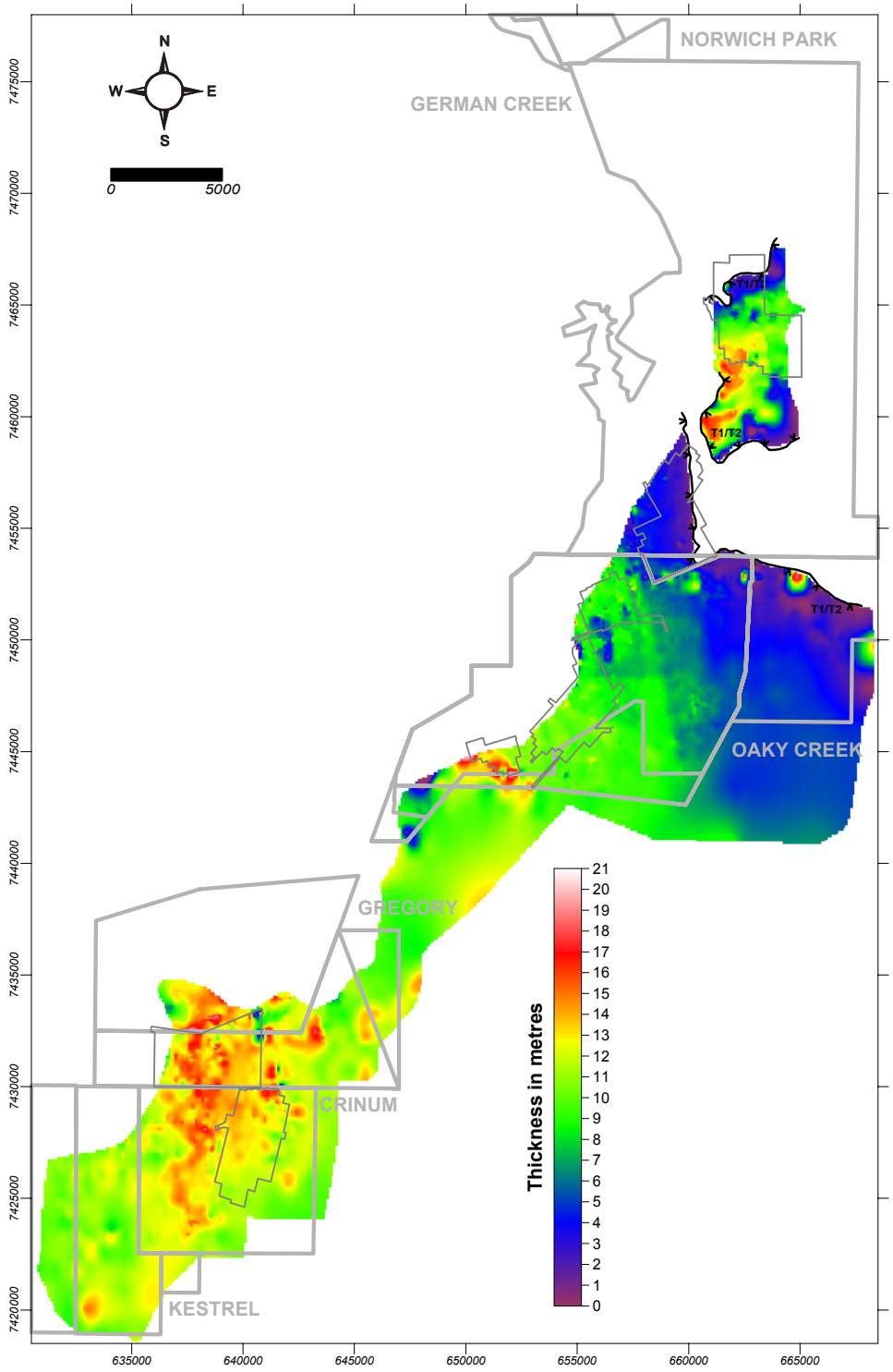

Figure 91 Tieri 2 to Tieri 1 interburden thickness distribution

5.5.8 Tieri 1 to Aquila Seam interburden thickness

Once again the focus of deposition shifted to the north. The distribution patterns suggest multiple overlapping distributary channel/mouth bar systems trending south-southwest that progressively migrated northward. Shoreline processes reworked the sediments and they exhibit bioturbation that indicates marine conditions. In the south the distributing system at Gregory/ Kestrel was still mildly active.

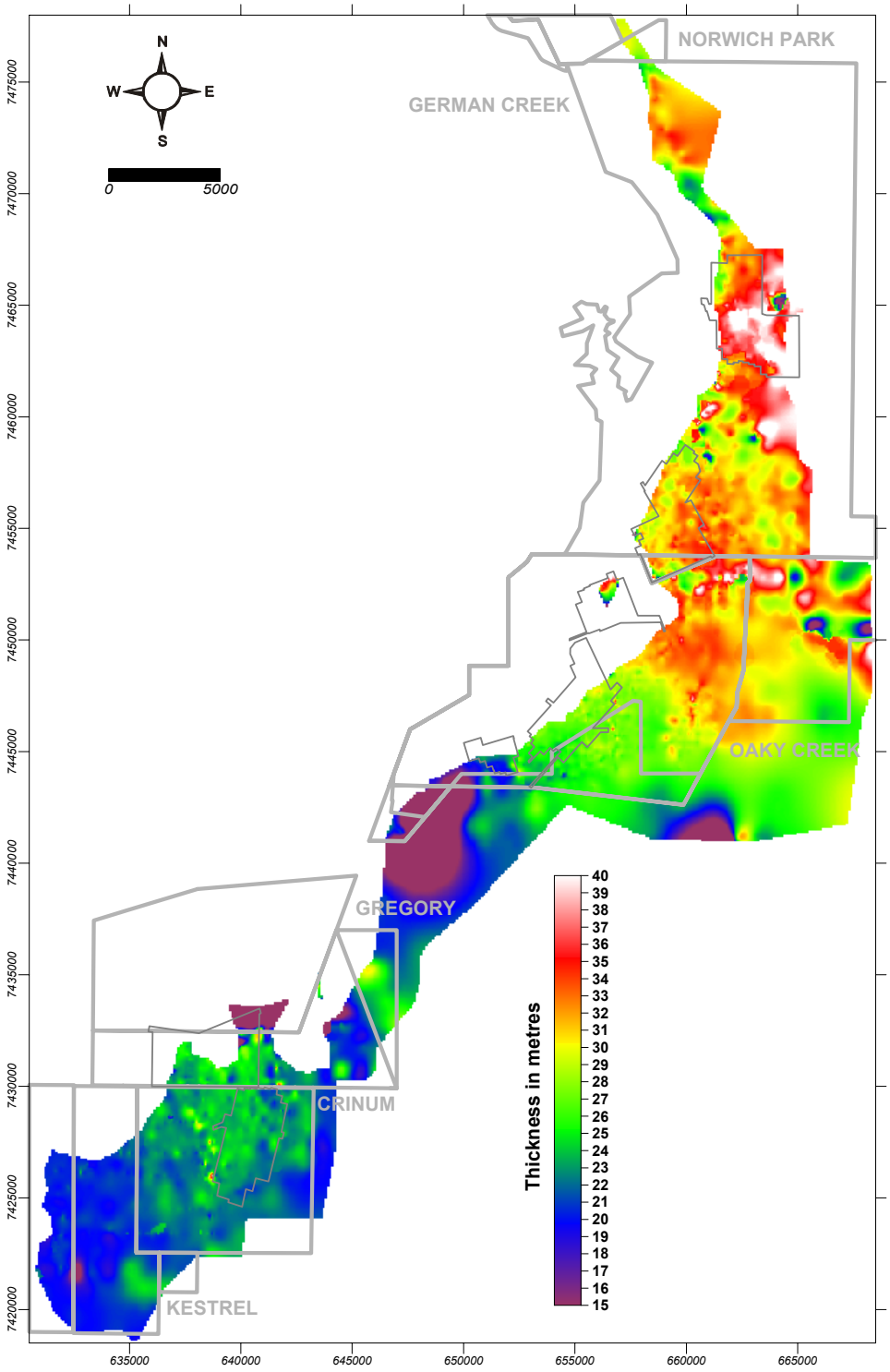

Figure 92 Tieri 1 to Aquila Seam interburden thickness distribution

5.5.9 Aquila Seam thickness

The Aquila seam is thickest (>1.2 m) at German Creek and thins considerably to the south. Split lines for the Aquila Lower seam in the floor trend northwesterly, suggesting southeasterly draining channel systems during the initiation of the peat mire. In general the seam is relatively thick where the underlying interburden is thick.

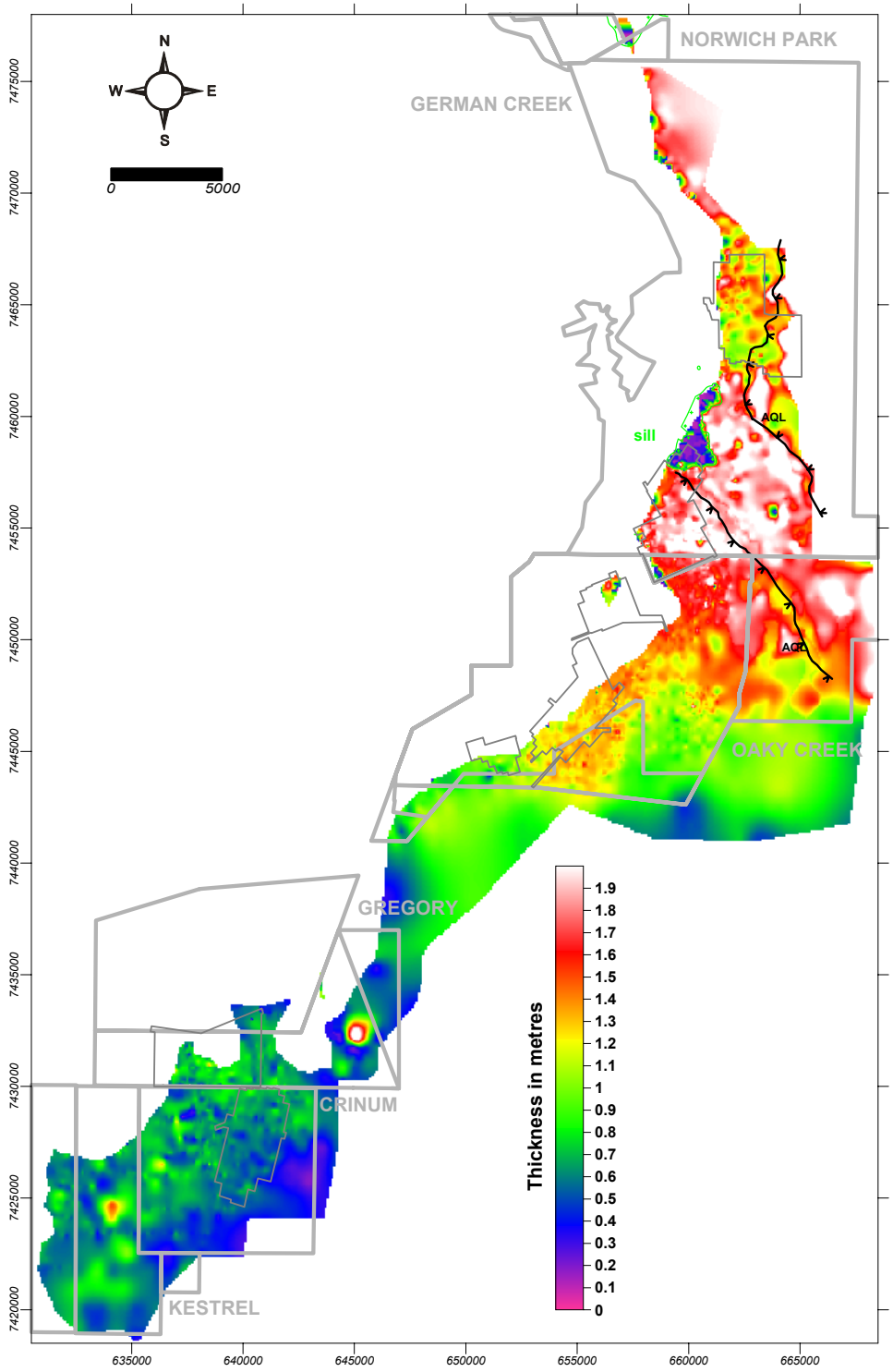

Figure 93 Aquila Seam thickness distribution.

5.5.10 Aquila to Pleiades 3 Seam interburden thickness

The interval above the Aquila seam is generally of constant thickness, except for an EW oriented meandering channel in the southern part of German Creek, and possibly a similar channel in the south of Oaky Creek. In the south the areas of thick interburden are aligned NESW, parallel to the palaeo-shoreline. This is the coastal extension of the middle superseam to P Tuff interval.

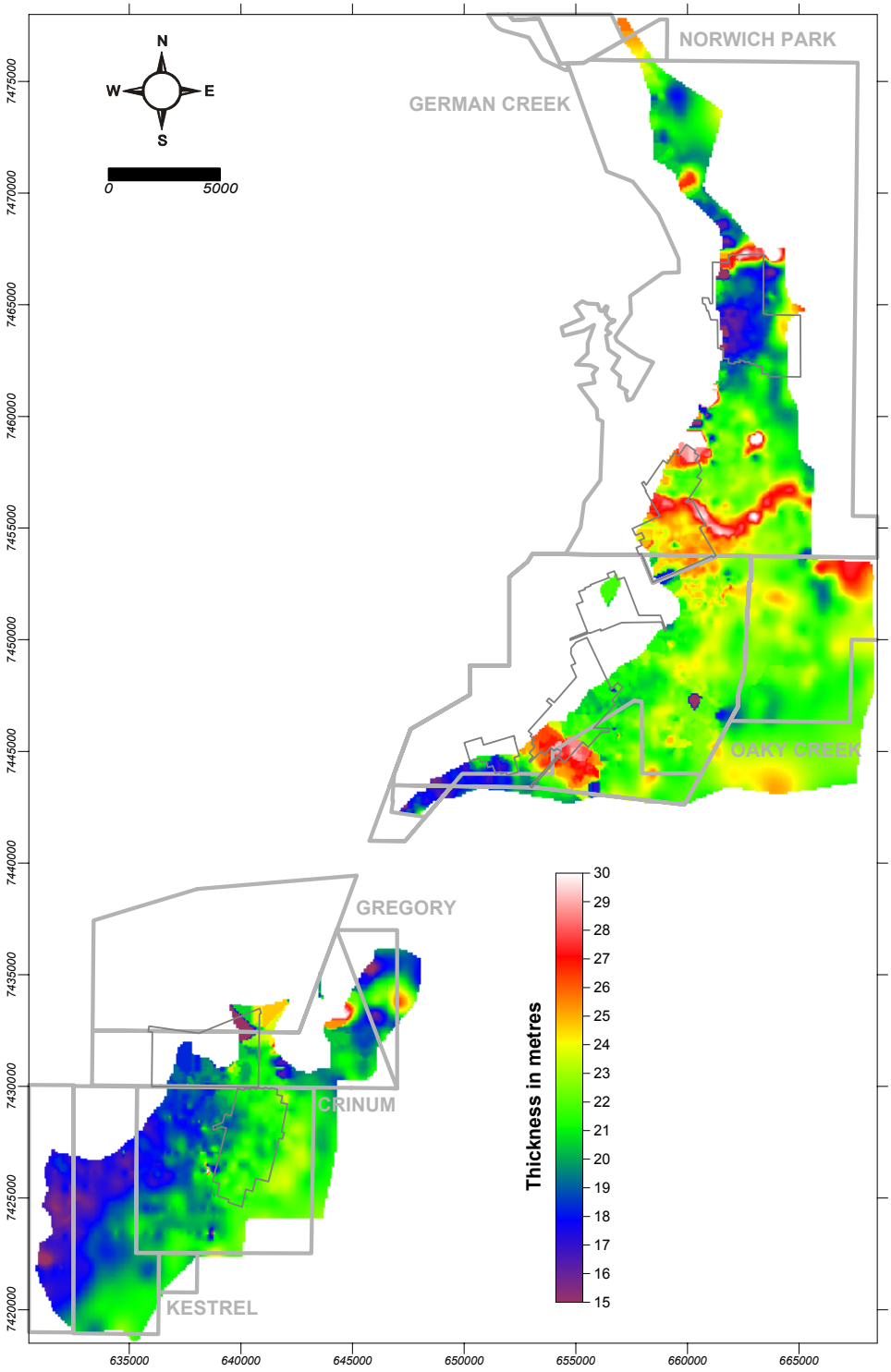

Figure 94 Aquila to Pleiades 3 Seam interburden thickness.

5.5.11 Sediment distribution and stacking patterns

Figure 95 shows the main interburden distribution maps above the Corvus 2 seam simplified and stacked on top of one another to highlight inheritance from lower interburden units on the following units. One or two contours were chosen for each interburden interval, to highlight the shape and position of the thickest accumulation of sediments.

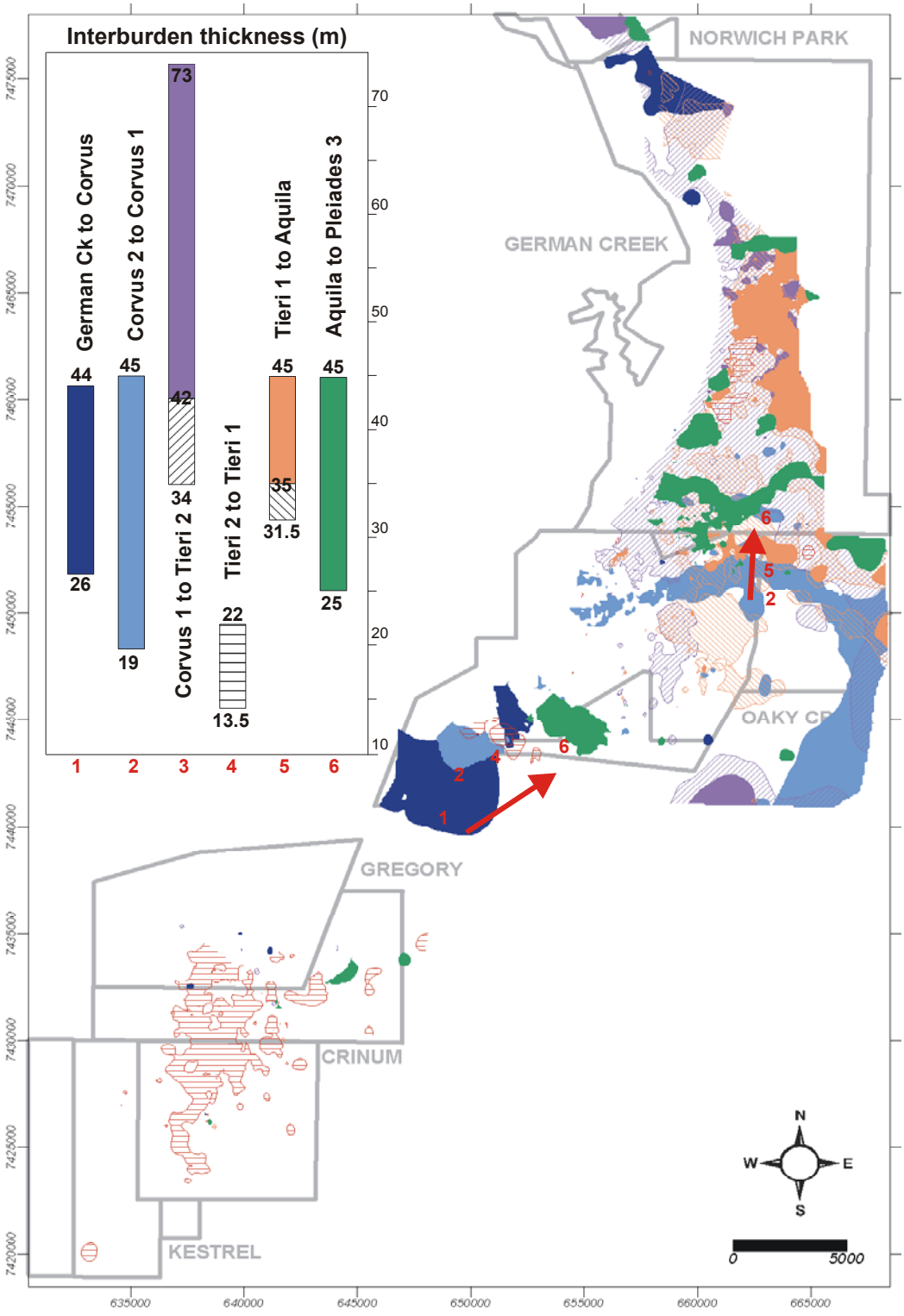

Figure 95 Synthesis of main sandstone distribution patterns above the Corvus 2 seam.

The patterns of the thickest interburden distribution are interpreted to represent complex channel assemblages. Two contrasting types of these assemblages occur in the tile: Large, thick E to SE trending belts, which are interpreted as channel belt complexes are contained in the GCWS/Corvus, C1/C2, T1/AQ and AQ/PL3 intervals. These channel belts are generally ~1 km wide, show low sinuosity and transect the entire study area. Some of the channel belts are associated with well-developed mouth bars. The other assemblage comprises thin, broad sheets with complex internal architecture, interpreted as distributary channel complexes. They occur within the C1/T2, T2/T1 and T1/AQ interburdens. These distributary channel systems trend NS and taper to the south. They contain high sinuosity channels and complex splay patterns.

There is a clear pattern of offset stacking with inheritance lasting for several intervals. For example the EW trending channel belt in the C1-C2 interval strongly controls sediment distribution within the C1/T2 and T1/AQ intervals.

There is a general trend for the thickest successive intervals to stack towards the N and NE (see arrows on map). This pattern is consistent with an overall regional transgression that culminates with the deposition of the marine Macmillan Formation.

5.6 Summary of regional sedimentation patterns in the Supermodel area

This image of the regional Bouguer gravity is overlain by the cumulative thickness of the Moranbah/German Creek CM between the top and bottommost coal seams that can be traced across the three tiles. These are the Goonyella Lower/ Dysart Lower/German Creek and GU2/P/Pleiades seams. Data from government boreholes outside the Supermodel area are shown as dots.

The cumulative thickness map demonstrates the overall thinning of the coal measures to the south and southwest over the Comet Ridge and Capella block. This correlates with a change from thick coal seams with complex splitting and highly variable interburden distributions to thinner seams with less complex splitting and more laterally persistent interburden thicknesses, as shown on the regional correlation diagram. The interval is thickest in areas associated with deep gravity lows in the northern part of the basin. Increased thickness is a function of complex splitting and the accumulation of thick interburden sandstones. Mechanisms were described in the Northern Tile section. The northernmost extent of the MacMillan Formation is also associated with the southern edge of the deep gravity low.

Interburdens attaining > 40 m thickness are generally sandstone dominated. These areas were numbered in the correlation diagram (Figure 42) and their distributions are shown in Figure 97. Seam splitting patterns for the relevant intervals are also shown. During the deposition of the Lower Goonyella (equiv. Dysart, German Creek, Corvus) seams and its associated overburden, the splitting patterns suggest a southerly draining channel system that deposited aerially extensive splays to the west throughout the northern and Middle Tiles. A possible reconstruction is shown in Figure 98. The thickest interburdens (1-4) are dispersed and restricted to north of Saraji. Immediately above these seams thick interburdens (5-6) are more widespread extending into the Southern Tile and are more extensive. Splitting in the Harrow Creek seam is confined to the northern end of the Middle Tile. The orientation suggests a continuation of the south to southwest trending drainage system that surrounds areas of thick peat accumulation. However, it is the interval above the Goonyella Middle (equiv. Harrow Creek) seam to the Goonyella Upper seams that contains the most well developed channel systems (7-9). These systems are offset-stacked and cover most of the area north of Saraji, abutting the

northernmost extent of the marine Macmillan Formation. These channel system are best observed in the Northern Tile and exhibit thick broad low sinuosity channel systems that have overbank splay deposits on their outer bends. These are overlain by the P seams and associated P tuff that merge to form the thick Pleiades interval in the Southern Tile. The interburden to the upper seam (10) is the thickest coal free interval in the system, and coincides with the northern extent of the MacMillan Formation. These upper sandstones are more quartz-rich than those in the lower part of the sequence and it is suggested that these upper sands would be reworked by coastal processes and formed easterly trending shoreline parallel sandstones similar to those observed in the German Creek CM.

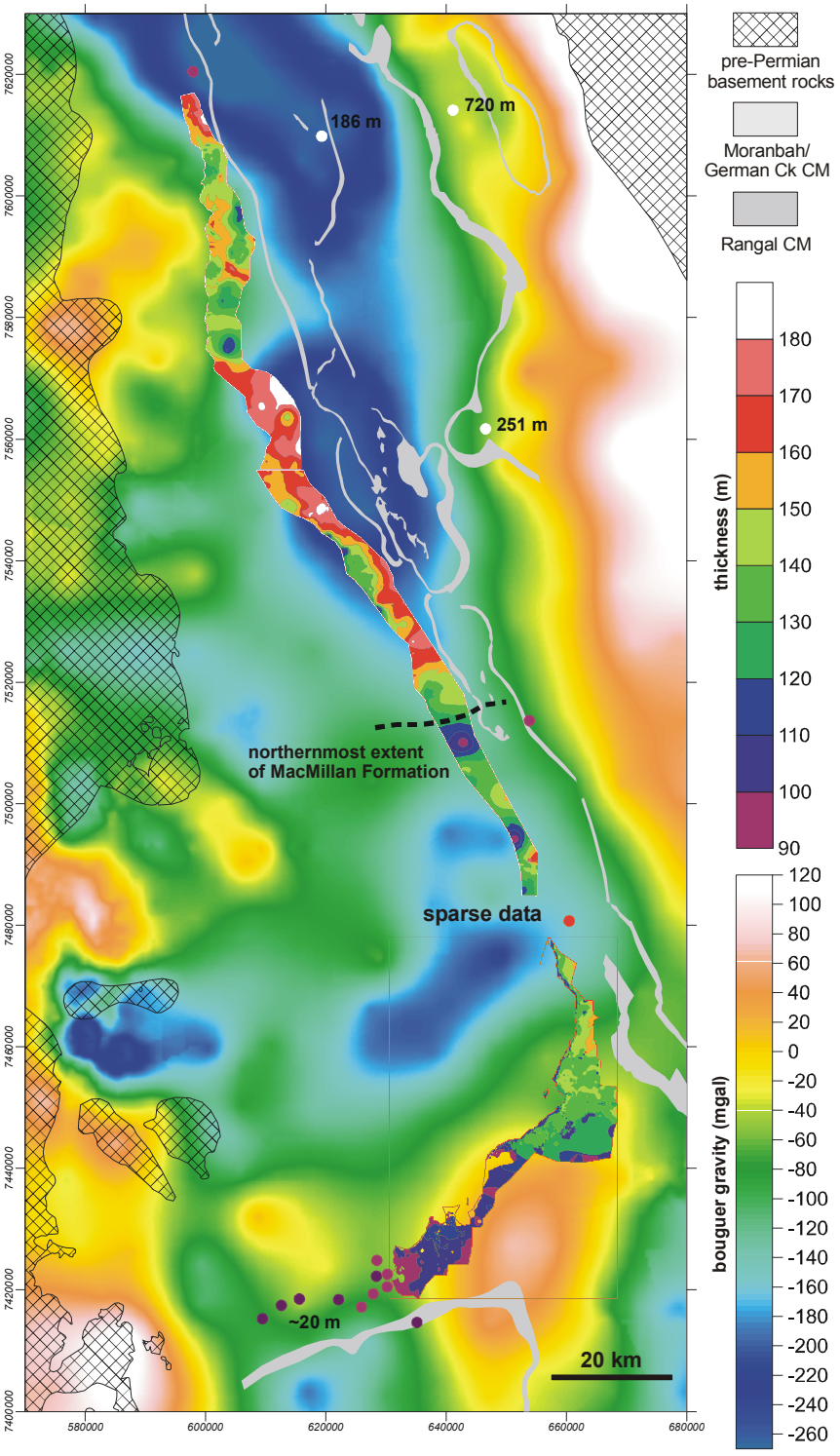

Figure 96 Total coal measure thickness overlain on Bouguer Gravity for the Supermodel region.

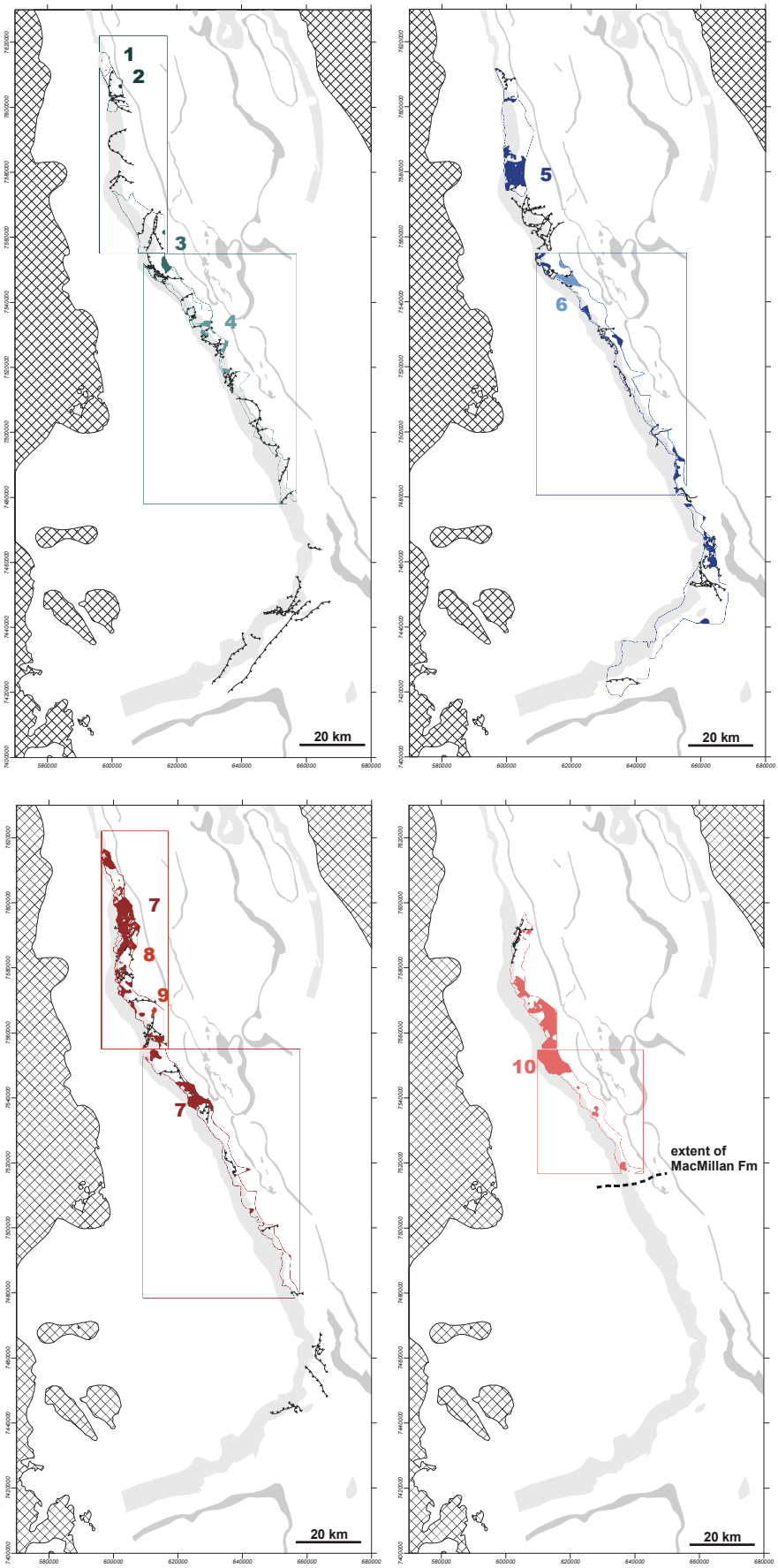

Figure 97 Distribution of thick interburdens (>40m) between superseams demonstrating the progradational nature of the Moranbah-German Creek CM and response to MacMillan transgression. Interburden numbers are located stratigraphically in Figure 42.

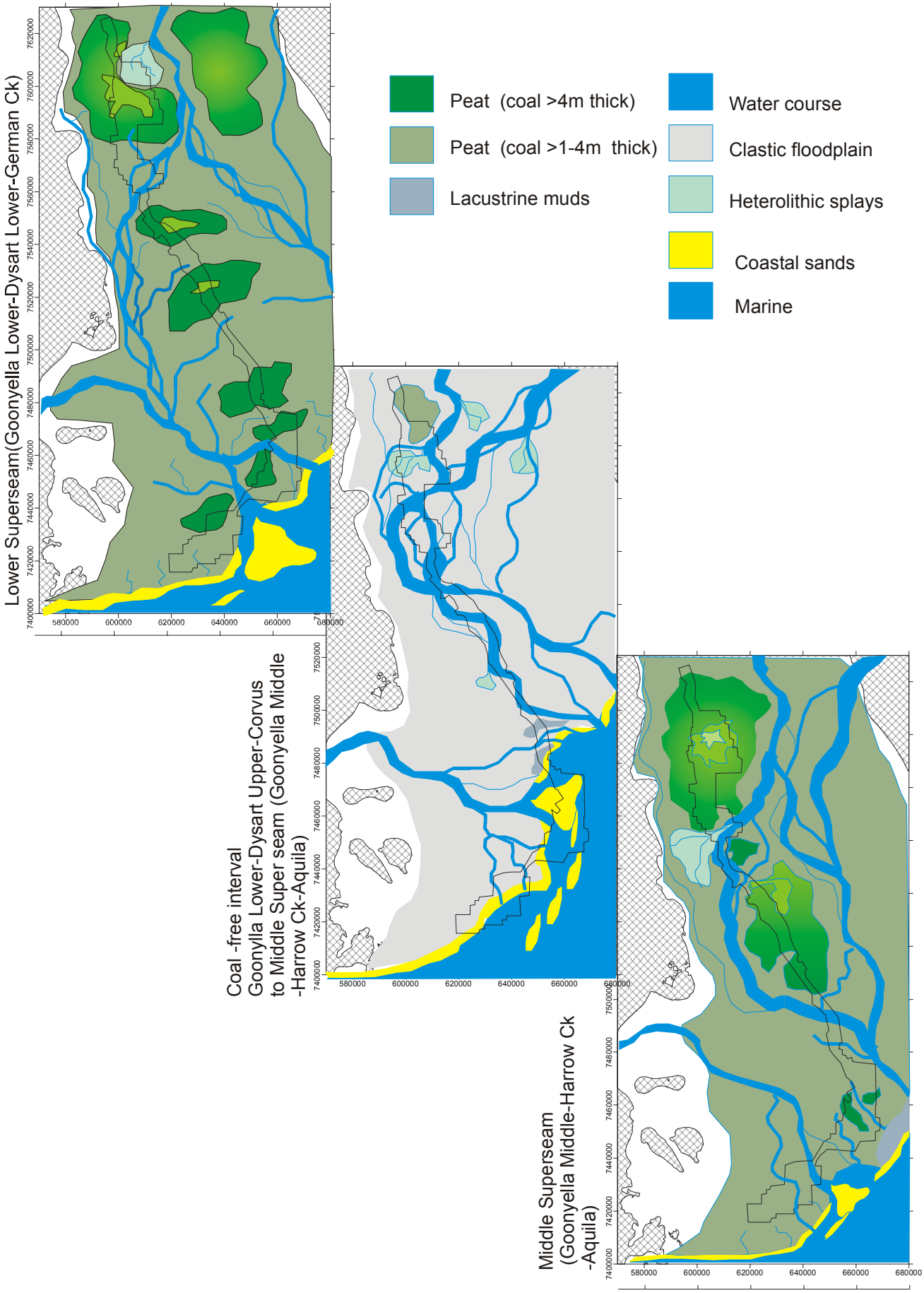
Peat (coal >4m thick)
Peat (coal >1-4m thick)
Lacustrine muds
Water course
Clastic floodplain
Heterolithic splays
Coastal sands
Marine
Lower Superseam(Goonyella Lower-Dysart Lower-German Ck)
Coal -free interval
Goonylla Lower-Dysart Upper-Corvus
to Middle Super seam (Goonyella Middle
-Harrow Ck-Aquila)
Middle Superseam
(Goonyella Middle-Harrow Ck
-Aquila)
580000
600000
620000
640000
660000
680000
7400000
7420000
7440000
7460000
7480000
7500000
7520000
7540000
7560000
7580000
7600000
7620000

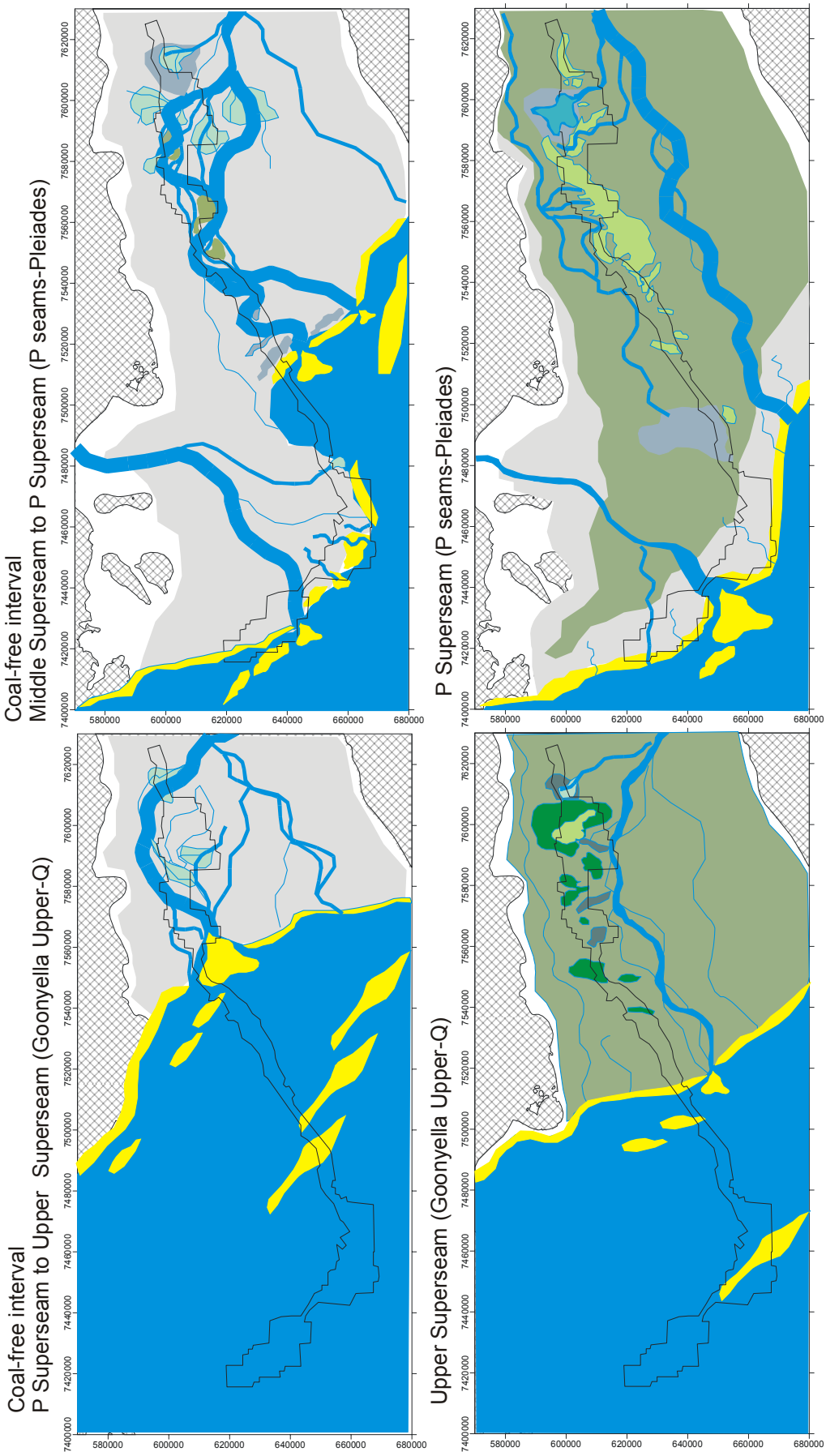

Figure 98 The schematic maps representing possible depositional environments at the time of depositional for superseams and coal-free clastic interburdens. The present basement outcrop and the outline of lease data overlie maps.

6 COAL SEAM GAS DISTRIBUTION

Joan Esterle and Ray Williams

6.1 Introduction

Coal seam gas is both a hazard and a potential resource for underground mines. Gas reservoir parameters vary widely in Bowen Basin coals. While gas content generally increases with depth of cover and permeability decreases there are significant differences in magnitude and variability, a consequence of geological history. Understanding geological controls on its distribution will aid in reservoir characterisation for drainage management and/or commercial production. Virgin gas content data for the Goonyella Middle seam in the Northern Tile and the German Creek seam in the Southern Tile were made available to the project to examine regional and local trends in gas parameters that could be related to the geology of the deposit. Sparse data were available for the Dysart seam in the Middle Tile.

6.2 Approach

All the gas content tests evaluated for this report directly measure the quantity of gas in the bore core (i.e. none are indirectly estimated from other coal quality parameters). Gas data were compiled and validated. Actual values are not reported due to confidentiality concerns. Trends in the data are presented which give some insight into geological controls that might be used as predictors of gas domains.

The basic approach involved:

- Compiling available data from participating mine sites, validation of data and deleting samples suspected of error;
- Aligning results collected by laboratories other than GeoGAS to that of GeoGAS to reduce variability due to operators;
- Calculating an average seam gas content at a normalised ash (15%), temperature (20°C) and pressure (101.3 kPa abs) for each borehole;
- Interpolating the composite seam data to develop trends and identify domains of similar gas content; and
- Comparing gas distributions to seam thickness, splitting patterns, rank and type, structure and stress to determine predictive relationships with geology.

6.3 Data

Gas data were available for 418 locations within the study area (Figure 100). All data used in this study were measured by either the fast or slow desorption techniques (AS3980-1999). The fast desorption method only varies from the slow desorption method in the time allowed for Q2 desorption (defined below). Instead of waiting up to 100 days for Q2 desorption to be completed, the core is taken "off line" and crushed to immediately release the remaining gas. In slow desorption testing, Q2 is normally the largest gas component, with Q3 being small (usually less than 2 m^3 /t). In fast desorption testing, Q3 is usually the largest gas component and it will vary with increasing total gas content. For CH_4 gas content coals, the measured gas content (Qm) is comparable with either test (Figure 99).

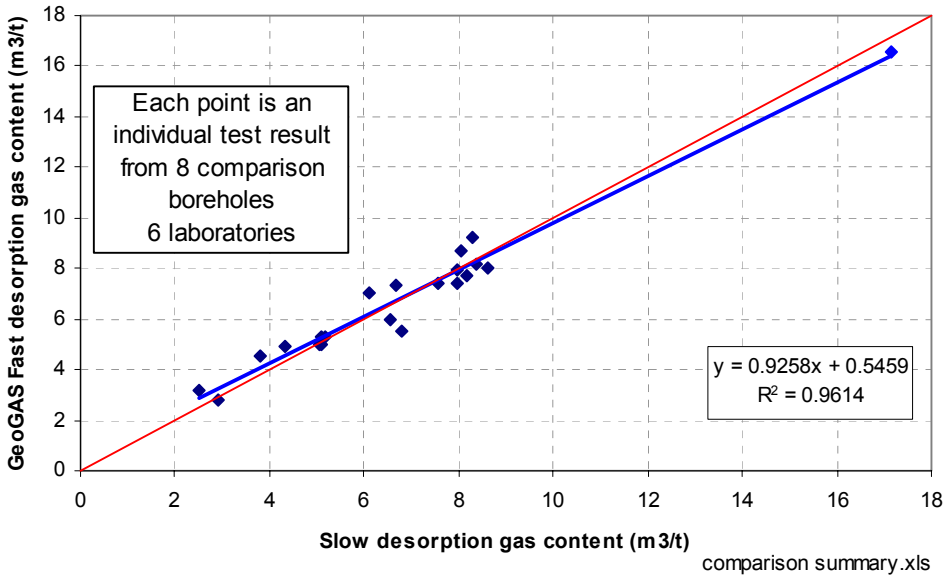

Figure 99 Comparison of slow desorption gas content testing with GeoGAS fast desorption testing 1997-2002.

Measured gas content Qm is the sum of Q1, Q2 and Q3 components that are measured as follows:

- Initial desorption in the field to determine the quantity of gas lost before sealing the core in the gas canister. The calculated quantity of lost gas per unit mass of coal is termed "Q1".
- The gas volume desorbed from the intact bore core per unit mass of coal, prior to removal of the core for crushing is termed "Q2".
- The gas volume released during crushing per unit mass of coal is termed "Q3".

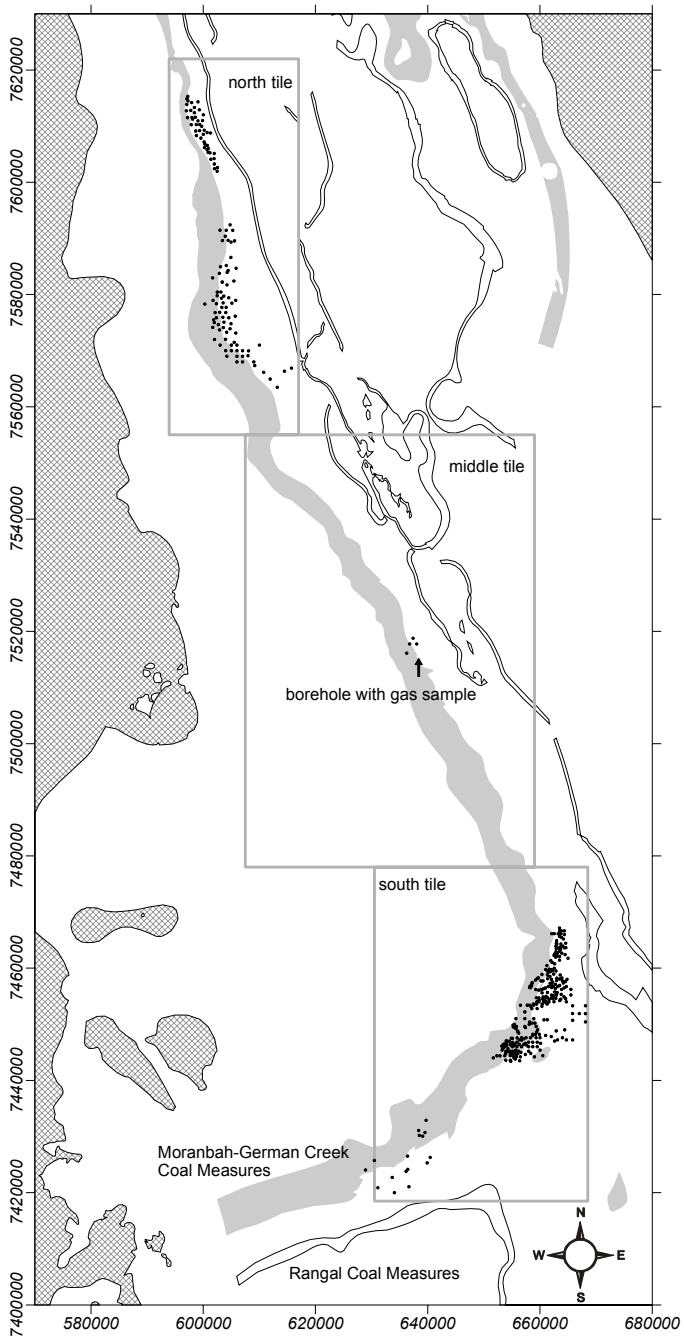

Figure 100 Map showing the location of boreholes for which gas content data were available in the study area.

6.4 Gas content variability within a single seam

Where multiple ply sample data were available for the Goonyella Middle seam in the northern tile, there was a tendency for the measured gas content to increase from the top to the bottom of the seam in the order of 1 to 2 m^3 /t, regardless of depth (Figure 101). The variability in gas content within a single seam is primarily related to changes in mineral matter content (ash), but is also thought to result from the change in coal lithotypes from dull to bright banded coals towards the base. This shift in coal type is coincident with a decrease in raw inherent ash yields and a decrease in stone partings. Although not universal, bright (vitrinite-rich) coals are often associated with increased adsorption capacity, particularly in high volatile bituminous coals (Beamish, et al, 1993; Faiz and Hutton, 1995;

Laxminarayana and Crosdale, 1999; Bustin and Clarkson, 1998). However, Ettinger et al (1967) originally stated that inertinite-rich coals had the greatest adsorption capacity (presumably on a comparable mineral matter basis). This relationship between coal type and adsorption capacity varies with rank (coal behaviour tends to converge around a rank of Rvmax 1.6%) due to the availability of pore space, in particular micro porosity, which can be occupied by moisture or mineral matter.

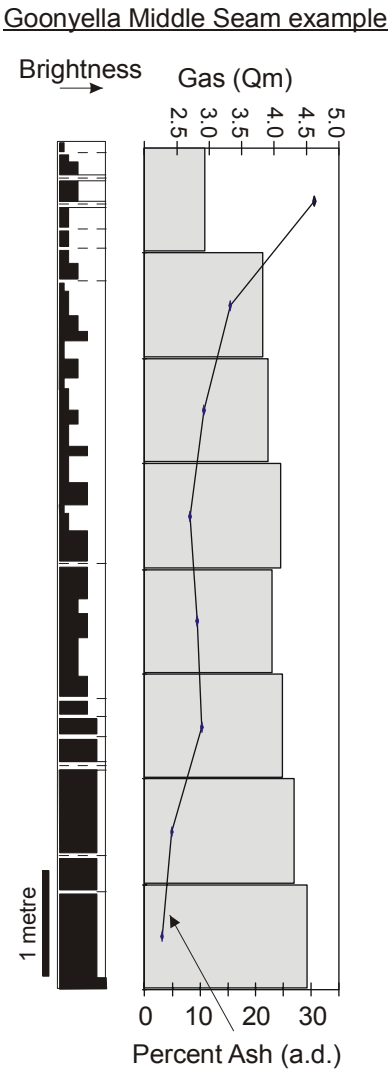

Figure 101 Variation in total measured gas content (Qm) within a single seam relative to coal type, ash yield (as determined) and depth in seam. Brightness profile increases in vitrain band content from left to right.

This trend is also observed in the Goonyella Lower seam where it also exhibits a "dulling up" sequence in its lithotype profile. For a given drill hole there is often an increase in gas content from the Middle to the Lower seam. This increase may be due to the increased adsorption capacity with increased rank, even at differences as small as Rvmax=1.1 to 1.2%. However, this increase in deeper seams is not consistent, even over short distances either due to the higher ash yields in the Lower seam or to gas loss through faulting (Figure 102).

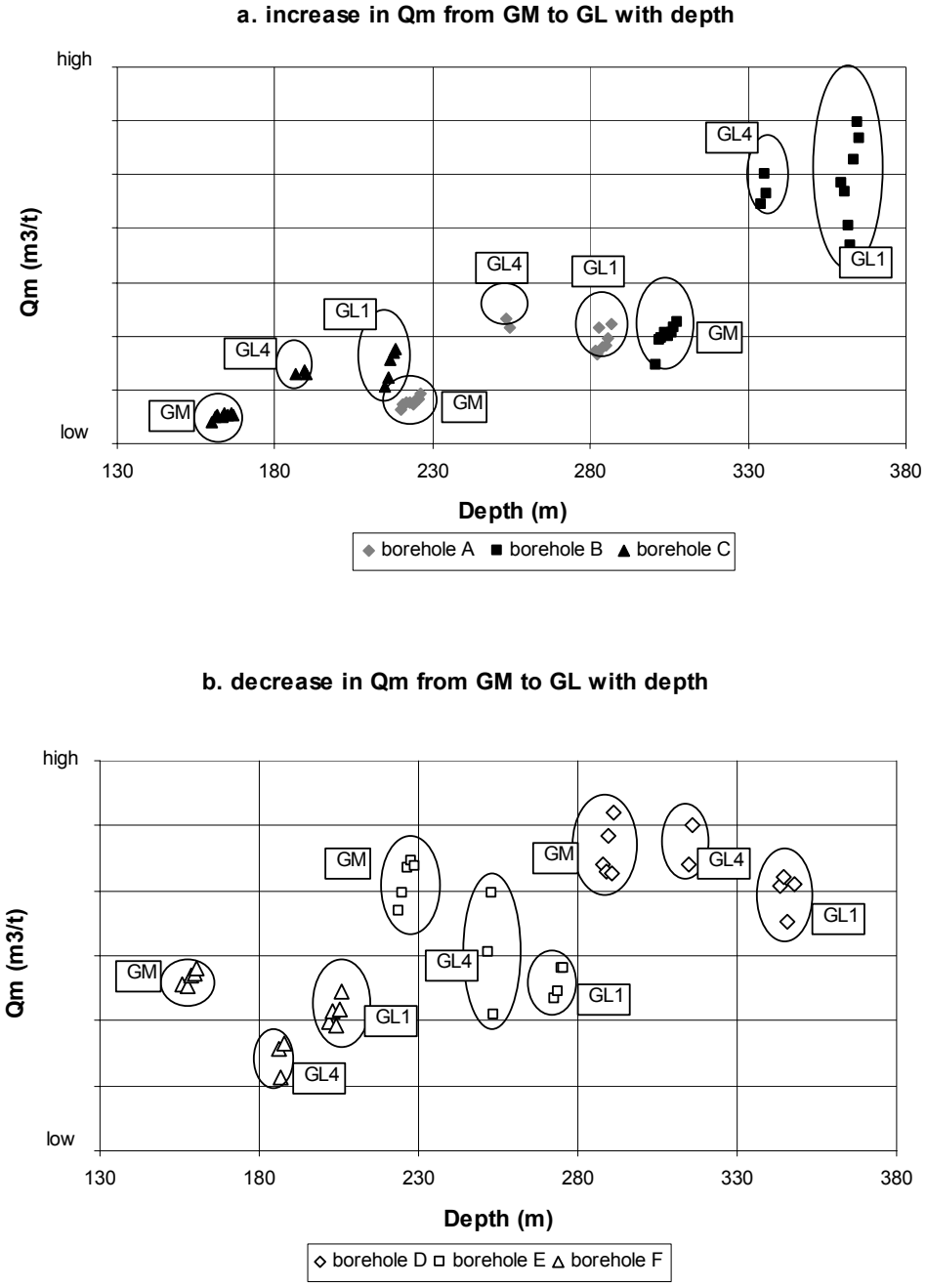

Figure 102 Change in measured gas content Qm with depth within and between the GM, GL4 and GL seams within a borehole demonstrating two different trends occurring in the Northern Tile.

Coal seams can generate gas at up to ten times their sorption capacity during coalification, but little of this is retained and many coals, particularly in Australian Permian measures are under saturated (Bustin and Clarkson, 1998). Seam gas can be lost at any point in the history of the coal seam, whether geological or present day as a consequence of uplift, reduced reservoir pressures or increased temperatures, faulting and fracturing or ground water movement through the seams.

6.5 Desorption rates

Desorption rate increases with increasing gas content, but for coals of similar gas content the rate can vary as a function of coal rank and type. Desorption rates, shown as IDR30 (the volume of gas desorbed after the first 30 minutes), are shown for the Goonyella Middle seam (Figure 103) and compared to data from the Bulli seam from the Sydney Basin. In both data sets, desorption rates increase with increasing measured gas contents, but are also affected by coal type and rank. Although of similar bituminous rank, the Bulli seam (Rvmax=1.2%) samples are duller and contain higher ash yields than the Goonyella Middle (Rvmax=1.1%) seam, and thus desorb more slowly for a given gas content. There could also be differences due to micro fracturing under differing tectonic histories, but this is not substantiated.

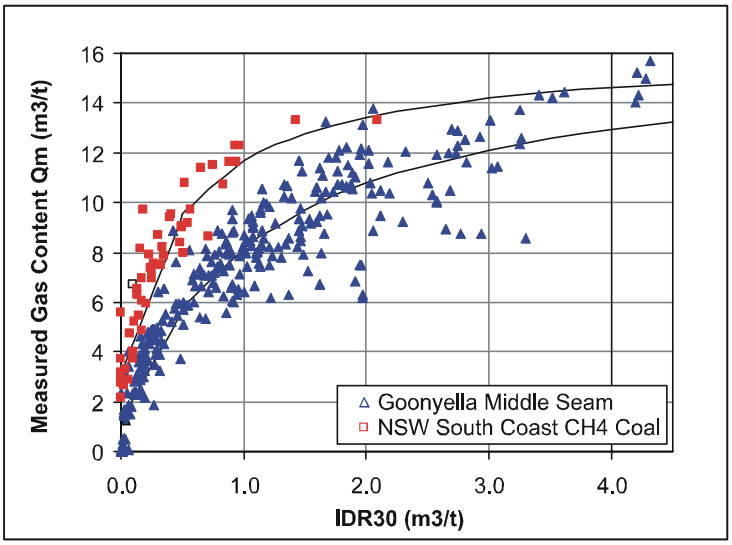

Figure 103 Graph showing variation in desorption rate (IDR30) with total measured gas content for the Goonyella Middle seam.

Although the available data set was small, the graph below suggests that desorption rates will increase with increasing vitrinite content (i.e. with increasing brightness) and with increasing rank (Figure 104). This is due to their increased fracture or cleat density. This behaviour would be enhanced where face cleat was open and aligned with principle horizontal stress direction.

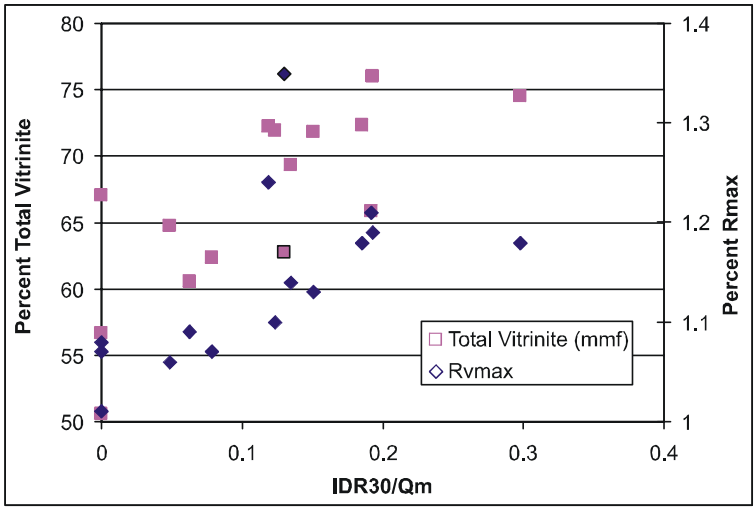

Figure 104 Graph of desorption rate (IDR30) normalised for total gas content (Qm) against vitrinite content and rank for a set of Goonyella Middle seam samples.

6.6 Variation in permeability

Gas drainage behaviour is a function of the measured gas content, desorption rates and coal permeability. Permeability decreases with increasing effective stress, which generally occurs with increasing depth of cover. Permeability also varies with coal type, fracture density/connectivity and mineral infilling. An example of the magnitude difference in permeability for bright-banded coals over dull coals for iso-rank samples from the Bulli seam in indicated in Figure 105 (Wold et al, 2001).

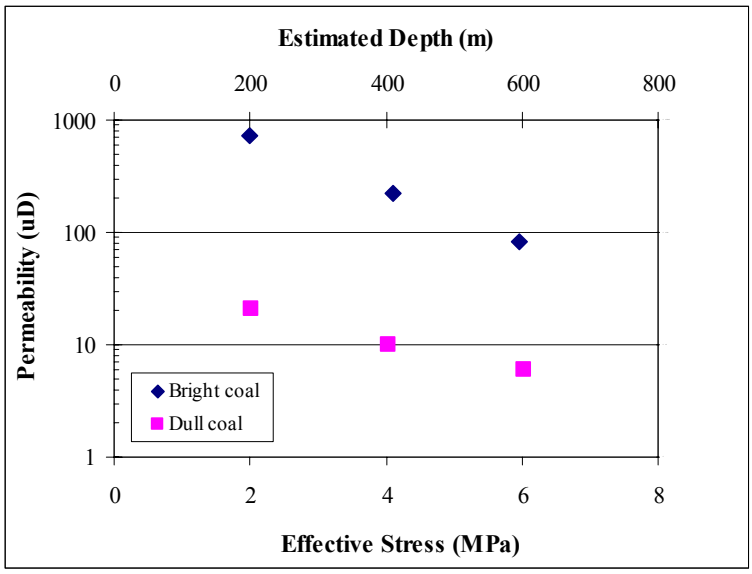

Figure 105 Graph of permeability vs. effective stress for bright banded and dull coals from the Bulli seam. Depth estimated from effective stress.

Due to issues of confidentiality, permeability measurements available for the Moranbah and German Creek CM seams in the study area could not be divulged directly, but examples of the variation observed between seams and areas as a function of coal rank and type are presented below (Figure 106). In these examples, permeability was measured *in situ* and it also decreased with depth of cover. Although not a predictive relationship, permeability generally increases with increasing vitrinite content, as observed in laboratory tests for the Bulli seam. Unexpectedly, the permeability also appears to increase with decreasing rank, but it is suggested that rank in these examples is overridden by coal type.

The direct associations between coal type, desorption rates and permeability suggests that, in the absence of direct permeability measurements, one could estimate areas of high and low permeability, relative to gas content, based on coal type.

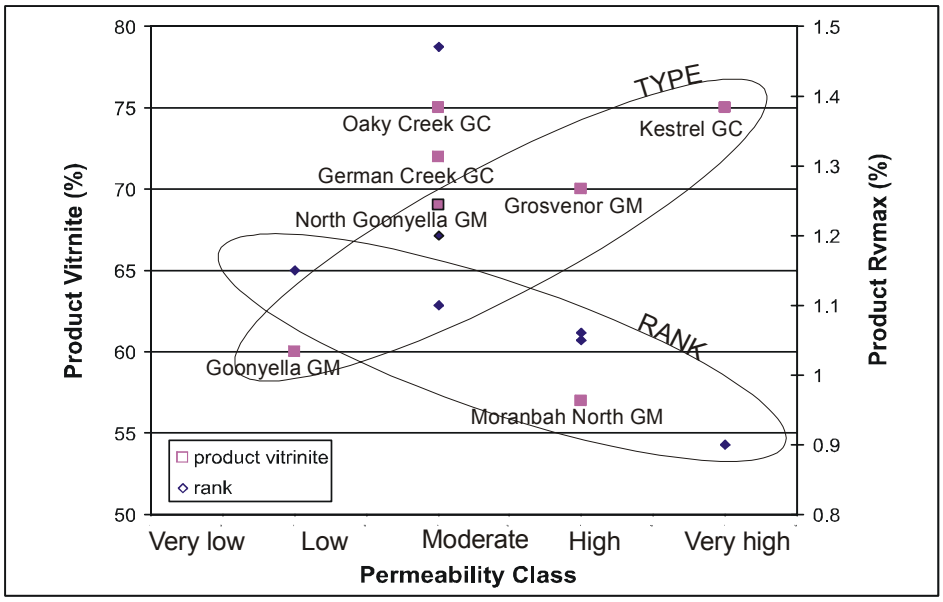

Figure 106 Graph showing variation in permeability classes for coals of different rank and type in the Moranbah and German Creek coal measures relative to a depth of 250m. Very low <1 mD; Low 1-5 mD; Moderate 5-40 mD; High 40-100 mD; Very high >100 mD. Seam labels for vitrinite only. GM=Goonyella Middle seam; GC=German Creek seam.

6.7 Relationship between measured gas content and depth

The general increase in gas content with increasing depth for seams in this study as well as published data for other Australian seams in indicated in Figure 107. Present day gas content is a function of a coal's ability to retain the generated gas. According to Eddy et al (1982), the relationship between gas content and depth is a function of increasing adsorption capacity with increasing reservoir pressure. A depth of 100 m is approximately equal to 1 MPa pore pressure, and laboratory tests have shown that optimum adsorption capacity occurs between 3 and 6 MPa, or 300 to 600 m depth. Higher rank coals also have a higher adsorption capacity for a given depth. Coal rank in along the western limb range from Rvmax=0.9% to 1.8% and as medium volatile coals have moderate storage capacities for their depth.

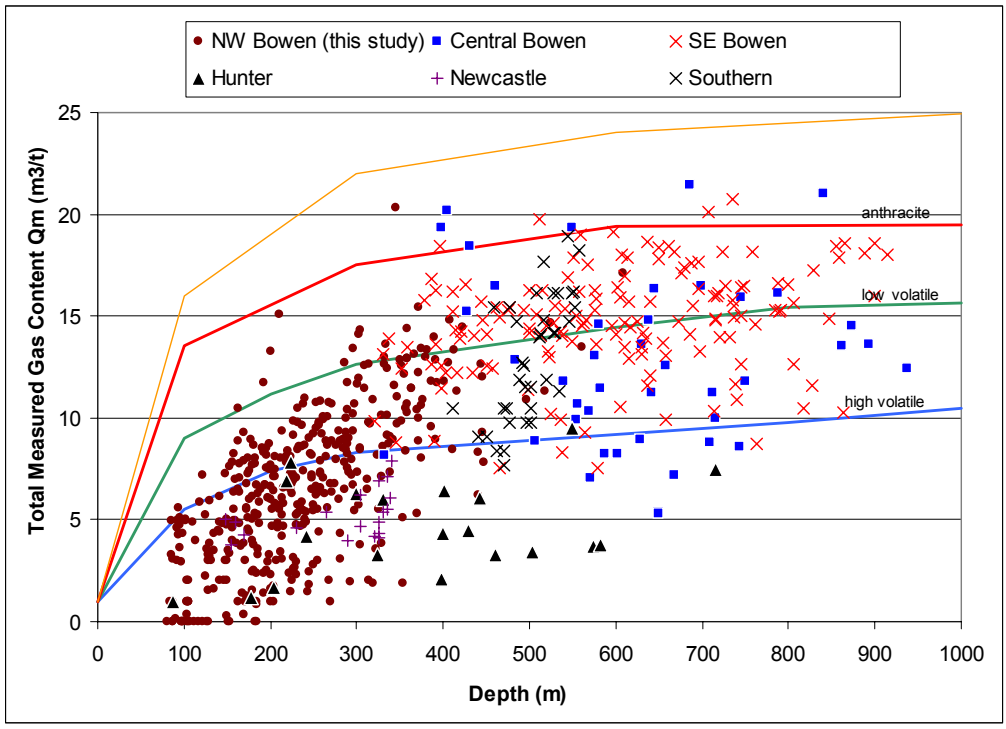

Figure 107 Graph of gas content vs. depth for data from this study and from other basins. Data overlain by generalised methane storage capacity as a function of rank from Eddy (1982). Data from this study presented at 15% ash; data from the central and SE Bowen Basin (Pattison et al *1993), and Central (Bocking & Weber 1991, 1993), Southern (Faiz & Cook 1991), Hunter Valley (Bocking & Weber 1991, 1993) and Newcastle (Creech 1991).*

6.8 Regional gas distribution

A comparison of gas contents for Goonyella Middle seam and the German Creek seam along the western limb of the basin with rank trends for the Goonyella Lower-Dysart-German Creek super seam in indicated in Figure 108. The highest measured gas content occurs at depths greater than 300 m in the northern and Southern Tiles. Data are sparse for the Middle Tile, but along with anecdotal evidence suggest low gas contents (eg < 2 m^3/t) at mineable depth (Sleeman, pers. comm.). Low gas contents in the Middle tile are coincident with the highest ranks seen on the western limb of the basin, particularly for the lowermost super-seam. All seams at the southern end of the Middle tile are densely intruded, which may serve to elevate rank locally. The areas of highest gas contents in the southern and Northern Tiles are coincident with coal ranks between Rvmax=1.2 and 1.6. In theory, this is an optimum range for gas generation, but more importantly gas retention.

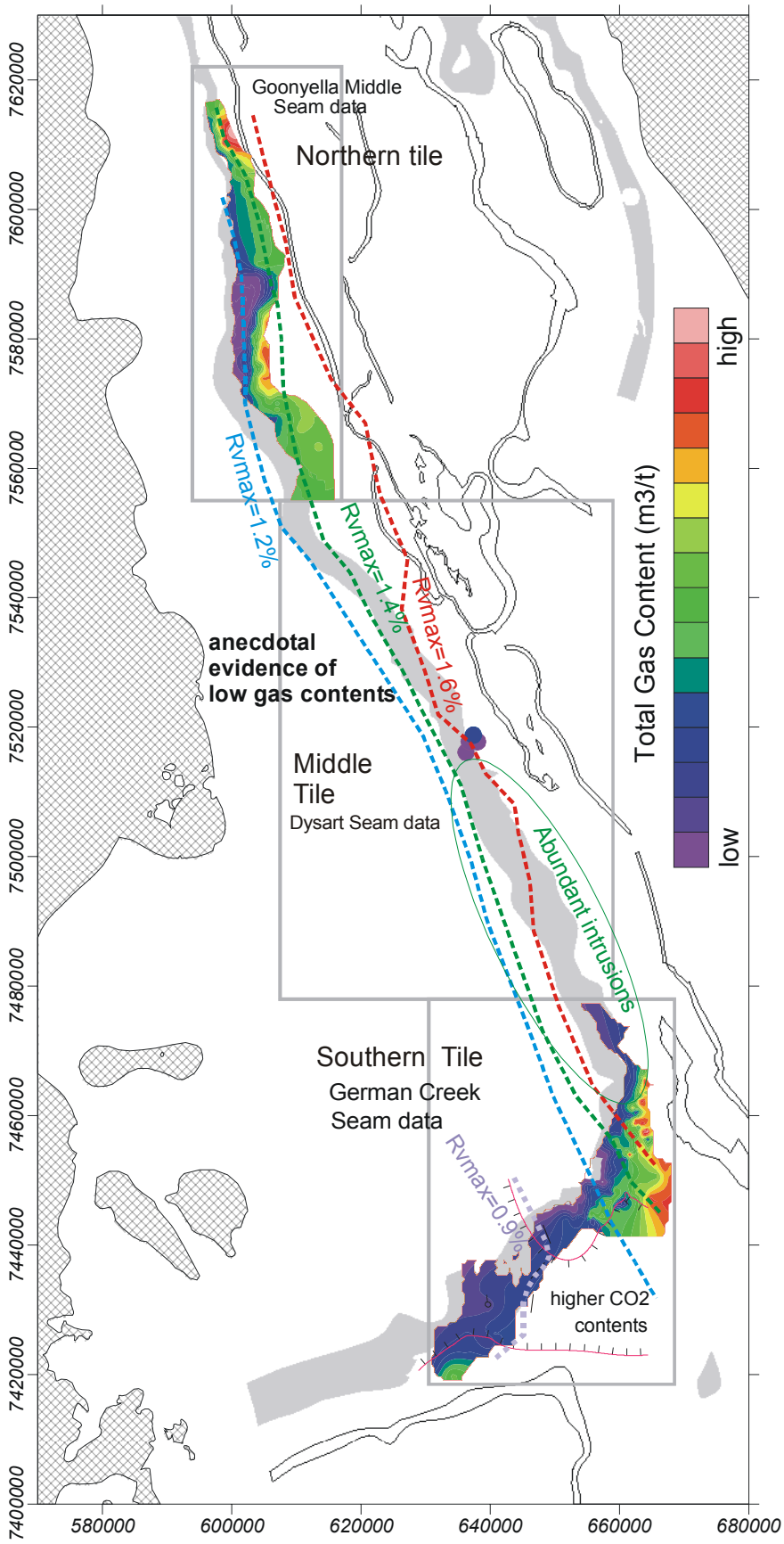

Figure 108 Map showing the distribution of low to high gas contents available for the study area. Note that the Northern Tile data are for Goonyella Middle seam, the Middle tile data are for Dysart seams and the Southern Tile data are for German Creek seam. Iso-reflectance lines (Rvmax) for the Goonyella Lower-Dysart-German Creek seam are overlain to give an indication of increasing rank with depth.

Gas is composed of >95% methane with minor amounts of carbon dioxide and nitrogen, except for areas in the Southern Tile. The high CO_2 concentration seen in the Southern Tile does not show a direct relationship with depth (Figure 109). The high concentration zone occurs in a relatively wide EW striking belt between Oaky Creek and Kestrel.

The origin of the CO_2 in this area is unknown. During gas generation, thermogenic CO_2 is expelled prior to CH_4 with increasing temperatures due to burial metamorphism. However, CO_2 can also be emplaced post-coalification, either regionally due to continental scale magmatisation (Baker et al, 1995), or locally due to intrusions (Faiz and Hutton, 1995). However, CO_2 can also be generated at shallow levels during coal oxidation (Gould et al, 1981) and be a remnant after the preferential desorption of CH_4. No obvious intrusions occur within the sequence in the high CO_2 area, but intrusions are prevalent further north from German Creek mine to Norwich Park mine, where CO_2 concentrations are very low. EW striking features that indicate deeply buried intrusives are observed within the aeromagnetic data, and these could be the progenitors. The magmatic, thermogenic or biogenic origins of the CO_2 can only be determined by isotopic analysis.

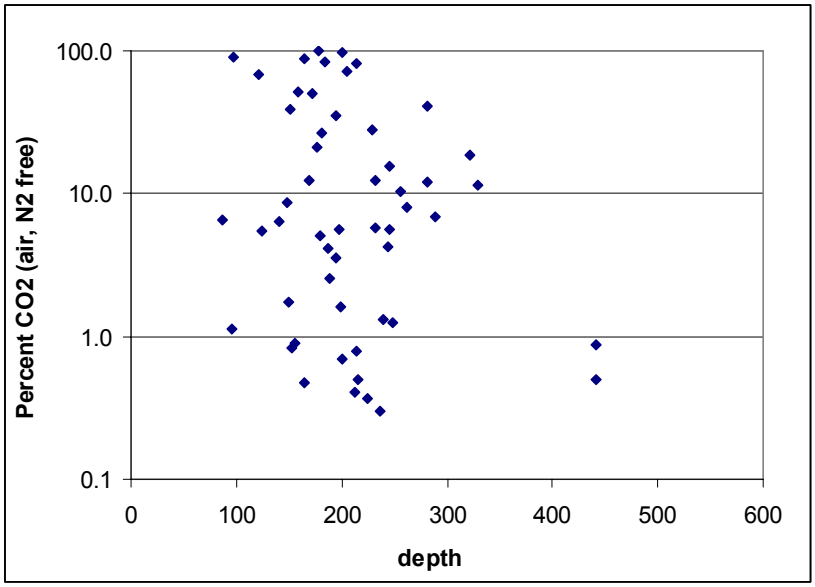

Figure 109 Graph showing the lack of relationship between CO2 content in gas and depth for the Southern Tile.

6.8.1 Gas distribution in the Goonyella Middle seam

The distribution of measured gas contents is presented in Figure 110 and overlain by elevation contours for the Goonyella Middle seam. The lowest gas contents occur in the shallow areas of the broad regional anticline from Goonyella through Moranbah North mine. The highest gas contents are associated within the steeper plunging synclines to the north and south of these areas at Wards Well and southeastern Moranbah North. In the Northern Tile, the iso-reflectance contours conform to the seam structure contours. As a result, gas content generally increases with both depth and rank, but is best retained in the synclines. These areas coincide with the hinge zones associated with the margins of the basement high discussed in previous sections of this report. This relationship is counter to conventional oil and gas exploration concepts in which anticlines are targeted for gas reservoirs.

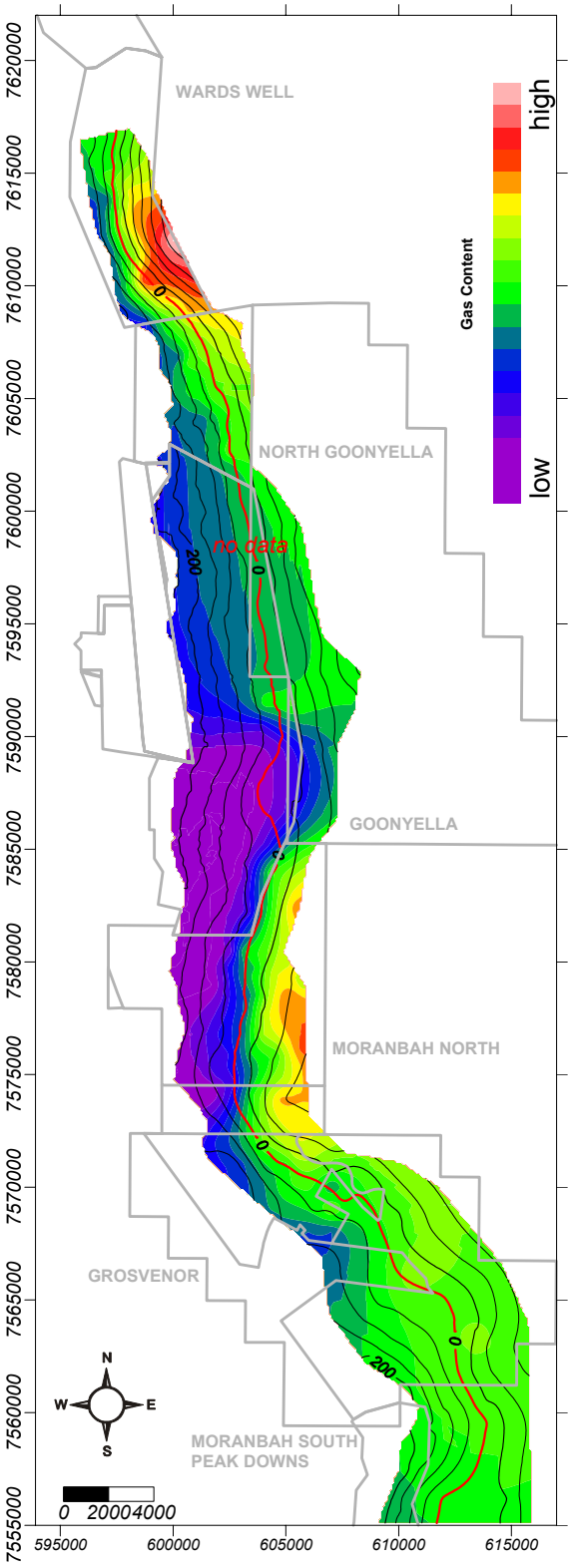

Figure 110 Distribution of measured gas content for the Northern Tile overlain by seam elevation. Zero elevation contours approximately 250m depth of cover highlighted in red. Data points presented in Figure 100.

Williams et al(2000) suggest that examining the consistency in relationship between gas content with depth can identify domains. Depths with lower than expected gas contents have been preferentially desorbed, whereas those with higher than expected contents may have been sites for preferential migration and/or retention. To determine this relationship, the measured gas content was divided by

depth to derive domains designated simply as low for depth, moderate for depth, high for depth and very high for depth (Figure 111).

An independent geostatistical analysis of gas/depth domains and their distribution is included in APPENDIX 3.

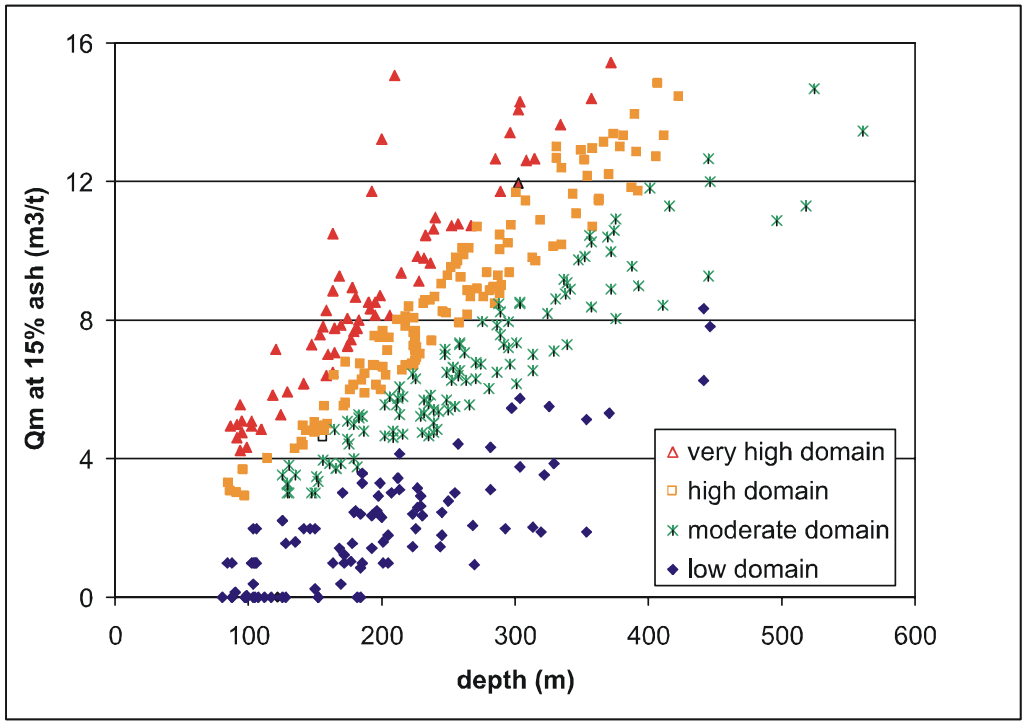

Figure 111 Graph of total measured gas content Qm versus depth of cover for samples in this study. Samples are colour coded by domain. Domains are contoured in following maps.

A very different distribution is observed when the gas data are plotted as domains normalised for depth (Figure 112). Data plotted in this manner should highlight anomalous areas requiring additional consideration, as gas is higher than expected for depth. Recent work by Bodden and Ehrlich (1998) demonstrates a predictive relationship between gas production and desorbed gas yield at 120 days divided by sample depth. This is due to better permeability at shallower depth. Overlain on the gas domain map are faults, face cleat orientation and an adjacent map shows vitrinite content that can potentially be used as an estimator of permeability.

More conventionally, the high gas for depth domains coincide with the local anticlines in the Grosvenor area and also with faulted zones in the North Goonyella area. In previous sections of this report it was noted that the face cleat orientation swings into alignment with principle horizontal stress direction to the south. Cleats in this NNE orientation should be open and enhance the permeability of the seam. The Goonyella Middle seam also becomes more vitrinite rich to the south as it splits and thins, increasing the fracture connectivity, and hence permeability of the seam.

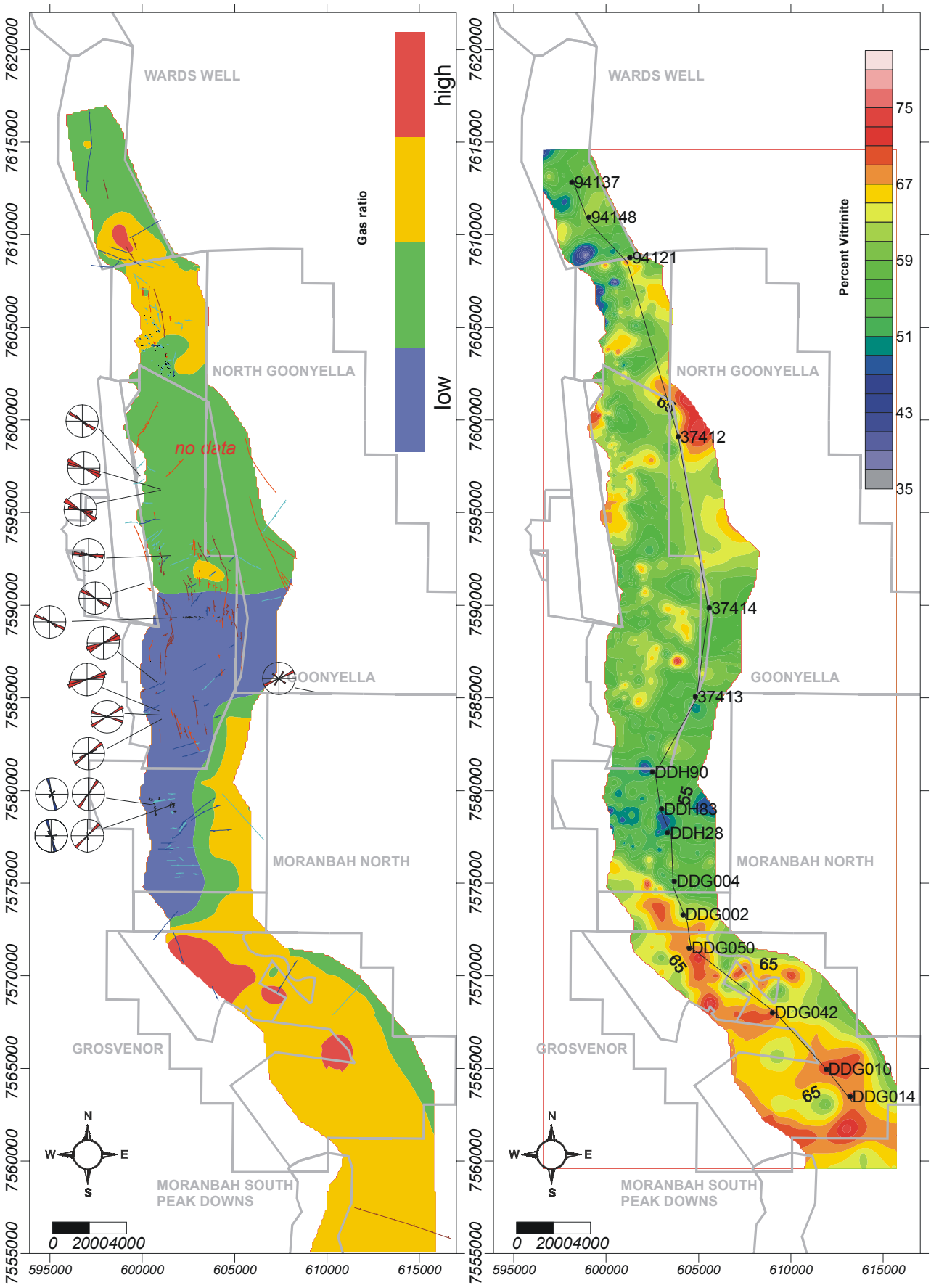

Figure 112 Maps showing the distribution of gas domains normalised for depth and overlain by faults and cleat (left) and total seam vitrinite content (as received). Section line for Figure 113 shown.

The relationships between seam geometry, vitrinite content and permeability allow a reservoir model to be presented for the Goonyella Middle seam (Figure 113). The figure below is a cross section through the Goonyella Middle seam demonstrating the vertical and lateral distribution of coal brightness lithotypes. Where thick, the base of the seam tends to be bright banded, but becomes duller up section. As the seam thins, the brighter banded leader and rider seams diverge from the main seam, and the main seam tends to become dominated by bright-banded coal. These bright-banded areas would tend to have better gas retention capacity, but also higher permeability for drainage. This lateral variability in the coal seam reservoir can potentially be used to assist in gas drainage design.

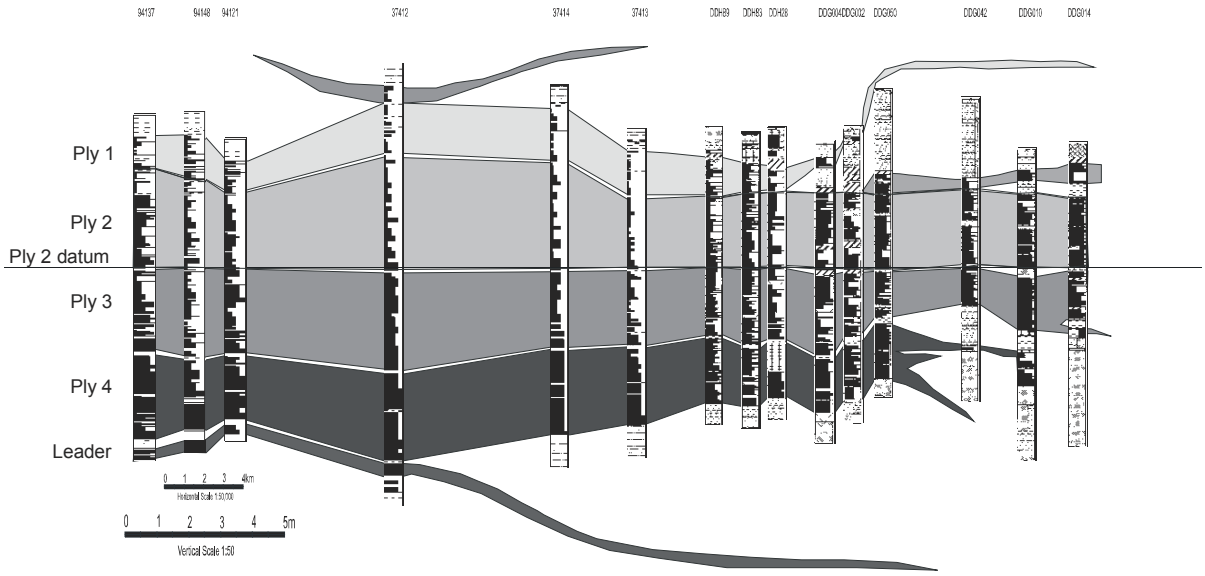

Figure 113 Cross-section through the Goonyella Middle seam showing the distribution of bright banded and dull coal within laterally correlative plies that split and thin from north to south.

6.8.2 Gas distribution Southern Tile German Creek seam

The distribution of gas content in the Southern Tile is more variable than in the Northern Tile, but still shows a general increase with depth, particularly in the higher rank areas where Rvmax >1.2%. Similar to the Northern Tile, gas contents are locally higher in synclines in the German Creek and Oaky Creek area (Figure 114). Low gas contents occur in shallow areas, but also at depth in the Kestrel area due to the lower rank and density of the seam.

At Oaky Creek, a small dome at depth, known as the Aquila High, also contains low gas contents. As previously discussed, gas contents are generally >95% methane, except in an EW striking belt between Oaky Creek and Kestrel leases.

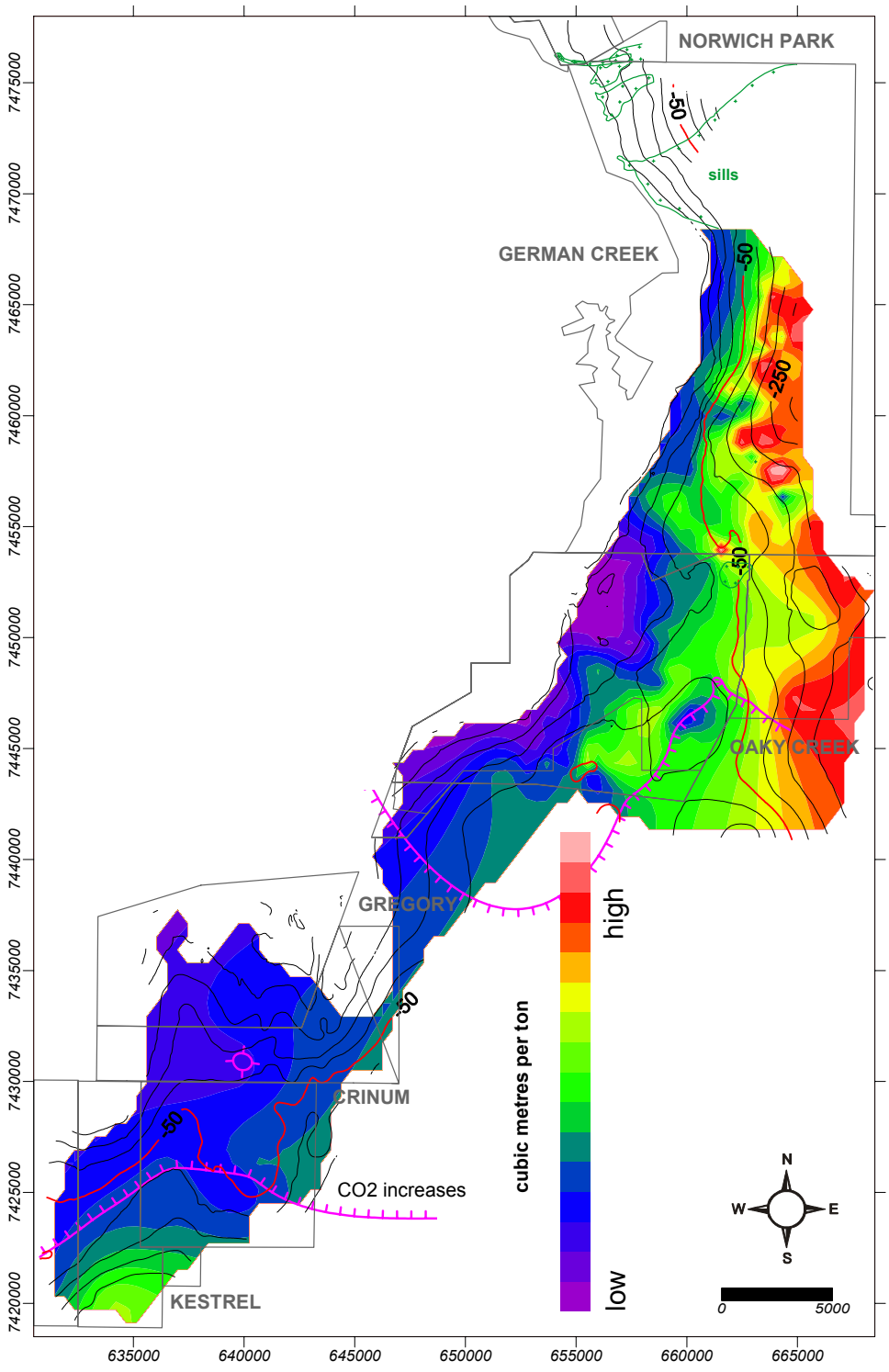

Figure 114 Map showing the distribution of measured gas contents for the German Creek seam in the Southern Tile, overlain by area of high CO2 in gas and elevation contours. The 50m line highlighted in red is the approximate 250m depth of cover.

Unlike the Northern Tile, the gas domains in the Southern Tile follow the general trends observed in the gas content, but also highlight migration up fault zones, creating areas with higher than expected gas contents for a given depth (Figure 115). This is true in the Oaky Creek area, although other fault swarms are not particularly higher in gas content.

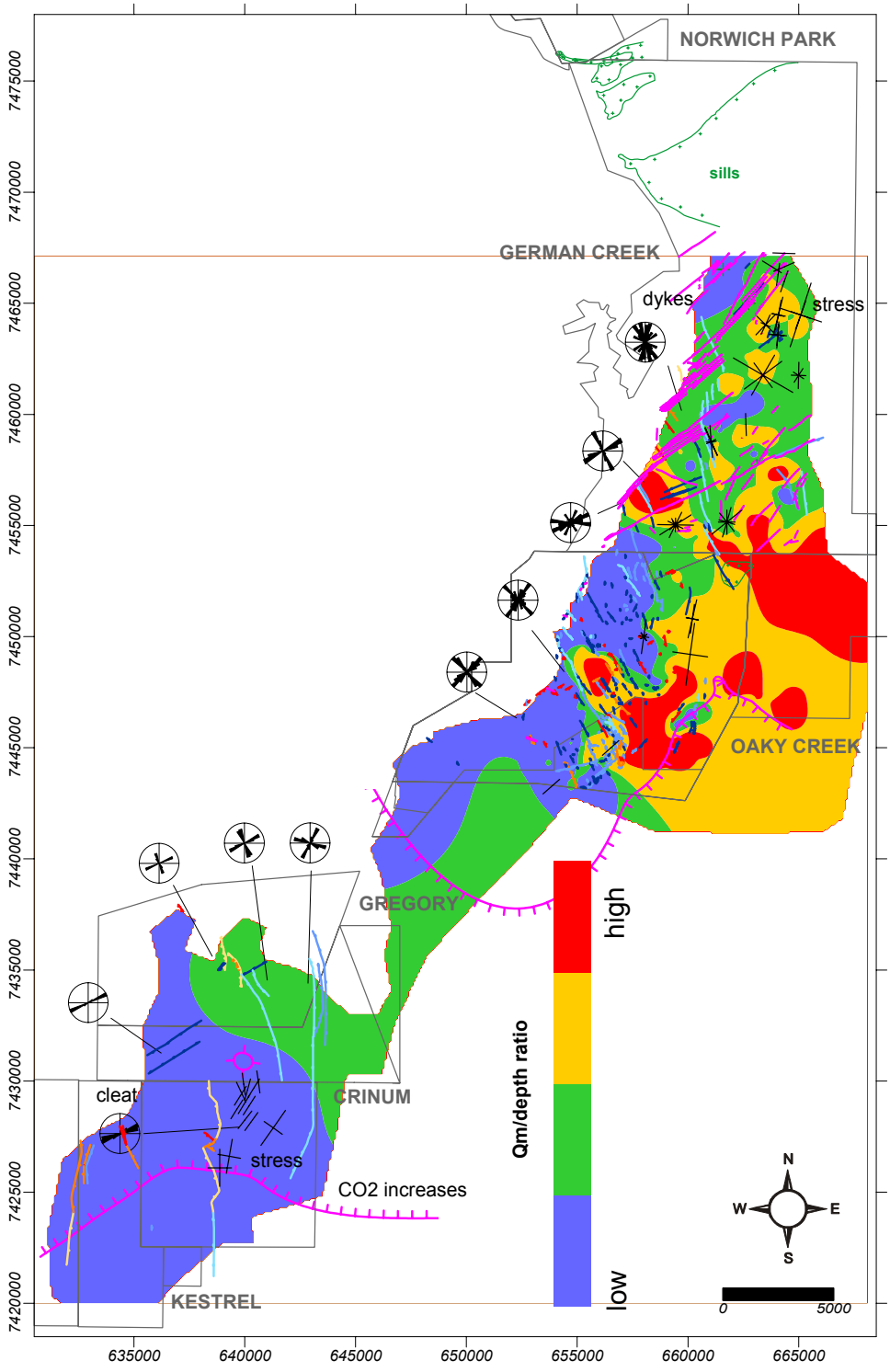

Figure 115 Map of gas domains overlain by faults, dykes, sills and cleat. Stress roses are also shown. Area of high CO2 is bounded by pink hatched lines.

Although there is local variability, the German Creek seam in the Southern tile is high in vitrinite content (>70%) relative to the Goonyella Middle seam in the Northern Tile. As a result, the general permeability of the seam is also higher in many cases. Principle horizontal stress is still generally NE-SW, but also shows variability in orientation and magnitude in the Oaky and German Creek areas. Both face and butt cleat are well developed. Face cleat is generally oriented NNW, orthogonal to the principle stress direction. As a result, some areas may be tighter than expected.

A closer look at the distribution of gas domains at Oaky Creek is used to develop another hypothesis for controls on gas distributions (Figure 116 and Figure 117). As previously stated, the higher gas contents are associated with synclines, particularly occurring between two domes (the lowermost named the Aquila High). Similar distributions have been observed at Oakgrove DSM field in Alabama (Pashin and Groshong, 1998).

The hypothesis is that the gas is lost over the anticlines due to fracturing, however gentle, during deformation. This is particularly true in the shallow areas and probably compounded by groundwater oxidation. Evidence for this occurs at German Creek where zones of higher hydrogen sulphide content form a halo around areas of low methane (Biggs, unpublished data). Microbial reduction of methane in the presence of sulphates can produce hydrogen sulphide, water and carbon monoxide.

Significant gas depletion of a coal seam reservoir can occur over geological time. In the case of coals occurring at shallow depths, leakage to the surface via tensile fractures associated with uplift and unloading is commonplace. Equally, in situations where the reservoir permeability is high, up-dip leakage along the seam could be anticipated (Pattison, 1998). As a result, deep seams can contain low gas contents even at depth. The association with the synclines, then, is one of retention under higher reservoir pressures, potentially with tighter fracture.

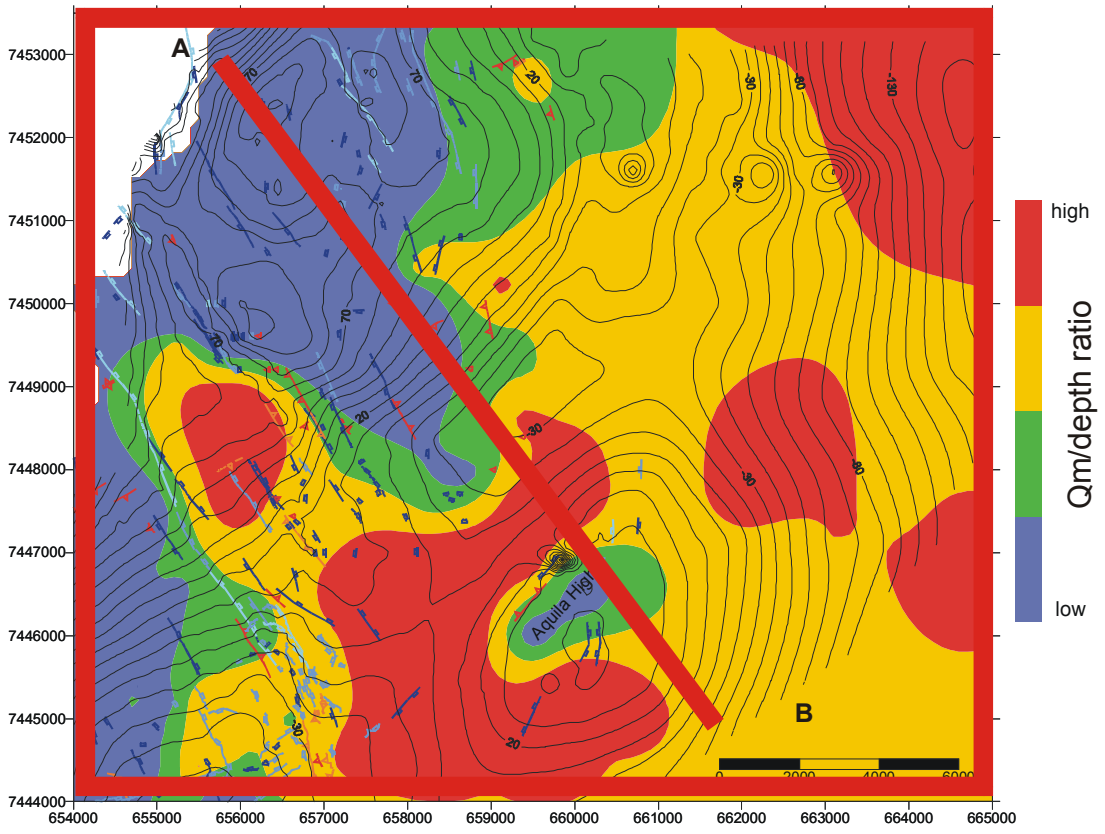

Figure 116 Map of gas domains at Oaky Creek mine, overlain by structure contours and faults. Cross-section line also shown.

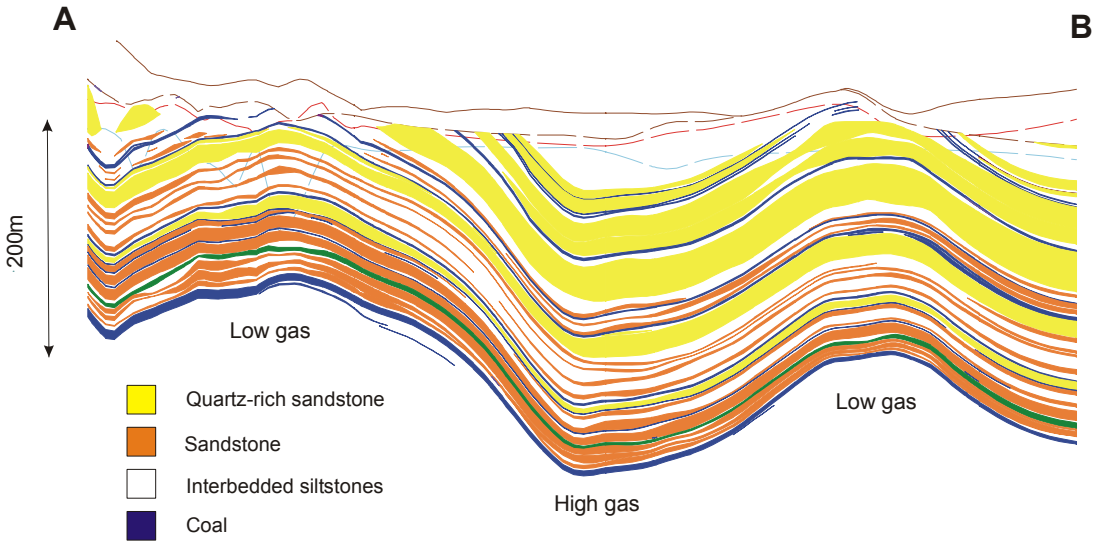

Figure 117 Cross section through the German Creek coal measures at Oaky Creek showing the distribution of seams and sandstone bodies relative to structure.

6.9 Discussion of gas generation and retention

Coal seam gas is generated as a by-product of the coalification process and it forms during both the initial low temperature (biogenic) phase of organic matter decomposition and later, with progressive burial and thermal maturation. With increasing burial over time thermogenic gases begin to form by progressive devolatilisation at about 100° C. As this process continues, large amounts of CH4, C02, N2 and water are generated. Consequently there is a positive relationship between the amount of gas generated and coal rank, as measured either by volatile matter content or vitrinite reflectance. The bulk of thermally generated methane starts in the rank range of medium volatile bituminous coals (Rvmax=1.2-1.4%), and continues up through the anthracite stage (Rvmax=3.0%).

Coals can generate up to 10x their gas retention capacity. Once generated, gas is stored in coal seams in either an adsorbed or absorbed state, and is contained within both the inherent micro pore (matrix) and macro pore (fracture/cleat) systems. Although some debate exists as to the exact mechanism of methane storage, evidence from adsorption isotherm experimentation indicates that the gas storage capacity of coal is governed by a combination of coal rank, reservoir temperature, the moisture content of the coal matrix, and reservoir pressure (Pattison, 1998).

Seam gas can be lost at any point in the history of the coal seam, whether geological or present day as a consequence of uplift, reduced reservoir pressures or increased temperatures, faulting and fracturing or ground water movement through the seams. Free gas will migrate preferentially to areas of lower pressure and/or higher permeability, making it difficult to use rank or present depth alone as a predictive tool for targeting gas. Conversely, gas can also be generated post-coalification, either during younger thermal events or as a by-product of microbial activity in ground water, thus re-saturating seams. The biogenic and/or thermogenic origins of gas in coal can only be determined by detailed studies of thermal history using isotopic characterisation.

7 SUMMARY AND CONCLUSIONS

The Supermodel 2000 project provides a compilation of current data and knowledge, as at December 2000, about the Moranbah-German Creek CM that occur along the western limb of the central Bowen Basin and how they fit into its evolution. The evolutionary sequence controlled the coal seam thickness and interburden distributions, gas generation and retention, and subsequent structural deformations that impact on coal mining conditions. The abundance of company drilling data contributed to the project allowed the three-dimensional geometries of these features to be mapped and presented for the first time at a regional scale.

The Bowen Basin formed during initial extension in a back arc rift setting that bequeathed a NE and NW trending structural grain that would influence the deposition and subsequent deformation of the coal measures. The coal measures developed during the onset of foreland loading in the Late Permian record the terrestrial infilling of the basin after a basin-wide marine transgression during the thermal sag phase. The Moranbah-German Creek CM form a wedge that decreases in thickness to the west and to the south and which grades into sediments deposited under coastal and marine conditions. The basin filled first from the west and then from the north and northeast through the seaward progradation of fluvio-deltaic to coastal environments, followed by an increasing transgression that culminated in the deposition of the McMillan Fm.

The most extensive, southerly progradation is capped by the Lower Superseam. The peat that formed the coal accumulated in vast, low-lying peat mires that initially tracked the coastal regression, as evidenced by the pervasive northeasterly trend both in floor splits and in the thickest pods of coal from Peak Downs to the south. Thick peats accumulate in an environment of slow subsidence devoid of clastic influx. With slow subsidence comes the possibility of increased oxidation, resulting in increasing dull coals in the thick non-split portions of coal seams. The bright-banded, or vitrininite-rich coal increases generally as seams split and thin, and in the Lower superseam, from the Middle tile southward. In the Northern Tile, we suggest that stable basement provided a platform to assist in the consistent accumulation of stacked peat mires with punctuated flooding from the adjacent channel systems traversing the more rapidly subsiding hinge zones of a basement block. Residence time for these peat-accumulating mires with minimal clastic sediment influx is estimated at around 100,000 years.

Increased influx of volcaniclastic sediments from the developing arc to the northeast of the basin and increased subsidence overwhelmed peat accumulation and massive to well bedded sandstones were deposited primarily in anastomosing, low-sinuosity channel networks that traversed floodplains and shallow lake systems on their way to the coast. A westerly sediment source and paralic conditions prevailed in the southern tile as evidenced by the quartz-rich nature of the sandstones and geometries of and sedimentary structures within sandstone bodies that formed as distributary mouthbar/channel complexes and reworked shoreline sands.

If thick, laterally extensive coal seams record periods of low subsidence and reduced clastic influx to the basin, and thick, relatively “coal-free” and sandstone-dominated interburdens that of higher subsidence and influx, then the above scenario can be generally applied to the remainder of the stratigraphic sequence of the Middle, P and Upper Superseams and their interburdens. At a local scale,

differential compaction of peat and mud versus sand created local accommodation space that attracted channel avulsion. This resulted in the "Z" splitting and offset stacking of sandstone bodies between thin coal seams up section so commonly seen. However, at the basin scale there is interplay between the continued fluctuations of sea level, which upon rising served to raise base level and back the system up, the pulses of great sediment supply shedding from the rising arc and inferred subtle movements in the basement that channelled sedimentation into areas of greater subsidence. The latter is evidenced by the increased occurrence of seam splitting, stacked channels and coals, and greater cumulative thickness of the Moranbah-German Creek CM over areas of gravity lows within the southerly decreasing wedge. The wedge thins over the present-day Comet Ridge that also forms a basement high in the gravity.

This sequence was progressively buried by continued terrestrial sedimentation and southward progradation of the systems that deposited the Ft Cooper Fm to Rangal Coal Measures during subsidence and escalating foreland loading and thrusting to the east of the basin. Maximum burial of the coal measures occurred during this time prior to basin closure and thrusting during the mid Triassic. Geothermal gradients were interpreted to be relatively high and burial coalification increases generally towards the east and northeast of the basin. Primary thermogenic gas would be generated during this period. Along the western limb, the local increase in rank (Rvmax >1.6%) and the abundance of intrusions in the southern part of the Middle Tile suggest that rank could have been subsequently elevated during the Cretaceous igneous activity and uplift.

Cleat formed early during the burial history, as suggested by clay mineral infill dated at ~245 Ma. Cleat orientation varies at a regional scale in response to subtle basement features, but there are no local anomalies correlated with faults, suggesting that these structures are younger. Overprinting cleats developed close to thrust faults and bedding-plane shears corroborates this.

Increased compression during basin closure resulted in the propagation of thin skinned thrust faults throughout the entire basin. The most significant of these in the Supermodel area is the Jellinbah Thrust system that occurs approximately 12 to 15 km to the east and extends from Collinsville to south of Blackwater with approximately 600 to 800 m of throw. The currently mined measures are positioned well within the footwall of this structure, and by comparison show only subsidiary and relatively minor faulting that none-the-less mimic the style of the north-trending regional structure. The thrust flats tend to occur within or at the top of coal seams and preferentially ramp up through seams along the margins of thick sandstone bodies. On their own, they can create poor mining conditions, but compounded with the transition between strong and weak roof, they form some of the most damaging structures. This compressional event served to reactivate many pre-existing normal faults, in particular the deep-seated basement structures inherited from the early Permian.

Throughout the Jurassic and Early Cretaceous, the Surat Basin developed over the Bowen Basin under relatively quiescent tectonism. Although the succession is thick, paleo-geothermal gradients are interpreted to be very much lower than during the Permian and Triassic periods. The break-up of Gondwanaland resulted in a marine transgression over the Surat Basin and the formation of fault-controlled extensional basins. During this period, extensional volcanism resulted in the intrusion of abundant dykes, sills and plugs into the Permian coal measures. Mild reactivation of shallow faults and bedding plane shear occurred at this time.

Up to 1500 m of uplift occurred in the eastern Bowen Basin during the Late Cretaceous accompanied by the formation of ubiquitous vertical joint sets. The new incised land surface along the western limb is preserved as the Tertiary unconformity, as sediments and large volumes of basalt of this age infill it. Subtle movements in the basement blocks are also thought to influence the distribution of Tertiary fill, as evidenced by thick sediments occurring over the basement hinges in the Northern Tile.

The present day stress regime evolved as a result of Tertiary plate movements, particularly the accretion of terranes in Papua New Guinea, and is currently a reflection of plate-boundary forces acting on the Australian continent. In the western limb of the basin the regional horizontal stress is a consistent NNE-NNW compression, with local variations near existing faults.

The development and subsequent deformation of the coal measures have had direct influence on the distribution of seam gas, that is both a hazard and a potential resource. In general, measured gas content increases with depth but variability is too high to use this relationship as a predictor. However, shallow areas with higher than expected measured gas contents should have better permeability for drainage or production due to reduced pressure. Seam gas can be lost at any point in the history of the coal seam, whether geological or present day as a consequence of uplift, reduced reservoir pressures or increased temperatures, faulting and fracturing or ground water movement through the seams. Seam gas can also be secondarily emplaced due to biogenic processes or to intrusive activity. In the Supermodel area, permeabilities within a seam can be related to increased vitrinite content and, more importantly open face cleat oriented in the position of maximum horizontal stress. Higher measured gas contents tend to be associated with synclines suggesting that the generated gas was retained due to hydrostatic pressure. Areas of higher gas domains for a given depth due occur in classical association with broad anticlines and faulted ground, but again not predictably. Except for an area in the southern tile, all gas is primarily methane. The origin of the high carbon dioxide levels in the gas, regardless of measured content in the southern tile is unknown at this time, but may be related to intrusions at depth that do not intersect the coal measures.

The impact of the development and subsequent deformation of the coal measures upon mining conditions is incumbent upon the distribution of thick seams, massive sandstone belts, faulting, maximum horizontal stress orientation and gas domains. The maps presented in this report are intended to give a regional picture of the development and distribution of the coal measures, their interburden character and structures. It provides a framework in which to examine differences in rock mass and gas behaviour that occur between individual minesites, but does not replace detailed work at the minescale. Many of the relationships observed can be used for area selection, but more importantly to prompt geologists and engineers to hypothesis test within their rich datasets prior to extraction of the coal.

8 REFERENCES

Australian Standards AS 3980-1999. Guide to the determination of gas content of coal - Direct desorption method.

Baker, J.C., Fielding, C.R., De Caritat, P. and Wilkinson, M.M., 1993. Permian evolution of sandstone composition in a complex back-arc extensional to foreland basin. the Bowen Basin, Eastern Australia. Journal of Sedimentary Petrology, 63 (5), 881-893.

Baker, J.C., Bai, Guo P., Hamilton, P.J, Golding, S.D., Keene, J.B., 1995. Continental-scale magmatic carbon dioxide seepage recorded by dawsonite in the Bowen-Gunnedah-Sydney Basin system, eastern Australia, Journal of Sedimentary Research, Section A. Sedimentary Petrology and Processes, 65 (3), 522-530.

Battino, S. and Hargraves, A.J., 1982. Seam gas pre-drainage at Ain, Cook, Leichardt, Metropolitan and Moura No 2 Collieries. Proceedings of Symposium on Seam Gas Drainage with particular reference to the working seam, Wollongong, NSW, Australia, 157-171.

Beamish, B.B., Crosdale, P. J. and Gamson, P.D., 1993. Characterising the methane sorption behaviour of banded coals in the Bowen Basin, Australia. Proceedings of the 1993 international Coalbed methane symposium, Birmingham, AL, United States, May 17-21, 1993, 145-150.

Beeston, J.W., 1986. Coal rank variation in the Bowen Basin, Queensland. International Journal of Coal Geology, 6 (2), 163-179.

Bocking, M.A. and Weber, C.R., 1991. The Electricity Commission's involvement in coalbed methane, with early results from the Sydney Basin. In W.J. Bamberry and A.M. Depers (eds). Gas in Australian Coals, GSA Symposium Proceedings, 13-18.

Bocking, M.A. and Weber, C.R., 1993. Coalbed methane in the Sydney Basin, Australia. Proceedings of the 1993 international Coalbed methane symposium, Birmingham, AL, United States, May 17-21, 1993, 15-23.

Bodden, W.R. III and Ehrlich, R., 1998. Permeability of coals and characteristics of desorption tests: Implications for coalbed methane production. International Journal of Coal Geology, 35, 333-347.

Bustin, R.M. and Clarkson, C.R., 1998. Geological controls on coalbed methane reservoir capacity and gas content. International Journal of Coal Geology, 38, 3-26.

Charleson, S.W. and Gray, I., 1999. Report on stress measurement at German Creek Mine during June 1999, Sigra Pty Ltd report, 22pp.

Clarkson, C.R. and Bustin, R.M., 1996. Variation in micropore capacity and size distribution with composition in bituminous coal of the Western Canadian Sedimentary Basin: Implications for coalbed methane potential. Fuel, 75 (13), 1483-1498.

Creech, M., 1992. Geological controls on gas distribution in the Newcastle Coalfield. 26th Newcastle Symposium on Advances in the study of the Sydney Basin, 80-86.

Desbarats A.J. and Dimitrakopoulos, R., 2000. Geostatistical simulation of regionalized pore-size distributions using Min/Max autocorrelation factors, Mathematical Geology, 32 (8), 919-942.

Devey, D.M., 1983. The influence of structure on the development of underground mines in the western Bowen Basin. In Proceedings of a symposium on the Permian Geology of Queensland, Geological Society of Australia (Queensland Division), Brisbane, 73-80.

Dimitrakopoulos, R., Li, S., Scott, J. and Mackie, S., 2001. Quantification of Fault Uncertainty and Risk Management in Underground Longwall Coal Mining. ACARP Project C7025 Report (Vol. I). W H Bryan Mining Geology Research Centre, The University of Queensland, Brisbane, Australia.

Draper, J.J. and Balfe, P.E., 1985. Late Permian stratigraphy - western Bowen Basin, Queensland. In Proceedings of the 19th Symposium on Advances in the Study of the Sydney Basin, Department of Geology, University of Newcastle, 106-109.

Draper, J J; Palmieri, V; Price, P L; Briggs, D J C; Parfrey, S M, 1990. A biostratigraphic framework for the Bowen Basin. In J.W. Beeston (ed), Proceedings of the Bowen Basin Symposium 1990, 26-35.

Eddy, G.E., Rightmire, C.T. and Bryer, C., 1982. Relationship of methane content of coal rank and depth. Theoretical versus observed. Proceedings of Conventional Gas Recovery Symposium, SPE/DOE 10800, 117-130.

Enever, J.R., 1992. Hydraulic fracture stress measurements data interpretation and analysis, Oaky Creek No.2 colliery - feasibility study. Strata-tek consulting report, 7pp.

Enever, J.R., Bocking, M.A. and Clarke, I. 1994. The application of in-situ stress measurements and numerical stress analysis to coalbed methane exploration in Australia. Conference Asia Pacific oil & gas conference, Melbourne, Australia, November 7-10, 1994, SPE Paper 28780, 373-381.

Enever, J.R., Pattison, C.I., McWatters, R.H. and Clark, I., 1993. The relationship between in situ stress and reservoir permeability as a component in developing an exploration strategy for coalbed methane in Australia. SPE/ISRM 28048, 163-171.

Enever, J., Wooltorton, B., Edgoose, J., Bride, J. and Sullivan, D., 1987. Notes accompanying summary of Bowen Basin stress measurements, CSIRO report, 20pp.

Esterle, J.S., Damen, P. and Laws, A., 1999. Updated Sedimentary Model. Moranbah North Underground Mine. CSIRO Exploration and Mining Confidential Report 638c.

Esterle, J., Sliwa, R., West, D. and Sommer, D., 2002. Integrated interburden and structure model for Oaky Ck coal mine, Bowen Basin. CSIRO Confidential Report 919F, 109pp.

Esterle, J.S. and Fielding, C.R., 1996. Sedimentological analysis of goafing interval for longwall mining, Goonyella mine, Bowen Basin. In C. Ward (ed), Geology in Longwall Mining, Conference Proceedings, 27-34.

Esterle, J.S., Leblanc Smith, G., and Yago, J.V.R., 2000. Geometry and connectivity of distributary channel sandstones in the Late Permian Moranbah Coal Measures, Bowen Basin, Australia. Journal 2000 - Australian Petroleum Production and Exploration Association, 381-392.

Esterle, J.S., LeBlanc Smith, G., Poulsen, B. and Cameron, J.L., 1998. Integrated geological model for BHPC Goonyella Riverside and SCOA Moranbah North minesites. CSIRO Exploration and Mining Confidential Report 520C.

Ettinger, I., Eremin, I., Zimakow, B., Yanovskaya, M., 1967. Natural factors influencing sorption properties. I: Petrography and the sorption properties of coal. Journal of Fuels, 45, 267-275.

Faiz, M.M. and Cook, A.C., 1991. Influence of coal type, rank and depth on the gas retention capacity of coals in the Southern Coalfield, NSW. In, W.J. Bamberry and A.M. Depers (eds), Gas in Australian Coals, GSA Symposium Proceedings 2, 19-29.

Faiz, M.M. and Hutton, A.C., 1995. Geological controls on the distribution of CH4 and CO2 in coal seams of the Southern Coalfield, NSW, Australia. In R.D. Lama (ed), International Symposium cum Workshop on Management and Control of High Gas Emissions and Outbursts, Wollongong, 375-383.

Falkner, A.J. and Fielding, C.R., 1992. Quantitative facies analysis of coal-bearing sequences in the Bowen Basin, Australia. Applications to reservoir description. In S.Flint, S. and I.D. Bryant (eds) Quantitative description and modelling of clastic hydrocarbon reservoirs and outcrop analysis. International Association of Sedimentologists Special Publications 15, 81-97.

Falkner, A.J. and Fielding, C.R., 1993. Geometrical facies analysis of a mixed influence deltaic system. the Late Permian German Creek Formation, Bowen Basin. International Association of Sedimentologists Special Publications, 17, 195-209.

Faraj, B.S.M., 1997. Cleat Mineralisation, coalification and tectonic history of Late Permian Blackwater Group in ATP364P, Northern Bowen Basin, Queensland. Implications for coalbed methane exploration. BHP Coal Ltd Business Development Department Report, 155pp.

Fielding, C.R., Sliwa, R., Holcombe, R.J. and Kassan, J., 2000. A new palaeogeographic synthesis of the Bowen Basin of central Queensland, Bowen Basin Symposium 2000. In J.W. Beeston, (ed), Bowen Basin Symposium 2000-the New Millenium-Geology, Geological Society of Australia Inc., Coal Geology Group and the Bowen Basin Geologists Group, Rockhampton, October 2000, 287-302.

Geoscience Australia, 2002. Gravity Anomaly Map of the Australian Region.

Godfrey, N.H.H., 1978. Instability factors in highwall overclays at an open pit strip coal mine. Unpubl. MSC thesis, James Cook Univ of North Qld.

Godfrey, N.H.H., 1985. Strip mine higwall geology in the Moranbah and Gemran Creek Coal Measures. Proceedings of the Bowen Basin Coal Symposium, Geological Society of Australia Coal Geology Group, 75-81.

Gould, K. W; Hart, G.N; Smith, J.W., 1981. Carbon dioxide in the Southern Coalfields; a factor in the evaluation of natural gas potential?. Proceedings - Australasian Institute of Mining and Metallurgy, Technical Note, 279, 41-42.

Gurba, L.W. and Ward, C.R., 2002. The influence of depositional and maturation factors on the three-dimensional distribution of coal rank indicators and hydrocarbon source potential in the Gunnedah Basin, New South Wales. In M. Mastalerz, M. Glikson, and S.D Golding, (eds), Coalbed methane: scientific, environmental and economic evaluation, Proceedings of the International conference on coal seam gas and oil, Brisbane, Queensland, Australia, March 23-25, 1998, 493-515.

Hammond, R. and Mallett, C.W., 1987. A tectonic framework for coal measure deformation in the southern Bowen Basin. Advances in the Study of the Sydney Basin. Proceedings of the Symposium, 21, 193-196.

Hill, T.W.C., 2000. Three-dimensional geometry and internal architecture of the Northern Norwich Park Coal Mine, Bowen Basin, Central Queensland. Honours Thesis, University of Queensland, St. Lucia.

Hillis, R.R., Enever, J.R. and Reynolds, S.D., 1999. In situ stress field map of eastern Australia. Australian Journal of Earth Sciences, 46, 813-825.

Holcombe, R.J., Stephens, C.J., Fielding, C.R., Gust, D.A., Little, T.A., Sliwa, R., Kassan, J. McPhie, J., and Ewart, A., 1997. Tectonic evolution of the Northern New England Fold Belt. the Permian-Triassic Hunter-Bowen event. In P.M. Ahsley, and P.G. Flood (eds), Tectonics and Metallogenesis of the New England Orogen, Special Publication of the Geological Society of Australia, 19, 52-65.

Jensen, A.R., 1971. Regional aspects of the Upper Permian regression in the northern part of the Bowen Basin. In: A.Davis (ed) Proceedings of the Second Bowen Basin Symposium, Queensland Department of Mines Geological Survey Report, 62, 7-20.

Johnson, D.P., 1984. Development of Permian fluvial coal measures, Goonyella, Australia. International Association of Sedimentologists Special Publication, 7, 149-162.

Kelly, M., Luo, X. and Craig, S., 2001. ACARP Project C7021 – The Extended Influence of Geological Conditions and Structure on Longwall Geomechanics. CSIRO Exploration And Mining Report 899F.

Khavari-Khorasani, G., Michelsen, J. K., Coal bed content and gas undersaturation. In M. Mastalerz, M. Glikson, and S.D Golding, (eds), Coalbed methane: scientific, environmental and economic evaluation. Proceedings of the International conference on coal seam gas and oil, Brisbane, Queensland, Australia, March 23-25, 1998, 207-231.

Koppe, W.H., 1978. Review of the stratigraphy of the upper part of the Permian succession in the northern Bowen Basin, Queensland Government Mining Journal, 79, 35-45.

Korsch, R.J., Johnstone, D.W. and Wake-Dyster, K.D., 1997. Crustal architecture of the New England Orogen based on deep seismic reflection profiling. In P.M. Ahsley, and P.G. Flood (eds), Tectonics and Metallogenesis of the New England Orogen, Special Publication of the Geological Society of Australia, 19, 52-65.

Laubach, S.E., Marrett, R.A. Olsen, J.E. and Scott, A.R., 1998 Characteristics and origins of coal cleat. A review. International Journal of Coal Geology, 35, 175-207.

Law, B.E., 1993. The relationship between coal rank and cleat density: implications for the prediction of permeability in coal. 1993 International Coalbed Methane Symposium, Birmingham, Alabama, Paper 9341.

Laxminarayana, C. and Crosdale, P.J., 1999. Role of coal type and rank on methane sorption characteristics of Bowen Basin, Australia coals. International Journal of Coal Geology, 40, 309-325.

Le Blanc Smith, G. and Esterle, J., 1998. Sedimentary and structural geology assessment for potential underground mining sites. Eureka and Goonyella No2 areas, Goonyella-Riverside Mine. CSIRO Exploration and Mining Confidential Report 506C, 150pp.

Le Blanc Smith, G. and Yago, J.V.R., 2000, Integrated geological model of the North Goonyella Coal Mine, Queensland. CSIRO Exploration and Mining Confidential Report 680.

Li, S., Dimitrakopoulos, R., Scott, J. and Mackie, S., 2001, Quantification of Fault Uncertainty and Risk Management in Underground Longwall Coal Mining. ACARP Project C7025 Report (Vol. II). W H Bryan Mining Geology Research Centre, The University of Queensland, Brisbane, Australia.

Lohe, E. and Sullivan, D., 1992. Geological structure of the central northern Oaky Creek Mine area, Bowen Basin, Qld. CSIRO Internal Report 156, 63pp.

Mallett, C.W., Hammond, R.L., Leach, J.H.J., Enever, J.R. and Mengel, C., 1988. Bowen Basin - stress, structure and mining conditions assessment for mine planning. NERDDC Project No. 901, 233pp..

Martini, I.P. and Johnson, D.P., 1987. Cold-climate, fluvial to paralic coal-forming environments in the Permian Collinsville Coal Measures, Bowen Basin, Australia. International Journal Coal Geology, 7, 365-388.

Miall, A. D., 1978. Lithofacies types and vertical profile models in braided rivers. a summary, in Fluvial Sedimentology, edited by A. D. MIALL. Canadian Society Petroleum Geologists Memoir 5, p. 597-604.

Miall, A. D., 1985. Architectural element analysis: a new method of facies analysis applied to fluvial deposits. Earth Science Reviews, 22, 261-308.

Michaelsen, P, 1999. Development of Uer Permian coal measures, northern Bowen Basin, Australia. Unpub. PhD thesis, James Cook University.

Michaelsen, P., Henderson, R.A., Crosdale, P.J. and Fanning, C.M., 2001. Age and significance of the Platypus Tuff bed, a regional reference horizon in the Uer Permian Moranbah Coal Measures, north Bowen Basin. Australian Journal of Earth Sciences, 48, 183-192.

Michaelson, P. and Henderson, R.A., 2000. Facies relationships and cyclicity of high-latitude, Late Permian coal measures, Bowen Basin, Australia. International Journal of Coal Geology, 44, 19-48.

Milligan, E.N., 1971. Geology and correlation in th German Creek Coal Measures. In. Davis, A. (e3d), Proceedings of the 2nd Bowen Basin Symposium. Publications of the Geological Survey of Queensland, 62, 77-85.

Milligan, E.N., 1975. German Creek-Goonyella District in Traves, D.M. and King, D., Economic Geology of Australia and Papua New Guinea, Volume 2, Coal. AusIMM Monograph Series 6, 92-98.

Murray, C.G., Scheibner, E. and Walker, R.N., 1989. Regional geological interpretation of a digital coloured residual Bouguer gravity image of eastern Australia with a wavelength cut-off of 250km. Australian Journal of Earth Sciences, 36, 423-449.

Pashin, J.C. and Groshong, R.H., Jr., 1998. Stuctural control of coalbed methane production in Alabama. International Journal of Coal Geology 38, 89-113.

Pattison, C., 1998. Coal seam methane exploration and development in Australia. Confidential report to CSIRO.

Pattison, C.I., 1990. Igneous Intrusions in the Bowen Basin. MScA thesis, Queensland Institute of Technology, unpublished.

Pattison, C.I., Fielding, C.R., McWatters, R.H. and Hamilton, L.H., 1995. Nature and origin of fractures in Permian coals from the Bowen Basin, and the relationship with in-situ permeability. In I.L Follington, J.W. Beeston, and L.H Hamilton (eds). Proceedings of the Bowen Basin Symposium, Mackay, Queensland, 217-234.

Pattison, C.I., Marshall, A.J., McWatters, R.H. and Brotherton, R.A., 1993. Gas content and composition in the Rangal (Baralaba) Coal Measures, ATP 524P, Bowen Basin. 15th PESA (Qld) Petroleum Symposium Proceedings, 41-53.

Prouza, V and Park, W J, 1973. Revision of Permian stratigraphy of the Emerald-German Creek-Comet area, Queensland Government Mining Journal, 74 (866), 433-438.

Pusch, R., 1995. Rock mechanics on a geological base. Elsevier, 498pp.

Queensland Coal Board, 2001. Queensland coals: physical and chemical properties, colliery and company information, 12th edition. Queensland Department of Mines and Energy.

Queensland Department of Mines, 1988. Bowen Basin Solid Geology. 1:500,000 map.

Raza, A., Hill, K., Korsch, R. and Brown, R., 1998. Geological evolution of the central eastern margin of Australia. Fission track thermochronology. Proceedings Australian Geodynamics Cooperative Research Centre Symposium - Mineral systems and the crust- upper mantle of SE Australia.

Rice, D. D., 1993. Controls of coalbed gas composition. Proceedings of the 1993 International Coalbed Methane Symposium, Birmingham, AL, United States 1993, 577-588.

Ronan, M.J., 2000. Three-dimensional modelling of external geometry and internal heterogeneity of sediment bodies, Norwich Park, Bowen Basin, Central Queensland. Honours Thesis University of Queensland, St. Lucia, unpublished.

Scheibner, E. and Veevers, J.J., 2000. Tasman Fold Belt System. In J.J. Veevers (ed), Billion-year earth history of Australia and neighbours in Gondwanaland, 154-234.

Shibaoka, M. and Bennett, A.J.R., 1976. Effect of depth of burial and tectonic activity on coalification. Nature, 259, 385-386.

Sliwa, R. and Le Blanc Smith, G., 2000. Enhanced highwall mining project. Report on geological/structural interpretation at Saraji. CSIRO Exploration and Mining Confidential Report No 767C, 19pp.

Smith, R., 1996. A comparative study of dykes and their effects on coal seams. QUT report, unpublished, 12pp.

Staines, H.R.E. and Koppe, W.H., 1979. The geology of the north Bowen Basin. Queensland Government Mining Journal, 80, 172-195.

Uysal, I.T., Golding, S.D., and Glikson, M., 2000. Petrographic and isotope constraints on the origin of authigenic carbonate minerals and the associated fluid evolution in Late Permian coal measures, Bowen Basin (Queensland), Australia. Sedimentary Geology, 136 (3-4), 189-206.

Veevers, J.J., Powell, C. McA. and Roots, S.R., 1991. Review of seafloor spreading around Australia. 1. Synthesis of the patterns of seafloor spreading. Australian Journal of Earth Sciences, 38, 373-389.

Ward, C., Hanson, C. and Biggs, M., 1997. Central Colliery extended project-geological and geotechnical status report. CapCoal Internal Report.

Weisenfluh, G.A. and Ferm, J.C., 1991. Roof control in the Fireclay Coal Group, Southeastern Kentucky. Journal of Coal Quality, 10 (3), 67-74.

Williams, R.J., Casey, D.A. and Yurakov, E., 2000. Gas reservoir properties for mine gas emission assessment. J.W. Beeston, J.W. (ed) Bowen Basin Symposium 2000-the New Millenium-Geology. Geological Society of Australia Inc., Coal Geology Group and the Bowen Basin Geologists Group, Rockhampton, October 2000, 325-334.

Wold, M.B. and Esterle, J., 2000. Measurements of permeability, fracture density and coal petrology on Bulli seam core, in the context of gas outburst risk assessment, CSIRO Petroleum Restricted Report No. 00-004, CSIRO Australia, August 2000, 16pp.

Zhao, S. and Müller, R.D., 2001. The tectonic stress field in Eastern Australia. Proceedings of the Eastern Australian Basins Symposium, 61-70.

APPENDIX 1 NOTES ON COAL SEAM MODELS

A1.1 Introduction

All the maps and sections presented in this report are based on three contiguous geological models, the "northern", "middle" and "southern tiles", which were built in Minescape 4. This appendix describes the data compilation, model building and map production procedures used in the building of the models.

A1.2 Data compilation for model

Due to the limitations of the geological modelling software, the Supermodel dataset was divided into three tiles. The geographical extent of the tiles and the data contributors in each tile are listed in Table 1.

Table 1 Geographic limits of Supermodel tiles and contributing datasets

	Northern tile	**Middle tile**	**Southern tile**
Northern limit (AMG)	7 622 000	7 555 000	7 478 000
Southern limit (AMG)	7 555 000	7 478 000	7 418 500
Western limit (AMG)	593 900	607 500	630 500
Eastern limit (AMG)	617 000	659 000	668 500
Contributing mines and prospects	Wards Well North Goonyella Goonyella Riverside Red Hill Moranbah North Grosvenor South Moranbah (Iscor) Peak Downs (partial) Government data	Peak Downs Saraji Norwich Park	German Creek Oaky Creek Crinum Gregory Kestrel Government data

The data for all the tiles compiled from the contributors is up-to-date to early 2001. The data include:

- Borehole surveys
- Coal picks
- Interburden sandstone picks (Northern tile only)

To reduce the dataset to a manageable size, all boreholes without coal seam intersections were rejected. In addition boreholes that were less than 10m apart were filtered out (keeping the borehole with the most information). This resulted in 45 384 boreholes included in Supermodel (Table 2).

Table 2 Number of boreholes supplied and included in models

	Northern tile	**Middle tile**	**Southern tile**
Total number of boreholes compiled	11 630	16 504	18 718
Number of boreholes included in model	10 113	15 799	12 308
Total number of boreholes modelled			38 220

To turn the data from the various sources into a single consistent "clean" dataset, several steps were taken:

1. Develop a coal (and sand body) correlation schema that is consistent across each tile, and matches with the schema of the adjacent tile (see detailed discussion below)
2. Delete any picks of units not to be modeled (eg. Tertiary basalt units)
3. Recode all picks to conform to the new schema
4. Turn all Tertiary interval picks into zero-thickness surfaces
5. Delete all coal seam zero-thickness picks (ie. Minex to Minescape conversion)
6. Compound all coal plies
7. Where thrust faults caused seam duplication, retain the lower set of picks
8. Delete super thick seam picks (obvious outliers)
9. Fix length of hole inconsistencies
10. Fix miscorrelations, "bullseyes" and other data errors. Keep a record of the changes in the data spreadsheets.

Several generations of preliminary models were built to help identify data problems, until the final models loaded and modeled with no data errors or warnings.

A1.3 Correlation schemas

Correlation schemas were developed for each tile internally, and then adjusted to be consistent across the three tiles. Coal seam codes from each minesite were replaced by Supermodel codes as shown in Table 3 to Table 5 below. Several minor coal seams with only few picks were excluded from the models.

Correlations were built up by tracking coal seam occurrences, thicknesses, and successions as well as interburden thicknesses across the tiles using GIS software.

All splitlines shown on the maps throughout the report were tracked by plotting the interburden thickness between the two seams and interpolating the 1m separation contour.

Table 3 Coal seam correlation schema for northern tile (NB. greyed out units are not included in model, light blue bars are the major working seams, "c" denotes forced continuity of seam)

Supermodel codes	WW North	Wards Well	North Goonyella	Goonyella	Riverside	Red Hill	Moranbah	South Moranbah	Peak Downs
BHWE	BHWE	BHWE			BHWE	BHWE			BHWE
BHWL		BHWL			BHWL				
BUTE	BUTE	BUTE	TER	BUTE	BUTE	BUTE	TER		BUTE
Fairhill									
FH		GF2				R	FH	FH	F02
R and Q seams									
R			R					R	
Q			Q			Q	QA	Q	Q01
QB		GF0				QB	QB	QB	
Goonyella Upper									
GU4				GU4		GU4			
GU5				GU5		GU5			
GUS	GU5	GU5	GUA	GU0,GU3	GUS	GU0,GU3,GU1?	GU	GUS	
GU0	GU0	GU0	GUB			GU9			
GU2		GP9	GXU	GU2		GU2	GR	GR	P08
P-seams									
GP3 \ **GP5**	GP3	GP3	GXL	GP3		GP3	PL1		
				GP5		GP5	P	P	P07
GP2	GP2	GP2	GP	GP2		GP2	PL2		
GP1		GP1	PSU	GP1		GP1		GP1	
PT	GP4	GP4	PT	GP4	GP4	GP4	PT	GP4	P01
GP0	GP0	GP0	PSL	GP0		GP0		GP0	
Goonyella Middle									
GM2			P3	GM2,CP3	GM2		GMR		H072
G1 \ **G12**							GM1		
							[GM1,GM2]		
G2							GM2		
GM0	GM0	GM0	GM0	GM0,GM1	GM0	GM0,GM1	[GM1-3,4,5]	GM1	H071/H06
G4A							GM4A		
G45							[GM4B,5T,5B]		
GM3			GML	GM3	GMS?		GML		
CL6				CL6		CL6	HL		
Harrow Creek									
HL1 \ **H01**							HL1	HL1	H03
									H01
HL2							HL2	HL2	H02
HL3							HL3	HL3	H00
Dysart Upper									
DYU1 \ **D42**							DYU1	DYU1	D40
									D42
DYU2							DYU2	DYU2	D39
Goonyella Lower									
GL5 \ **D04**		GMF	GLA1	GL5		GL5	DYR1	DYR1	
									D04
GL4				GL4	GLU	GL4	DYR2	DYR2	
D03									D03
GL3 \ **GL6**	GL3	GL3	GLA2	GL3					
				GL6		GL6			
GL2		GL2	GLB1	GL2					
GL0	GL8	GL8,GL7	GLB2	GL0,GL1,GL7,GL8	GL0	GL0,GL7	GL	GLL	D02
GLL							GLL	GLL1	D00

Table 4 Coal seam correlation schema for middle tile (NB. greyed out units are not included in model, light blue bars are the major working seams, "c" denotes forced continuity of seam)

Supermodel codes elements	compounds	Peak Downs	Saraji	Norwich Park	Government Holes
BHWE	(Base of weathering)	BHWE	BHWE	BHWE	
BHWL	(Base of Tertiary)	BHWL	BHWL	BHWL	
BUTE	(Standing water level)	BUTE	BUTE	BUTE	
Fairhill					
F02		F01			
	FH	FH			
F01		F02			
S and Q seams					
SU					S UPPER
	S	S01			S SEAM
SL					S LOWER
R01		R	R01		R SEAM
Q03			Q03		Q UPPER
	Q01	Q01,Q			
Q02			Q02		Q LOWER
P-seams					
QB		QB			
GUS		GUS			
P19		GU2	P19,P08	P26	P1
	P17	P02	P17		
P18		GP5	P18,P07	P25	P2
GP1		GP1			
PT		GP4,P01			P TUFF
P14		GP0	P14,P06	P14	HARROW CK UPPER
Harrow Ck					
H352				H352	
	H35			H35,H331	
H351				H351	
H072		H072,GM2			
H162		H162			
	HC	GM1,H071,H07,H13,H16,H05	H16	H16,H33,H332	HARROW CK
H161		H161			
GM3		GM3			
Harrow Ck Lower					
H21		H21			
H32				H32	
H06		H06			
H03		H03,HL1			
	HL	H15,H08,H01	H15	H24,H25,H31	HARROW CK LOWER
H02		H02			
H20		GL2	H20		
H18			H18		
	H19	H00,HL3	H19	H23,H30	J SEAM, H CK LOWER 2
H17			H17		
Dysart Upper					
D43		D43	D17,D53		
D49		D51,D401	D49,D52,D53,D532	D56,D58	
	DU	GL5,D40,D42,D44,D46,D47	D17,D18,D19,D49,D52,D53	D54,D55,D56,D57,D58	K SEAM,DYS RIDER,DYS UPPER
D19		D50,D402	D17,D19,D531	D55,D57	
D23		GL5L	D17,D23,D31		
D45		D45,D39,GL3			DYSART UPPER
D59				D59	
Dysart Lower					
DYR1		DYR1			
	D04	D04	D142		
DYR2		DYR2			
	DL	D05,D11,D13,D14	D14,D24,D27,D29,D30	D30,D45,D37,D35,D33,D38,D34	DYSART
D03		D03			
GL7		GL7			
	D02	D02	D141		
GL9		GL9			
D28			D28		
D22			D22,D26		
	D12	D12		D36	DYSART LOWER
D21			D21,D25		
D01		D01			
D20		D00	D20		

Table 5 Coal seam correlation schema for southern tile (NB. greyed out units are not included in model, light blue bars are the major working seams, "c" denotes forced continuity of seam)

Supermodel codes elements	compounds	Norwich Park	German Ck	Oaky Ck	Crinum - Gregory	Government Holes	Kestrel
BOW	(Base of weathering)	BHWE	BOW	BOW	BHWE		BHLW
BOT	(Base of Tertiary)	BUTE	BOT	BOT	BUTE	TERT	BUTE
BHWL	(Standing water level)	BHWL	BHWL	SWL	BHWL		THWL
Virgo							
VI							VI
Leo							
LEO							LEO
Aquarius							
AUU							AUU
	AU						AU
AUL							AUL
Hercules							
			~~HE?~~	~~HERCR~~			
HERCU			HEU	HERCU			HEU
	HERC						HERC
HERCL			HEL				HEL
Canis/Lepus							
CANIS			CN	CANIS			CA
	CALP						CALP
LEPUS				LEPUS			LP
Fair Hill							
FHU							FHU
	FH		FH	FH			FH
FHL				FHL			FHL
Pleiades							
PX			PX				
PL1			PU	PL1			
			~~PT (P Tuff)~~	~~PL2R~~			
PL2			PM	PL2	PL0	PLAD	PU
			~~PTL~~	~~PL3R~~			
PL3			P	PL3	PL1		PL
			~~PS,AS (sills)~~				
Aquila							
AQ		H33	AQ	AQ	AQ0	AQUIL	AQ
AQL			AQL	AQL			
Tieri							
T1U			T1U	T1U			T1U
	T1			T1	TI1	TIR1	T1
T1L			T1L	T1L			T1L
			~~TS (sill)~~	~~T2R~~			
T2U				T2U			T2U
	T2		T2	T2	TI2	TIR2	T2
T2L				T2L			T2L
Corvus							
C1U			C1U				
				~~C1R~~			
	C1	D58	C1	C1	CV0	CRVS,CRS1	CO
C1L			C1L				
				~~CMR~~			
CM			CM	CM			
CM2				CM2			
C2		D59	C2	C2			
				~~C2L~~			
German Creek							
GCG				GCG			
	GCFG		GU	GCFG	LV2		
GCF				GCF			
				~~GCWSR~~			
GCWS		D34	GC	GCWS	LV0	GMCK,GMK1	GC,GCU,GCU1,
GCE				GCE			GCU2,GCU3
GCD				GCD			GCC
GCB1							GCB1
	GCBK						GCB
GCB2							GCB2
GCA1							GCA1
	GCC						GCA
GCA2				GCC			GCA2
	GCBC		GL	GCBC,GCAB		GMK2	
GCB				GCB			
GCL1							GCL1
	GCA			GCA	LV1		GCL
GCL2							GCL2

APPENDIX 2 GEOSTATISTICAL ANALYSIS OF FAULT PATTERNS

Shuxing Li and Roussos Dimitrakopoulos

A2.1 Introduction

This study deals with the quantitative analysis of faults compiled within the Southern Tile in Supermodel 2000 project. It includes (a) the quantitative analysis of fault characteristics and comparison to existing information for parts of the Northern Tile (ACARP C7025 Dimitrakopoulos et al, 2001; Li et al, 2001); and (b) the simulation of faults with the related spatial quantification of fault risk in the Southern Tile.

The work reported in this section integrates the qualitative aspects of fault identification and understanding in the Southern Tile into qualitative fault risk maps that may assist in aspects of long wall mine design and planning. It is worth stressing that key use of fault simulation studies and fault risk quantification is to reduce the effect of geological uncertainty and risk on the exploration and mining of underground coal deposits. Typical examples of the use of fault probability maps are shown in Figure 118 and Figure 119.

Figure 118 shows the quantification of geological uncertainty in (a) mined-out panels in a long wall mine; and (b) an area where a long wall mine is being planned to suggests that the mine under development is substantially less risky (34% versus 61%). However, long wall panel layout will also need to consider principle stress orientation and variability in grade.

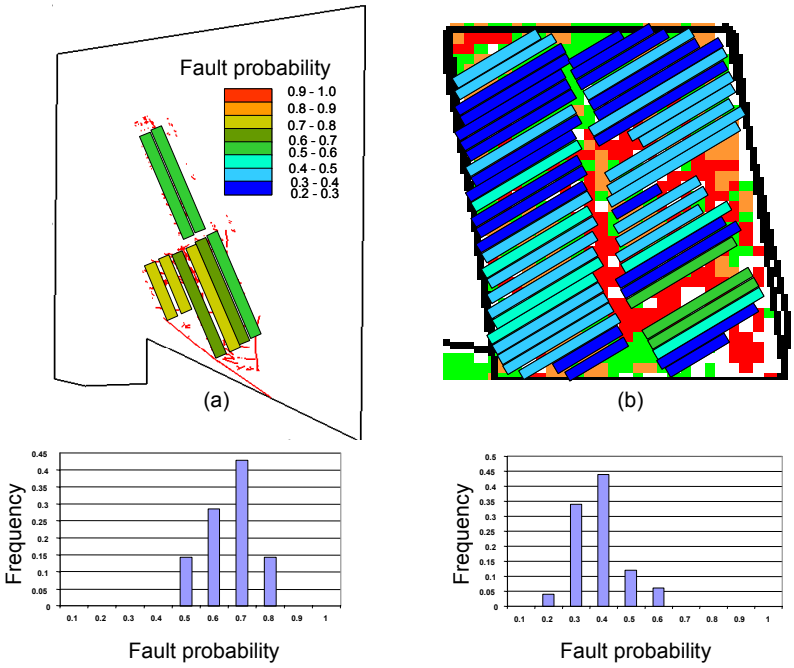

Figure 118 Fault probability maps and histograms for (a) a mined out long wall mine with mapped faults ≥ 1m and comparison of average fault risk (61%) to (b) a long wall mine being planned with average risk at 34%. Panel size equivalent 0.2 x 2km and coloured by probability. (ACARP C7025).

Figure 119 shows an example of integrating quantified geological uncertainty into long wall design and planning. The layout of long wall panels can be optimised to manage fault uncertainty. In this example, changing the panel layout resulted in a reduction of fault risk and an increase in coal resource recovery.

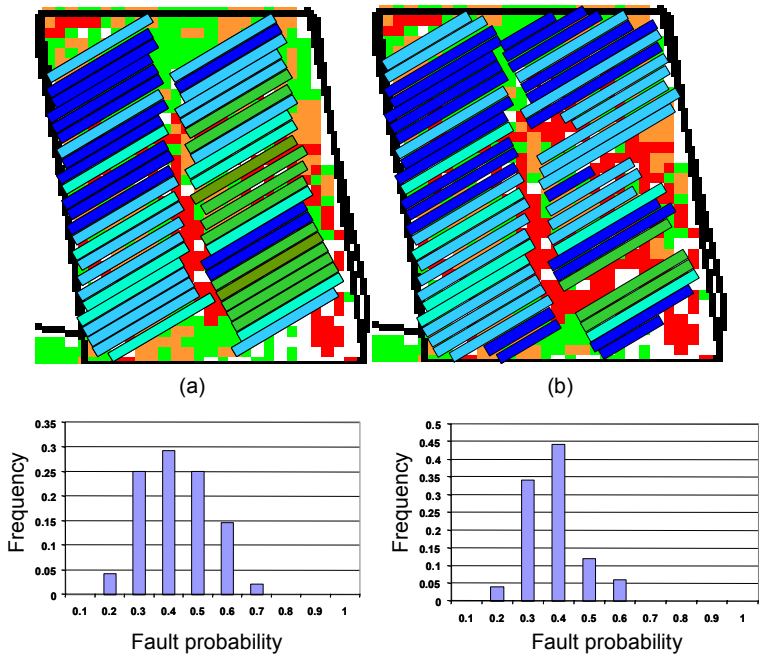

Figure 119 Examples of different panel layouts designed to minimise loss of reserves and potential downtime using fault probability maps. (a) A non-optimal of a layout; (b) improved design minimising reserve loss and potential downtime. Average fault risk in (a) is 40% and in (b) 34% with 5% increase in resources. Panel size and colour scheme as in Figure 118. (ACARP C7025).

The previous ACARP 7025 study also developed methods for characterising faults using power-law models of fault size, length and throw distributions which can be used for regional analysis of fault patterns and comparisons to other parts of the Bowen Basin. These methods and software developed for ACARP project C7025 (Dimitrakopoulos et al, 2001; and Li et al, 2001) were used to analyse the fault distributions for the Southern Tile.

A2.2 Fault data analysis and modelling

The faults compiled and categorised for the Southern Tile are shown in Figure 120 (a) and are referred to as the "complete fault dataset". Only faults ≥1 m were compiled and they comprise faults mapped in open cut and underground mine exposures, faults interpreted from seismic survey and faults interpreted from drilling. The fault strike distributions are shown in Figure 120 (b). Based on the fault orientation, the faults are grouped into two populations: Population 1 (oriented towards NE) and Population 2 (oriented towards NNW). The power-law models fitted for each fault population are shown in Figure 121(a) and (b) for Population 1 and Population 2 respectively. The power-law model shows the relation of log (fault throw in metres) and log (cumulative number of faults). Recall that the log (0)=1 m, log (1)=10 m, log (2)=100 m and so on. In all of the following graphs T=throw and L=length.

The relationship between fault throw and length are modelled for each of the two populations shown in Figure 122. The NE Population 1 shows a poorer relationship than NNW Population 2. The latter are the more persistent features interpreted as inherited from deep basement structures.

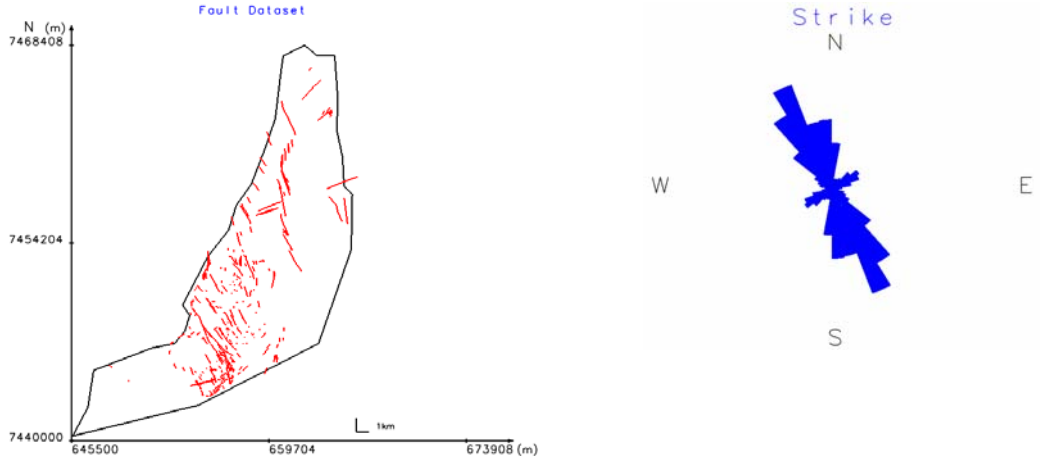

(a)

(b)

Figure 120 Complete fault data (a) and their strike distribution (b) for the Southern Tile.

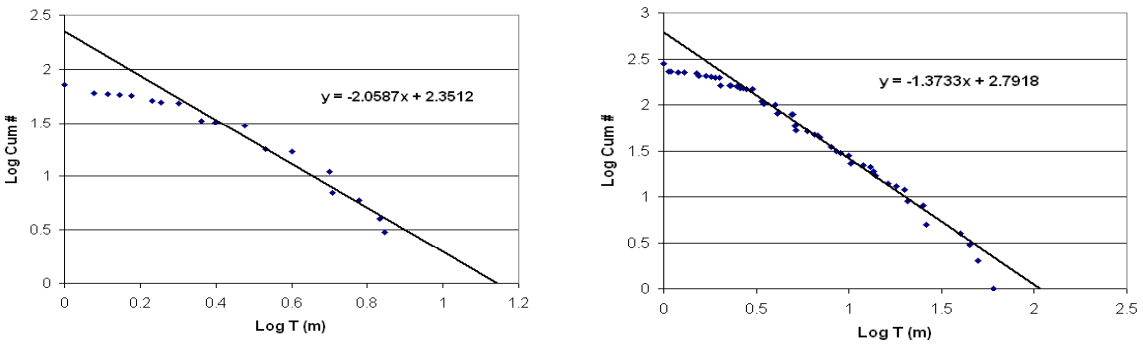

(a)

(b)

Figure 121 Power-law models using complete dataset: (a) Population 1; (b) Population 2.

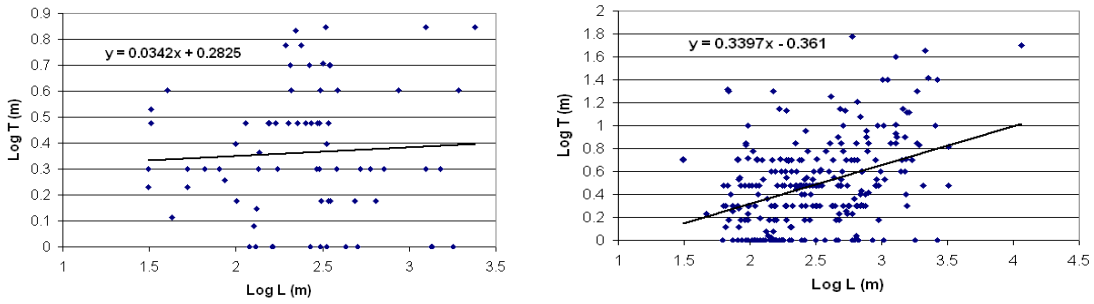

(a) (b)

Figure 122 The relationship between fault length and throw using complete fault dataset: (a) Population 1; (b) Population 2.

A2.3 Modelling spatial characteristics of faults

The spatial characteristics of faults are investigated using geostatistical tools as developed in ACARP C7025 and results are as follows.

Firstly, the fault density is calculated based on the known faults. Figure 123 shows the fault density maps of each fault population.

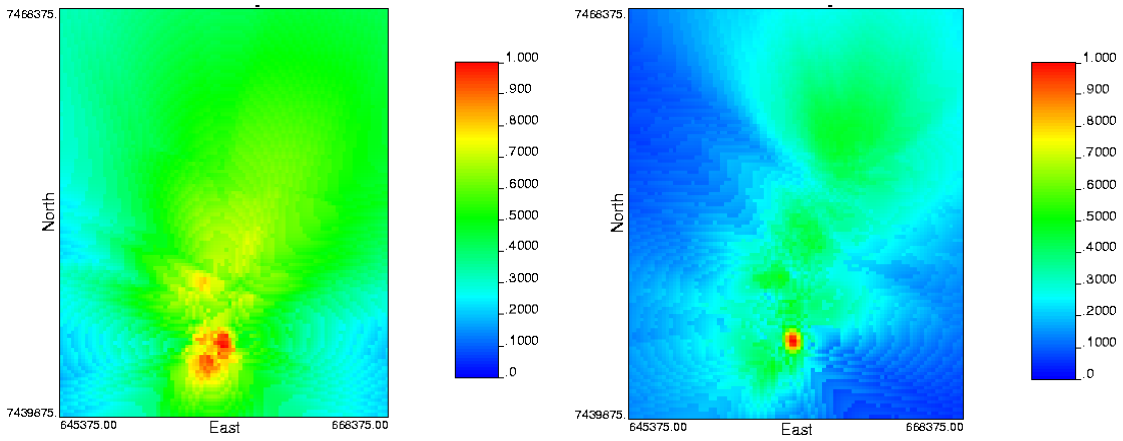

(a) (b)

Figure 123 Normalized fault density image using complete fault dataset:(a) Population 1; (b) Population 2.

Next, the variogram of each population is modelled and presented in maps to determine the anisotropy directions. Figure 124 shows the variogram maps for individual fault populations.

Thirdly, based on the variography maps and anisotropy directions, the variograms are calculated and modelled. Figure 125 shows the variograms of individual fault populations.

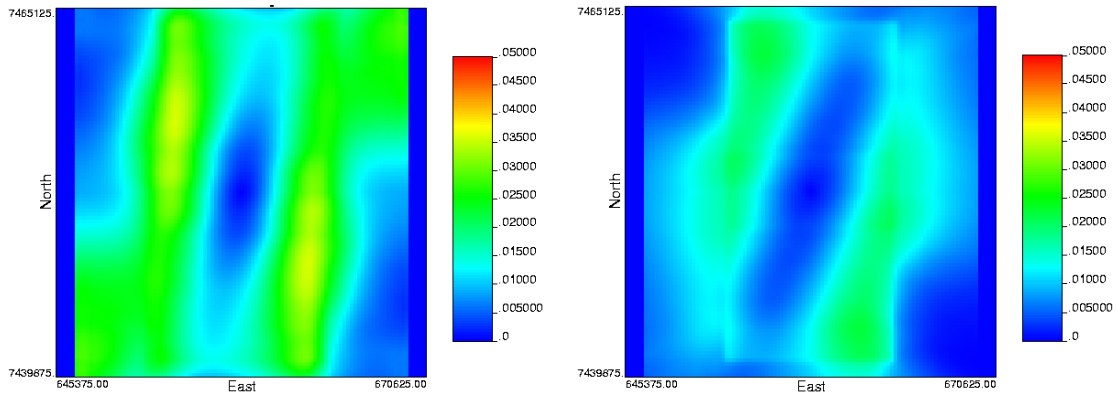

(a) (b)

Figure 124 Variography map using complete fault dataset: (a) Population 1; (b) Population 2.

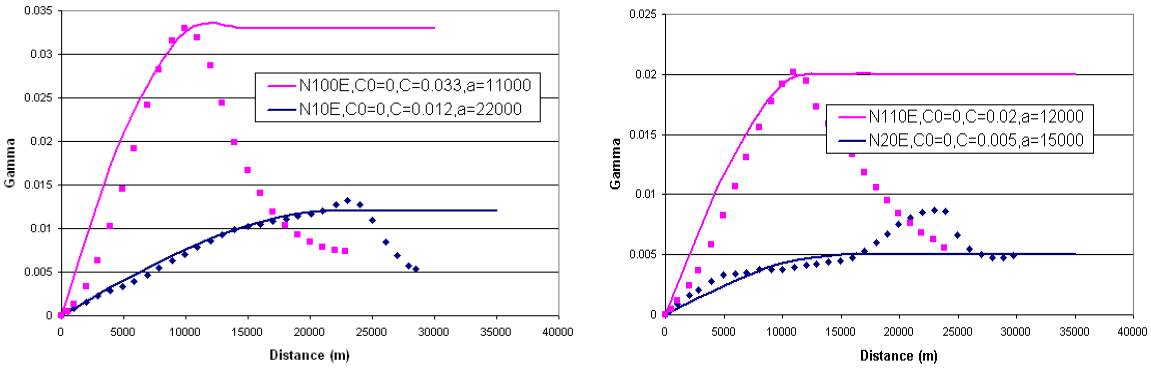

(a) (b)

Figure 125 Variogram using complete fault dataset: (a) Population 1; (b) Population 2.

A2.4 Results of fault simulations

Based upon the characterisation of each fault population and its spatial characteristics, the faults are simulated to generate the equal-probable fault realisations. The simulations reproduce the statistical characteristics of faults as well as the fault data.

Figure 126, Figure 127 and Figure 128 show the results of fault simulations using the complete fault dataset.

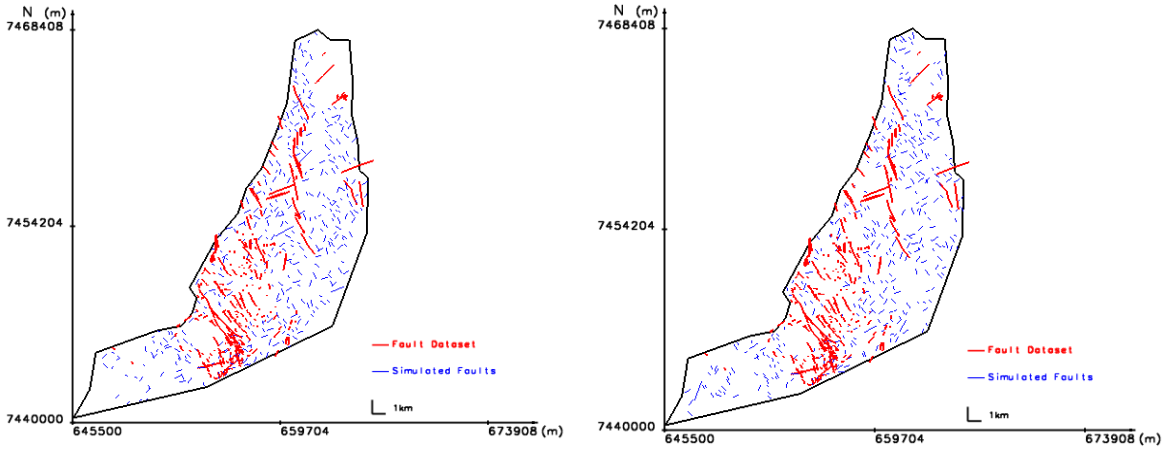

Figure 126 Two simulated fault realisations using complete dataset.

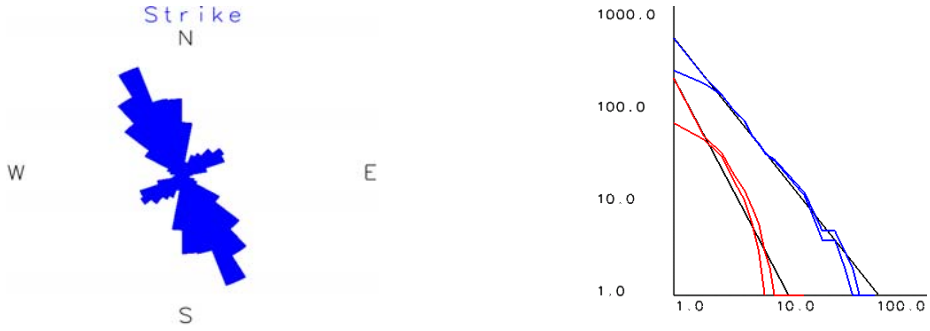

Figure 127 Strike distribution and power-law model reproduced in above simulations. Red is the fault dataset and blue are the simulated faults.

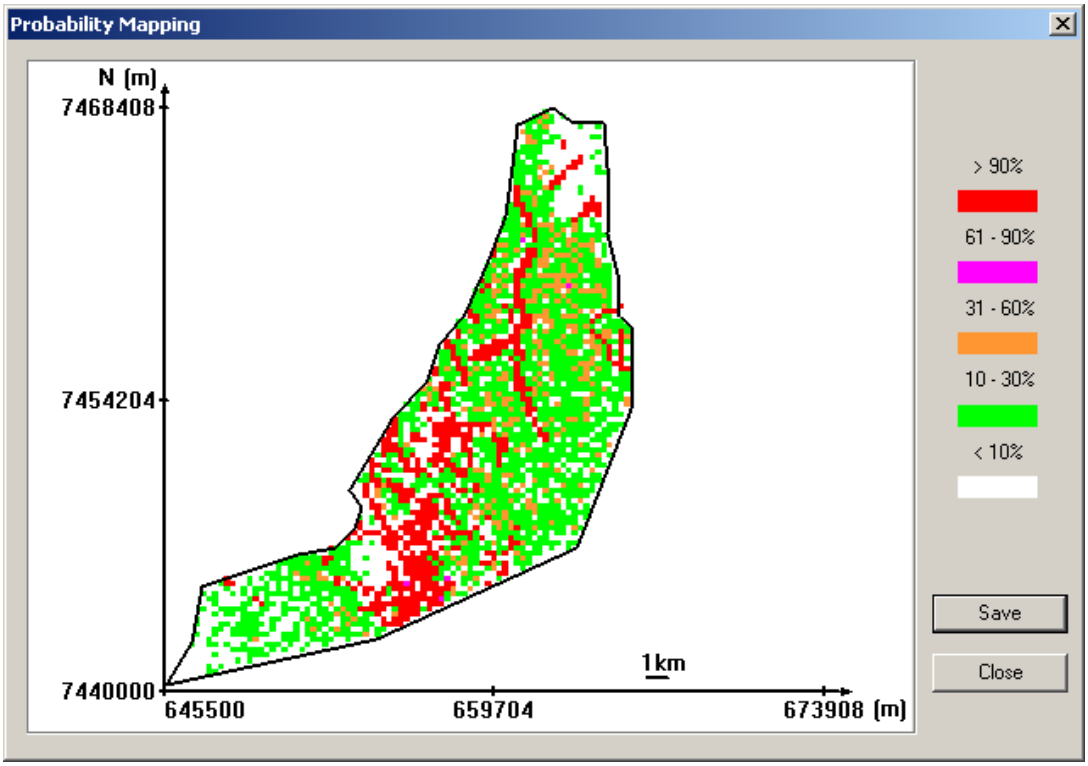

Figure 128 Fault probability mapping using the complete fault dataset.

Figure 129, Figure 130 and Figure 131 show the results of fault simulations of Population 1 using the complete fault dataset.

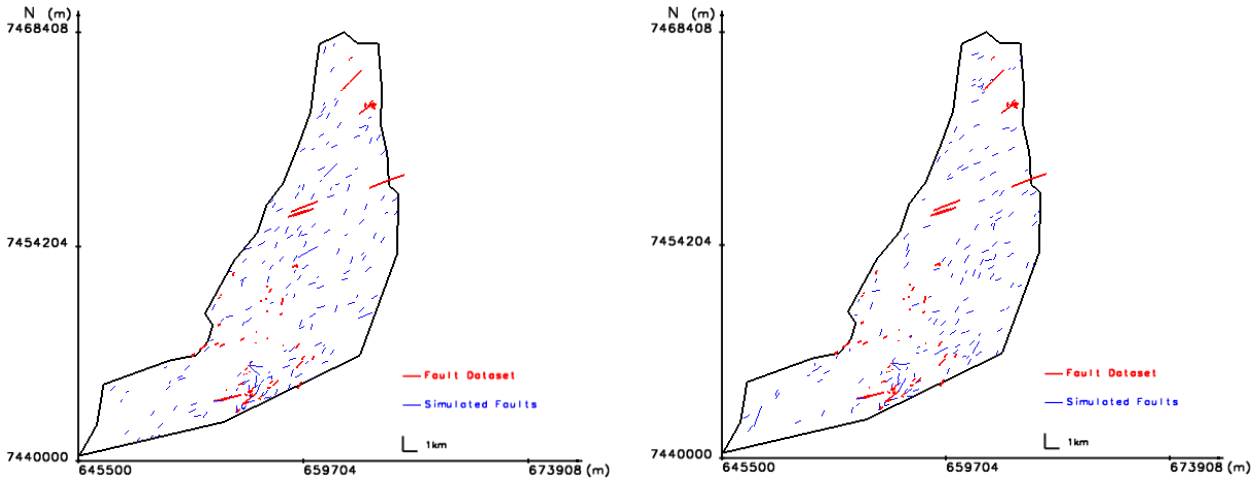

Figure 129 Two simulated fault realisations using complete dataset for Population 1.

Figure 130 Strike distribution and power-law model reproduced in the above simulations for Population 1.

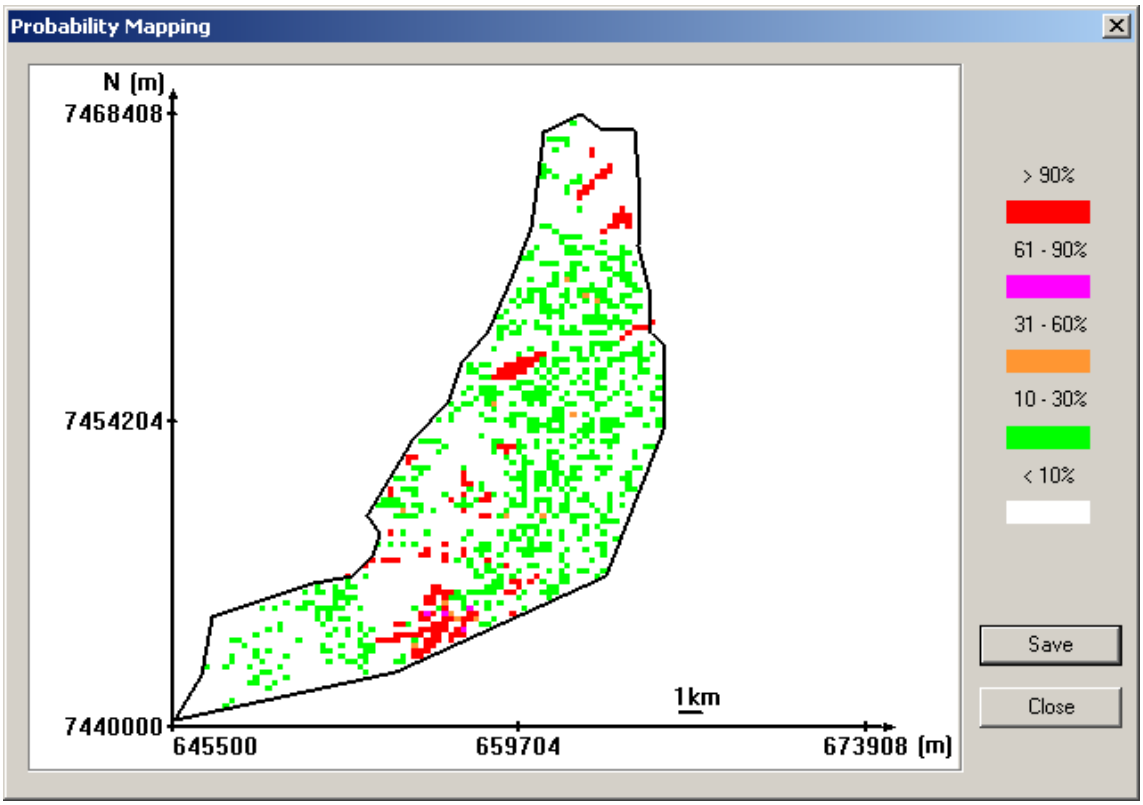

Figure 131 Fault probability map of Population 1 using complete fault dataset.

Figure 132, Figure 133 and Figure 134 show the results of fault simulations of Population 2 using the complete fault dataset.

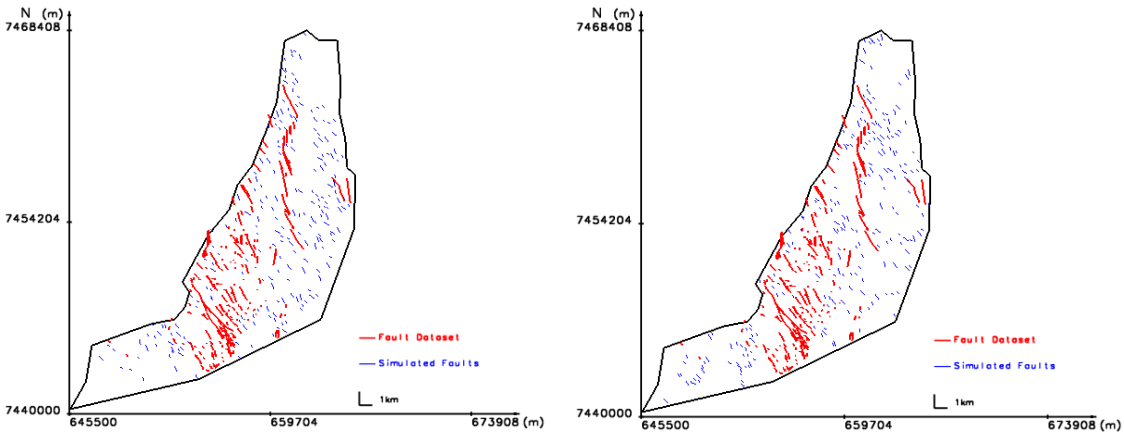

Figure 132 Two simulated fault realisations using complete dataset for Population 2.

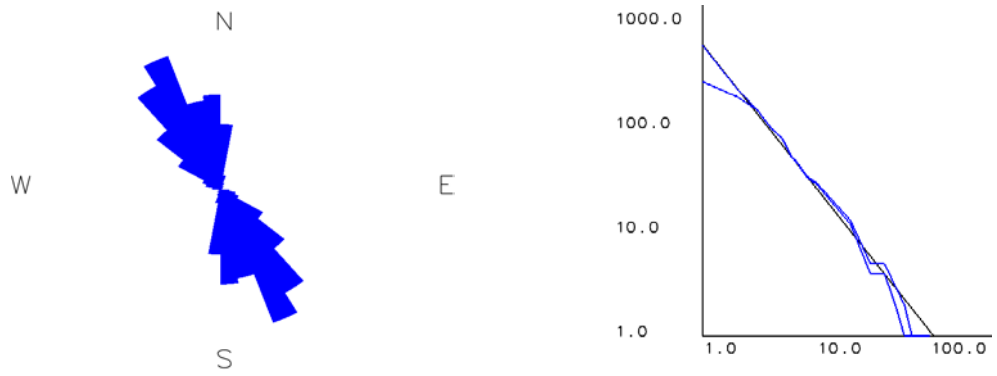

Figure 133 Strike distribution and power-law model reproduced in the above simulations for Population 2.

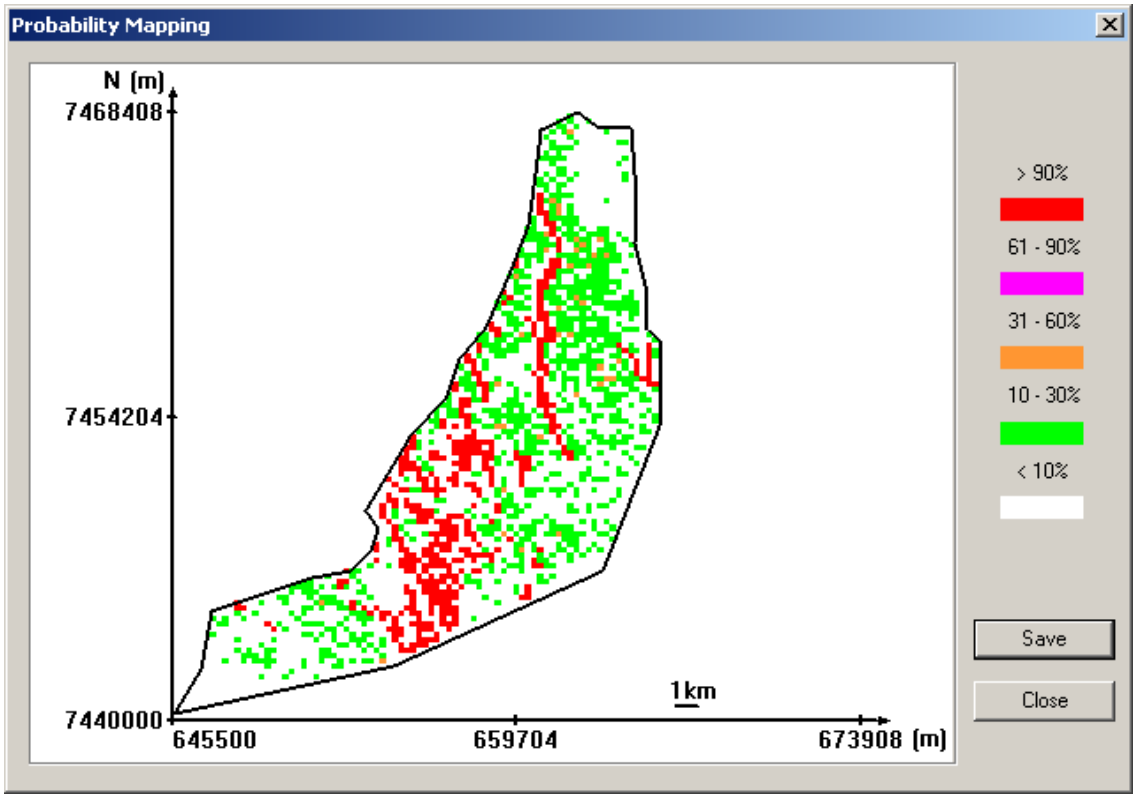

Figure 134 Fault probability map of Population 2 using complete fault dataset.

A2.5 Comparison of simulations with the interpretations

The fault data come from three sources, surface and underground mapping, seismic surveys and drilling interpretations. The confidence level of the data and their characteristics including length and throw, are different for each source. Generally, faults and fault attributes obtained from mapping and seismic surveys have higher level of confidence than the faults interpreted using drilling data. Thus, the mapped and seismic faults may be used to simulate and predict probabilities for the presence of faults. In this study, comparisons are made to assess the simulation results based on mapped and seismic faults with respect to the faults interpreted from drilling data.

Figure 135 shows the realisations of fault simulation based on mapped and seismic faults. Figure 135 (a) depicts the mapped and seismic faults. Figure 135 (b) shows one realisation of fault simulation using mapped and seismic faults. Figure 135 (c) presents the interpreted faults from drilling. Figure 135 (d) shows a second realisation of fault simulation using mapped and seismic faults.

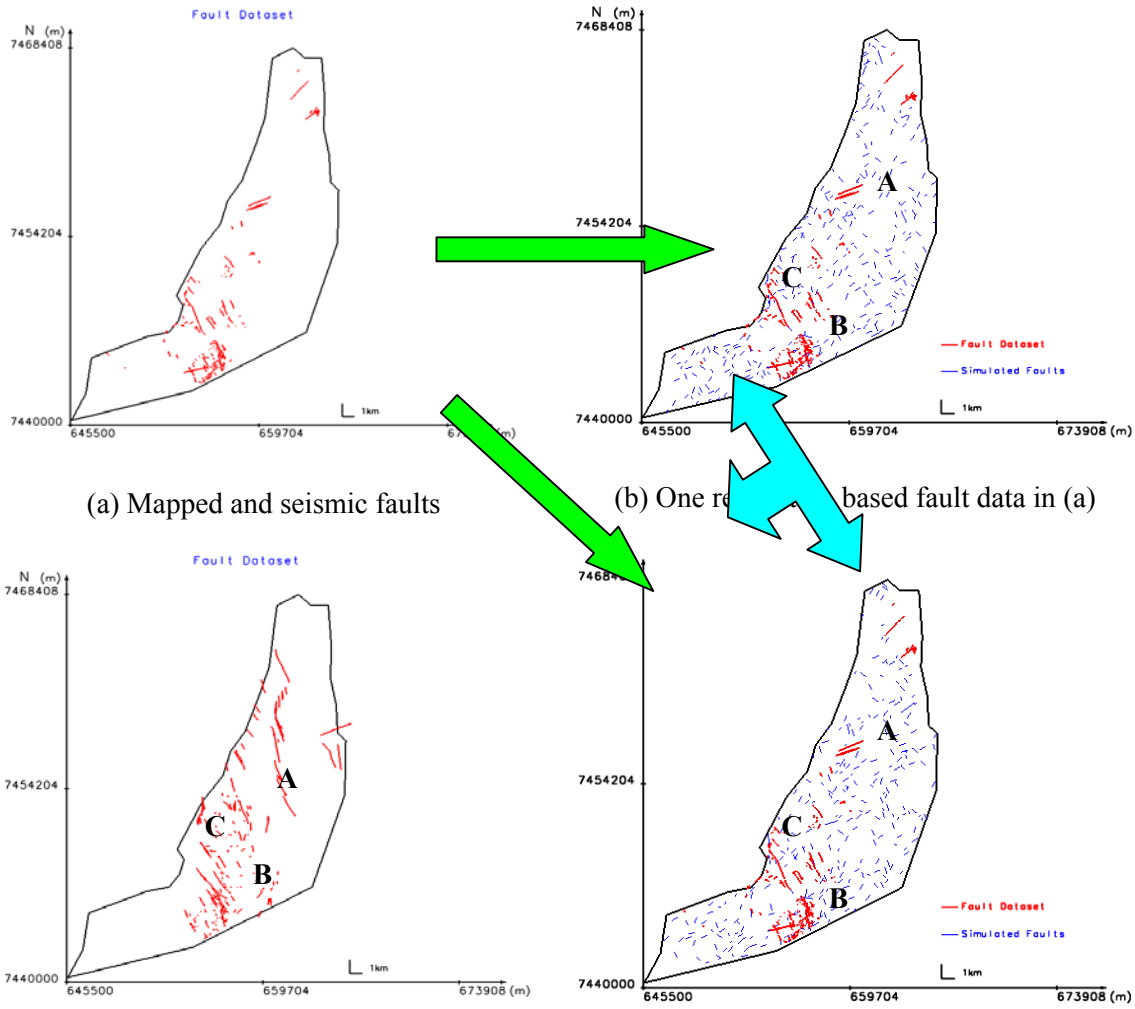

(a) Mapped and seismic faults

(b) One realisation based fault data in (a)

(c) Interpreted faults

(d) Second realisation based fault data in (a)

Figure 135 Comparison of simulated faults and interpreted faults.

It is interesting to note that the Part A, B and C of the realisations in Figure 135 (b) and (d) are consistent in placing additional faults in approximately the same areas (see Part A, B and C in Figure 136 (c)).

Figure 136 shows the comparison of mapped and seismic fault data of Population 2 and corresponding simulated faults. Figure 136 (a) shows the mapped and seismic fault data. Figure 136 (c) presents the interpreted fault dataset. Figure 136 (b) and (d) are two realisations of fault simulation based on mapped and seismic fault data.

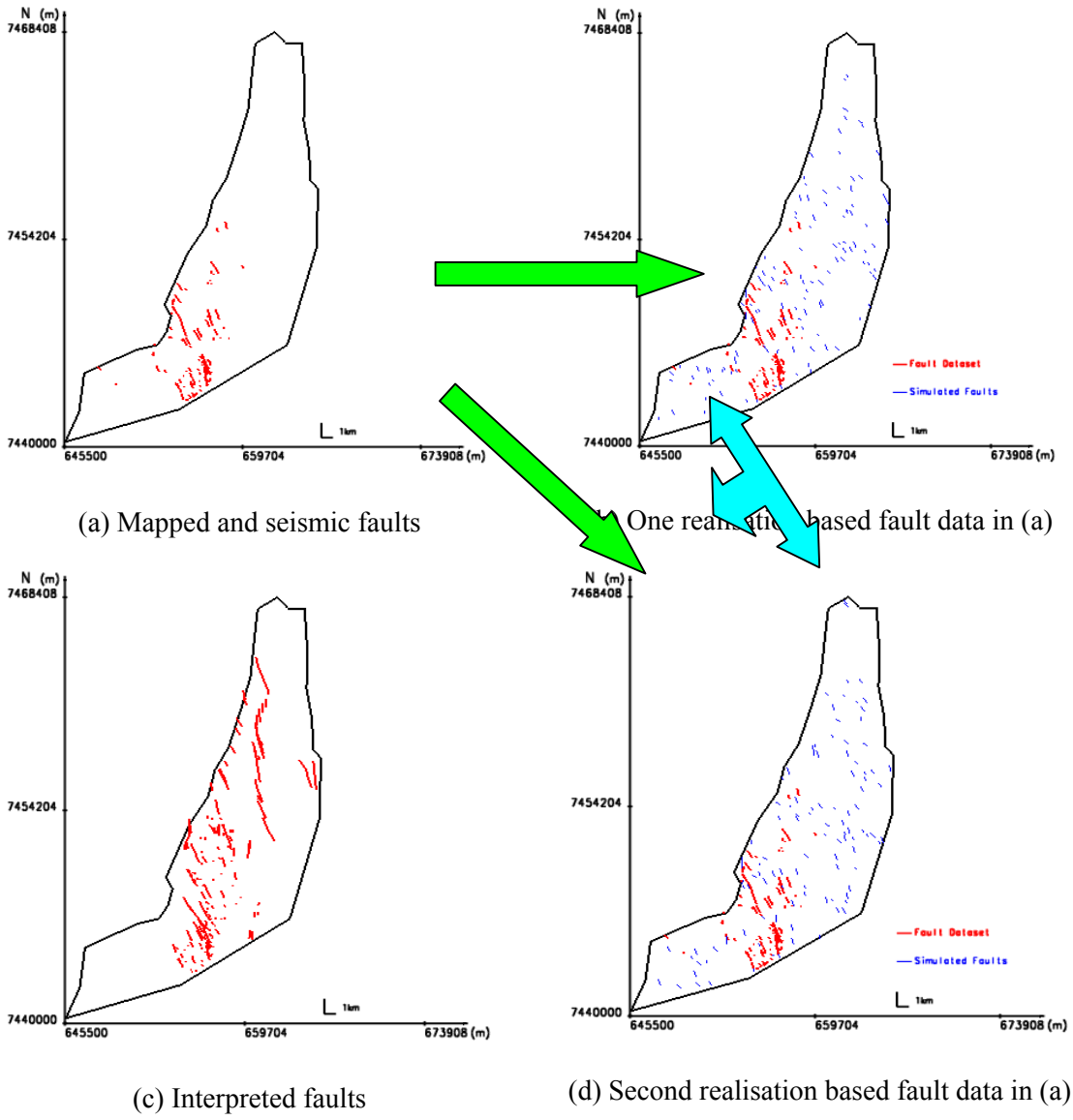

(a) Mapped and seismic faults

(b) One realisation based fault data in (a)

(c) Interpreted faults

(d) Second realisation based fault data in (a)

Figure 136 Comparison of fault simulation based on mapped and seismic fault data of Population 2 with complete fault dataset of Population 2.

The comparison shows that the simulation may extend the faults towards NE in a manner similar to the interpreted faults as they reflect the distribution pattern of interpreted fault dataset.

A2.6 Comparison of fault statistics and simulations between the southern and Northern Tiles

The results of the current study are compared to the study results in at the Goonyella-Riverside, Northern Tile, undertaken by BRC in the ACARP project C7025 (Dimitrakopoulos et al, 2001). The results of the comparison are as follows.

A2.6.1 Strike distributions

Figure 137 shows the strike distributions in (a) the Southern tile and (b) Goonyella-Riverside, part of the Northern Tile. The figure shows that the fault orientations are similar. Population 1 is oriented towards NE and Population 2 towards NNW.

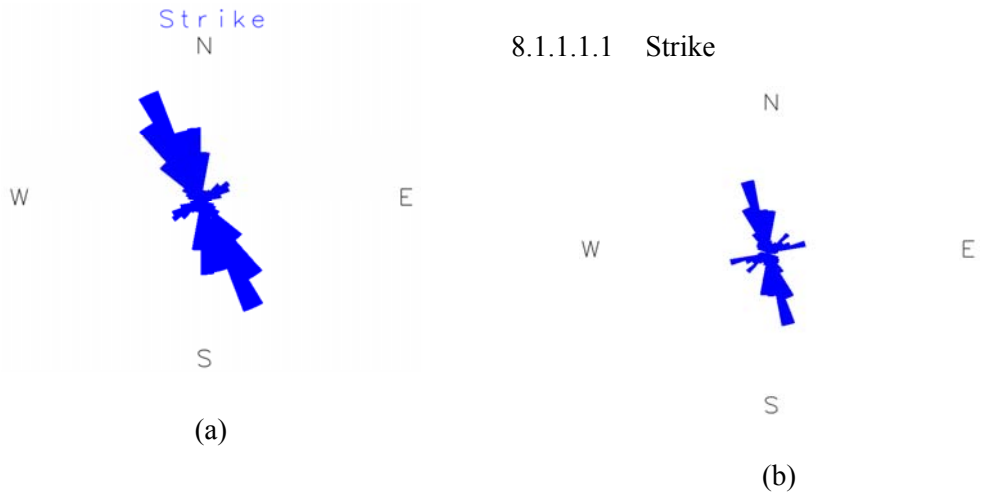

Figure 137 Fault strike distribution in (a) the Southern tile and (b) Goonyella-Riverside.

A2.6.2 Power-law model for the fault size distribution

The power-law model of the Southern tile is presented in Table 6. The corresponding plots are shown in Figure 138 (a) and Figure 139 (a). Note that the data used for modelling are as included in the complete fault dataset.

Power-law models of fault size distribution for each population in Goonyella-Riverside are reported in Table. The plots of these models are shown in Figure 138 (b) and Figure 139 (b) respectively.

Table 6 Power-law models of fault size distribution in the Southern tile

Population/ Orientation	Power-law Model	Number of Faults	
	$\text{Log}(N_s) = -\beta \log(S) + \alpha$	Identified	Predicted
1/ NE	$\text{Log}(N_s) = -2.0587 \log(S) + 2.3512$	74	224
2/ NNW	$\text{Log}(N_s) = -1.3733 \log(S) + 2.7918$	277	619

Table 7 Power-law models of fault size distribution in Goonyella-Riverside

Population/ Orientation	Power-law Model Log (N_s)= - β log (S) + α	Number of Faults	
		Identified	Predicted
1/ NE	$\log(N_s) = -1.783\log(S) + 2.33$	30	213
2/ NNW	$\log(N_s) = -1.492\log(S) + 2.275$	41	188

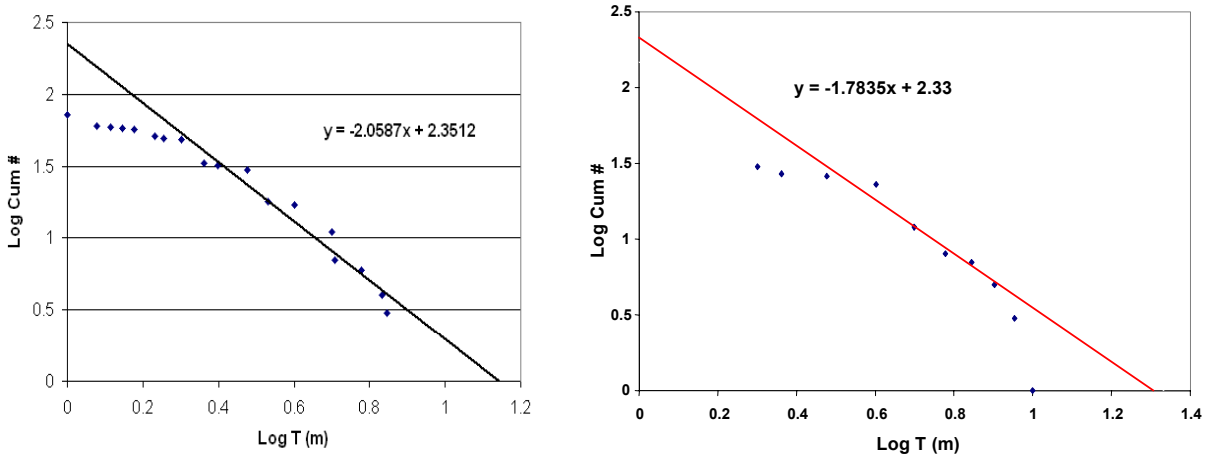

(a) (b)

Figure 138 Power-law model of fault throw distribution of Population 1: (a) Southern tile, and (b) Goonyella-Riverside.

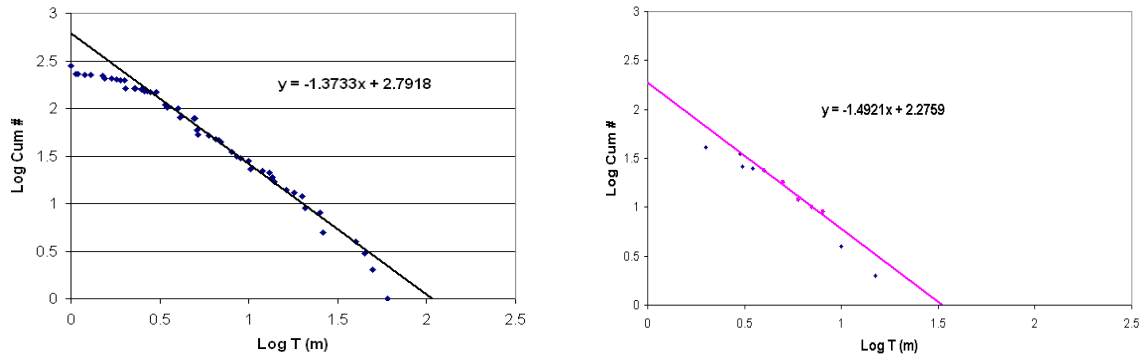

(a) (b)

Figure 139 Power-law model of fault throw distribution of Population 2: (a) Southern tile, and (b) Goonyella-Riverside.

The comparison of the power-law models shows that the slope of the Southern tile model for Population 1 is higher than that in Goonyella-Riverside. It means that the proportion of faults with smaller throw in Southern Tile is greater than that in Goonyella-Riverside. For Population 2, the slope of the Southern Tile model is slightly lower than that in Goonyella-Riverside, which indicates that the proportion of faults with larger throw in the Southern Tile is more than that in Goonyella-Riverside. These latter are the deep basement derived structures.

The study area in the Southern Tile is approximately 226 km^2, and the study area in Goonyella-Riverside is about 104 km^2. The size of study area in the Southern Tile is about 2.17 times of the size of Goonyella-Riverside study area. Based on the power-law models for the two study areas, the number of predicted faults in Southern Tile is about 2.1 times of that in Goonyella-Riverside. That is, the number of faults is proportional with the study area covered. The above comparisons suggest that the fault populations in these two areas have comparable fractal characteristics.

A note on power-law models from mined out long walls to assist the reader, the power-law models for a fully known dataset in North Goonyella mine (Northern Tile) are shown in Figure 140. The faults included have been mapped in mined out long walls and include faults with throws less than 1 m (i.e. log (0)).

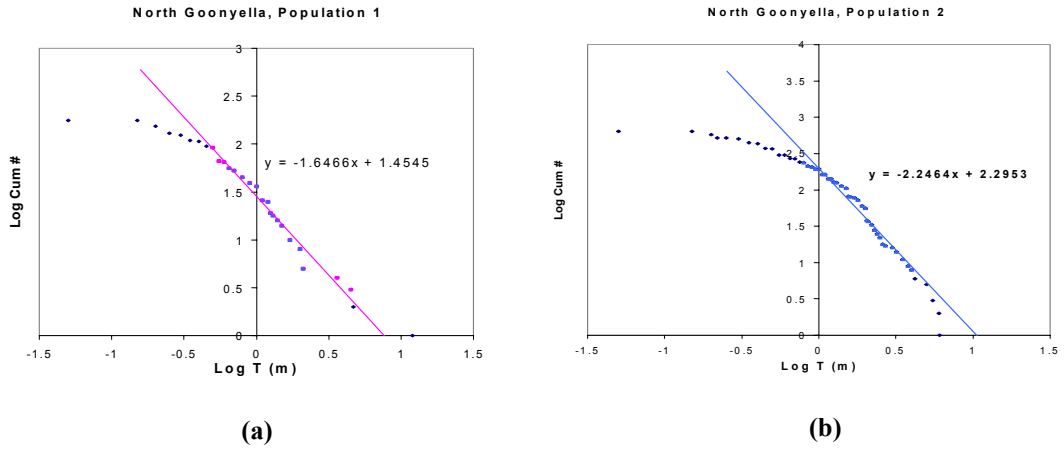

(a) **(b)**

Figure 140 Power-law model of fault throw distribution: (a) Population 1 and (b) Population 2.

The figure shows that the above power-law models for Population 1 and Population 2 using fully known fault dataset in North Goonyella, Northern Tile, concludes that the fault populations follow the power-law relationship for fault size distribution. The faults with throw greater than and equal to 1 m fit to the models very well. The decline from the model suggests that small faults may not be consistently mapped.

A2.6.3 Power-law relationship between fault length and throw

The power-law models of the relationship between fault length and throw for each population in the Southern Tile are reported in Table 8. The plots of these models are shown in Figure 141 (a) and Figure 142 (a) respectively.

Table 8 Power-law models of relationship between fault lengths and throw in the Southern Tile

Population/ Orientation	Power-law models $Log\ (T_{max}) = N\ log(L) - c$
1/ NE	$\text{Log } (T_{max})=0.0342\log(L)+0.2825$
2/NNW	$\text{Log } (T_{max})=0.3397\log(L)+0.361$

The power-law models of the relationship between fault length and throw for each population in Goonyella-Riverside are reported in Table 9. The plots of these models are shown in Figure 141 (b) and Figure 142 (b) respectively.

Table 9 Power-law models of relationship between fault lengths and throw in Goonyella-Riverside

Population/ Orientation	Power-law models $Log\ (T_{max}) = N\ log(L) - c$
1/ NE	$\log(T_{max}) = 0.296\log(L) - 0.214$
2/ NNW	$\log(T_{max}) = 0.311\log(L) - 0.28$

The figures show that for Population 1 the length and throw data do not correlate. This is the result of substantial number of interpreted faults in the dataset. It is suggested that the interpreted faults, specifically length and throw character need to be re-examined in the context of fault statistics and inference.

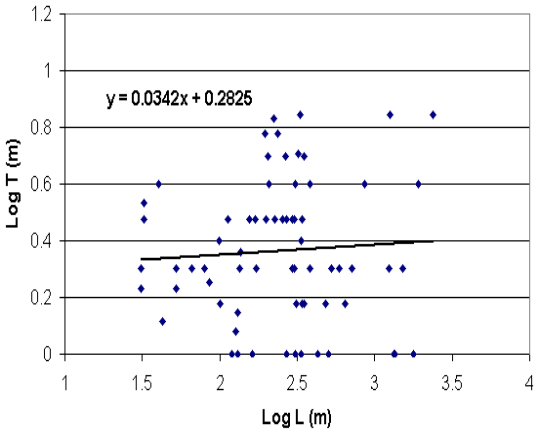

(a)

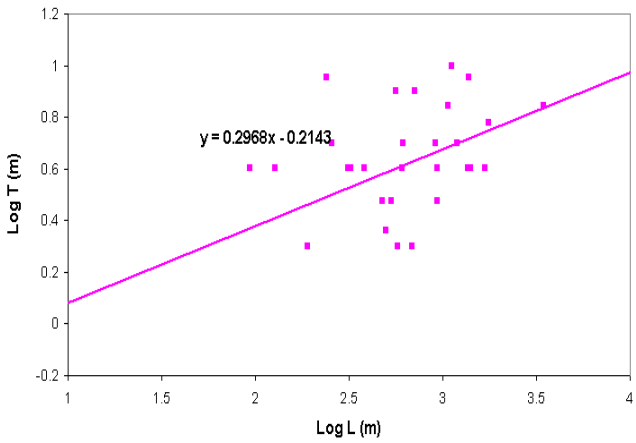

(b)

Figure 141 The relationship between fault length and throw for Population 1: (a) the Southern Tile, and (b) Goonyella-Riverside.

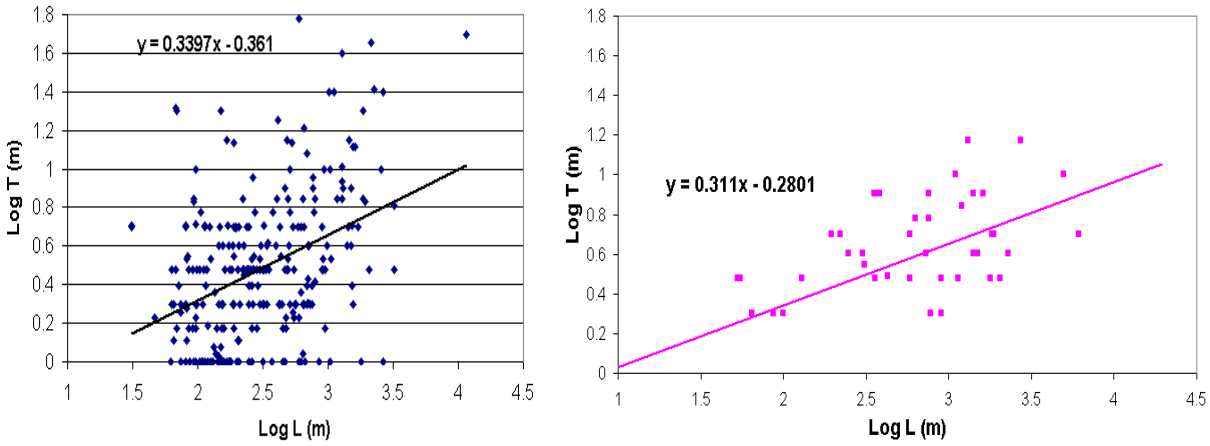

(a) (b)

Figure 142 The relationship between fault length and throw for Population 2: (a) the Southern Tile, and (b) Goonyella-Riverside.

A2.7 The simulated fault probability

Figure 143 and Figure 144 show the simulated fault probability in the study area of Southern Tile and in Goonyella-Riverside respectively.

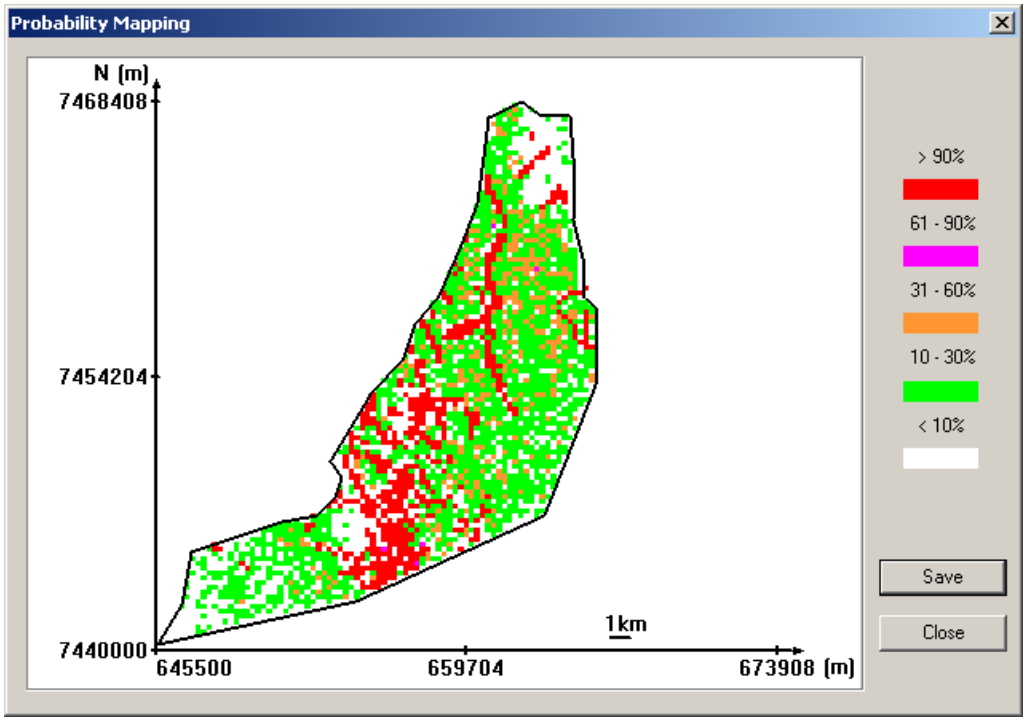

Figure 143 Maps of probability of occurrences for faults over or equal to 1 m in the study area of Southern Tile.

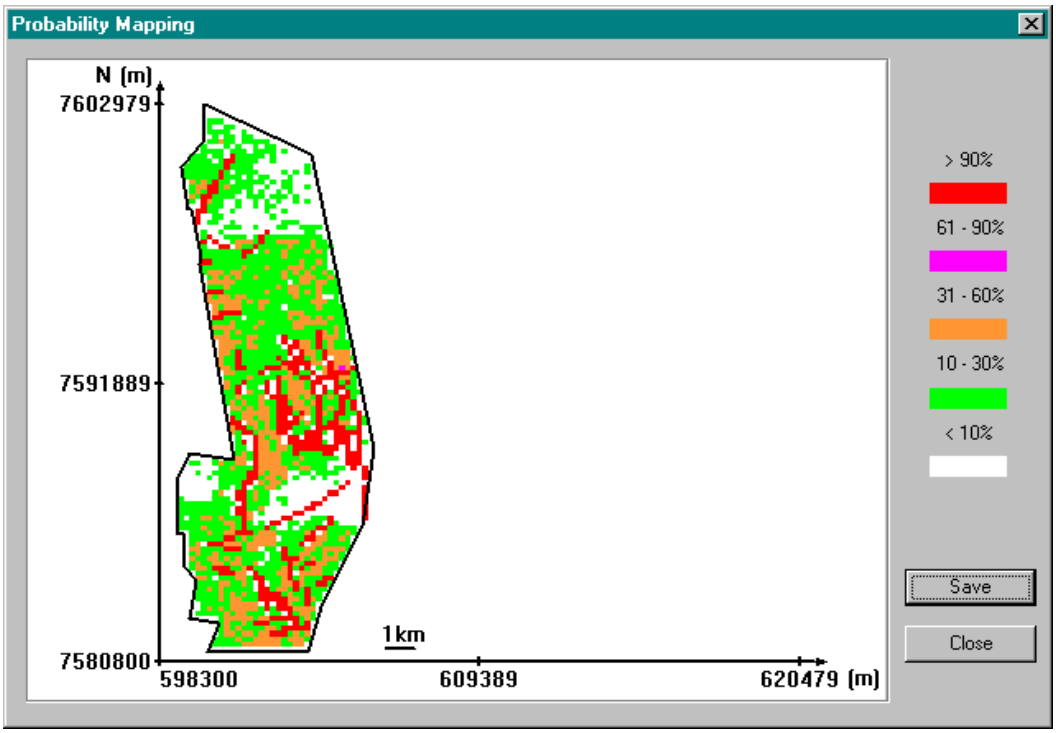

Figure 144 Maps of probability of occurrences for faults over or equal to 1 m in the study area of Goonyella-Riverside.

The fault probability in both study areas demonstrates that the intensity of faulting in these two areas is similar. Fault probability in most part of both study areas is from 10-30%. The areas with fault probability of 30-60% are noticeable in both cases.

A2.8 Conclusions

The fault populations at Southern Tile in Bowen Basin were investigated using stochastic simulations. The study shows that the power-law model of faults based on the complete fault dataset predicts the probability for the presence of an additional 450 faults with throw above 1 m in the area of the tile. The fault system in the Southern Tile has comparable fractal characteristics as that in Northern Tile. Maps of fault probabilities have been generated for the tile and using various combinations of fault populations and data options.

APPENDIX 3 GEOSTATISTICAL ANALYSIS OF GAS/DEPTH DOMAINS

Shuxing Li and Roussos Dimitrakopoulos

A3.1 Regionalised modelling of gas domains

The aim of this study is to regionally model the cross-plots of gas quantity vs. seam depth using multivariate geostatistical methods so as to assist with the understanding of the spatial characteristics of gas domains. The objective was to test the stability of domains and their areal extent and to improve estimation in areas of sparse data. In this case study we defined domains by gas quantity versus seam depth relationships, as per Figure 111.

A3.1.1 Joint simulation of correlated variables with Min/Max autocorrelation factors

Minimum/Maximum Autocorrelation Factors or MAF is a principle components-based approach incorporating global spatial statistics of the data in addition to the non-spatial statistics of the lag-zero variance-covariance matrix (Desbarats and Dimitrakopoulos, 2000). The MAF procedure de-correlates the transformed variables at all lags so that conditional simulations can be performed independently on MAF factors. The independent MAF factors simulated are then transformed to correlated variables.

The method of joint simulation of correlated variables with Min/Max autocorrelation factors or MAF follows the steps:

- Normalisation of variables.
- Generation of non-correlated MAF factors.
- Variography for each factor.
- Conditional simulation of each MAF factor.
- Back-rotation and normalisation of MAF factors to variables.

A3.1.2 Characterising gas domains using regionalised gas vs. depth cross-plots

Gas domains in coal seam may be characterised using cross-plots of gas quantity vs. seam depth. To better understand the spatial distribution of cross-plots in a coalfield, a methodology has been developed to model the regionalised cross-plots of gas quantity vs. seam depth. The method of spatial modelling gas domains is as follows:

- Jointly simulate gas quantity and seam depth at a fine scale.
- Consider gas quantity vs. seam depth cross-plots for a basic unit (2 by 2 km).

- Generate maps of gradient and intercept from the gas quantity vs. seam depth cross-plots for the basic unit.
- Repeat for a bigger unit (3x3, 4x4, 5x5, 5x10 km, etc.) and stop at the size that identifies region with given gradient and intercept.
- Repeat for a number of different simulations to test the stability of the above regions.
- Repeat for a number of different simulations with the shifting of modelling window to test the stability of above regions.
- Generate gas quantity vs. seam depth cross-plots for each of the identified regions.

A3.2 Case study Southern Tile

The study area and available data are shown in Figure 145. Figure 145 (a) shows the seam depth measured from borehole drilling at Southern tile in Bowen Basin. Figure 145 (b) depicts the gas quantity obtained from the corresponding boreholes. The gas quantity is measured in m^3/t at 20°C and 101.3kPa. Each sample borehole has a record of seam depth and corresponding gas quantity.

Figure 146 (a) shows a realisation of seam depth simulations. Figure 146 (b) shows the corresponding realisation of gas quantity simulations. They are obtained from joint simulation using available data.

The cross-plots of gas quantity versus seam depth are spatially referenced and defined by their gradients and intercepts. To model the cross-plots is to obtain their gradients and intercepts. The generation of gradient and intercept maps start from a smaller modelling window. With the increase of modelling window size, the regions with distinct gradient and intercept can be identified. Figure 147 shows the spatial distribution of gradient identified using different sizes of modelling windows. In Southern tile, the window size 4x4 km or 5x5 km will maintain a stable cross-plots.

To analyse the sensitivity of cross-plots modelling, a number of simulations are conducted and used to model the cross-plots. Figure 148 shows the spatial distribution and variation of gradients from the different simulations. It indicates that the gradient distribution is relatively stable from realisation to realisation.

In addition, the gradient and intercept may also sensitive to the location of modelling window in spite of the same window size. The sensitivity analysis is also carried out to test the sensitivity of regions using moving windows. Figure 149 shows the spatial distribution of gradients with the shifting of windows used. The results show that there are no major shifts.

Figure 150 shows the spatial distribution of the gradient of cross-plots. There are marked differences within Southern tile. The middle part has higher gradient than that in southern part. It means the gas quantity increases faster than that in southern part. These differences may help to characterise the gas domains.

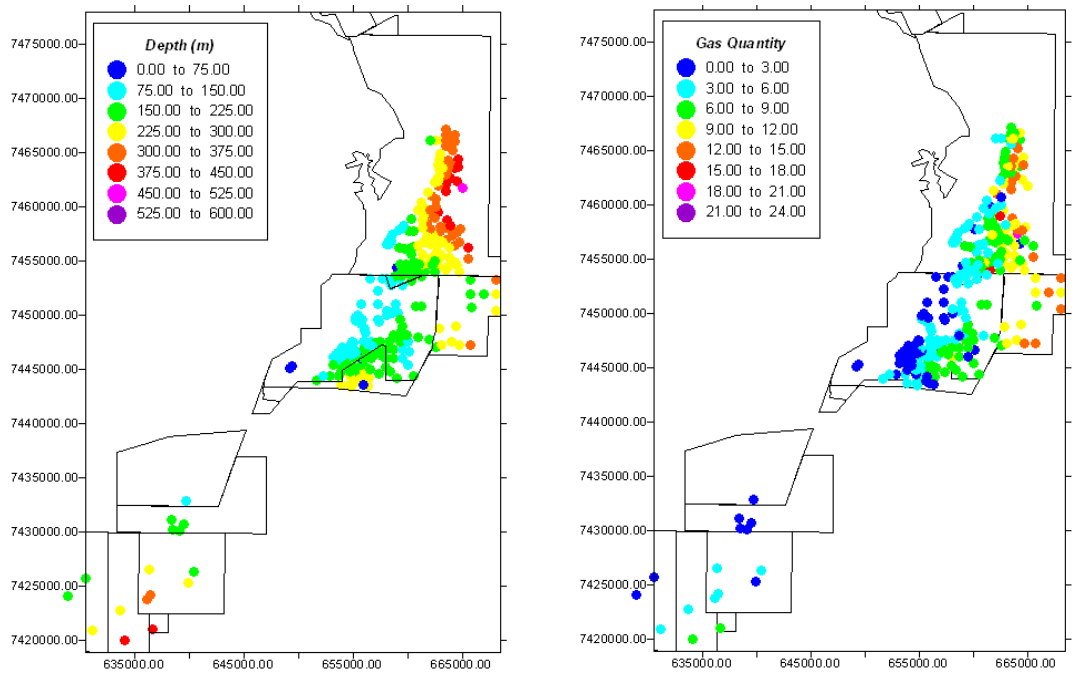

(a) (b)

Figure 145 Data measurement from borehole drilling: (a) seam depth; (b) gas quantity

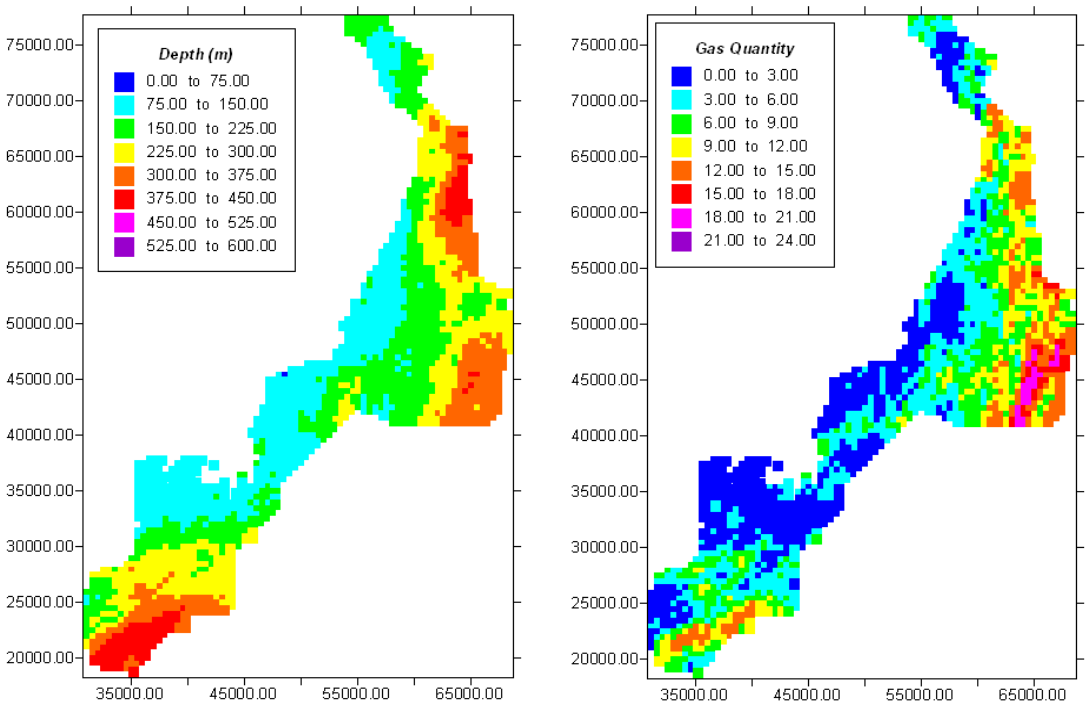

(a) (b)

Figure 146 (a) Simulated seam depth values and (b) simulated corresponding gas quantity values at Southern tile in Bowen Basin

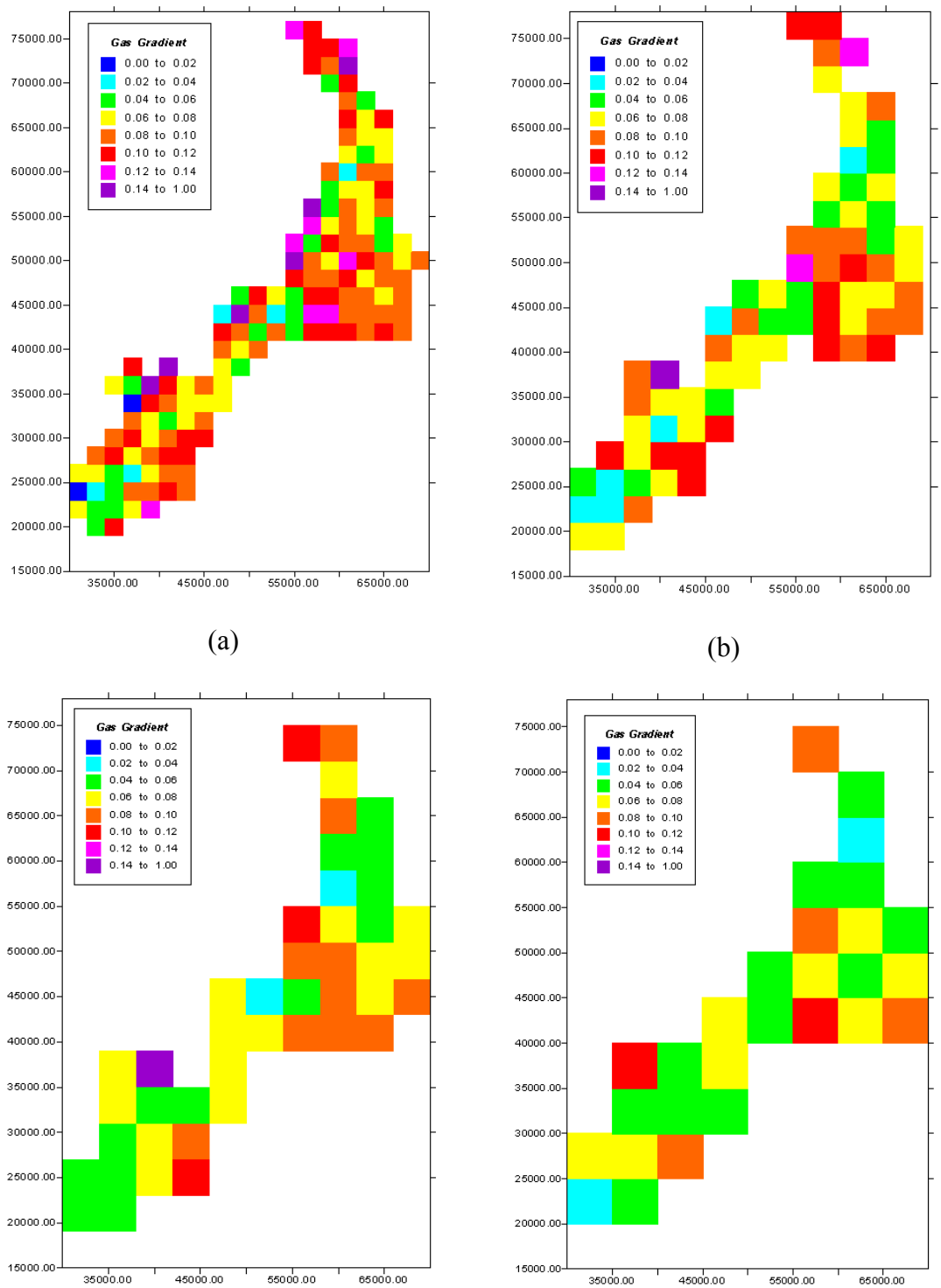

Figure 147Gradient of gas vs. depth cross-plots in different modelling window sizes: (a) 2x2km, (b) 3x3km, (c) 4x4km, (d) 5x5km

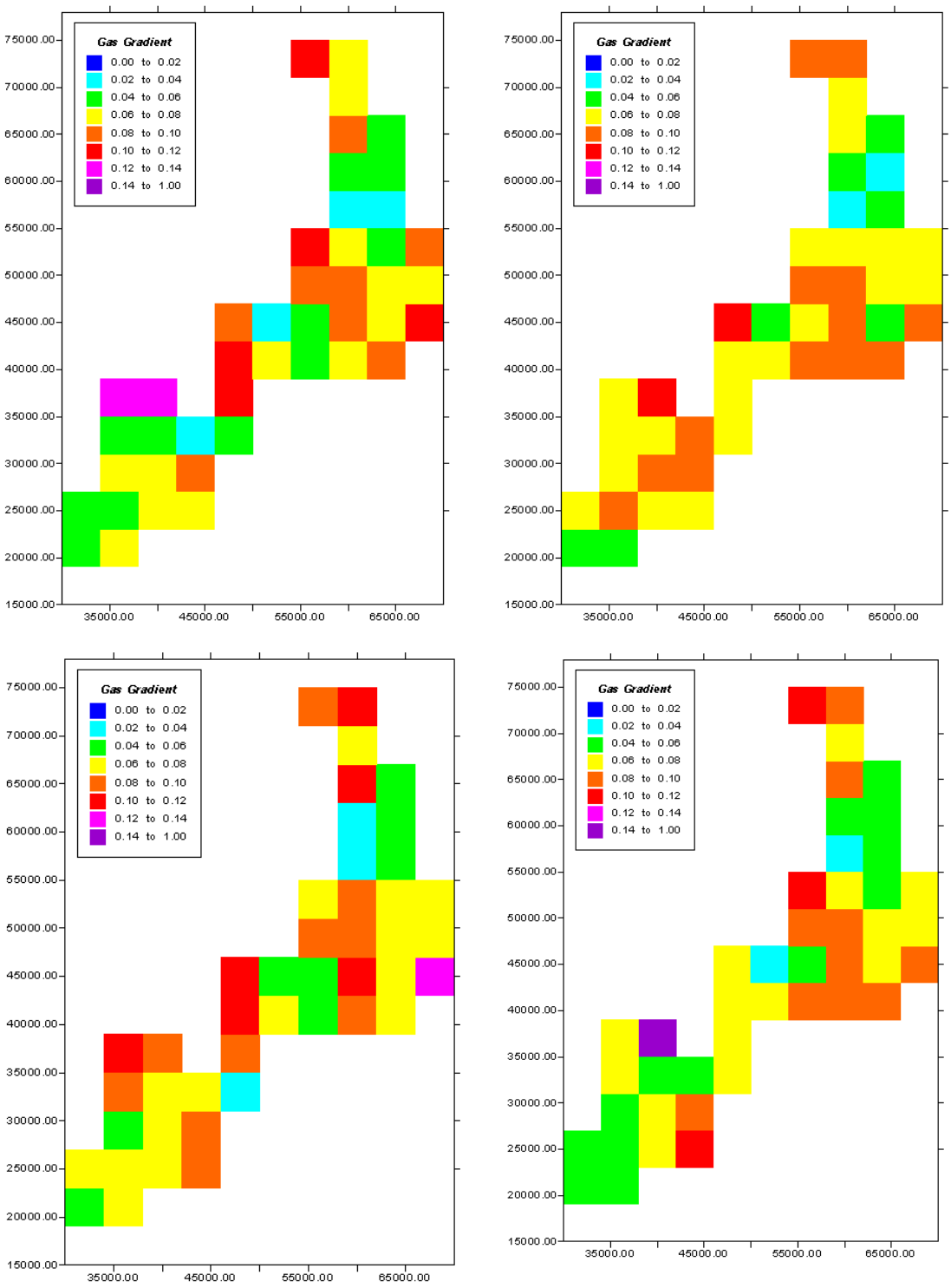

Figure 148 Gradient of cross-plots of gas quantity vs. seam depth obtained from different simulations (modelling window sizes 4x4km)

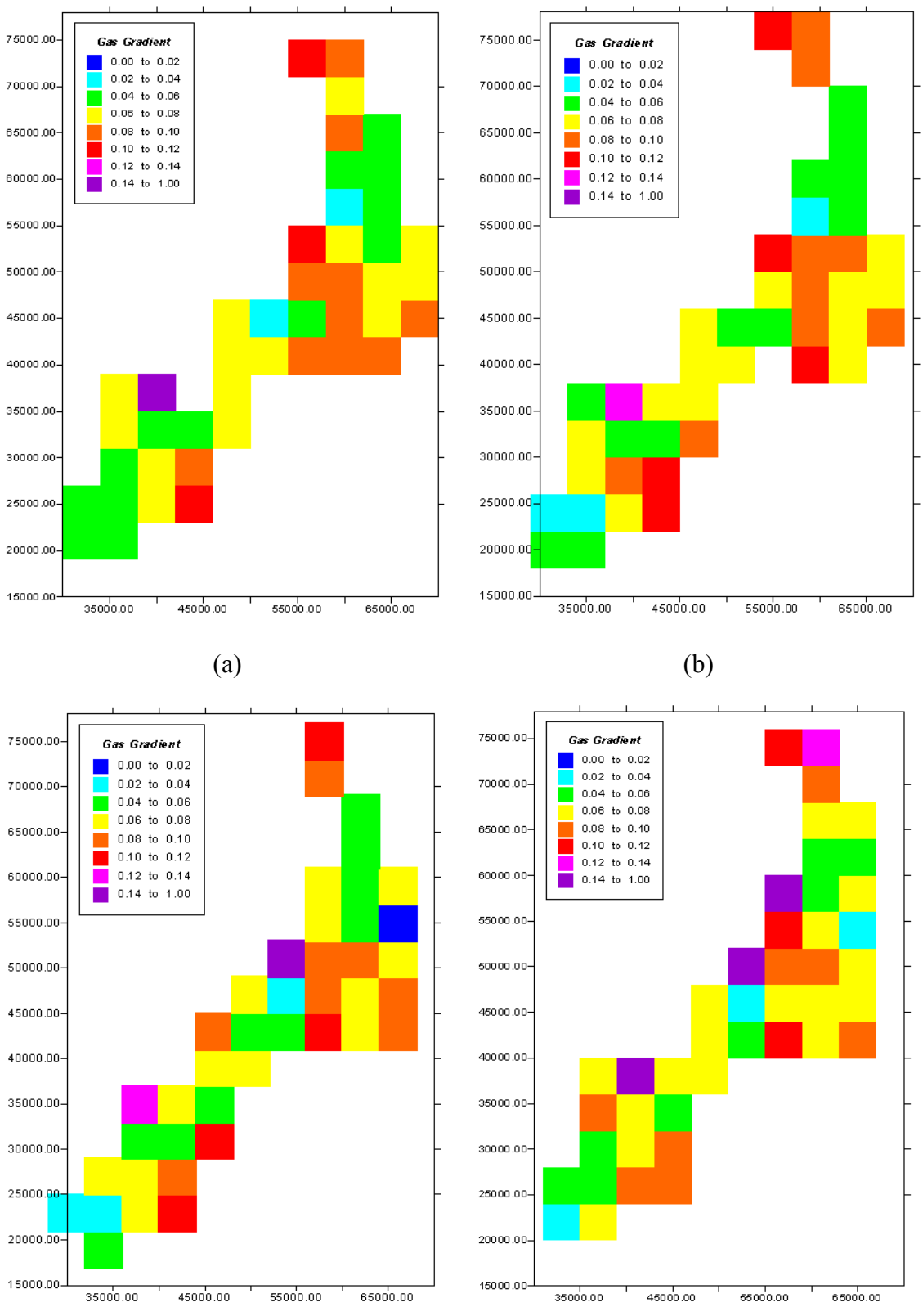

Figure 149 Gas gradient obtained based on above simulation in window size 4x4km with different shifting distance toward to s-w direction: (a) original state, (b) 1km, (c) 2km, (d) 3km.

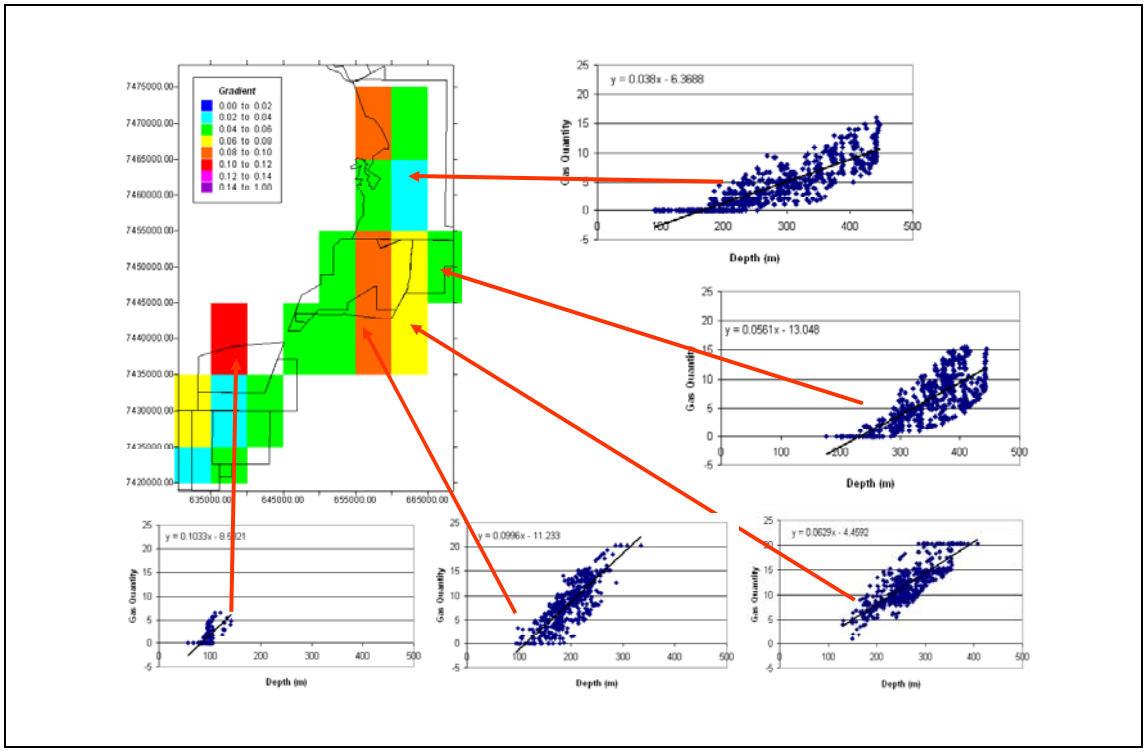

Figure 150 Identified regions and their gas quantity vs. seam depth cross-plots

A3.3 Case study at Northern Tile

The study area and gas data at Northern tile in Bowen Basin are shown in Figure 151. Figure 151 (a) shows the seam depth measured from borehole drilling. Figure 151 (b) shows the gas quantity obtained from the corresponding boreholes.

Using the available data of seam depth and gas quantity, the joint simulations are conducted at Northern tile. Figure 152 (a) shows a realisation of seam depth simulations. Figure 152 (b) shows the corresponding realisation of gas quantity simulations.

Based upon a realisation of seam depth and gas quantity, the regionalised cross-plots of seam depth vs. gas quantity are modelled. Figure 153 shows the spatial distribution of gradient identified using different sizes of modelling windows. In Northern tile, a stable spatial distribution of cross-plots will be identified using the window size above 2x2 km.

There are two aspects that have been identified for sensitivity analysis. One is the sensitivity of different realisations. Other is the sensitivity of the locations of modelling windows. To analyse the sensitivity of different realisations, a number of simulations are conducted to model the cross-plots. Figure 154 shows the spatial distribution of gradients from the different

simulations. It indicates that the gradient distribution is very stable from realisation to realisation.

The sensitivity of the locations of modelling windows is analysed by testing the sensitivity of regions using moving windows. Figure 155 shows the spatial distribution of gradients with the shifting of windows used. The figure indicates that there are no major shifts from the movement of modelling windows.

Figure 156 shows the spatial distribution of the gradient of cross-plots at Northern tile. There are some differences from area to area within Northern tile. The middle part has higher gradient values than that in southern and upper middle parts. Although the differences of gradient are not as large as that at Southern tile, these differences may also help to characterise the gas domains at Northern tile.

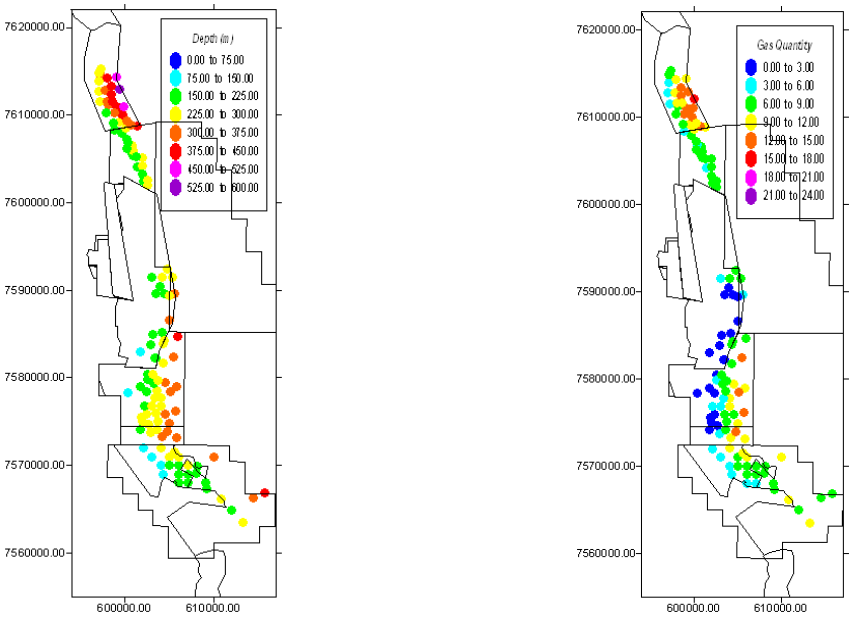

(a) (b)

Figure 151 Data measurement for borehole drilling: (a) seam depth; (b) gas quantity

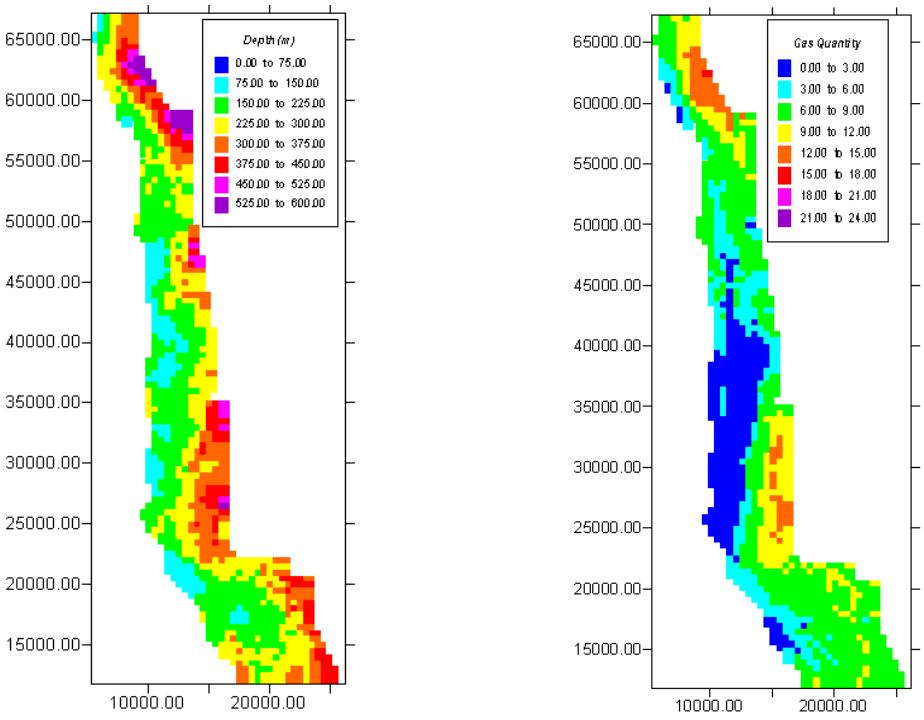

(a) (b)

Figure 152 (a) Simulated seam depth values and (b) simulated corresponding gas quantity values at Northern tile in Bowen Basin

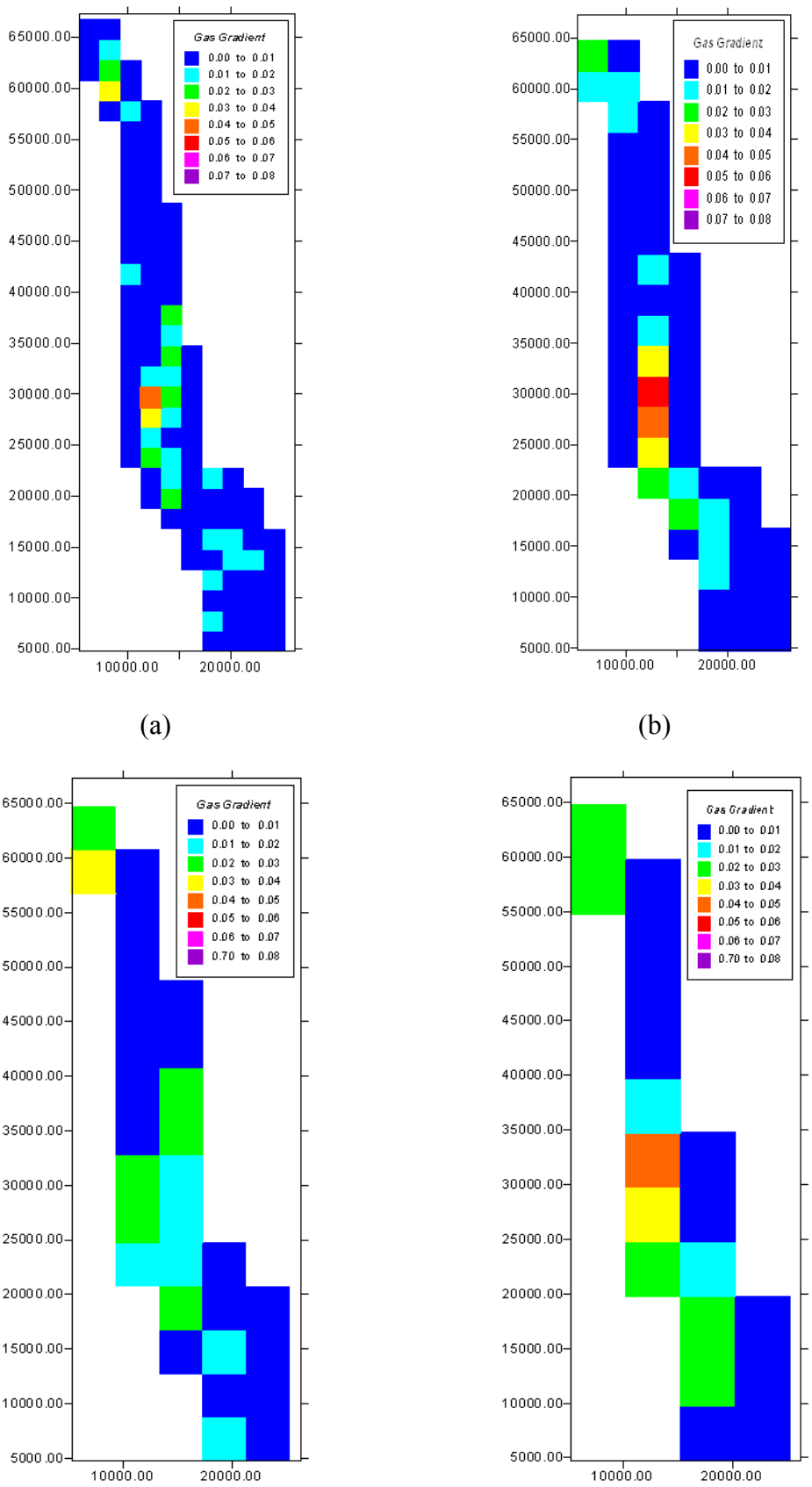

Figure 153 Gradient of gas quantity vs. seam depth cross-plots in different window size at northern tile: (a) 2x2km, (b) 3x3km, (c) 4x4km, (d) 5x5km.

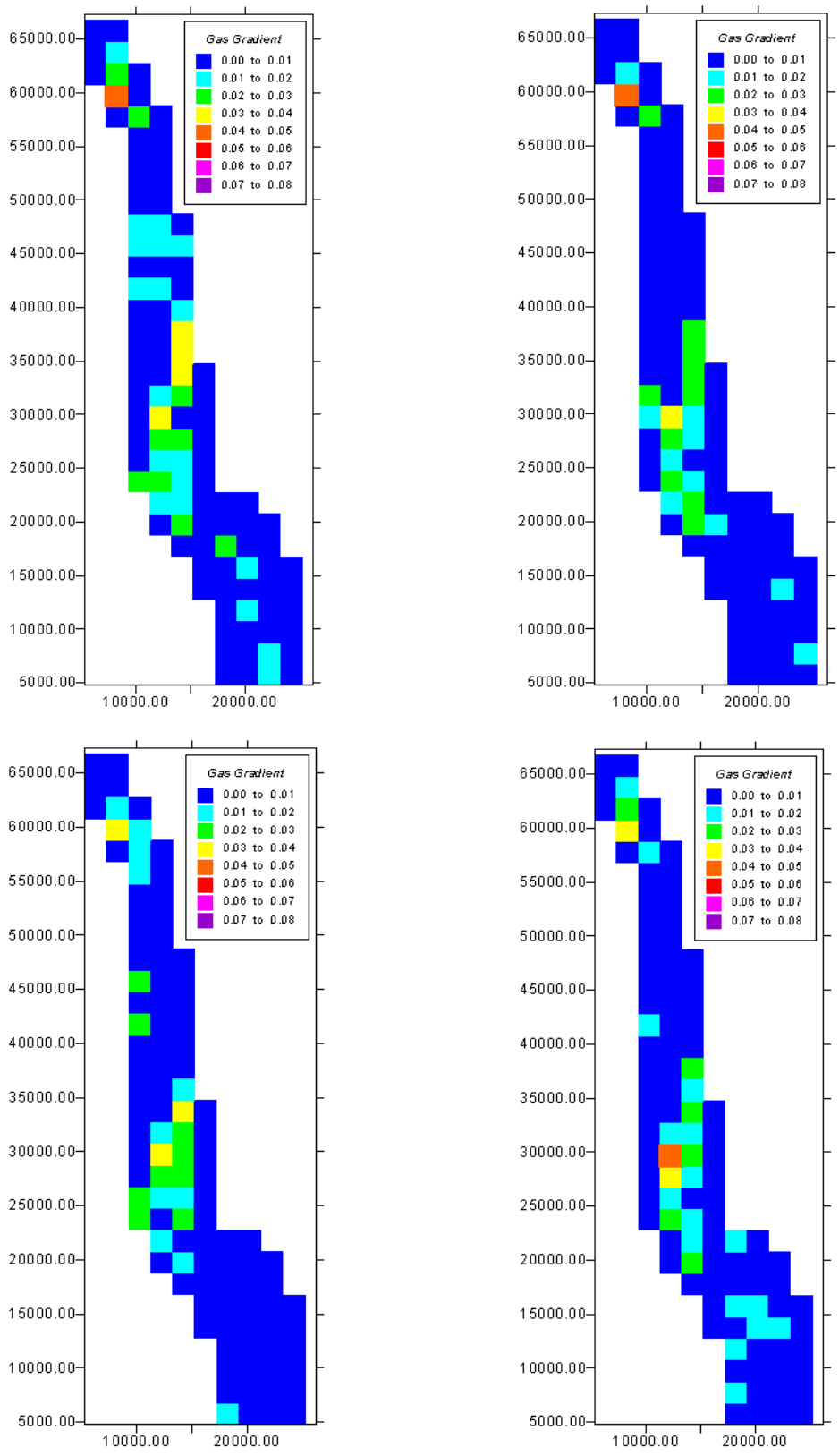

Figure 154 Gradient of gas quantity vs. seam depth cross plots in different simulations (modelling window size 2x2km)

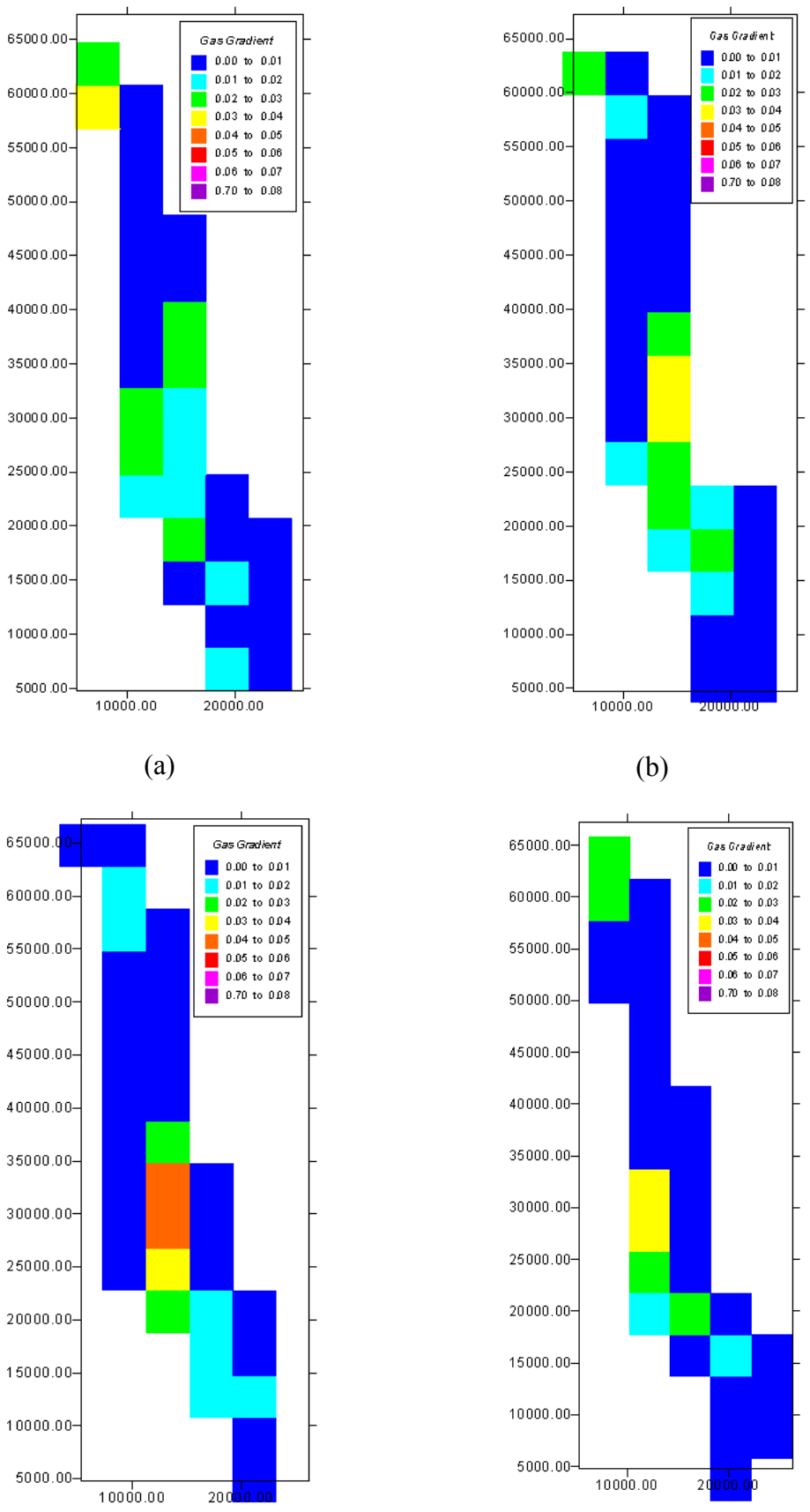

Figure 155 Gradient of gas quantity vs. seam depth cross-plots in different shifting distance with window size of 4x4km (a) Original mapping, (b) 1km, (c) 2km, (d) 3km

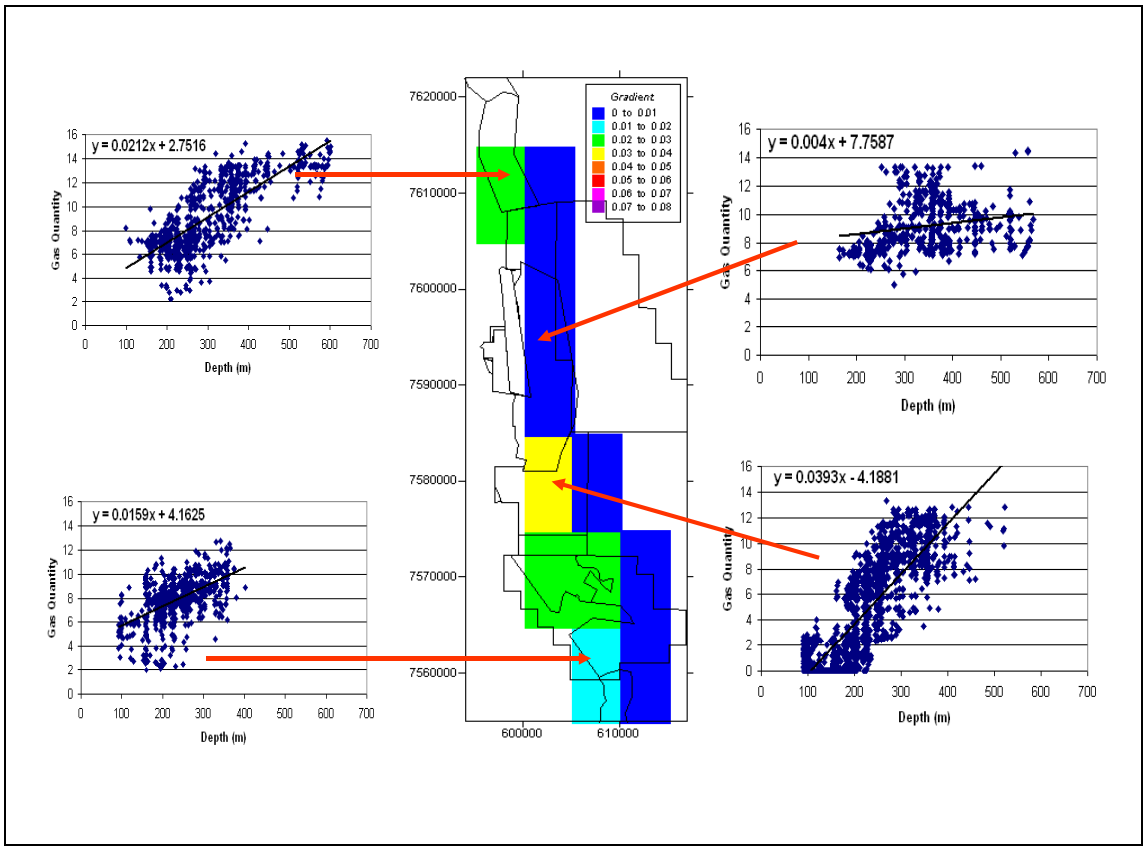

Figure 156 Identified regions and their gas quantity vs. seam depth cross-plots at Northern tile in Bowen Basin

A3.4 Comparison of the Northern and Southern Tiles

From above modelling results, a comparative analysis has been done. The following differences were found:

1) The gradients at Northern tile are much lower than that in the Southern Tile.

2) The intercepts tend to be positive in the Northern tile.

3) ntercepts are negative in the Southern tile.

4) The gradient variations within Northern tile are less.

5) The gradient variations within Southern tile tend to be large.Figure 157 shows the comparison of cross-plots of gradient vs. intercept at Northern tile and Southern tile in Bowen Basin. There are marked differences between these two tiles. Figure 157 can be used to characterise large regions like a tile.

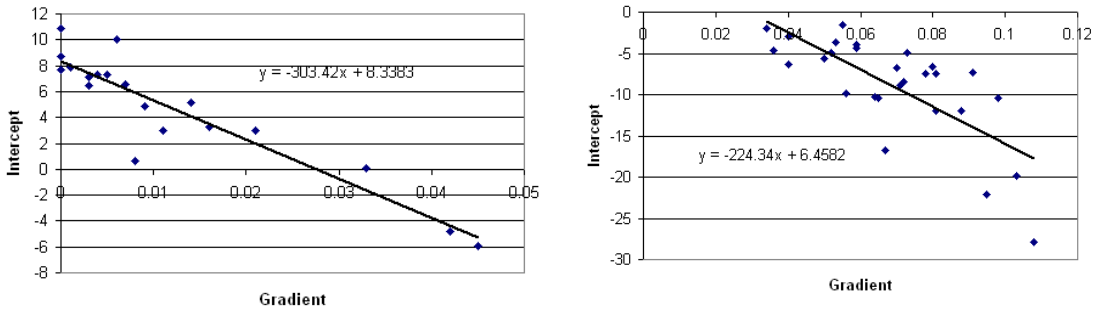

(a) (b)

Figure 157 Cross-plot of gradient vs. intercept (a) at Northern tile; (b) at Southern tile

A3.5 Conclusions

The results suggest that:

1) Spatial modelling of gas quantity vs. seam depth cross-plots allows the identification of regions with distinct gas vs. depth relationships.

2) Spatial modelling of gas quantity vs. seam depth may also assist geological interpretations when combined with other layers of information within a study area.

3) A first example was shown; more complex data sets may substantially contribute to assessing the gas distribution in any region of interest.The identified regions with distinct gradient can be used in characterising gas domains in a coalfield.